

TYPE III DEEP EUTECTIC SOLVENTS (DESS) AS BASE LUBRICANTS

**Thesis submitted for the degree of
Doctor of Philosophy
at the University of Leicester**

by

**Essa Ismaeil Ahmed MSc
Department of Chemistry
University of Leicester**

**Supervisors
Prof Andrew P. Abbott
Prof Karl S. Ryder**

July 2015



ABSTRACT
TYPE III DEEP EUTECTIC SOLVENTS (DESS) AS BASE LUBRICANTS

ESSA ISMAEIL AHMED
UNIVERSITY OF LEICESTER
2015

Mineral oils are the most commonly used fraction of formulated lubricating oils except for some specialised applications where synthetic oils are employed. An alternative approach has been suggested using ionic liquids (ILs) due to their high viscosity index and high thermal stability. The aim of this study is to examine the use of a different type of ionic liquids in the form of Deep Eutectic Solvents (DESS) as base lubricants as these have significantly improved environmental credentials.

The first stage of the study involved the investigation of thermo-physical properties such as heat capacity, thermal stability, surface tension, viscosity index, melting point, conductivity and density to determine if the liquids are suitable fluids as lubricants. The data for a variety of imidazolium based ILs and standard mineral base oil were also determined and used for comparison sake. In addition the properties of DES mixtures with water were determined and self-diffusivity were measured using NMR spectroscopy. It was shown for the first time that aqueous DES mixtures are not homogeneous but instead they form bicontinuous micro-emulsions.

This study has also been the first to quantify the corrosion rates of metals in DESS and ionic liquids. The corrosion of iron, aluminium and nickel was studied in four DESS and four ILs using both Tafel slope analysis and electrochemical impedance spectroscopy. The corrosion rate was found to change over time for some liquids and so the corrosion product films were characterised using Raman spectroscopy.

The interfacial properties of DES and ILs are shown to be totally different from mineral base oil and the wettability in terms of contact angle and interfacial energies for various metals have been studied. The friction coefficient and wear volume were measured for DESS for dissimilar sliding couples. Finally, the change of both thermo-physical and mechanical properties due to the inclusion of two common surfactants sodium dodecylsulfate and cetyltrimethylammonium bromide are characterised in three DESS and shown to decrease the wear volume.

PUBLICATIONS

A) Papers

- 1- A. P. Abbott, E. I. Ahmed, R. C. Harris and K. S. Ryder, *Green Chem*, 2014, **16**, 4156-4161.
- 2- C. D'Agostino, L. F. Gladden, M. D. Mantle, A. P. Abbott, E. I. Ahmed, A. Y. M. Al-Murshedi and R. C. Harris, *Phys Chem Chem Phys*, 2015, **17**, 15297-15304.

b) Conferences:

(1) Talks:

- 1- E. I. Ahmed, A. P. Abbott and K. S. Ryder, Lubrication and Corrosion Studies of Deep Eutectic Solvents (DESSs), *Midlands Electrochemistry Group Meeting (MEG) 2014*, 1st April 2014, Loughborough University, Loughborough.
- 2- E. I. Ahmed, A. P. Abbott and K. S. Ryder, using Deep Eutectic Solvents (DESSs) as base lubricants, *Department Of Chemistry Postgraduate Research Day*, 14th April 2015, University of Leicester, Leicester.

(2) Posters:

- 1- E. I. Ahmed, A. P. Abbott and K. S. Ryder, Corrosion of metals in ionic liquids, *Electrochem Conference, September 1-3, 2013 Southampton University*, Southampton, Royal society newsletter issue two 2013, p184.
- 2- E. I. Ahmed, A. P. Abbott and K. S. Ryder, Lubrication studies of some Deep Eutectic Solvents (DESSs), *the Molten Salt Discussion group*, 10th January 2014, WMG International Digital Laboratory University of Warwick Coventry University of Warwick, Coventry.
- 3- E. I. Ahmed, A. P. Abbott and K. S. Ryder, Lubrication studies of some Deep Eutectic Solvents (DESSs), *Iraqi Cultural Attaché Conference*, 28th February 2014, University of Nottingham, NG7 2RD, Nottingham.

STATEMENT

The accompanying thesis submitted for the degree of Ph. D entitled "Type III Deep Eutectic Solvents (DESs) as Base Lubricants" is based upon work conducted by the author in the Department of Chemistry at the University of Leicester during the period between October 2012 and July 2015.

All the work recorded in this thesis is original unless otherwise acknowledged in the text or by references. None of the work has been submitted for another degree in this or any other university.

Signed:

Date:

ACKNOWLEDGEMENTS

Firstly, my sincere gratitude and appreciation to my supervisor, Prof Andrew Abbott, for all of his ideas, continued support and encouragements during the past three years. It has been an absolute pleasure to have been able to work within his group and has been a very memorable experience. I find myself extremely fortunate to have him as my supervisor.

I also would like to thank my second supervisor Prof Karl Ryder for his insightful suggestions, ideas, and time for serving in our discussions.

I am thankful to all the Materials Centre Group members both past and present, that I have had the pleasure of working with, but most notably Dr Robert Harris, Dr Alex Goddard, Dr Andrew Ballantyne and Stefan Davis for their unforgettable help and guidance. I would also like to thank Dr William Wise for all his help during my second year DSC and TGA data measurements and Dr Luka Wright, Dr Jennifer Hartley and Mahmud Khoshnaw in proof reading a great deal of this thesis.

I am thankful to all my colleagues Dr Azeez Abdulla, Jamil Juma, Idrees Qadir and Jalil Kareem for their individual contributions socially and academically to my experience.

A scholarship and living costs granted by The Higher Committee for Education Development in Iraq (HCED) and the Ministry of High Education in the Iraqi Kurdistan Region and University of Salahaddin-Hawler is also gratefully acknowledged.

My immeasurable appreciation and thanks is for my mother and my father's pure soul, thank you for all your prayers, support and unconditional love. I am very thankful to all my brothers and sisters who have helped me out not just throughout the PhD, but through all my life especially at the undergraduate and MSc stages.

Most of all, I would like to thank my wife, Bokan for her patience and for staying up with me throughout all those tiredness and to my beloved son Kewan and both my precious daughters Kave and little Laya, who are my continuous inspiration and joy and challenging players in the truly delightful and ever-evolving game of father-children relations.

DEDICATION

I dedicate this thesis to the memory of my dearly loved father, who would have been proud to see me at this time.

Essa Ismaeil Ahmed Khoshnaw

Leicester, 2015

CONTENTS

Abstract.....	i
Publications.....	ii
Statement.....	iii
Acknowledgements.....	iv
Dedication.....	v
Thesis contents.....	vi

CHAPTER ONE: BACKGROUND INFORMATION

1	Introduction.....	2
1.1	Lubricants.....	2
1.2	The history of lubrication.....	2
1.3	Lubricating oil.....	3
1.3.1	Base oils.....	4
1.3.2	Classification of base oils.....	7
1.3.3	Additive packages	8
1.3.4	Classification of additive package	8
1.4	Lubrication regimes.....	16
1.5	Ionic Liquids (ILs) and their applications.....	17
1.6	Deep Eutectic Solvents (DESs) and their applications	19
1.7	Using ILs and DESs as lubricants.....	22
1.8	Research objectives.....	32
1.9	References.....	33

CHAPTER TWO: EXPERIMENTALS

2	Experimental.....	40
2.1	Chemicals.....	40
2.2	Preparation of DESs.....	41
2.3	Measurements.....	41
2.3.1	Physical properties.....	41
2.3.2	Thermal properties.....	43
2.4.3	Corrosion studies.....	44
2.5.4	Measurements of mechanical and wetting properties.....	46
2.6	References.....	49

CHAPTER THREE: BULK PROPERTIES

3	Rheology and thermo-physical properties of DESs.....	52
3.1	Introductions.....	52
3.2	Thermal properties.....	53
3.2.1	Differential scanning calorimetry (DSC).....	53
3.2.2	Phase behaviour of DESs.....	55
3.2.3	Heat capacity of liquids.....	57
3.2.4	Enthalpy of formation of DESs.....	60
3.2.5	Thermal stability.....	61
3.3	Physical properties.....	63
3.3.1	Viscosity of ILs.....	64
3.3.2	Surface tension.....	68
3.3.3	Conductivity.....	71
3.3.4	Density.....	74

3.4	Rheological properties.....	75
3.4.1	Flow characteristics of liquids.....	75
3.4.2	Flow characteristics of DESs.....	77
3.5	Conclusions.....	85
3.6	References.....	86

CHAPTER FOUR: CORROSION STUDIES

4	Corrosion studies.....	92
4.1	Introductions.....	92
4.1.1	Corrosion.....	92
4.1.2	Corrosion requirements.....	93
4.1.3	Corrosion types.....	94
4.1.4	Uniform corrosion.....	94
4.2	Corrosion process.....	94
4.3	Electrochemical studies of corrosion.....	95
4.3.1	Linear Polarization Resistance (LPR).....	97
4.3.2	Corrosion rate calculations.....	99
4.3.3	Results from LSV measurements.....	100
4.3.4	Effect of water on corrosion.....	106
4.3.5	Corrosion thermodynamics.....	108
4.3.6	Electrochemical Impedance Spectroscopy (EIS).....	109
4.4	Results from EIS measurements.....	113
4.5	Characterizations of corrosion products.....	117
4.6	Conclusions.....	123
4.7	References.....	124

CHAPTER FIVE: MECHANICAL PROPERTIES

5	Lubrication studies.....	127
5.1	Introductions.....	127
5.2	Frictions	127
5.2.1	Friction coefficient.....	128
5.2.2	Friction coefficient results.....	129
5.2.3	Wear and wear volume.....	132
5.3	Wettability.....	134
5.3.1	Contact angle	136
5.4	Surface energy and interfacial tension.....	139
5.4.1	Thermodynamics of wetting.....	140
5.4.2	Surface roughness.....	142
5.5	Additive studies.....	144
5.5.1	Surfactants.....	144
5.5.2	Adsorption of surfactants.....	146
5.5.3	Viscosity index.....	147
5.5.4	Conductivity.....	148
5.5.5	Density.....	150
5.5.6	Contact angle.....	151
5.5.7	Friction coefficient.....	152
5.5.8	Wear volumes.....	154
5.6	Conclusions.....	155
5.7	References.....	157

CHAPTER SIX: CONCLUSIONS

6	Conclusions and future works.....	162
6.1	Conclusions.....	162
6.2	Further work.....	165
6.3	Appendixes.....	166

CHAPTER ONE: BACKGROUND INFORMATION

CONTENTS

1. INTRODUCTION	2
1.1 LUBRICANTS	2
1.2 THE HISTORY OF LUBRICATION	2
1.3 LUBRICATING OIL	3
1.3.1 BASE OILS	4
1.3.2 CLASSIFICATION OF BASE OILS	7
1.3.3 ADDITIVE PACKAGES	8
1.3.4 CLASSIFICATION OF ADDITIVE PACKAGE	8
1.4 LUBRICATION REGIMES	16
1.5 IONIC LIQUIDS (ILS) AND THEIR APPLICATIONS	17
1.6 DEEP EUTECTIC SOLVENTS (DESS) AND THEIR APPLICATIONS	19
1.7 USING ILS AND DESS AS LUBRICANTS	22
1.8 RESEARCH OBJECTIVES	32
1.9 REFERENCES	33

1. INTRODUCTION

1.1 Lubricants

A lubricant is a material used to assist the relative motion of sliding bodies by offering a protective thin film between their surfaces in order to reduce wear and friction between contacting sliding surfaces. Furthermore, a lubricant helps to maintain the ability of engineering machines to produce more power and work more efficiently. In addition a lubricant performs a number of other functions, such as; cooling lubricated surfaces during use, avoiding corrosion, increasing power transfer, offering a liquid seal at sliding contacts and the removal, neutralization and suspension of wear and combustion products.

There are three types of lubricants;

- 1) Liquid lubricants, such as hydraulic and motor oil,
- 2) Semi-solid lubricants such as greases and
- 3) Solid lubricants such as graphite or molybdenum disulfide.¹⁻⁵

Lubricants can also be classified according to their applications e.g. automotive engine oils, industrial oils, metal working fluids, aviation oils and greases.^{1, 6}

1.2 The history of lubrication

The history of lubrication dates back to more than 3500 years ago when people from ancient Egypt and China employed oils from animals and plants to handle and move large materials e.g. stones for construction.⁴ Essentially all lubricating oils until the mid-19th century had been derived from natural sources such as animal fats, vegetable oils, and marine oils. During the industrial revolution in the mid-19th century the demand for lubricants increased rapidly due to the high use of heavy equipment which was mainly powered by steam and coal fire. The development of the internal combustion engine which was powered by gasoline in the late of 19th century promoted an increase in demand for a new generation of lubricants. This requirement was in addition to a shortage of natural oils. Therefore, by 1880 the manufacture of lubricating

oil from crude oil started to become the main source and this remains the major part of today's lubricants.^{1, 4, 5}

1.3 Lubricating oil

Unlike other crude oil fractions, lubricating oils possess high viscosities and have boiling points (usually more than 670 K). From the refinery, lubricating oils are produced through a number of processes including distillation to remove light compounds followed by hydrogenation or solvent extraction to remove constituents other than hydrocarbons. Dewaxing is performed to improve low temperature fluidity and finally clay- or hydrogen-treatment is performed to increase stability.¹ Generally formulated lubricating oils are prepared from a mixture of two or more base stocks (mineral oil, bio-based oil or synthetic oil) together with the inclusion of a number of additives.

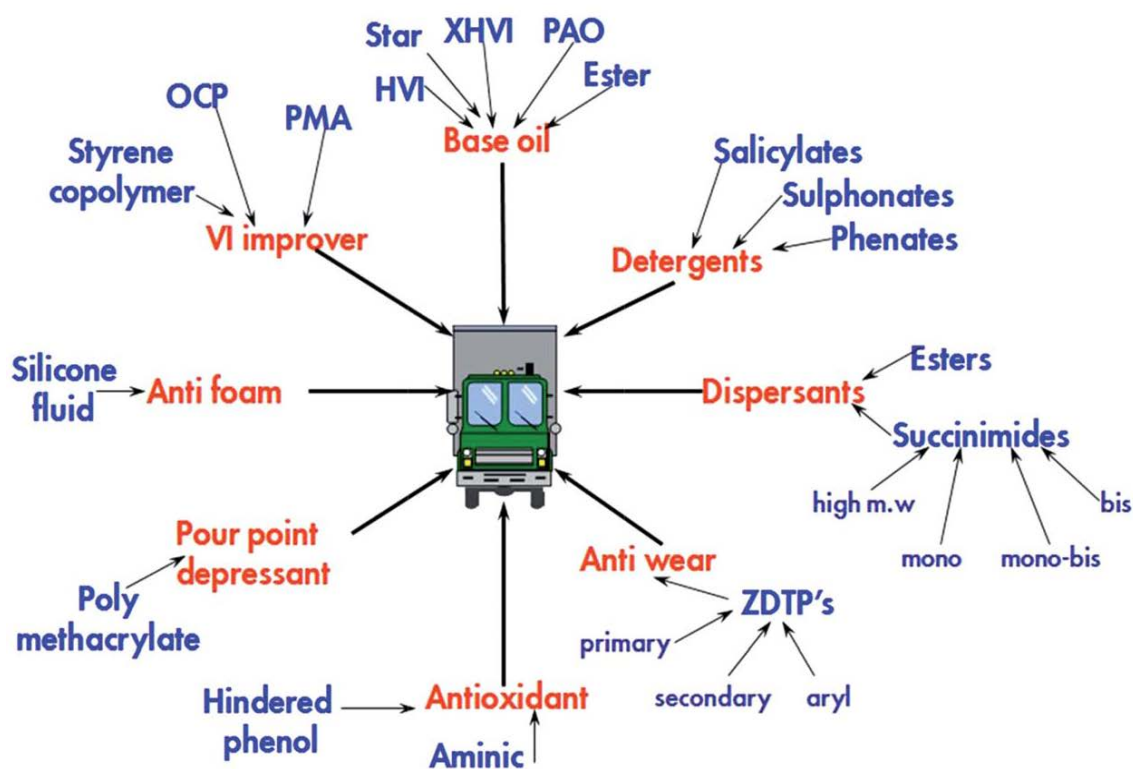


Figure 1-1 : Additives for formulated engine oil.⁷

Common additives which are used in lubrication are intended to perform a variety of roles, some of them are used to protect the surface of sliding solids, some others are aimed to enhance the performance of the lubricant itself and others are used to maintain the lubricant properties the same as before use.⁷ Examples of common additives include dispersants, antioxidants, friction modifiers, anti-wear agents, detergents and viscosity index (VI) improvers. Figure 1-1 shows schematically most available constituents of modern engine oils.^{2, 3, 8}

Table 1-1: Weight percentage of formulated SAE 30 or SAE 40 components.³

Materials	Weight %
Base oil	71.5-96.2
Detergents	2-10
Anti-wear/oxidant	0.1-2
Dispersant	1-9
Pour point depression	0.1-1.5
Anti-foam	2-15 ppm
Friction modifiers	0.1-3
ZDDP	0.5-0.3

The base oil and viscosity index improvers form the main components of the oil which are in the range of (72-96 w%) and the other component is the additive package (28-4 w%).³ Typical additives concentration ranges for formulated engine oils SAE30 or SAE40 are shown in Table 1-1.

1.3.1 Base oils

Generally, there are three different base oils used in the formulation of lubricating oil, these are; mineral, bio-based (natural) and synthetic base oils.^{2, 6}

1.3.1.1 Mineral base oil

Mineral base oils used in engineering machines, are a mixture of paraffinic, naphthenic, and aromatic hydrocarbons derived from one of the distillation fractions of crude oil containing (C₂₀-C₅₀) hydrocarbons. It should be noted that the mixtures contain different molecules having different number of side chains, rings, molecular weight, and hydrogen/carbon ratios. Based on the final application, different quantities of these hydrocarbons are mixed together to meet the desired properties. Generally, the percentage of aromatic hydrocarbons range between 10-40 %, the naphthenic content is 25-80% and the iso-paraffins are 15-75 % depending on the source of the crude oil. However, the base oil will be predominantly iso-paraffinic and naphthenic hydrocarbons if the fraction boiling is under 723 K together with a few percent of mono aromatic hydrocarbons.^{6, 9, 10}

1.3.1.2 Renewable base oil

Recently, the development of new products from renewable bio-based materials has become important in the area of lubricant manufacture. Having some attractive properties, derivatives of seed oil are valued as important alternatives to petroleum-derived mineral base oils. Lubricants based on biological sources are often nontoxic, biodegradable, and due to having high molecular tri-glyceride concentrations, they have low vapor pressures, as well as exhibiting small changes in viscosity, as a function of temperature. Additionally, they are able to adhere to metal surfaces, enabling improved boundary lubrication. Moreover, vegetable oils are able to dissolve additives and polar contaminants. However, their drawbacks are associated with their high sensitivity to oxidation, hydrolytic instability and high pour points.^{6, 11-13}

1.3.1.3 Synthetic base oil

The use of lubricants for long periods of time and their ability to reduce undesirable emissions to the environment are two key factors which govern the growing quest for new lubricants. The disadvantages of mineral oils used under severe conditions include the ready emission of poisons to the environment and the oxidation

of mineral oils at high temperatures leading to the formation of corrosive bi-products and high molecular weight condensed products. Therefore, the demand for alternatives especially for applications at high temperature or under low pressure, such as in aerospace applications.⁶

The history of synthetic lubricants starts with the first observation of a viscous liquid in 1877 by Friedel and Crafts when they obtained a viscous hydrocarbon from hydrolyzing the product obtained from reaction of amyl chloride with Al or AlCl_3 . This was followed by Balsohn in 1879 who prepared lubricating oil from treating ethylene with AlCl_3 followed by hydrolysis to produce the first synthetic lubricating oil. The first commercially available synthetic lubricating oil was developed by the Standard Oil Company in 1929.^{9, 14} The demand for synthetic lubricants grew rapidly during the Second World War for applications in gas turbines, space vehicles and rocket motors.¹⁵ Since then a large number of synthetic lubricants have been commercialized.

Many synthetic lubricants have been produced and some of them have been applied very successfully such as poly-alphaolefins (PAOs). General examples of synthetic oils are; synthetic hydrocarbon polymers (such as poly-alphaolefins, poly-butenes, alkylated aromatics), poly-phenyl ethers, halogenated hydrocarbons, carboxylate esters, aliphatic esters, polyol esters, phosphate esters, poly-alkylene glycols, silicon compounds (such as silicones, silicate esters). Examples including perfluoropoly-ether (PEPE), poly-alphaolefin, polyesters, multiply-alkylated cyclopentanes and cyclotriphosphazene (X-IP) as conventional synthetic oils are shown in Figure 1-2.¹⁵⁻¹⁸

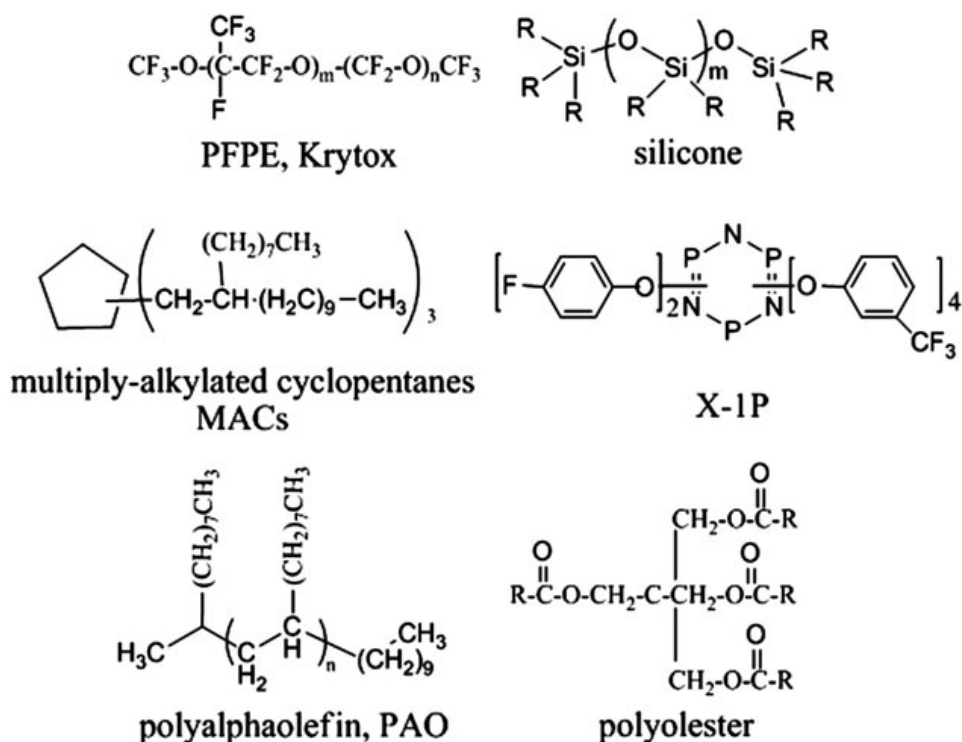


Figure 1-2 : Some examples of synthetic oils.¹⁵

1.3.2 Classification of base oils

Base oils have been categorized into seven groups and sub groups as shown in Table 1-2 according to the American Petroleum Institute (API). The classification is based on three measurable values which are sulfur content, viscosity index and saturate percentage.

Table 1-2: Base oil categories according to API.¹⁹

Group	Sulfur Mass %	Saturates, Mass %	VI
I	>0.03	<90	≥80 to <120
II	≤0.03	≥90	≥80 to <120
II+	≤0.03	≥90	≥110 to <119
III	≤0.03	≥90	≥90 ≥120
III+	≤0.03	>90	≥130<150
IV	All polyalphaolefins (PAOs)		
V	All stocks not included in groups I–IV (e.g., esters, pale oils)		

Measurements of sulfur and saturate mass percentages and VI should be made according to standard test methods which are listed in Table 1-3.

Table 1-3 : Standard test methods used for measuring properties.^{6, 20}

properties	Test methods
Saturate percent	ASTM D2007
Sulfur percent	ASTM D1552, D2622, D3120, D4294, D4927
Viscosity index	ASTM D2270

1.3.3 Additive packages

Today the development of new engines and transmission technologies have become possible through the inclusion of additives since the durability and efficiency of engines is directly related to the quality of the lubricant employed. Although, base oils constitute the basic structure of lubricating oils, their qualities have to be upgraded in order to perform efficiently during use. Therefore, a number of additives need to be incorporated into these base oils to meet the final specification requirements.^{2, 3}

1.3.4 Classification of additive package

Different additives are incorporated into the lubricating oil in an attempt to improve their already existing properties or to increase new properties. Additives are categorized into three main classes which include; performance improving, surface protecting and additives for protecting the lubricating oil itself.³ The most well-known additives together with their influence on lubricating oil properties are described below:

1.3.4.1 Performance additives

Viscosity index (VI) improvers

The ability of lubricating oils to efficiently minimize wear and friction is significantly influenced by its viscosity change as a function of temperature (viscosity index) since the viscosity governs an oil's performance when the temperature varies.⁵ Viscosity is affected by temperature, pressure and shear in some cases.⁷ The viscosity of a lubricant should change as little as possible with temperature. Therefore, from 1929 onwards, various polymers have been inserted into lubricating oils to improve their viscosity index.

Common viscosity index improvers include; styrene-butadiene co-polymers, poly-methacrylates, olefin co-polymers (OCPs), and hydrogenated poly-isoprene.^{2, 3} Poly n-alkyl methacrylates are commonly used as an additive for mineral base lubricating oils, because the side chain (n-alkanes) in a polymer provides multifunction ability. For instance, methacrylates having lateral alkyl (C₁₀–C₁₄) groups improve the viscosity index only.

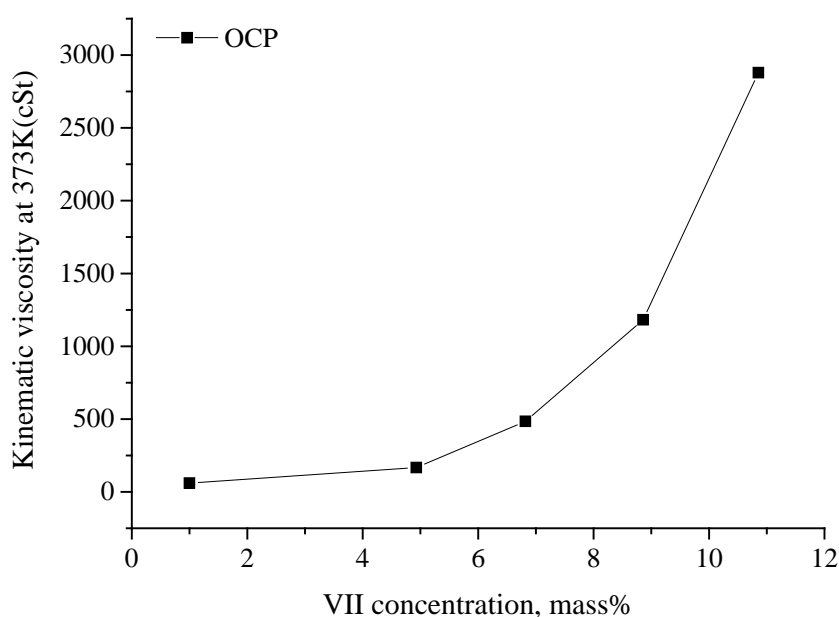


Figure 1-3: Effect of viscosity index improver on kinematic viscosity at 373K.²

On the other hand, using longer-chains (C16–C18), improves the viscosity index in addition to acting as a pour point depression additive.²¹ The influences of viscosity index improver additives are different for each additive/base oil mixture. Figure 1-3 shows a typical viscosity/concentration relationship of amorphous OCP dissolved in group I 100N mineral base oil at 373K.

Pour point depression additives (PPD)

The pour point is defined as a minimum temperature at which the oil is able to move. Mineral oils derived from petroleum naturally thin out when their temperature is raised and thicken when their temperature is lowered. This property depends on the nature of the crude oil and the refining process. However, for the purpose of a wide range of applications lubricating oils must stay liquid within a wide range of temperature.

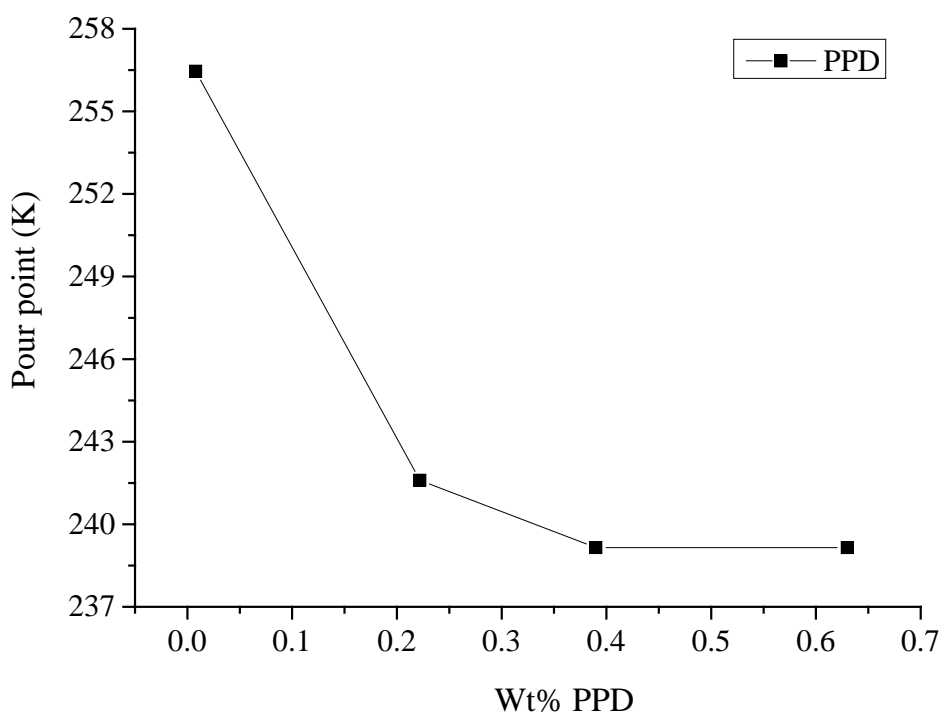


Figure 1-4: *Effect of PPD on pour point of typical group I mineral base oil.*²

Oil movement stops at low temperatures due to the existence of paraffin waxes in the oil which crystallize at reduced temperature. Therefore, pour point depression additives such as condensation products of chlorinated waxes, poly-methacrylates or long chain alkyl groups are added to the oil to maintain oil fluidity since these additives

co-crystallize with the paraffin wax molecules to break the interlocking network of wax crystals which consequently prevents the oil from solidifying.^{3, 21} The effect of PPD additive and its optimized concentration on group I 100N mineral base oil are shown in Figure 1-4.²

1.3.4.2 Surface protective additives

Friction modifier additives

The inclusion of a friction modifier to lubricating oils is intended to change the mode of friction which occurs at solid surfaces. A number of additives are used for this purpose including long chain organic amines, amides and their derivatives, long chain organic alcohols, compounds of molybdenum and phosphoric acids or their derivatives. These compounds preferentially adsorb on different surfaces by the action of polarity and hydrogen bonding as shown in Figure 1.4. As in the case of anti-wear activities, friction modifier additives are able to adsorb onto a surface by attraction displaying adsorbing forces ≥ 13 kcal/mole; forming a protection film. However, the film is produced under relatively mild loads and temperature conditions.²

Anti-wear additives

In a mechanical device there are four types of wear which happen to metal surfaces. Firstly, corrosion wear, in which corrosive agents in the oil, such as acids produced by oxidation reactions are a source of corrosion for metallic surfaces. Secondly, abrasions (ploughing) wear which comes from solid particles. Thirdly, adhesive wear produced by the adhesion tendency of very clean surfaces to each other. Finally, fatigues wear which results from metal to metal contact.

Anti-wear additives are always used to reduce abrasive and solid contacts wear.⁷ There are a number of anti-wear additives such as, sulfur and chlorine compounds, crown ethers, sulfide and disulfides, organic phosphates, and zinc dithiophosphates. Friction reduction occurs by the formation of tribo-film on the metal surface during the chemical reaction of these additives with the metal surface.

Zinc dialkyldithiophosphate (ZDDP) has commonly been used as a multifunctional and inexpensive additive for more than half a century. Figure 1-5 shows the different structures of ZDDP which exist in different conditions i.e. whether it is in solution or it is as a crystal or with the other additive compounds. Under tribo-chemical

conditions, ZDDP forms a complex film which has a thickness in the range 10-200 nm and consequently the friction coefficient of the oil is greatly influenced. Besides its anti-wear ability, ZDDP behaves as an anti-oxidant and anti-corrosion agent in media of extreme pressure.^{2, 3, 8}

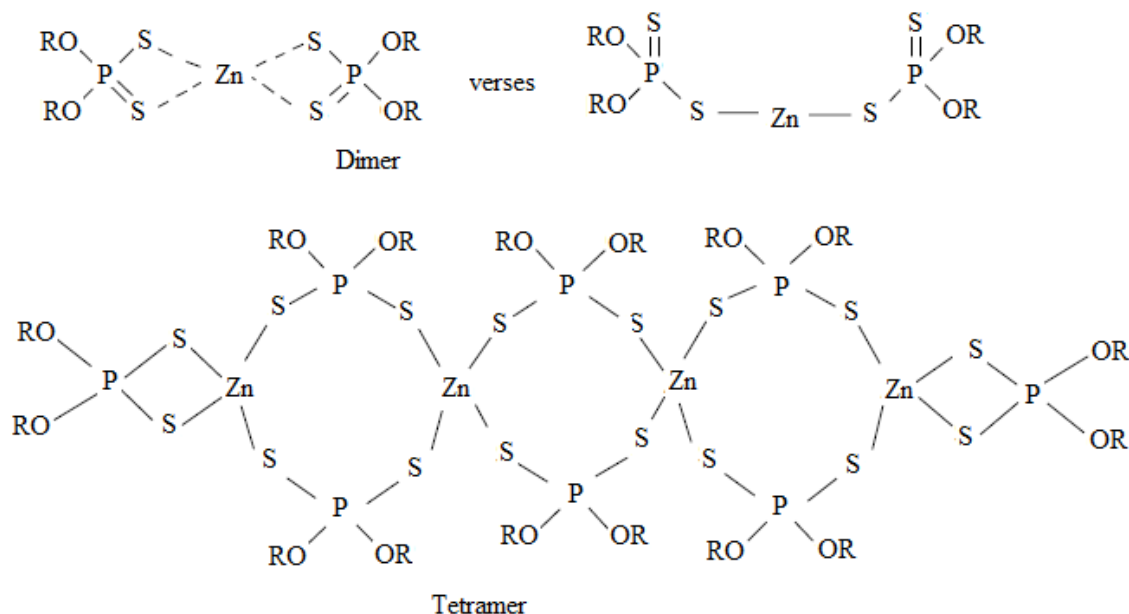


Figure 1-5 : different structures of ZDDP.²

Dispersants and Detergents

The terms dispersants and detergents are frequently used interchangeably when engine oils are discussed. Both of them have a polar head group and a long hydrocarbon chain. A polar head group in detergents is made from an alkaline metal salt of an organic acid. However, in dispersants the polarity of the head group comes from oxygen and nitrogen. These additives affect the suspension and dissolution of particulate matter in the lubricant oil, as well as neutralization of acidic products formed during fuel oil combustion to keep metal surfaces as clean as possible either by forming a protective film on the surface Figure 1-6 or by suspension Figure 1-7.³

When a distinction between detergent and dispersant is used, dispersants are added into a lubricant to avoid sludge formation at low temperatures which sometimes leads to the shut-down of an engine. Some examples of dispersants are succinate esters, succinimides, Mannich bases, phosphorus compounds and macrocyclic, polycyclic and bicyclic polyamines. Their addition is aimed to keep the surface as clean as possible

from deposits. They also help to avoid accumulation of carbon, sludge, and dispersed particles in the oil.³

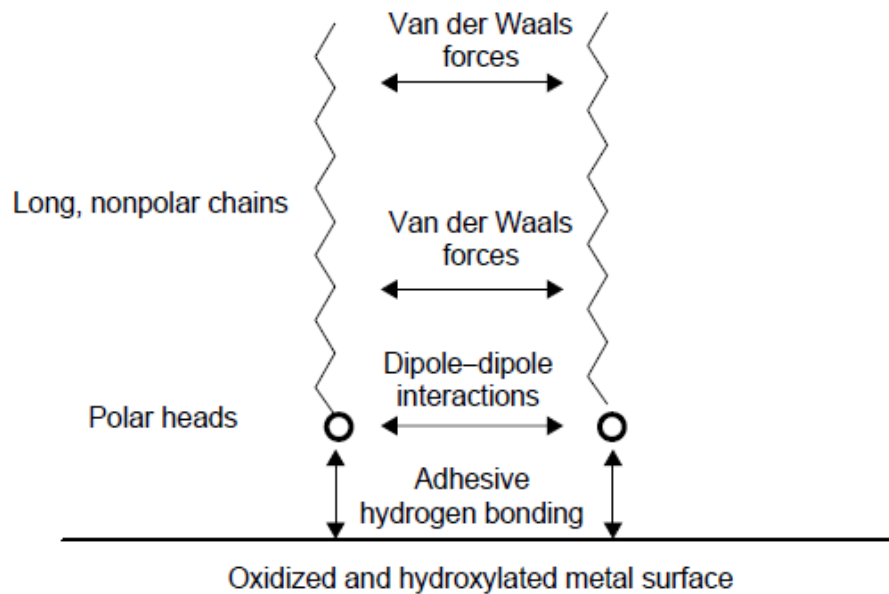


Figure 1-6 : Formation adsorbed film.^{2, 3}

Deposit formation is controlled at high temperature by the presence of detergents. These additives produce reverse micelles which solubilize organic acids and neutralizing strong acids.

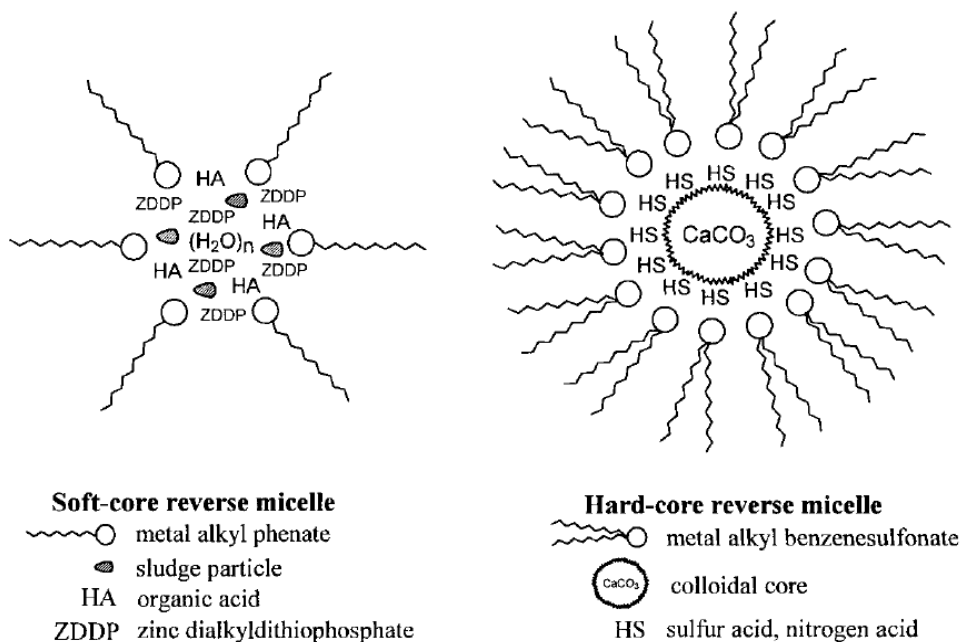


Figure 1-7 : Example of sulfonate detergents.^{2, 3}

Examples of detergents are phenates (alkyl phenate sulfides), sulfonates (Figure 1-7) phosphonates, and salicylates. Inclusion of a dispersant along with a detergent is intended to maintain an engine working as efficiently as possible and hence improve fuel efficiency. Furthermore, dispersants decrease exhaust emissions from the engine, and increasing engine life time.^{2, 3}

1.3.4.3 Lubricant Protective Additives

Anti-oxidants

The stability of lubricating oil towards oxidation is considered as one of the most important requirements. When an oil is exposed to air at ambient or higher temperatures it can undergo a number of reactions; producing peroxides as a primary product. Subsequently, these decompose to give ketones and alcohols. With this degradation additional oxidation and condensation reactions occur to produce esters, lactones and organic acids.^{2, 22} Free radicals (R^\bullet) can be formed by the removal of hydrogen atoms (H^\bullet) from hydrocarbon (RH) chains, then the highly reactive radicals react with oxygen to form peroxi-organic radicals (ROO^\bullet) which attacks other molecules as shown in Figure 1-8.³

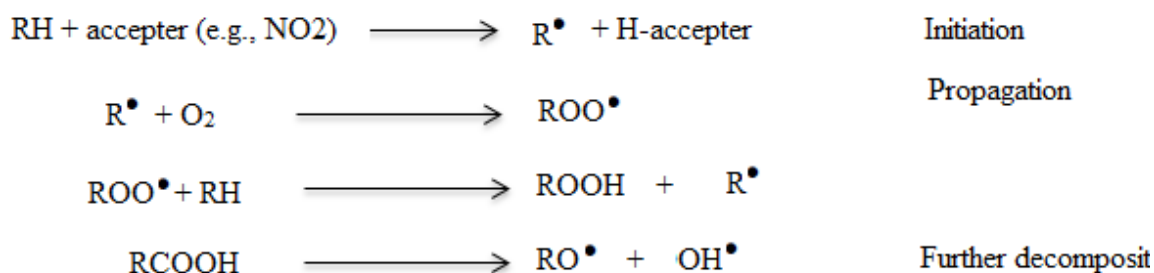


Figure 1-8: Hydrocarbon oxidation reaction steps.

To terminate these reactions and stop the deleterious aging of lubricating oils, two types of anti-oxidants are employed, including peroxide decomposers and radical scavenger additives. Examples of anti-oxidants are zinc dialkyldithiophosphates (ZDDP), alkylated diphenylamine, substituted phenols, sulfur compounds and zinc dialkyldithiocarbamates. The mode of action of radical scavengers is either via single electron transfer (SET) redox reactions or by transfer of hydrogen to free radicals thus

terminating the chain reaction. For instance the mechanism of the radical scavenger for ZDDP is illustrated in the following three steps as illustrated in Figure 1-9.²

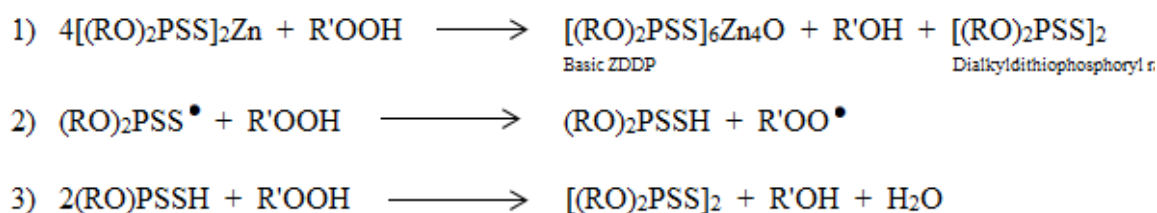


Figure 1-9: Termination of propagation steps by ZDDP additive.

However, the peroxide decomposes converting hydro-peroxides to radical free alcohols. Although, these compounds are altering themselves to another form of free radical (albeit more stable) during the termination reactions, they are still stopping undesirable chain propagation reactions. The mechanism of peroxide decomposer activity of substituted phenols and diarylamine are shown in Figure 1-10.²

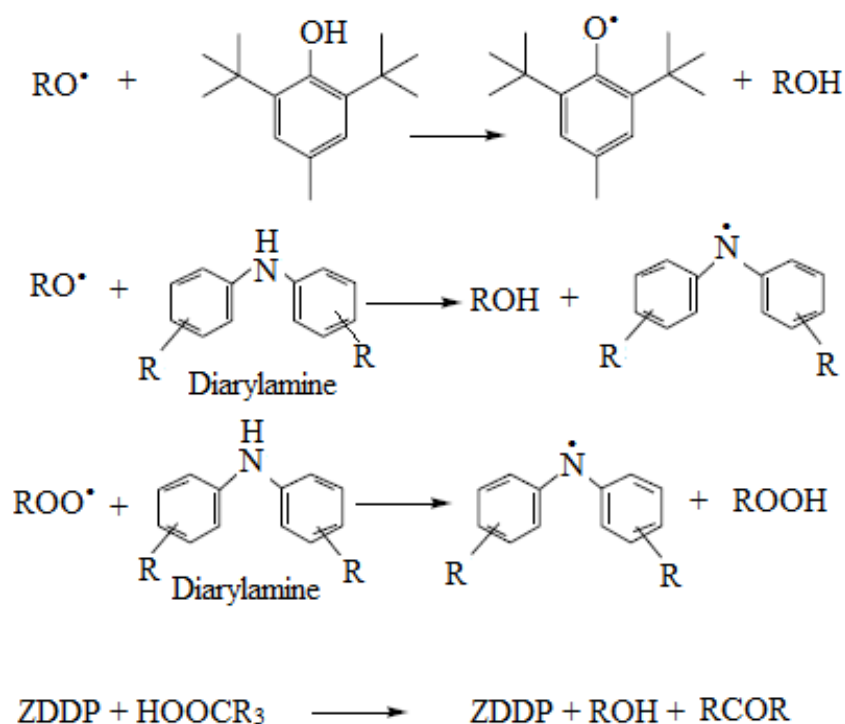


Figure 1-10 : Examples peroxide decomposer antioxidant.²

1.4 Lubrication regimes

Based on the applied load (distance between sliding pairs) lubrication in mechanical devices is divided into different regimes which are shown clearly in Figure 1-11a.^{2, 3, 8, 23}

1- Hydrodynamic/ elasto-hydrodynamic lubrication regime

In this regime a sufficient amount of oil exists between moving surfaces which survives the load.

2- Mixed lubrication regime

In the mixed regime, only a molecular thin layer of oil remains between moving surfaces since the load pushes out most of the lubricating oil Figure 1-11b.

3- Boundary lubrication regime

In boundary lubrication (which appears in circumstances such as low viscosity oils, low speed or high load,) metal to metal contact occurs due to rupture of the lubricant film.

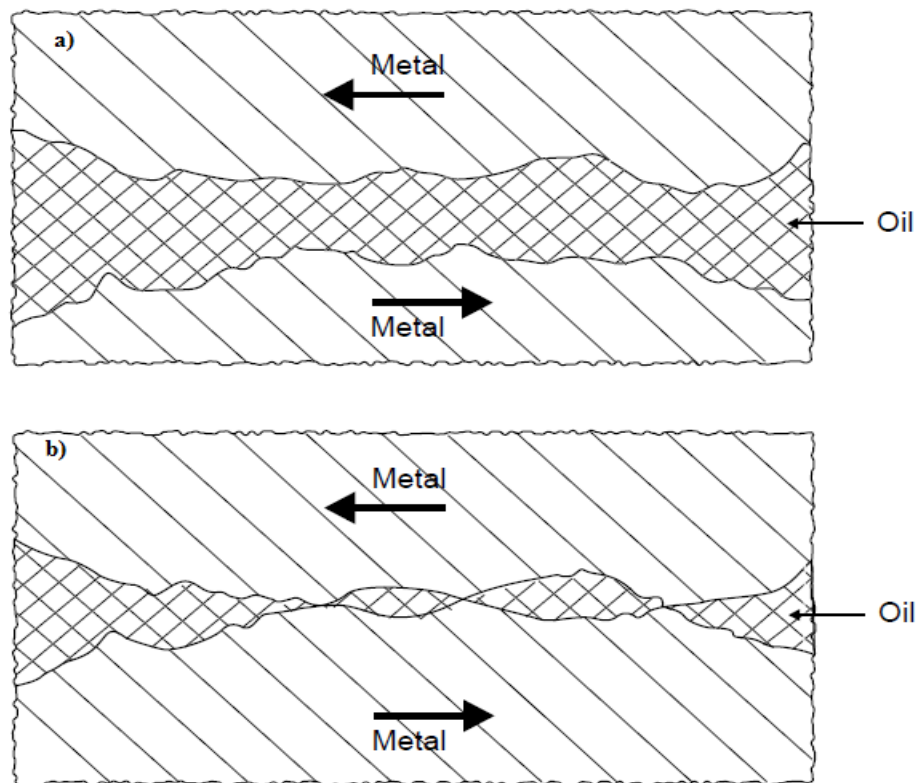


Figure 1-11 : Lubrication regimes in machinery devices a) full film hydrodynamic lubrication. b) Mixed film lubrication /boundary lubrication.²

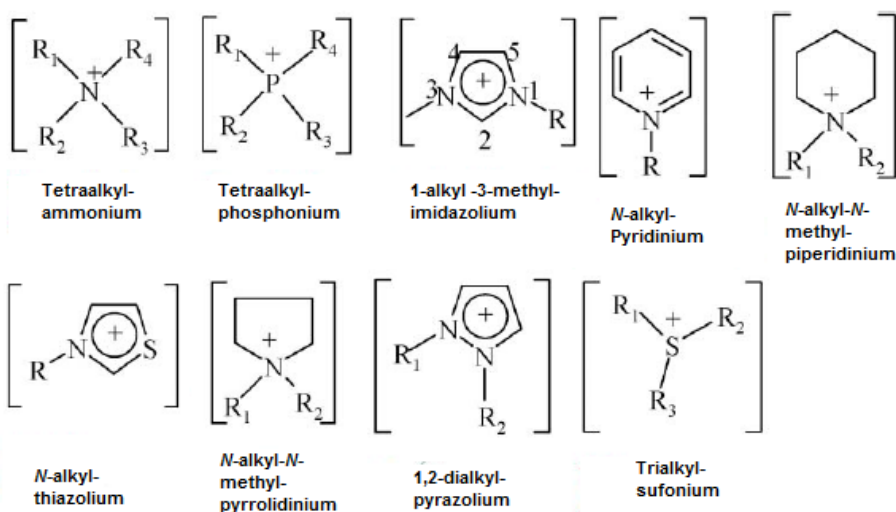
Commercially, in most formulated oil the boundary additives are inserted to maintain a protective film between moving surfaces preventing direct contact between two surfaces.^{3, 8, 23} In some cases such as between a cylinder wall and a piston ring in an internal combustion engine when metal to metal contact occurs, the energy is released in the form of heat, which helps the chemical reaction to occur between boundary additive elements like chloride phosphors or sulphur containing compounds and metal surface. The chemical reaction results in a film which protects the surface from wear.³

1.5 Ionic Liquids (ILs) and their applications

Ionic liquid are defined as a class of fluid that consist entirely of ions and demonstrate ionic conductivity. Typically ILs are salts having large nitrogen or phosphorous containing organic cations with linear alkyl side chains as shown in Figure 1-12. They can have a variety of anions but the most common are inorganic as shown in Figure 1-12.^{24, 25} Broadly the term ionic liquid includes all fused salts as in the case of sodium chloride which is liquid at temperatures above 1073 K. However, the term is more commonly applied solely to salts having melting points lower than 373 K.^{26, 27}

ILs have attracted growing attention, owing to their attractive properties when compared to molecular solvents.^{28, 29} Generally, ionic liquids consist of one or two bulky ions having a low melting point due to the low level of symmetry and charge delocalization resulting in a decrease in crystalline lattice energy. ILs have found application in synthesis, electrochemical engineering and analytical processes.^{29, 30, 31}

a)



$R_{1,2,3,4} = \text{CH}_3(\text{CH}_2)_n$, ($n=1,3,5,7,9$); aryl; etc.

b)

water - immiscible



water - miscible

$[\text{PF}_6]^-$

$[\text{NTF}_2]^-$

$[\text{BR}_1\text{R}_2\text{R}_3\text{R}_4]^-$

$[\text{BF}_4]^-$

$[\text{OTf}_2]^-$

$[\text{N}(\text{CN})_2]^-$

$[\text{CH}_3\text{CO}_2]^-$

$[\text{CF}_3\text{CO}_2]^-$

Br^- , Cl^- , I^-

$[\text{Al}_2\text{Cl}_7]^-$, $[\text{AlCl}_4]^-$ (Decompose)

Figure 1-12 : a) Most commonly cations. b) Some possible anions.^{4, 32}

The importance of ILs can be seen from the exponential growth in the number of academic publications and patents issued in this field every year.^{33,34} Indeed, the number has grown to more than 36,700 articles in the last five years. The reason for this growth is due in part to the almost limitless combinations of cations and anions possible, and this has led to the concept of ILs being designer solvents.^{32,35} Most common cations and anions which have been combined to design ionic liquids are shown in Figure 1-12.

Regarding the industrial role of ILs, their importance is apparent in a number of marketable routes and yields based on their current availability in the market as well as their wide range of commercial use and applications.^{32, 34, 36}

As predicted by Plechkova and Seddon, the most important areas for ILs to be applicable in the future are shown here.³²

- **Engineering** Lubricants, plasticisers, compatibilisers, coatings, dispersing agents
- **Electrochemistry** Metal plating, electrolyte in batteries, , ion propulsion, solar panels, electro-optics, fuel cells
- **Physical chemistry** Thermodynamics, refractive index, binary and ternary systems
- **Biological uses** Biocides, ,drug delivery, personal care, embalming, biomass processing
- **Solvents and catalysis** Multiphasic reactions and extractions, catalysis, microwave chemistry, nano-chemistry, synthesis
- **Analysis** Stationary phase for HPLC, matrices for mass spectrometry, gas chromatography columns

A detail about their properties and applications of ionic liquids can be found in the reviews by Plechkova and Seddon,³² Hallett and Welton³⁷ and Welton.³⁸

1.6 Deep Eutectic Solvents (DESS) and their applications

Deep eutectic solvents, DESs are commonly recognized as a novel class of ILs although the two are distinctly different.^{27, 39} Deep eutectic solvents are compounds prepared from a mixture of Lewis or Brønsted acids and simple quaternary ammonium salts. On the other hand, the system of ILs contains only one discrete of cation and anion. Thus, it is expected that even though the physical properties of both liquids are analogous, the difference in their chemical properties suggests their applications will not be the same.

Most common hydrogen bond donor and hydrogen bond acceptor species which have been studied in the synthesis of DESs and some are shown in Figure 1-13.³⁹

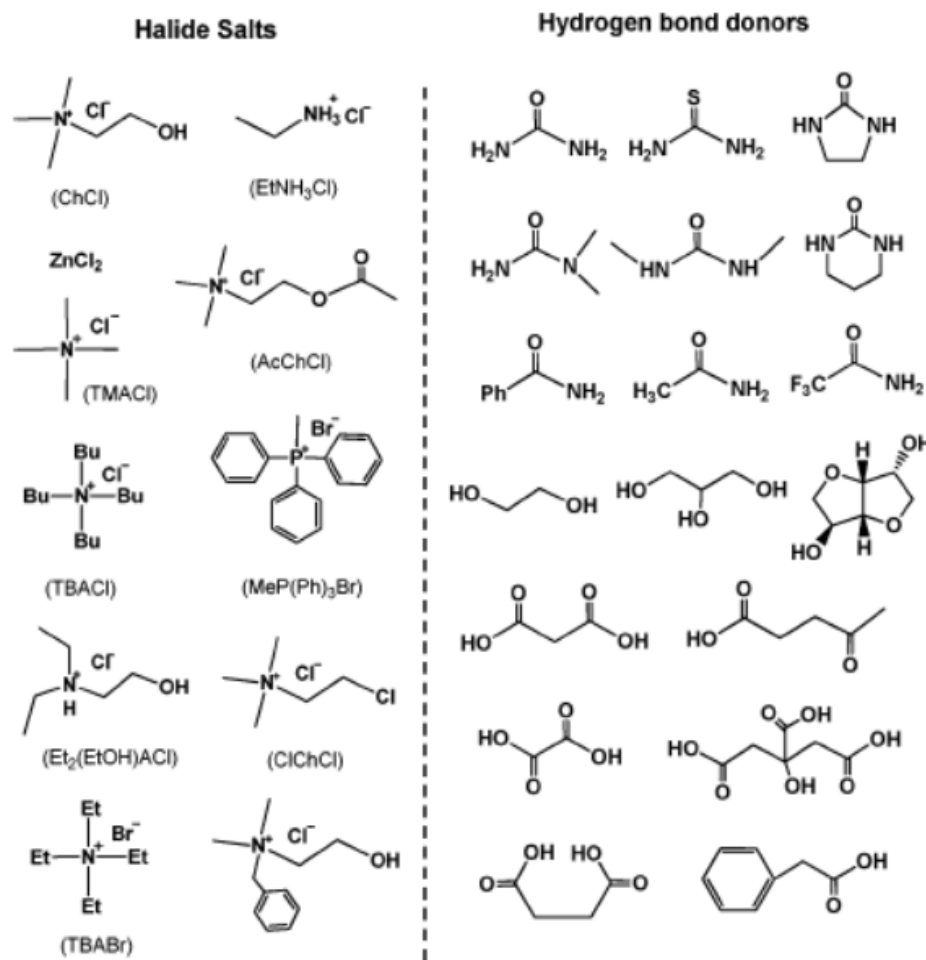


Figure 1-13: Some common hydrogen bond donors and accepters used for preparation of DESs.³⁹

DESs are formed between simple hydrogen bond donors (HBD), a metal or hydrated metal halide salt with a quaternary ammonium salt.^{27, 39, 40} As shown in Figure 1-13 most hydrogen bond donors are amides, carboxylic acids and alcohols which frequently are used because they possess a complexing ability with a halide (X^-) anion in a quaternary ammonium salt.⁴¹⁻⁴⁴ Commonly, DESs are recognized by a substantial reduction of lattice energy and hence lowering the freezing point of mixture at eutectic temperature which is in the range of 423 K and up to 543 K in some cases therefore, most DESs have fluidity between ambient temperature and 343 K.^{27, 39}

The reduction of lattice energy which occurs is originated from the charge density reduction due to the delocalization of charge through the formation of hydrogen bonding between halide ion and the moiety of hydrogen bond donor which is responsible for a decrease in melting point of a mixture in comparison with the melting point of both pure constituents of hydrogen bond system.²⁸

Being inexpensive, nontoxic, biodegradable and readily available among all quaternary ammonium salts, Choline Chloride $[(CH_3)_3NC_2H_4OH]Cl$ (ChCl) is used widely as a hydrogen bond acceptor which is produced by an efficient reaction in gas phase between trimethylamine, HCl and ethylene oxide producing almost no waste.⁴⁵ The salt is able to form DESs easily and rapidly with readily available HBDs such as renewable polyols e.g. carbohydrates, glycerol, carboxylic acids e.g. succinic acid, citric acid, oxalic acid, amino acids, and amides such as urea. Consequently, the final product of most type III DESs is thought to be biodegradable.

DESs are classified into four categories which are summarized in Table 1-4 with their general formula.

Table 1-4: Types of DESs and their general formula.^{27, 46}

<u>Types</u>	<u>General formula</u>	<u>Terms</u>
Type I	$Cat^+X^- + zMCl_x$	M= Zn, In, Zn, Sn, Al, Fe
Type II	$Cat^+X^- + zMCl_x \cdot yH_2O$	M=Cr, Ni, Cu, Fe, Co
Type III	$Cat^+X^- + zRZ$	Z= OH, COOH, CONH ₂
Type IV	$MCl_x + zRZ$	M=Zn, Al Z=OH, CONH ₂

In comparison with ILs, DESs possesses many advantages over ILs which includes their ease of preparation. DESs require only a simple mixing at moderate temperature (323- 533K). Hence they thought to be less hazardous to the environment as there is no waste associated with their preparations. Therefore, the valuable properties of DESs in terms of industrial applications make these liquids cheaper and greener than ILs.^{27, 39, 47}

DESs have been studied in different electrochemical processes such as electroplating, electropolishing, processing of metal oxides and metal recycling because these liquids are possesses essential properties which are required for electrochemical solutions such as high conductivity, low Ohmic loss, great solubility of metals and metal (oxides, salts, and hydroxides), low cost, high electrochemical stability and non-flammability. The applications of DESs have been reviewed in depth by Smith et.al.²⁷

1.7 Using ILs and DESs as lubricants

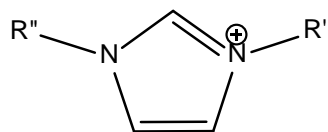
ILs possess valuable properties which make them appropriate candidates for a variety of applications, as their properties can be tuned through the different cations and anions exist for specific applications. For instance, they are used as electrolytes for electrodeposition and batteries, suitable agents for gas absorption, as a solvent in chemical synthesis, pharmaceutical ingredients, for gas purification, media for biological reactions, supercritical fluids, plasticizers, extraction of nanomaterials, removal of metal ions and as lubricants and lubricant additives.^{15-17, 48, 49}

ILs have been studied as lubricants by a number of researchers as shown in Table 1.5. Unlike synthetic oils, ILs are very polar liquids which adhere better to many metal surfaces. Additionally, they possess properties which make them suitable for the purpose of lubrication such as low freezing point, non-flammable, high thermal stability, non-volatile, and high conductivity.¹⁵ Commonly used cations and anions which combined for the purpose of lubrication by ILs are shown in Figure 1-14.

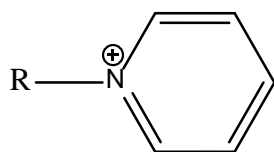
Taking into consideration their appropriate characteristics, ILs have been used for a variety of lubrication purposes such as neat lubricants as additives in synthetic lubricants, forming tribo-film, as an additive in aqueous lubricant and inclusion of additives in ILs for lubrication. Table 1.5 gives a summary of the purpose of use, contact pairs, combined cations and anions and lubrication conditions which have been addressed in these studies. Most of articles in Table 1.5 have been reviewed in references (16, 17 and 50). In general it could be said that the anionic moieties are responsible for lubrication and thermo-oxidative properties. Higher alkyl substituted imidazolium improves lubrication more than short alkyl substituted however; they have reverse effect on thermo-oxidative stabilities. Due to the cost it is preferred to use ILs as lubricant additive rather than neat lubricant unless the cost is not an issue.

Typical Cations

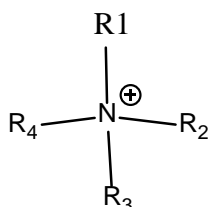
Monovalent cations



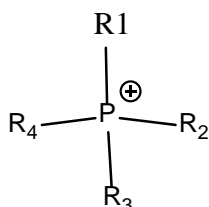
alkylimidazolium



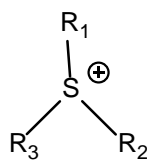
N-alkyl-pyridinium



Tetraalkyl-
ammonium

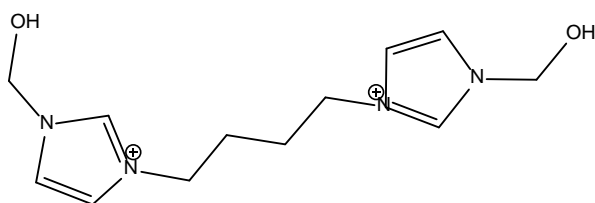


Tetraalkyl-
phosphonium



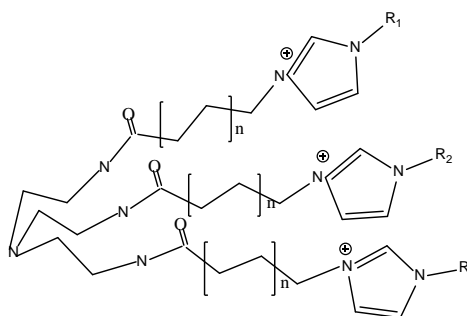
Trialkyl-
sulphonium

Di-cations



Imidazolium-derived dication

Tri-cations



Imidazolium-derived trication

Typical Anions

Monovalent anions

Bromide ion

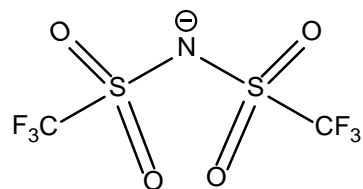
Chloride ion

Perchlorate

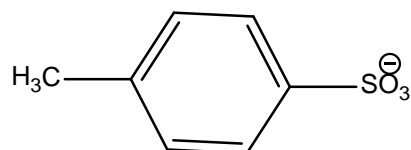
Hexafluorophosphate

Tetrafluoroborate

Nitrate

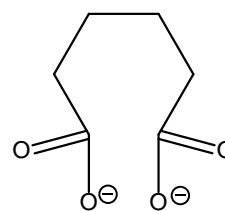


Bis(trifluoromethylsulfonyl)amide
(triflamide)



Toluene-4-sulfonate (Tosylate)

Di-anions



Adipate

Figure 1-14: The structure of cations and anions used commonly for designed ILs as lubricants.^{17, 48, 50}

Table 1.5: Lubrication studies of ILs.

Lead Author (Year)	Cation and Anion	Contact pairs	Purpose of use and condition
Smith P.G. (1961) ⁵¹	(Li ⁺ , U ⁴⁺ , F ⁻)	Ni-Mo alloy / Ni-Mo alloy	neat lubricant at room temperature (RT), 117, 230, 980 °C
Ye C. (2001) ⁵²	imidazolium, (BF ₄ ⁻ , PF ₆ ⁻)	steel/steel , steel/Al , steel/Cu , steel/sialon, steel/SiO ₂ , Si ₃ N ₄ /sialon Si ₃ N ₄ /SiO ₂ , steel/Si,	neat lubricant at RT
Liu W.M. (2002) ⁵³	imidazolium, phosphazene (BF ₄ ⁻)	steel/dy-sialon	neat lubricant at RT
Liu W.M. (2002) ⁵⁴	imidazolium, phosphazene (BF ₄ ⁻)	SAE 52100 steel/ SAE 52100 steel,	neat lubricant at RT under high vacuum
Chen Y. (2003) ⁵⁵	imidazolium, (BF ₄ ⁻)	steel / aluminum	neat lubricant at RT
Lu Q. (2004) ⁵⁶	imidazolium, phosphazene bis(trifluoromethylsulfonyl)imide (TFSI)	SAE 52100 steel / SAE 52100 steel	neat lubricant at RT
Phillips B.S.(2004) ⁵⁷	imidazolium, (BF ₄ ⁻ , PF ₆ ⁻)	ceramic Si ₃ N ₄ / Si ₃ N ₄	ILs as an additive in aqueous lubricant at RT
Omotowa, B. A. (2004) ⁵⁸	Phosphazene, I ⁻⁶	Si ₃ N ₄ / Si ₃ N ₄	IL as an additive in synthetic lubricant at RT
Mu Z. (2005) ⁵⁹	imidazolium, (BF ₄ ⁻ , PF ₆ ⁻)	Al2024 / steel	neat lubricant at RT
Xia Y. (2006) ⁶⁰	imidazolium, (PF ₆ ⁻)	plasma nitrided 1Cr18Ni9Ti stainless steel / SAE52100 steel	neat lubricant at RT

Table 1.5: Continued

Bo Y. (2006) ⁶¹	imidazolium, (PF ₆ ⁻)	SAE52100 steel / Si ₃ N ₄	thin film study of IL lubricant at RT
Sanes J. (2006) ⁶²	imidazolium, (BF ₄ ⁻ , PF ₆ ⁻ , (CF ₃ SO ₃) ⁻ , (4-CH ₃ C ₆ H ₄ SO ₃) ⁻)	SAE52100 steel/polystyrene and poly amide coated SAE52100 steel	neat lubricant at RT
Qu J. (2006) ⁶³	imidazolium and ammonium, (Cl ⁻ , Br ⁻ , PF ₆ ⁻ , TFSI ⁻ , [(C ₂ F ₅ SO ₂) ₂ N] ⁻)	52100 steel /aluminum alloy 6061-T6511	IL as an additive and neat lubricant at RT
Liu X. (2006) ⁶⁴	imidazolium, (PF ₆ ⁻)	steel / Cu–Sn alloy	benzotriazole as additive in IL lubricant at RT
Yu G. (2006) ⁶⁵	imidazolium, (PF ₆ ⁻)	SAE52100 steel / single crystal silicon (P100)	thin film study of IL lubricant at RT
Kamimura H. (2006) ⁶⁶	imidazolium, (TFSI ⁻)	SUJ2 steel/ SUJ2 steel	carboxylic acid as friction modifier in ILs lubricant at RT
Jimenez A.E. (2007) ⁶⁷	imidazolium, (BF ₄ ⁻)	aluminum Al 2011 / AISI 52100 steel	neat lubricant at -30, 100 and 200 °C
Weng L. (2007) ⁶⁸	phosphonium, imidazolium,(BF ₄ ⁻ , PF ₆ ⁻)	AISI52100 steel / AISI52100 steel	neat lubricant at RT
Kamimura H. (2007) ⁶⁹	alkyl pyridinium imidazolium, (TFSI ⁻ , BF ₄ ⁻)	SUJ2(JIS) steel / SUJ2(JIS) steel	fatty alcohols , acids, phosphorous , sulfur compounds , and ZDDP as additives in ILs lubricant at RT
Phillips B.S. (2007) ⁷⁰	imidazolium, (TFSI ⁻ , BF ₄ ⁻ , PF ₆ ⁻)	steel / oxidized iron	neat lubricant at RT, 100 and 300 °C
Suzuki A. (2007) ⁷¹	imidazolium, (BF ₄ ⁻ , PF ₆ ⁻)	JIS SUS440C stainless/ JIS	Neat lubricant at RT under high vacuum

Table 1.5: Continued

		SUS440C stainless	
Yu B. (2008) ⁷²	imidazolium, (PF ₆ ⁻)	SAE52100 steel / SAE52100 steel	benzotriazole as friction modifier in ILs lubricant at RT, 100, 150, 1nd 200 °C
Murakami T. (2008) ⁷³	alkylperidinium, (TFSI ⁻)	ASTM 52100 steel/ Fe ₇ Mo ₆ -based alloy, Mo, Fe, ASTM class no. 45 cast iron	neat lubricant at RT
Zhu M. (2008) ⁷⁴	imidazolium, (adipate, BF ₄ ⁻ , PF ₆ ⁻)	52100 steel/ silicon wafers from ILs	thin film study of ILs lubricant at RT
Xia Y. (2008) ⁷⁵	imidazolium, (BF ₄ ⁻ , PF ₆ ⁻)	AISI 52100 steel / Ni on AISI 1045 steel	Neat lubricant at RT
Minami I.(2008) ⁷⁶	imidazolium phosphate, (TFSI ⁻)	SUJ2 steel/ SUJ2 (JIS)steel	carboxylic acids as friction modifier in IL lubricant at RT
Kondo H. (2008) ⁷⁷	PFPE ammonium, (COO ⁻)	(SUS304) stainless steel/ magnetic polyethylene terephthalate (PET)	thin film study of IL lubricant at RT
Xia Y. (2008) ⁷⁸	imidazolium, (PF ₆ ⁻)	AISI 52100 steel /phosphor bronze coated with nano-crystalline Ni	neat lubricant at RT

Table 1.5: Continued

Mo Y. (2008) ⁷⁹	imidazolium, (Cl ⁻)	Si ₃ N ₄ /silicon/(100 P doped)	neat lubricant at RT
Zhuo Z. (2008) ⁸⁰	di cationic ills of di-imidazolium, (sulfonate, TFSI ⁻ , BF ₄ ⁻)	AISI52100 steel/ AISI52100 steel	neat lubricant at 300 °C
Zhao W. (2009) ⁸¹	imidazolium, (BF ₄ ⁻)	AISI-52100 steel / silicon	neat lubricant at RT
Jime'nez A. E. (2009) ⁸²	imidazolium, ammonium, (BF ₄ ⁻ , Cl ⁻)	AISI 52100 steel/ AISI 52100 steel	neat lubricant at RT, 100, 200 and 300 °C
Jime'nez A. E. (2009) ⁸³	imidazolium, ammonium, (PF ₆ ⁻ , BF ₄ ⁻ , Cl ⁻)	AISI52100 steel /titanium grade 3	neat lubricant at RT and 100 °C
Zhang L. (2009) ⁽⁸¹⁾⁸⁴	imidazolium, (PF ₆ ⁻ , BF ₄ ⁻ , phosphate)	SAE52100 steel / SAE52100 steel	neat lubricant at RT and 80 °C
Lin Z. (2009) ⁽⁸²⁾⁸⁵	imidazolium, (phosphate)	steel / steel	neat lubricant at RT
Ju. Q. (2009) ⁸⁶	imidazolium, (TFSI ⁻)	engine piston ring coated with Cr-plating/cast iron	neat lubricant at RT
Nooruddin N. S. (2009) ⁸⁷	di-cationic ionic liquids, imidazolium, (PF ₆ ⁻ , BF ₄ ⁻)	steel/ hydroxylated silicon surface of single crystal silicon	neat lubricant at RT
Zhang H. (2009) ⁸⁸	imidazolium, (BF ₄ ⁻)	silicon oxide LTO/Si ₃ N ₄ poly Si/ Si ₃ N ₄	neat lubricant at RT
Yao M. (2009) ⁸⁹	dicationic ILs imidazolium, (PF ₆ ⁻ , BF ₄ ⁻ , TFSI ⁻)	AISI 52100 steel/ AISI 52100 steel	IL as an additive in synthetic oils

Table 1.5: Continued

Xie G. (2009) ⁹⁰	imidazolium, butylpyridinium (BF ₄ ⁻)	silicon oxide LTO/Si ₃ N ₄ poly Si/Si ₃ N ₄ Si ₃ N ₄ /Si ₃ N ₄	neat lubricant at RT
Arora H. (2010) ⁹¹	imidazolium, (PF ₆ ⁻ , BF ₄ ⁻)	M52100 steel / polished steel	neat lubricant at RT
Jimenez, A.E. (2010) ⁹²	imidazolium, (PF ₆ ⁻ , BF ₄ ⁻)	titanium / 52100 steel	neat lubricant at RT, 200 and 300 °C
Jimenez, A.E. (2010) ⁹³	imidazolium, (TFSI ⁻)	titanium Ti6Al4V / 52100 steel	neat lubricant at RT and 100 °C
Somers A. E. (2010) ⁹⁴	phosphonium,(diphenylphosphate(DPP) , phosphenate)	100Cr6 steel/ AA2024 aluminum	neat lubricant under different applied loads
Cai M. (2010) ⁹⁵	imidazolium, (PF ₆ ⁻ , BF ₄ ⁻)	AISI 52100 steel/ AISI 52100 steel	ILs as an additive in Poly urea grease at RT and 150 °C
Minami I. (2010) ⁹⁶	phosphonium, imidazolium, (TFSI ⁻ , Phosphate)	SUJ2(JIS) steel/SUJ2(JIS) steel	neat lubricant at RT
Lawes S. D. A. (2010) ⁹⁷	ChCl, urea, ethylene glycol	M2 steel/ M2 steel	neat lubricant at RT (low speed-high load and high speed-low load)
Cai M. (2010) ⁹⁸	imidazolium, (PF ₆ ⁻ , BF ₄ ⁻)	AISI 52100 steel/ AISI 52100 steel	ILs as an anti-oxidant in synthetic oils
Perkin S. (2010) ⁹⁹	imidazolium, (sulfate)	mica/ mica	thin film study of IL lubricant at RT under different shear stress
Wang B. (2010) ¹⁰⁰	imidazolium, (PF ₆ ⁻)	AISI 52100 steel/ AISI 52100 steel	formulated multi-walled carbon nanotubes as an additive in ILs lubricant under different load ranges 200-800 N

Table 1.5: Continued

Blanco D. (2011) ¹⁰¹	methoxyethylammonium tris(penta-fluoroethyl) (trifluorophosphate)	chrome steel /ASTM A-569 steel coated with TiN	ILs as an additive in Poly-alphaolefin
Li D. (2011) ¹⁰²	imidazolium, (PF ₆ ⁻ , BF ₄ ⁻)	AISI 52100 steel/AISI 52100 steel	neat lubricant at RT, 100, 150, 200 °C lubricant
Francisco. J. (2011) ¹⁰³	imidazolium, (Cl ⁻)	polycarbonate (PC) disc/AISI 316L stainless steel	single walled carbon nanotubes (SWCNTs) as an additive in ILs lubricant
Blanco D. (2011) ¹⁰⁴	ammonium, tris(penta-fluoroethyl) (trifluorophosphate)	chrome steel/ ASTM A-569 steel coated with CrN	ILs as an additive in poly-alphaolefin
Jiang D. (2011) ¹⁰⁵	crown imidazoliums, (Cl ⁻ , BF ₄ ⁻)	AISI 52100 steel / polished SAE52100	neat lubricant at RT
Xiao H. (2011) ¹⁰⁶	imidazolium, (PF ₆ ⁻)	steel / sapphire disk	neat lubricant at RT
Qu J. (2011) ¹⁰⁷	ammonium, (TFSI ⁻)	AISI 52100 steel / cast Iron	thin film study of neat lubricant at RT
Cai M. (2011) ¹⁰⁸	imidazolium, (PF ₆ ⁻ , BF ₄ ⁻ , TFSI ⁻)	AISI 52100 steel/ AISI 52100 steel	ILs as an additives in Polyethylene glycol and Polyuria grease at RT
Liu J. (2011) ¹⁰⁹	imidazolium, (PF ₆ ⁻ , BF ₄ ⁻ , TFSI ⁻)	SAE52100 / silicone	ultra-thin film lubrication of monolayer assembled catecholic biomimet ILs at RT
Pu J. (2011) ¹¹⁰	imidazolium, (PF ₆ ⁻ , BF ₄ ⁻)	AISI 52100 steel / single-crystal Si(100)	thin film study of neat lubricant at RT

Table 1.5: Continued

Amann T. (2012) ¹¹¹	imidazolium,(PF ₆ ⁻ , BF ₄ ⁻ , TFSI ⁻ , Cl ⁻ , Br ⁻)	steel/steel	influence of rheological properties on the tribological behavior of ILs and ionic liquid crystals ILCs at RT
Zhang C. (2012) ¹¹²	imidazolium, (BF ₄ ⁻)	AISI 52100 steel/ AISI 52100 steel	ILs as neat lubricant at RT and 80 °C and as lubricant additive in liquid paraffin
Zhao Q. (2012) ¹¹³	ammonium, (diethyldithiocarbamate)	AISI 52100 steel/ AISI 52100 steel	ILs as additive in lithium complex based grease at RT
Wang Z. (2012) ¹¹⁴	imidazolium, (PF ₆ ⁻ , BF ₄ ⁻)	AISI 52100 steel/AISI 52100 steel	IL as greases at RT, 75 and 150 °C
Espejo C. (2012) ¹¹⁵	imidazolium ,(tosylate (Ts))	AISI 316L stainless steel /polycarbonate (PC) disc	multi-walled carbon nanotubes (MWCNTs) as additive in ILs lubricant at RT
Morales W. (2012) ¹¹⁶	imidazolium, (sulfate)	440c stainless steel/ 440c stainless steel	ILs as neat lubricant under ultra- high vacuum condition at RT
Song Y. (2012) ¹¹⁷	imidazolium, (TFSI ⁻)	steel/ steel	neat lubricant at RT
Gabler C. (2012) ¹¹⁸	ammonium, phosphonium, sulfonium and imidazolium, (TFSI ⁻)	100Cr6 steel/ 100Cr6 steel	neat lubricant at RT
Fan M. (2012) ¹¹⁹	in-situ formation of ILs between LiTFSI and synthetic ester	AISI 52100 steel/AISI 52100 steel	ILs as additive in ester based lubricants at RT
Werzer O. (2012) ¹²⁰	ammonium, nitrate(NO ₃)	silica /mica	neat lubricant at RT

Table 1.5: Continued

Somers A. E. (2012) ¹²¹	ammonium, phosphonium, sulfonium and imidazolium, (TFSI ⁻ , phosphate, BF ₄ ⁻)	100Cr6 steel/AA2024 aluminum	neat lubricant at RT
Cai M. (2012) ¹²²	imidazolium, (phosphate)	AISI 52100 steel / Cu–Sn alloy	ILs as additives in PEG based lubricants at 100 °C
Fan M. (2012) ¹²³	in-situ formation of ils from lithium halide and poly ethylene glycol (PEG)	AISI 52100 steel / AISI 52100 steel	ILs as anti-wear and anti- corrosion additives in PEG based lubricants at RT
Asencio R.Á. (2012) ¹²⁴	ammonium, nitrate (NO ₃)	silica/ silica or polytetrafluoroethylene alumina/ silica or polytetrafluoroethylene	neat lubricant at RT
Battez A. H. (2013) ¹²⁵	ammonium, (phosphate)	chrome steel / ASTM A-569 PVD coated steel with TiN, CrN or diamond like carbon DLC	IL as additive and neat lubricant at RT in poly-alphaolefin (PAO)
Song Z. (2013) ¹²⁶	in-situ formation of ILs in synthetic oils and grease	AISI 52100 steel / AISI 52100 steel	ILs as additive in polyether, polyester and poly-urea grease at RT
Watanabe S. (2013) ¹²⁷	imidazolium, (sulfonate, BF ₄ ⁻)	SUJ2 steel / calcium fluoride	neat lubricant at RT
Zhao W. (2013) ¹²⁸	imidazolium, (TFSI ⁻)	AISI-52100 / silicon wafer	thin film study of neat lubricant at RT
Ana C. F. (2013) ¹²⁹	ammonium, (sulfonate)	iron / iron	neat lubricant at RT
Shi Y. (2013) ¹³⁰	Propaline, Ethaline, Reline	stainless steel 302 / carbon fiber composite	neat lubricant at RT

1.8 Research objectives

Some ILs are thought to have better lubrication properties, lower environmental impact and can be cost effective compared with existing synthetic lubricants. Table 1.4 shows that the lubricant properties of a wide range of ILs and DESs have been studied including imidazolium, ammonium, and phosphonium alkyl derivatives. By comparison studies using DESs as lubricants are very limited. Lawes in 2010 studied DESs as a lubricant for steel/steel lubrication for the first time,⁹⁷ and in 2013 other study has been done by Shi Y. et al.¹³⁰ DESs are biodegradable, non-toxic, easy to prepare and readily available therefore,²⁷ it is important to study in detail how these liquids perform as base lubricants.

The aim of this research is to evaluate how some type III DESs formed between ChCl and HBDs such as di and tri functional alcohols, amides and di-carboxylic acids perform as base lubricants. Their thermo-physical, rheological, corrosion and lubrication properties are compared with standard mineral base oil and some other imidazolium based ionic liquids.

To fully understand the lubrication behaviour of these liquids it is important to study firstly, the physical properties, such as viscosity and viscosity index, conductivity, surface tension and density. Secondly, thermal properties such as phase behaviour, thermal stability, heat capacity and enthalpy of formation will be evaluated. In addition to these properties, corrosion rates will be determined for common metals such as iron and aluminum which are commonly used to design engine blocks and their components. This is important due to the considerable presence of chloride and proton donors in the DESs, Furthermore, the change in corrosion rate with time is measured and a corrosion mechanism is postulated.

In terms of lubrication, the friction coefficient and wear volume for different contact pairs for lubricated and dry surfaces will be addressed together with wettability in terms of the contact angle, surface roughness and surface energy of all couples used in this study. Finally, the effect of some additives such as anionic and cationic surfactants upon the mechanical and thermo-physical properties is taken into consideration.

1.9 REFERENCES

1. J. G. Speight, *Handbook of Petroleum Product Analysis*, Wiley, 2015.
2. L. R. Rudnick, *Lubricant Additives: Chemistry and Applications, Second Edition*, Taylor & Francis, 2009.
3. Z. Pawlak, *Tribochemistry of Lubricating Oils*, Elsevier Science, 2003.
4. A. Mohammad, Inamuddin and Editors, *Green Solvents II Properties and Applications of Ionic Liquids*, Springer Science+Business Media Dordrecht 2012.
5. S. Boyde, *Green Chem*, 2002, 4, 293-307.
6. S. P. Srivastava, *Developments in Lubricant Technology*, Wiley, 2014.
7. R. I. Taylor, *Faraday Discuss*, 2012, 156, 361-382.
8. J. Qu, D. G. Bansal, B. Yu, J. Y. Howe, H. M. Luo, S. Dai, H. Q. Li, P. J. Blau, B. G. Bunting, G. Mordukhovich and D. J. Smolenski, *Acs Appl Mater Inter*, 2012, 4, 997-1002.
9. J. F. W. Sullivan, V. Voorhees, A. W. Neeley, R. V. Shankland, *Industrial and engineering chemistry*, 1931, 23, 604-611.
10. H. B. P. Ferreira and P. J. S. Barbeira, *Energ Fuel*, 2009, 23, 3048-3053.
11. A. Adhvaryu, B. K. Sharma, H. S. Hwang, S. Z. Erhan and J. M. Perez, *Ind Eng Chem Res*, 2006, 45, 928-933.
12. S. Z. Erhan, B. K. Sharma, Z. S. Liu and A. Adhvaryu, *J Agr Food Chem*, 2008, 56, 8919-8925.
13. B. K. Sharma, J. M. Perez and S. Z. Erhan, *Energ Fuel*, 2007, 21, 2408-2414.
14. B. H. Shoemaker, *117th meeting of American chemical society* 1950, 2414.
15. F. Zhou, Y. Liang and W. Liu, *Chemical Society reviews*, 2009, 38, 2590-2599.
16. M. D. Bermudez, A. E. Jimenez, J. Sanes and F. J. Carrion, *Molecules*, 2009, 14, 2888-2908.
17. I. Minami, *Molecules*, 2009, 14, 2286-2305.
18. S. Q. A. Rizvi, *A Comprehensive Review of Lubricant Chemistry, Technology, Selection, and Design*, ASTM International, 2009.
19. T. R. Lynch, *Process Chemistry of Lubricant Base Stocks*, Taylor & Francis, 2007.
20. API, *Engine oil licensing and certification system, Appendix E* 2011.
21. I. Šoljić Jerbić, J. Parlov Vuković and A. Jukić, *Ind Eng Chem Res*, 2012, 51, 11914-11923.

22. A. Singh, R. T. Gandra, E. W. Schneider and S. K. Biswas, *J Phys Chem C*, 2013, 117, 1735-1747.
23. A. T. Mario Campana, Stuart Clarke, Roland Steitz, John. R. P. Webster and and A. Zorbakhsh, *Longmuir*, 2011, 27, 6085–6090.
24. M. Freemantle, *An introduction to ionic liquids*, Royal Society of Chemistry, 2009.
25. D. Coleman and N. Gathergood, *Chemical Society reviews*, 2010, 39, 600-637.
26. Gerhard Laus, Gino Bentivoglio, Herwig Schottenberger, Volker Kahlenberg, Holger Kopacka, Thomas Röder and H. Sixta, *Lenzinger Berichte*, 2005, 84.
27. E. L. Smith, A. P. Abbott and K. S. Ryder, *Chem Rev*, 2014, 114, 11060-11082.
28. A. P. Abbott, G. Capper, D. L. Davies, H. L. Munro, R. K. Rasheed and V. Tambyrajah, *Chem Commun (Camb)*, 2001, DOI: Doi 10.1039/B106357j, 2010-2011.
29. M. J. Earle and K. R. Seddon, *Pure Appl Chem*, 2000, 72, 1391-1398.
30. A. P. Abbott, G. Capper, D. L. Davies, R. K. Rasheed and V. Tambyrajah, *Chem Commun (Camb)*, 2003, DOI: Doi 10.1039/B210714g, 70-71.
31. R. B. Leron, D. S. H. Wong and M.-H. Li, *Fluid Phase Equilibria*, 2012, 335, 32-38.
32. N. V. Plechkova and K. R. Seddon, *Chem Soc Rev*, 2008, 37, 123-150.
33. J. A. P. Coutinho, P. J. Carvalho and N. M. C. Oliveira, *RSC Advances*, 2012, 2, 7322.
34. S. Aparicio, M. Atilhan and F. Karadas, *Ind Eng Chem Res*, 2010, 49, 9580-9595.
35. J. Jacquemin, R. Ge, P. Nancarrow, D. W. Rooney, M. F. C. Gomes, A. A. H. Padua and C. Hardacre, *J Chem Eng Data*, 2008, 53, 716-726.
36. M. Petkovic, K. R. Seddon, L. P. Rebelo and C. Silva Pereira, *Chemical Society reviews*, 2011, 40, 1383-1403.
37. J. P. Hallett and T. Welton, *Chemical Reviews*, 2011, 111, 3508-3576.
38. T. Welton, *Chemical Reviews*, 1999, 99, 2071-2083.
39. Q. Zhang, K. De Oliveira Vigier, S. Royer and F. Jerome, *Chem Soc Rev*, 2012, 41, 7108-7146.
40. S. L. Perkins, P. Painter and C. M. Colina, *J Chem Eng Data*, 2014, 59, 3652-3662.
41. K. Shahbaz, S. Baroutian, F. S. Mjalli, M. A. Hashim and I. M. AlNashef, *Thermochim Acta*, 2012, 527, 59-66.
42. K. Shahbaz, F. S. Mjalli, M. A. Hashim and I. M. AlNashef, *Fluid Phase Equilib*, 2012, 319, 48-54.
43. A. P. Abbott, D. Boothby, G. Capper, D. L. Davies and R. K. Rasheed, *Journal of the American Chemical Society*, 2004, 126, 9142-9147.

44. R. B. Leron, A. N. Soriano and M. H. Li, *J Taiwan Inst Chem E*, 2012, 43, 551-557.
45. A. P. Abbott, R. C. Harris, K. S. Ryder, C. D'Agostino, L. F. Gladden and M. D. Mantle, *Green Chem*, 2011, 13, 82-90.
46. A. P. Abbott, A. A. Al-Barzinjy, P. D. Abbott, G. Frisch, R. C. Harris, J. Hartley and K. S. Ryder, *Phys Chem Chem Phys*, 2014, 16, 9047-9055.
47. E. L. Smith, C. Fullarton, R. C. Harris, S. Saleem, A. P. Abbott and K. S. Ryder, *T I Met Finish*, 2010, 88, 285-291.
48. M. Palacio and B. Bhushan, *Tribol Lett*, 2010, 40, 247-268.
49. A. Somers, P. Howlett, D. MacFarlane and M. Forsyth, *Lubricants*, 2013, 1, 3-21.
50. Anthony E. Somers, Patrick C. Howlett, D. R. MacFarlane and M. Forsyth, *Lubricants* 2013, 1, 3-21.
51. P. G. Smith, *A S L E Transactions*, 1961, 4, 263-274.
52. C. F. Ye, W. M. Liu, Y. X. Chen and L. G. Yu, *Chem Commun*, 2001, DOI: Doi 10.1039/B106935g, 2244-2245.
53. W. Liu, C. Ye, Y. Chen, Z. Ou and D. C. Sun, *Tribology International*, 2002, 35, 503-509.
54. W. M. Liu, C. F. Ye, Q. Y. Gong, H. Z. Wang and P. Wang, *Tribol Lett*, 2002, 13, 81-85.
55. Y. Chen, Ye, Chengfeng, Wang, and L. Haizhong, Weimin, *Journal of Synthetic Lubrication*, 2003, 20, 217-225.
56. Q. Lu, H. Wang, C. Ye, W. Liu and Q. Xue, *Tribol Int*, 2004, 37, 547-552.
57. B. S. Phillips and J. S. Zabinski, *Tribol Lett*, 2004, 17, 533-541.
58. B. A. Omotowa, B. S. Phillips, J. S. Zabinski and J. M. Shreeve, *Inorg Chem*, 2004, 43, 5466-5471.
59. Z. Mu, F. Zhou, S. Zhang, Y. Liang and W. Liu, *Tribol Int*, 2005, 38, 725-731.
60. Y. Xia, S. Wang, F. Zhou, H. Wang, Y. Lin and T. Xu, *Tribol Int*, 2006, 39, 635-640.
61. B. Yu, F. Zhou, Z. Mu, Y. Liang and W. Liu, *Tribol Int*, 2006, 39, 879-887.
62. J. Sanes, F. J. Carrion, M. D. Bermudez and G. Martinez-Nicolas, *Tribol Lett*, 2006, 21, 121-133.
63. J. Qu, J. J. Truhan, S. Dai, H. Luo and P. J. Blau, *Tribol Lett*, 2006, 22, 207-214.
64. X. Liu, F. Zhou, Y. Liang and W. Liu, *Tribol Lett*, 2006, 23, 191-196.
65. G. Yu, S. Yan, F. Zhou, X. Liu, W. Liu and Y. Liang, *Tribol Lett*, 2006, 25, 197-205.
66. H. Kamimura, T. Chiba, N. Watanabe, T. Kubo, H. Nanao, I. Minami and S. Mori, *Tribology Online*, 2006, 1, 40-43.

67. A.-E. Jiménez and M.-D. Bermúdez, *Tribol Lett*, 2006, 26, 53-60.
68. L. Weng, X. Liu, Y. Liang and Q. Xue, *Tribol Lett*, 2006, 26, 11-17.
69. H. Kamimura, T. Kubo, I. Minami and S. Mori, *Tribol Int*, 2007, 40, 620-625.
70. B. S. Phillips, G. John and J. S. Zabinski, *Tribol Lett*, 2007, 26, 85-91.
71. A. Suzuki, Y. Shinka and M. Masuko, *Tribol Lett*, 2007, 27, 307-313.
72. B. Yu, F. Zhou, C. Pang, B. Wang, Y. Liang and W. Liu, *Tribol Int*, 2008, 41, 797-801.
73. T. Murakami, K. Kaneda, M. Nakano, A. Korenaga, H. Mano and S. Sasaki, *Tribol Int*, 2008, 41, 1083-1089.
74. M. Zhu, J. Yan, Y. Mo and M. Bai, *Tribol Lett*, 2008, 29, 177-183.
75. Y. Xia, L. Wang, X. Liu and Y. Qiao, *Tribol Lett*, 2008, 30, 151-157.
76. I. Minami, M. Kita, T. Kubo, H. Nanao and S. Mori, *Tribol Lett*, 2008, 30, 215-223.
77. H. Kondo, *Tribol Lett*, 2008, 31, 211-218.
78. Y. Xia, L. Wang, X. Liu and Y. Qiao, *Tribol Lett*, 2008, 31, 149-158.
79. Y. Mo, W. Zhao, M. Zhu and M. Bai, *Tribol Lett*, 2008, 32, 143-151.
80. B. S. P. Zhuo Zeng, Ji-Chang Xiao, Jean'ne M. Shreeve, *Chem. Mater.*, 2008, 20, 2719-2726.
81. W. Zhao, Y. Mo, J. Pu and M. Bai, *Tribol Int*, 2009, 42, 828-835.
82. A. E. Jiménez, M. D. Bermúdez and P. Iglesias, *Tribol Int*, 2009, 42, 1744-1751.
83. A. E. Jiménez and M.-D. Bermúdez, *Tribol Lett*, 2008, 33, 111-126.
84. L. Zhang, D. Feng and B. Xu, *Tribol Lett*, 2009, 34, 95-101.
85. L. Zhang, D. Feng, B. Xu, X. Liu and W. Liu, *Science in China Series E: Technological Sciences*, 2009, 52, 1191-1194.
86. J. Qu, P. J. Blau, S. Dai, H. Luo and H. M. Meyer, *Tribol Lett*, 2009, 35, 181-189.
87. N. S. Nooruddin, P. G. Wahlbeck and W. R. Carper, *Tribol Lett*, 2009, 36, 147-156.
88. H. Zhang, Y. Xia, M. Yao, Z. Jia and Z. Liu, *Tribol Lett*, 2009, 36, 105-111.
89. M. Yao, Y. Liang, Y. Xia and F. Zhou, *ACS applied materials & interfaces*, 2009, 1, 467-471.
90. G. Xie, Q. Wang, L. Si, S. Liu and G. Li, *Tribol Lett*, 2009, 36, 247-257.
91. H. Arora and P. M. Cann, *Tribology International*, 2010, 43, 1908-1916.
92. A. E. Jiménez and M. D. Bermúdez, *Tribol Lett*, 2009, 37, 431-443.
93. A. E. Jiménez and M. D. Bermúdez, *Tribol Lett*, 2010, 40, 237-246.
94. A. E. Somers, P. C. Howlett, J. Sun, D. R. MacFarlane and M. Forsyth, *Tribol Lett*, 2010, 40, 279-284.

95. M. Cai, Z. Zhao, Y. Liang, F. Zhou and W. Liu, *Tribol Lett*, 2010, 40, 215-224.
96. I. Minami, T. Inada, R. Sasaki and H. Nanao, *Tribol Lett*, 2010, 40, 225-235.
97. S. D. A. Lawes, S. V. Hainsworth, P. Blake, K. S. Ryder and A. P. Abbott, *Tribol Lett*, 2010, 37, 103-110.
98. M. Cai, Y. Liang, M. Yao, Y. Xia, F. Zhou and W. Liu, *ACS applied materials & interfaces*, 2010, 2, 870-876.
99. S. Perkin, T. Albrecht and J. Klein, *Phys Chem Chem Phys*, 2010, 12, 1243-1247.
100. X. W. Baogang Wang, Wenjing Lou, and Jingcheng Hao, *J. Phys. Chem. C*, , 2010, 114, 8749–8754.
101. D. Blanco, R. González, A. Hernández Battez, J. L. Viesca and A. Fernández-González, *Tribol Int*, 2011, 44, 645-650.
102. D. Li, M. Cai, D. Feng, F. Zhou and W. Liu, *Tribol Int*, 2011, 44, 1111-1117.
103. F. J. Carrión, J. Sanes, M.-D. Bermúdez and A. Arribas, *Tribol Lett*, 2010, 41, 199-207.
104. D. Blanco, A. H. Battez, J. L. Viesca, R. González and A. Fernández-González, *Tribol Lett*, 2010, 41, 295-302.
105. D. Jiang, L. Hu and D. Feng, *Tribol Lett*, 2010, 41, 417-424.
106. H. Xiao, D. Guo, S. Liu, G. Pan and X. Lu, *Tribol Lett*, 2010, 41, 471-477.
107. J. Qu, M. Chi, H. M. Meyer, P. J. Blau, S. Dai and H. Luo, *Tribol Lett*, 2011, 43, 205-211.
108. M. Cai, Y. Liang, F. Zhou and W. Liu, *ACS applied materials & interfaces*, 2011, 3, 4580-4592.
109. J. Liu, J. Li, B. Yu, B. Ma, Y. Zhu, X. Song, X. Cao, W. Yang and F. Zhou, *Langmuir : the ACS journal of surfaces and colloids*, 2011, 27, 11324-11331.
110. J. Pu, S. Wan, W. Zhao, Y. Mo, X. Zhang, L. Wang and Q. Xue, *The Journal of Physical Chemistry C*, 2011, 115, 13275-13284.
111. T. Amann, C. Dold and A. Kailer, *Soft Matter*, 2012, 8, 9840.
112. C. Zhang, S. Zhang, L. Yu, P. Zhang, Z. Zhang and Z. Wu, *Tribol Lett*, 2012, 46, 49-54.
113. Q. Zhao, G. Zhao, M. Zhang, X. Wang and W. Liu, *Tribol Lett*, 2012, 48, 133-144.
114. Z. Wang, Y. Xia, Z. Liu and Z. Wen, *Tribol Lett*, 2012, 46, 33-42.
115. C. Espejo, F.-J. Carrión, D. Martínez and M.-D. Bermúdez, *Tribol Lett*, 2012, 50, 127-136.

116. W. Morales, K. W. Street, R. M. Richard and D. J. Valco, *Tribology Transactions*, 2012, 55, 815-821.
117. Y. Song, Y. Xia and Z. Liu, *Tribology Transactions*, 2012, 55, 738-746.
118. C. Gabler, E. Pittenauer, N. Dörr and G. Allmaier, *Anal Chem*, 2012, 84, 10708-10714.
119. M. Fan, Z. Song, Y. Liang, F. Zhou and W. Liu, *ACS applied materials & interfaces*, 2012, 4, 6683-6689.
120. M. Fan, Z. Song, Y. Liang, F. Zhou and W. Liu, *ACS applied materials & interfaces*, 2012, 4, 6683-6689.
121. O. Werzer, E. D. Cranston, G. G. Warr, R. Atkin and M. W. Rutland, *Phys Chem Chem Phys*, 2012, 14, 5147-5152.
122. M. Cai, Y. Liang, F. Zhou and W. Liu, *Faraday Discussions*, 2012, 156, 147.
123. M. Fan, Y. Liang, F. Zhou and W. Liu, *RSC Advances*, 2012, 2, 6824.
124. R. Á. Asencio, E. D. Cranston, R. Atkin and M. W. Rutland, *Langmuir : the ACS journal of surfaces and colloids*, 2012, 28, 9967-9976.
125. A. Hernández Battez, R. González, J. L. Viesca, A. Fernández-González and M. Hadfield, *Tribol Int*, 2013, 58, 71-78.
126. Z. Song, M. Fan, Y. Liang, F. Zhou and W. Liu, *Tribol Lett*, 2012, 49, 127-133.
127. S. Watanabe, K. Takiwatari, M. Nakano, K. Miyake, R. Tsuboi and S. Sasaki, *Tribol Lett*, 2013, DOI: 10.1007/s11249-013-0130-1.
128. W. Zhao, Z. Zeng, S. Peng, X. Wu, Q. Xue and J. Chen, *Tribology Transactions*, 2013, 56, 480-487.
129. A. C. F. Mendonça, A. A. H. Pádua and P. Malfreyt, *Journal of Chemical Theory and Computation*, 2013, 9, 1600-1610.
130. Y. Shi, L. Mu, X. Feng and X. Lu, *Tribol Lett*, 2012, 49, 413-420.

CHAPTER TWO: EXPERIMENTALS

CONTENTS

2	EXPERIMENTAL	40
2.1	CHEMICALS	40
2.2	PREPARATION OF DESS:	41
2.3	MEASUREMENTS.....	41
2.3.1	<i>PHYSICAL PROPERTIES.....</i>	<i>41</i>
2.3.2	<i>THERMAL PROPERTIES.....</i>	<i>43</i>
2.3.3	<i>CORROSION STUDIES.....</i>	<i>44</i>
2.3.4	<i>MEASUREMENTS OF MECHANICAL AND WETTING PROPERTIES.....</i>	<i>46</i>
2.4	REFERENCES:	49

2 EXPERIMENTAL

2.1 Chemicals

The source of chemicals and their purity are shown in Table 2.1.

Table 2.1: List of chemicals and their specifications.

Chemicals	Source	Purity %
choline chloride	Sigma-Aldrich	≥ 98
glycerol	Fischer	98
urea	Sigma-Aldrich	99.9
ethylene glycol	Sigma-Aldrich	≥ 99
oxalic acid	Fischer	99
potassium nitrate	Sigma-Aldrich	≥ 99
potassium chloride	Fischer	99-100
1,6-Hexanediol	Sigma-Aldrich	97
1,5-Pentanediol	Sigma-Aldrich	96
1;4-Butanediol	Sigma-Aldrich	99
xylitol	Sigma-Aldrich	98
D-sorbitol	Sigma-Aldrich	≥ 98
graphite powder	Alfa Aesar	99.9995
sodium dodecyl sulfate	Sigma-Aldrich	99
cetyltrimethylammonium bromide	Sigma-Aldrich	CAS 57-09-0
1-ethyl-3-methylimidazolium ethylsulfate	Basif	CAS 342573-61-5
1-ethyl-3-methylimidazolium hydrogensulfate	Basif	CAS 412009-61-1
1-ethyl-3-methylimidazolium thiocyanate	Basif	CAS 331717-63-6
1-ethyl-3-methylimidazolium acetate	Basif	CAS 143314-17-4

2.2 Preparation of DESs:

The DESs were prepared as follows; Glyceline was prepared by mixing choline chloride and glycerol in a 1:2 molar ratio. The mixture was stirred and heated at *c.a.* 353 K, until a clear liquid was formed. The same procedure was used for Ethaline however, instead of glycerol, ethylene glycol has been used and the mixture was heated to about 333 K.

Reline was prepared by mixing choline chloride and urea in a 1:2 molar ratio. The mixture was stirred and placed in an oven at 320 K. Every half hour, the mixture was stirred, until a clear liquid was formed. Oxaline was prepared by the same procedure used for Reline, however the molar ratio of a mixture was 1:1(ChCl:Oxalic acid).

2.3 Measurements

2.3.1 Physical properties

- **Viscosity**

The viscosity of all DESs was measured using both Quartz Crystal Microbalance (QCM) and rotational (Brookfield DV-II+ Pro) viscometers. For rotating viscometer the spindle was rotated in each liquid between 5 and 200 rpm to ensure the appropriate torque and the resultant dynamic viscosities have been converted to kinematic viscosity using their densities at the same temperature to be used for calculating viscosity index.

The viscosity has also been measured using QCM in which a polished gold crystal was mounted on top of a glass tube in which only one face of a crystal to be exposed to the liquid. A tube holding the crystal was immersed in a liquid until the preferred temperature was achieved. Then the oscillating frequency of the crystal was measured at least three times for each liquid.

The frequency of a crystal is influenced by the temperature. The frequency of a free crystal (a crystal in air) was measured at the same temperature as the liquid. Later the frequency of the free crystal was subtracted from the crystal in a liquid to obtain the net frequency of the crystal.

For both viscosity measurements the viscosity was converted to a viscosity index according to the ASTM D2270 test method.¹ According to this standard test method the kinematic viscosity of a liquid should be measured at 313 K and 373 K. Then both constant values H and L corresponding to viscosity at 373 K are extracted from the table of the test method which required for calculations as follows;

$$VI = (L - U / L - H) * 100$$

Where;

U is the kinematic viscosity at 313.15 of the unknown oil; L is the kinematic viscosity at 313 K of an oil ($VI = 0$) having the same viscosity at 373 K as the unknown oil; H is the kinematic viscosity at 313 K of an oil ($VI = 100$) having the same viscosity at 373 K as the unknown oil.

- **Surface Tension and Density**

Both density and surface tension were measured with a Krüss Tensiometer K9 model K9MK1. A liquid sample was placed in a glass dish surrounded by a water jacket. The temperature was controlled by a thermostat connected to the jacket. Surface tension was recorded using a Pt–Ir alloy plate (Krüss, part number PL01). The density was measured every 5 K between 298 and 333 K as follows; A silicon log of known density (2.330 g cm^{-3}) was placed on a Pt-Ir cradle and submerged into a liquid then the density was recorded from the instrument. However, for surface tension measurements a Pt-Ir alloy plate (Krüss, part number PL01) was used wherein the plate was moved downward to be in contact with the surface layer of a liquid then the surface tension was read from the screen.

- **Conductivity**

The conductivity of all DESs used in this study was measured with a Jenway 4510 conductivity meter as follows; the conductivity meter probe has been immersed in a liquid and left until the temperature reached equilibrium, and the conductivity was recorded at least three times for each temperature. The conductivity was later converted to molar conductivity by dividing by the molarity of a liquid.

2.3.2 Thermal properties

- **Heat capacity and enthalpy of formation**

All heat capacity, phase behaviour and enthalpy of formation data of DESs were measured using a Mettler Toledo Differential Scanning Calorimetry (DSC). A baseline was recorded with an empty (blank) crucible made from aluminium and this data was used for heat transfer calculations. The pans with and without sample were heated at a fixed heating rate $5\text{-}10\text{ K min}^{-1}$ within the same range of temperature under an inert atmosphere of nitrogen ($75\text{ cm}^3\text{ min}^{-1}$).

A liquid or solid sample (5-10 mg) was weighted in to a sapphire pan and placed on the specified area of sample holder of the DSC and the empty pan was placed on the reference holder as shown in Figure 2-1. The sample and empty pans were heated or cooled together according to the requirements of the procedure.



Figure 2-1: Places of sample and blank pans for DSC measurements.

The data was analysed using STAR^e system software which enabled melting points, glass transition T_g temperatures and the amount of heat energy absorbed or released during the measurements to be determined.

- **Thermal stability**

Thermal stability measurements were performed using thermogravimetric analysis (TGA). Thermal stability of samples was measured using a Mettler Toledo

TGA/DSC 1 machine fitted with a sample robot. The TGA was able to detect a very small change in the mass c.a. 0.1 μg could be detected in a 15-25 mg sample. The instrument utilises the same STAR^e system software for data analysis as used for DSC machine.

2.3.3 Corrosion studies

- **Linear sweep polarization**

Corrosion studies were carried out using AUTOLAB instruments (Autolab PGSTAT12 and FRA2 μ AUTOLAB Type III). In all experiments the metal samples (Al, Fe and Ni) were used as a working electrode and Pt electrode as a counter electrode however, the reference electrode was (Ag/AgCl in 1M KCl_(aq)). Working electrodes were made in the form of disc shape electrodes. For corrosion rate measurements the electrodes were polished with micro-polish alumina particles 0.05 μm diameters. The calculations of corrosion rates were made as shown in Figure 2-2:

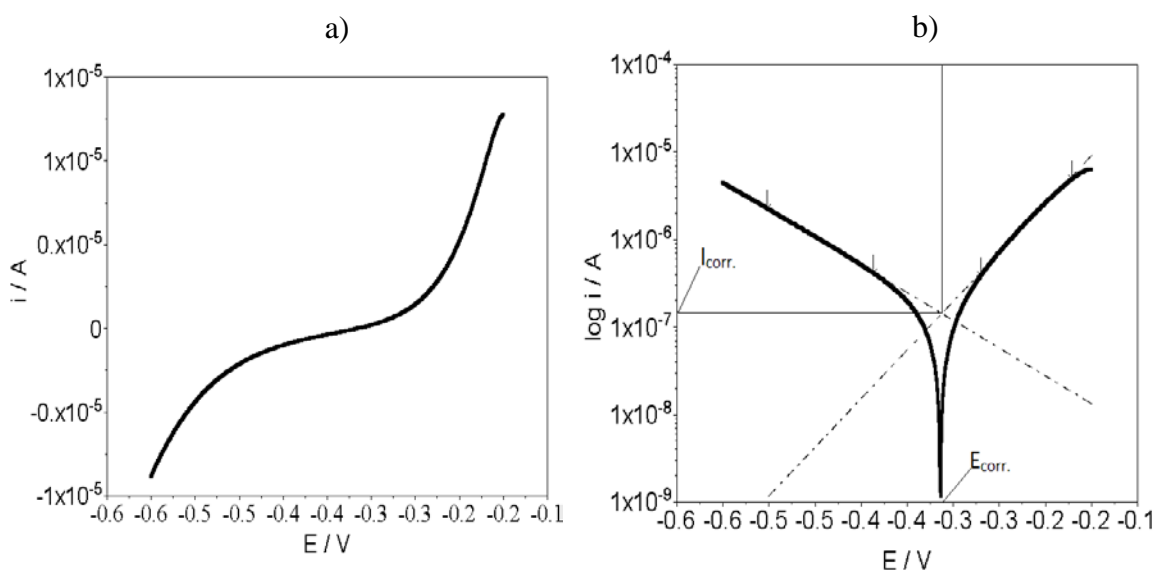


Figure 2-2: Measurement of corrosion rate and Tafel slopes.

- 1- Working electrodes were polarized linearly using 5-10 mV s^{-1} sweep rate at 298 K at least 300 mV cathodic and anodic on both sides of the corrosion potential as shown in Figure 2.2a.

2- From the software analysis options Tafel slope analyser was chosen to calculate cathodic and anodic slopes as shown in Figure 2-2 in which two points from both sides were required to draw a baseline slope measurement. After entering corrosion rate requirements such as electrode surface area, density and equivalent weight of the metal the corrosion rate in mm year^{-1} was calculated.

- **Electrochemical impedance spectroscopy**

For electrochemical impedance spectroscopy studies, electrodes were left in a liquid for periods of (1, 2, 4, 6, 8, 24, 28, 32 and 48 hours) at 298 K without polishing between measurements. The polarisation resistance was calculated as shown in Figure 2-3 by selecting three points on a semi-circular Nyquist plot and using fitting software to extract the polarisation resistance and solution resistance.

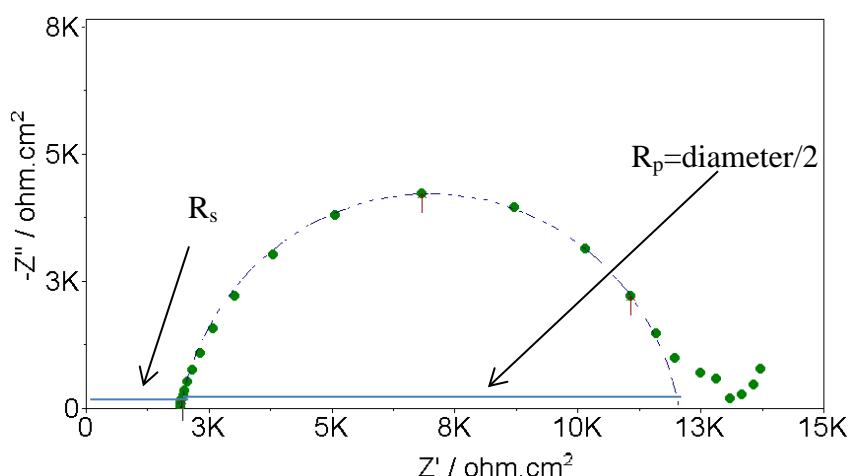


Figure 2-3: Nyquist plot showing solution resistance and polarisation resistance.

- **Investigation of corrosion products**

Corrosion products were identified using Raman spectroscopy wherein the spectrum of corrosion products was recorded by using a HORIBA Jobin Yvon Raman spectrometer. The corrosion products were collected as follows; metal plates were immersed in aerated DES s for 3 months – 1 year. Excitation of the surface was made with a small single frequency green laser beam of 532 nm with a power of (3.5 - 35 mW) using a sample area of $0.3\text{-}0.5 \text{ mm}^2$ for periods between 10 - 100 s in order to avoid thermal-transformation of corrosion products especially for iron oxides. The laser power was modulated by a set of filters. An Olympus microscope was used to observe samples with 10X, 50X and 100X Leitz lenses.

2.3.4 Measurements of mechanical and wetting properties

- **Friction coefficient**

Friction coefficient data were determined using the standard ball on sheet technique using a Teer Coatings ST-200 wear tester. In all cases the friction coefficient–time profile remained flat over 4000 cycles (2.3 hour at 0.005 ms^{-1} under a load of 30 N at 293 -298 K). The friction test has two components; a flat substrate (which moves) and a spherical ball specimen. As illustrated in Figure 2-4 both components are in relative linear sliding (back and forth) motion under prescribed conditions of applied load, temperature, speed, time (number of strokes or cycles) and the length of cycle. Through the carbon steel ball the load have been vertically applied downward against horizontally mounted substrates such as stainless steel, mild steel, aluminium, copper and bronze substrates. All friction tests were carried out with and without lubricant to address the extent of reduced friction in the presence of lubricants under the same conditions.

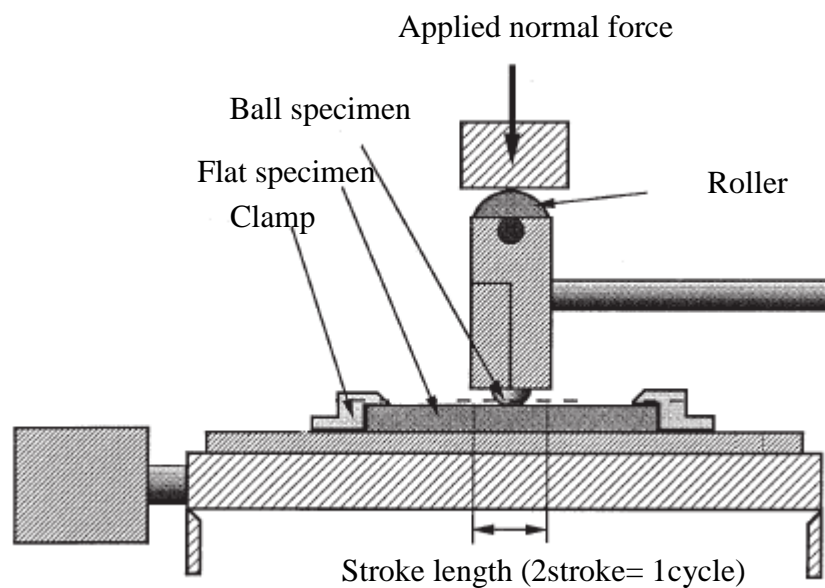


Figure 2-4: *The design of Friction and wear tester.*²

- **Contact angle and Wettability**

The wettability of substrate surfaces were made using contact angle measurements in which all tests carried out using CAM 100 contact-angle meter (Edmund industrial optics) and Attention Theta Optical Tensiometer from Biolin Scientific Company using Oneattention software to analyse the data. The contact angle measurements were done as follows; ³ droplets of 4.9 - 5.10 μL size from mineral base oil, DESs and ILs were formed at the end of a needle and brought into contact with substrate specimen surface of mild steel, bronze, copper, aluminium and stainless steel sheets. As illustrated in Figure 2-5 the reading was carried out after 10 seconds of the droplet contacting the metal surface. Later the mean values of the right and left contact angles were taken and the tests repeated at least for three droplets were studied for each liquid.

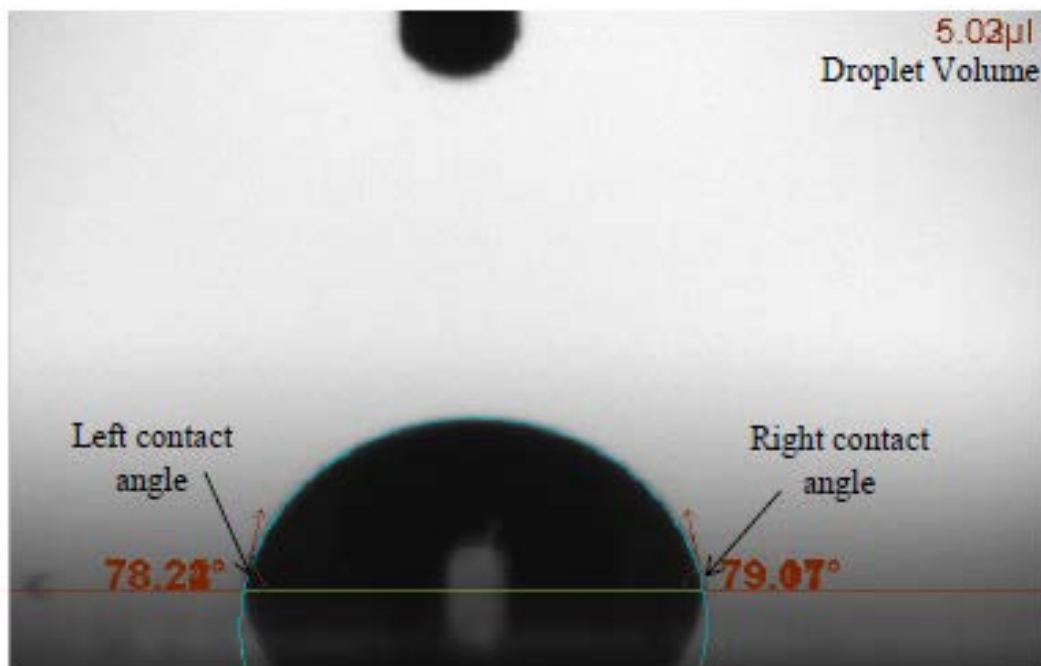


Figure 2-5: Measurement of contact angle the image represents Reline on stainless steel substrate.

- **Surface roughness**

A Zeta 20 optical profiler from Zeta instruments was used to measure the surface roughness and obtain optical images using version 1.8.5 of Zeta3D software for all metal and alloy substrates. The roughness and wear images of substrate surfaces which have been used to measure both wettability and friction tests have been carried as

follows; 3D images having $250 \times 200 \mu\text{m}$ for surfaces were recorded by combining smaller images taken automatically for the covered area. Then the roughness of a surface was calculated for five vertical and five horizontal cross section lines.

- **Wear area and wear volume**

Wear volume measured with the Zeta 2000 optical profiler, 3D images shown in Figure 2-6a, b and c having $6000 \times 2000 \mu\text{m}$ were made from combining smaller images having $400 \times 400 \mu\text{m}$ taken over the area of scratch. To obtain the volume of scratch a reference surface have been selected which represent the flat surface of a metal as shown in Figure 2-6b by choosing 3 points(blue squares) around scratches area since for calculated volume, any point under this reference surface is considered as a scratch. Followed by the drawing a line (the red line) in Figure 2-6c around the area of scratch to calculate the volume of intended area only.

Finally, the software will calculates the total volume of scratch being made during the experiment by considering any points within the red line reflects the light under the reference surface level.

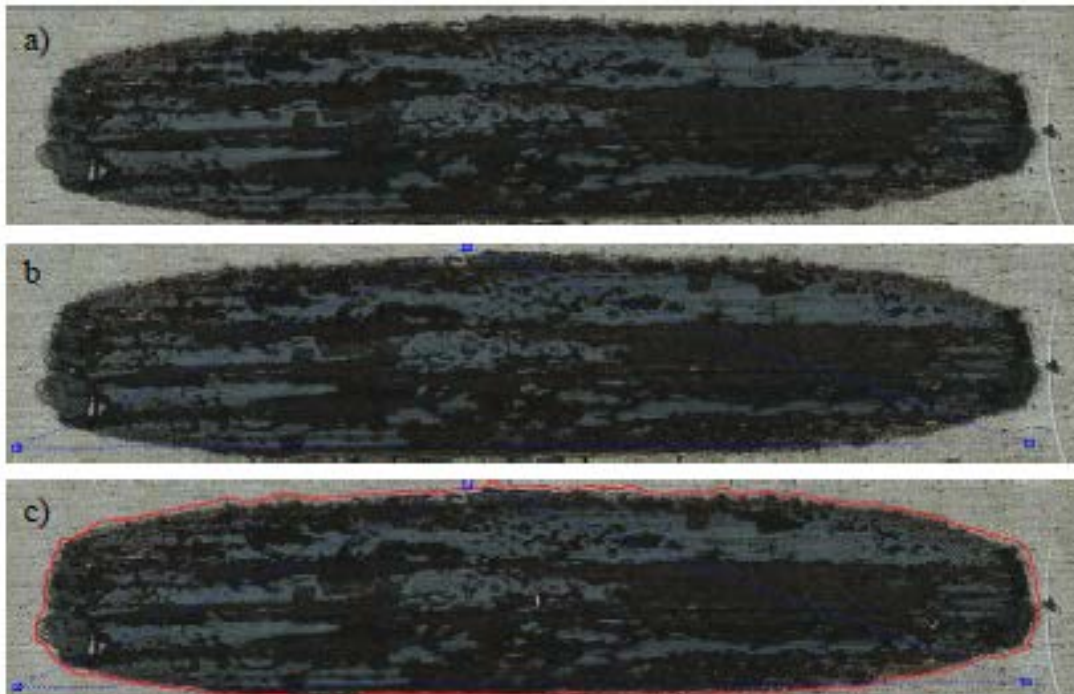


Figure 2-6: calculation of wear area and wear volume a) original scratched surface, b) defining of reference surface and c) determination of scratched area.

- **Substrate hardness**

Hardness tests were made using a Buehler micromet 5100 series hardness tester which is a microindentation technique used to measure hardness in Vickers. As shown in Figure 2-7 a pyramidal square shape diamond having a 136° point was pressed against a metal specimen surfaces using predetermined (300-1000) gram force for 10 s. The average of length dimensions of a diagonal has been measured automatically and converted to Vickers hardness number in $\text{g } \mu\text{m}^{-2}$ taking into consideration the applied force. The Vickers hardness number later converted to kilogram force (kgf) kg mm^{-2} which has used for calculations of wear coefficient (k) and anti-wear number (AWN).

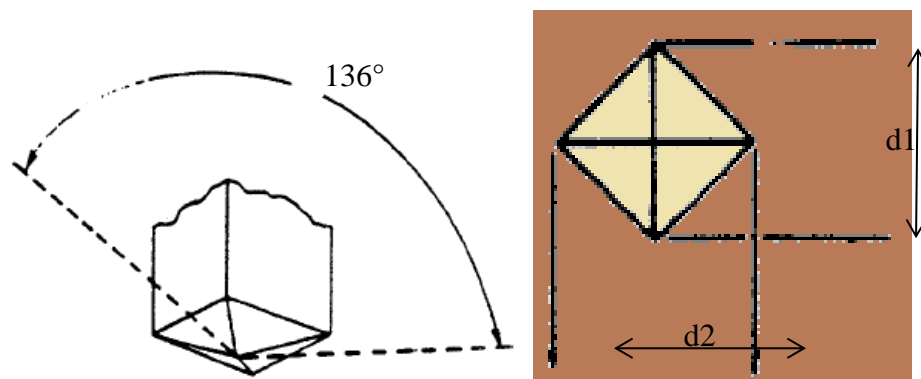


Figure 2-7: Vickers indenter tip and the resulted diagonal length dimensions.⁴

2.4 References:

1. *Annual Book of ASTM Standards, ASTM D2270, Standard Practice for Calculating Viscosity Index From Kinematic Viscosity at 40 and 100°C*, ASTM International, 100 Barr Harbor Drive, PO Box C700, West Conshohocken, PA 19428-2959, United States., Vol 05.01, 2004.
2. *Annual book of ASTM standards , ASTM G 133, Standard Test Method for Linearly Reciprocating Ball-on-Flat Sliding Wear*, ASTM International, 100 Barr Harbor Drive, PO Box C700, West Conshohocken, PA 19428-2959, United States., Vol. 03.02, 2004.
3. *Annual book of ASTM standards , ASTM D 5725, Standard Test Method for Surface Wettability and Absorbency of Sheeted Materials Using an Automated Contact Angle Tester*, ASTM International, 100 Barr Harbor Drive, PO Box C700, West Conshohocken, PA 19428-2959, United States., Vol.15:09, 2004.

4. *Annual book of ASTM standards* , *ASTM E384, Standard Test Method for Microindentation Hardness of Materials*, ASTM International, 100 Barr Harbor Drive, PO Box C700, West Conshohocken, PA 19428-2959, United States., Vol. 03.01, 2004.

CHAPTER THREE: BULK PROPERTIES

3 RHEOLOGY AND THERMO-PHYSICAL PROPERTIES OF DESS

3.1	INTRODUCTION.....	52
3.2	THERMAL PROPERTIES	53
3.2.1	<i>Differential scanning calorimetry (DSC)</i>	53
3.2.2	<i>Phase behavior of DESs</i>	55
3.2.3	<i>Heat capacity of liquids</i>	57
3.2.4	<i>Enthalpy of formation of DESs</i>	60
3.2.5	<i>Thermal stability</i>	61
3.3	PHYSICAL PROPERTIES	63
3.3.1	<i>Viscosity of ILs</i>	64
3.3.2	<i>Surface Tension</i>	68
3.3.3	<i>Conductivity</i>	71
3.3.4	<i>Density</i>	74
3.4	RHEOLOGICAL PROPERTIES	75
3.4.1	<i>Flow characteristics of liquids</i>	75
3.4.2	<i>Flow characteristics of DESs</i>	77
3.5	CONCLUSIONS	85
3.6	REFERENCES	86

3 RHEOLOGY AND THERMO-PHYSICAL PROPERTIES OF DESs

3.1 Introduction

Thermo-physical properties and flow characteristics of a liquid are governed strongly by molecular structure and molecular association forces. Despite the fact that mineral base oil and DESs are totally different in their molecular structure and intermolecular forces, they have comparable lubrication behaviour. Paraffinic mineral oils are long chain molecules which are able to make coil and uncoil at low and high temperatures respectively.^{1, 2} Consequently, at low temperature the effect of long chain molecules on viscosity is very small as they are coiled. In contrast at high temperatures the molecules uncoil and the long chain molecules will become more entangled.^{1, 3}

The dependence of liquid properties on both intermolecular forces and the structure of molecules are related to the fact that the more spherical the molecules, the smaller the tendency to become entangled, making them much easier to move over each other and vice versa, thereby reducing liquid viscosity without considering the existing of intermolecular forces. This dependence of viscosity on the structure of molecules and more specifically on the chain lengths reduces the correlation between intermolecular forces and viscosity index in mineral base oils.

In contrast to mineral oils the intermolecular forces in DESs are dominated by Coulombic and hydrogen bonding interactions which are much stronger than the van der Waals forces in mineral oils.⁴ These interactions will be less affected by temperature and hence they should retain high viscosity indexes.⁵ Therefore, although DESs and mineral base oil both show high viscosity-temperature relationships they have different intermolecular forces it is thought to be related to this phenomenon.³

In this Chapter the suitability of using DESs for lubricants will be ascertained. To do this the thermal properties are characterised including phase behaviour, heat capacity, thermal stability and enthalpy of formation. Next the physical properties were measured including the viscosity and viscosity index, density, conductivity and surface tension. Finally, the flow characteristics were characterized including Newtonian or non-Newtonian behaviour, the effect of water and temperature on this behaviour and self-diffusivity in the presence of water. In all cases the properties are compared with standard mineral base oil without additives.

3.2 Thermal properties

3.2.1 Differential scanning calorimetry (DSC)

According to the International Confederation for Thermal Analysis and Calorimetry (ICTAC) DSC is defined as:

“A technique in which the heat-flow rate (power) to the sample is monitored against time or temperature while the temperature of the sample, in a specified atmosphere, is programmed”.⁶

As a universal technique DSC is employed to monitor heat effects accompanying either chemical reactions or physical transition as a function of temperature. For example synthetic or biological polymers, nanoparticles, bulk materials and crystalline solids could be studied by DSC.^{6, 7} The instrument is able to measure a number of thermodynamic properties easily such as phase transitions, glass transitions, specific heat and enthalpy changes owing to the fact that the heat flow is directly related to electrical output.^{8, 9} Alumina or aluminum pan as inert materials are used commonly as a reference. Here the temperature is increased or decreased at constant rate for both sample and reference.

DSC works under constant pressure so the heat flow is equal to the enthalpy change:⁶

$$\left(\frac{dq}{dt}\right)_p = \frac{dH}{dt} \dots\dots\dots(3.1)$$

Where; dH/dt is the difference in heat flow measured in mWs^{-1} or mcal s^{-1} which is necessary to maintain the same temperature for both sample and reference pan. The difference between heat flow to the sample and reference is:

$$\Delta \frac{dH}{dt} = \frac{dH}{dt}(\text{sample}) - \frac{dH}{dt}(\text{reference}) \dots\dots\dots(3.2)$$

Accordingly depending on the physical transition or chemical reaction the value could be either negative or positive. For phase changes such as melting, boiling or glass transition in which the heat flows to the sample is more than the heat flows to the reference (endothermic) in which the energy absorbed by the transition, the value of

$\Delta dH/dt$ will be positive. On the other hand, if heat flow to the sample is lower than heat flow to the reference such as in crystallization and oxidation the value of $\Delta dH/dt$ will be negative named (exothermic) from which the energy released by the transition. Both sample mass and scan speed affects the difference between endothermic and exothermic data from which the difference will be small for low scan rate and low sample masses.^{9,}

¹⁰ Recording the difference between heat flow rate into both sample and reference material under the same conditions of experiment as a function of temperature, enables the direct measurement of specific heat of a sample, because this heat flow rate is proportional to the instantaneous specific heat of the sample when it is heated or cooled at linear temperature change at constant pressure provided that there are no chemical reaction or phase change occurs.^{11, 12}

$$\frac{dH}{dt} = mCp \frac{dT}{dt} \dots\dots\dots(3.3)$$

Where m ; is sample mass (g), Cp ; is specific heat in ($J\ g^{-1}.K^{-1}$), dT/dt ; is heat flow ($J\ s^{-1}$).

The enthalpy is a function of all temperature (T), pressure (p) and composition (ξ);

$$H = H(T, p, \xi) \dots\dots\dots(3.4)$$

Accordingly the total differential of enthalpy is;⁶

$$dH = \left(\frac{\partial H}{\partial p}\right)_{T, \xi} dp + \left(\frac{\partial H}{\partial T}\right)_{p, \xi} dT + \left(\frac{\partial H}{\partial \xi}\right)_{p, T} d\xi \dots\dots\dots(3.5)$$

Calorimetrically, the measured differential heat is;

$$dQ_m = \left[\left(\frac{\partial H}{\partial p}\right) - v\right]_{T, \xi} dp + \left(\frac{\partial H}{\partial T}\right)_{p, \xi} dT + \left(\frac{\partial H}{\partial \xi}\right)_{p, T} d\xi + \sum_i dE_i \dots\dots\dots(3.6)$$

The differentiation of equation 3.6 yields equation 3.7 for heat flow rate provided that the ideal condition is offered ($p \approx 0$ and $\sum_i dE_i \approx 0$).⁶

$$\frac{dQ_m}{dt} = C_{p, \xi}(T) \frac{dT}{dt} + \left(\frac{\partial H}{\partial \xi}\right)_{p, T} \frac{dH}{d\xi} \dots\dots\dots(3.7)$$

The kinetic evaluation of DSC curves are based on equation 3.7 from which the heat capacity C_p could be obtained by plotting dQ_m/dt against dT/dt , providing that the mass of the sample is known and the experiment proceeds under the constant pressure. This principle has been based in the data below for heat capacity calculations and determination of phase transitions.

3.2.2 Phase behavior of DESs

While some data exists in the literature on the phase behaviour of DESs it only exists for a limited compositional range and was in general determined using a melting point apparatus. In this section differential scanning calorimetry will be used across the full compositional range and the phase behaviour is compared to the strength of the hydrogen bonding existing between the two components.

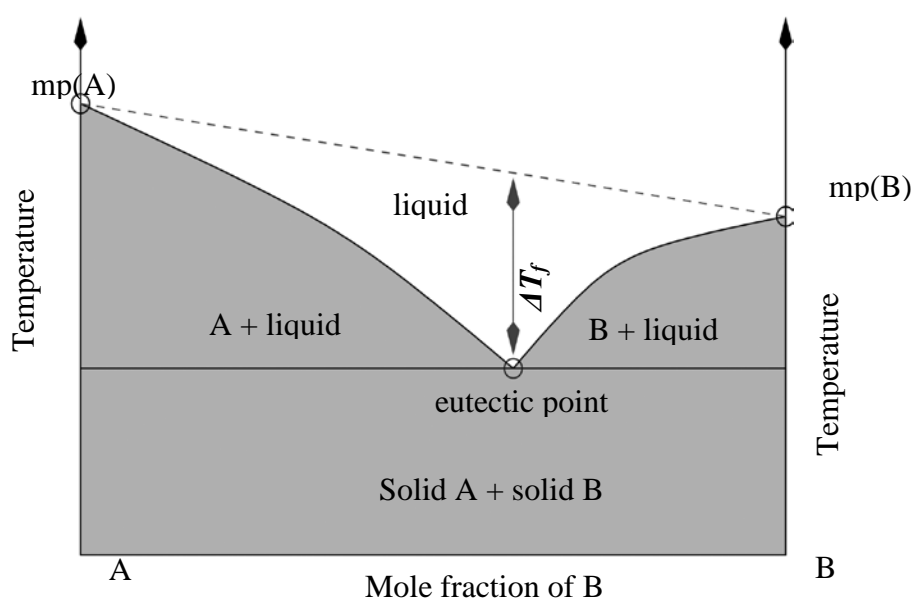


Figure 3-1: Schematic representation of a two component phase diagram ⁴.

The molar composition at which a mixture has the lowest freezing point is termed the eutectic composition as shown in Figure 3-1. The depression of freezing point ΔT_f is the difference in freezing point between ideal and eutectic freezing points of a mixture.

For mono-functional hydrogen bond donors the eutectic composition is made by mixing 1ChCl and 2 hydrogen bond donors (for this study; glycerol, ethylene glycol

and urea) however, for di-functional hydrogen bond donors e.g. oxalic acid the eutectic point occurs at a 1:1 mole ratio. It has been suggested that the formation of eutectic mixtures is based on hydrogen bonding interactions between hydrogen bond donors and chloride ion.¹³⁻¹⁸.

Figure 3-2 shows the phase diagram for ChCl and urea determined using DSC as a function of mole fraction of urea. The data are relatively similar to those previously reported but over a wider compositional range. It contains data for compositions of 10 to 50 mol% urea which have not been previously reported and these data show a much shallower freezing point curve than previously expected.

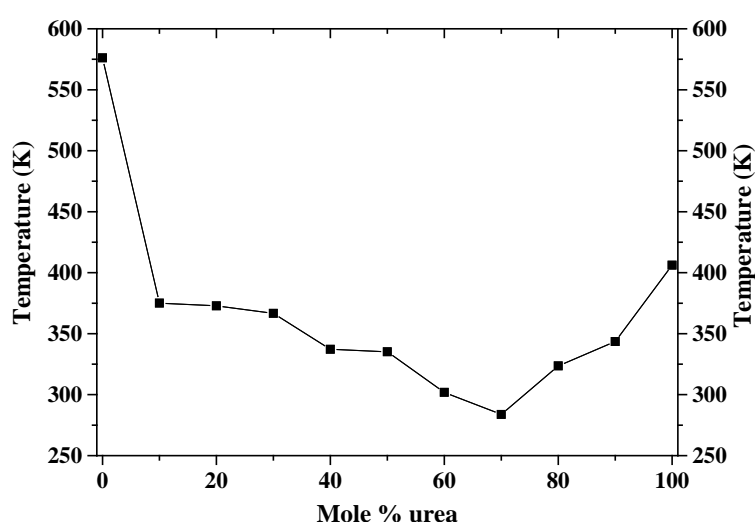


Figure 3-2: Phase diagram of urea/ ChCl as a function of mole composition.

Type III DESs are made between ChCl and hydrogen bond donors. In this study the hydrogen bond donors were glycerol, ethylene glycol, urea and oxalic acid. For these systems it was confirmed that all had a eutectic point a 1ChCl: 2HBD except oxalic acid where the eutectic occurred at 1ChCl: 1HBD. The depressing of freezing point in mixtures of ChCl with these materials are shown in Table 3-1 and agree closely with those already presented in the literature.¹⁹

Table 3-1: Freezing point data for the 4 liquids used in this study.

Temperature (K)	Ethaline	Glyceline	Reline	Oxaline
T^* (HBD)	260	291	406	375
$T_{eutectic}$	212	238	285	255
ΔT_f	97	102	125	145

In principle the depression of freezing point should be related to the deviation from ideality of the mixture i.e the greater the interaction between ChCl and the hydrogen bond donor the larger should be the depression of freezing point. The hydrogen bond donating parameter, α , has previously been determined for three of the liquids. The α -values for Reline were found to be 0.922, Glyceline was 0.937 and Ethaline was 0.903. But this is only an empirical measure of the hydrogen bonding ability.

The depression of freezing point can be estimated using Blagden's Law:

$$\Delta T_f = K_f b I \dots\dots\dots(3.8)^{20}$$

Where, K_f , is the cryoscopic constant, which depends on the solvent properties but not the solute. b is the molality and i is the Van 't Hoff factor which is the number of ion particles per solute molecule e.g. for ChCl $i = 2$. This approach is only valid for dilute solutions. An alternative approach has been proposed by Ge and Wang.^{21, 22}

$$\Delta T_f = \frac{\Delta H - 2RT^* \ln a - \sqrt{2\Delta C_p RT^{*2} \ln a + \Delta H^2}}{2\left(\frac{\Delta H}{T^*} + \frac{\Delta C_p}{2} - R \ln a\right)} \dots\dots\dots(3.9)$$

where, T^* is the normal freezing point of the pure component a is the activity of the eutectic mixture, ΔH is the enthalpy change of interaction between the two components and ΔC_p is the differences in heat capacity between the liquid and solid phases at T_f . This approach cannot be used exactly for the liquids studied here as the activity of the solution is unknown. It can however be seen that the depression of freezing point will be related to the enthalpy of interaction between the two components. In the next section this enthalpy of interaction will be determined calorimetrically and compared to the depression of freezing point of the mixtures.

3.2.3 Heat capacity of liquids

Heat capacity of a fluid is the amount of heat required to raise the temperature by 1 K and it can be expressed in molar or mass terms.^{23, 24} For the liquid to be applicable as a lubricant or as a heat transfer fluid, it is important to evaluate its heat capacity as it has to be able to remove heat from a system.²⁵⁻²⁸

Determination of heat capacity is necessary for a liquid as a lubricant because it indirectly influences fluid rheology especially when the temperature changes and it influences elasto-hydrodynamic lubrication. Additionally, knowledge of heat capacity is important for heat transfer fluids in order to estimate a critical heat storing capacity in applications such as solar power systems.^{26, 29-32} The reason is that the efficiency of heat transfer of the liquid depends on its capability to remove as much heat as possible for a specific quantity of liquid.³³

Figure 3-3 shows the specific heat capacity for a number of type III DESs and mineral base oil. The values for all liquids are relatively similar (1.95-2.2 J/g.K) at 298 K. The higher the specific heat capacity the better the fluid is at dissipating heat from the lubricated surface. However, when the temperature is increased this behavior changes and the heat capacity of the DESs increases more significantly than the mineral oil.

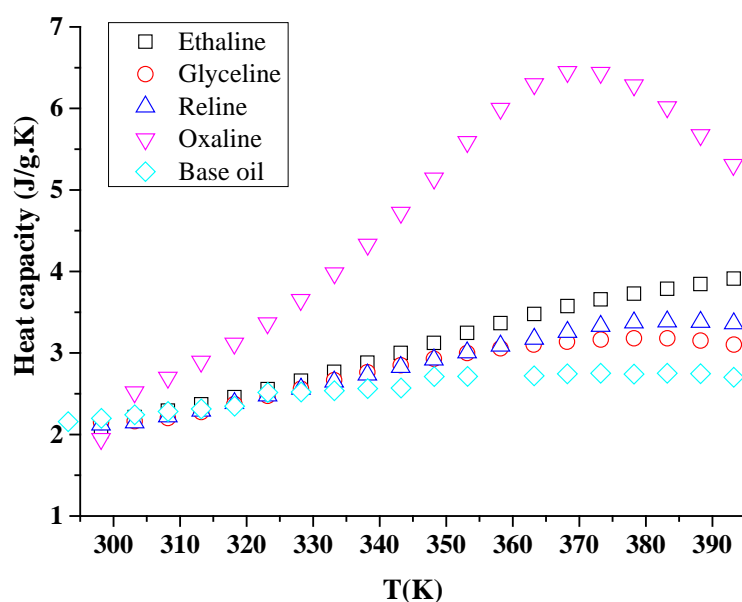


Figure 3-3 : Specific heat capacity of DESs and mineral base oil as a function of temperature.

This may be related to the existence of different cohesive forces among molecules in these liquids since the main factors influencing heat capacity of liquids are rotational, vibrational and translational energy storing modes within the molecule and these modes are influenced greatly by the coulombic interactions and hydrogen bonding.^{23-25, 34} Therefore, since the value of specific heat capacity of DESs increases

more than mineral base oil when the liquids are heated it is probable that hydrogen bonding or coulombic interactions significantly influence the heat capacity.²⁴

The unusual behavior of Oxaline in Figure 3.3 is thought to be due to two factors. Firstly, as DESs are hygroscopic materials it is not possible to obtain totally dry liquids even with a very careful preparation therefore; some water will be associated with them. As a consequence aluminum and aluminum oxide when present together react with water within a wide range of alkali and acid pH ($2 < \text{pH} < 11$) and the rate of reaction increases as the temperature increases from 283- 363 K.³⁵ As shown in Figure 3.3 the increase of heat capacity for Oxaline is different from other liquids with a maximum close to the boiling point of water. This is probably due to the pan reacting with the oxalic acid forming non- passive film of Al_2O_3 .³⁵



Figure 3-4 shows nickel, iron and aluminum plates in which they corroded in Oxaline for long time. Oxidation products of aluminum is unlike iron and nickel form a suspension in the liquid rather than a solid sheet which mean the oxidation products of aluminum are not passivating in low pH medium which supports the phenomenon of instability of aluminum passive films in Oxaline.

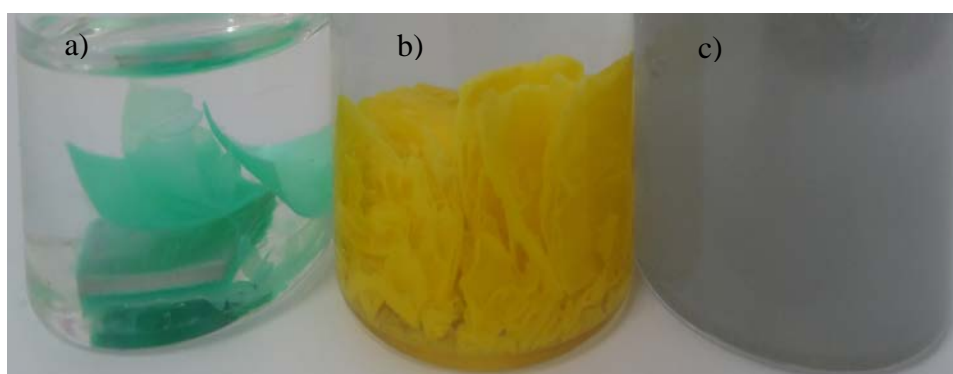


Figure 3-4: Behavior of passive film on a) nickel, b) iron and c) aluminum in Oxaline.

Secondly, the unusual change in heat capacity could be due to partly the corrosion reaction being accelerated by temperature, consequently the amount of heat transferred to the sample is much more than the heat needed to heat up the liquid.

The heat capacity of most mineral base oils is about half that of water at 373 K.²³ Likewise, polar synthetic hydrocarbons have heat capacities that are about 10% higher than most pure hydrocarbons.²⁴ In a number of industrial applications the heat capacity of liquids can be improved by the inclusion of additives to increase heat absorption and improve heat transfer.^{32, 36, 37} For example silica, graphite, CuO and Al₂O₃ nanoparticles with different particle sizes (1-100 nm) have been used widely with base oil, poly-alpha-olefins, eutectic mixtures of alkali metal carbonates and chlorides, ethylene glycol and water to improve their heat capacity and thermal conductivities.^{33, 37-41}

3.2.4 Enthalpy of formation of DESs

The depression of freezing point observed when a eutectic forms is related to the Enthalpy of interaction occurring between the two components in the mixture. It is therefore important to know the extent the enthalpy changed when ChCl and hydrogen bond donors are mixed to obtain different DESs.

Direct measurement of the enthalpy of interaction between the HBD and ChCl may be difficult but calorimetric data can be used together with a Hess cycle to calculate a value.⁴² Hydrogen bonds are a good method of storing energy and these tend to increase the heat capacity of a liquid.^{23, 25, 26, 34} This increase in heat capacity can be calculated by measuring the heat capacity of the eutectic mixture and subtracting that for the two pure components. So for Reline the heat capacity of the hydrogen bond C_p (HB)

$$C_p \text{ (HB)} = C_p \text{ (Reline)} - (C_p \text{ (ChCl)} + C_p \text{ (urea)}) \dots\dots\dots(3.11)$$

Accordingly the enthalpy of hydrogen bonding in these liquids is given by equation 3.12.⁴²

$$\Delta H = C_p \Delta T \dots\dots\dots(3.12)$$

By measuring the C_p data and using equations 3.11 and 3.12 the enthalpy of formation of the DESs and accordingly the enthalpy of hydrogen bonding could be determined. These data are listed in Table 3-2.

Table 3-2: ΔfH^0 data of some DES as a function of temperature.

Temperature	Enthalpy change (kJ mol ⁻¹)			
(K)	Ethaline	Glyceline	Reline	Oxaline
303	10.70	5.08	17.10	35.95
308	12.06	5.61	16.97	42.39
313	13.55	7.44	8.04	49.60
ΔT_f	97	102	125	145

As shown in Table 3-2 the change in enthalpy could be attributed to the formation of hydrogen bonding when ChCl is mixed with different hydrogen bond donors since the energy change in the process typical of what would be expected for hydrogen bonding formation.^{18, 43} Table 3-2 also shows that the enthalpy of hydrogen bond formation appears to correlate with the depression of freezing point observed in Section 3.2.1. This shows that HBDs with the strongest hydrogen bonding ability show the largest depression of freezing point they also correlate with the heat capacities of the liquids.

3.2.5 Thermal stability

The thermal stability of a lubricant is the resistance to either molecular rearrangement or molecular breakdown at high temperatures in the absence of air.²³ For simple organic compounds when the temperature is raised the vibrational energy of bonds rises until the vibrational energy become similar to the bond strength and bond rupture can take place. For more complex organic compounds with more than one type of chemical bonds, the weakest bond will determine the thermal stability.^{44, 45}

In general the bond strength is inversely proportional to the bond length which is related to resonance and hybridizations.⁴⁴ Therefore, liquids such as mineral base oils with a considerable fraction of C–C single bonds as the weakest point for failure display a thermal stability in the range of (616 to 644 K). Synthetic polymerized hydrocarbons formed by oligomerization or polymerization followed by hydrogenation used as VI improvers they have similar general structure as smaller molecules in mineral base oil, are 28 K or more lower thermal stable than mineral base oil.^{23, 24}

Hydrocarbons with aromatic moieties such as poly (phenyl ethers), chlorinated biphenyls and condensed aromatic rings such as alkylated naphthalene display higher thermal stability (727 to 755 K) than mineral base oils. However, esters of organic acids are less thermally stable (530 to 590 K) due to weaker bonds within the ester functional groups. Moreover, methyl esters have similar thermal stability to mineral base oils. Generally, polymers used as viscosity index modifiers tend to have thermal stabilities lower than smaller molecules having the similar general structure. Finally, lubrication improver additives are less thermal stability than mineral base oils for example, zinc dialkyldithiophosphates degrade between (477 and 533 K), while poly(methacrylate) decomposes at 505 K and polybutenes degraded at around 561 K.^{23, 24}

Figure 3-5 shows the thermal stability of some DESs compared with mineral base oil. When DESs are heated beyond the boiling point of water most DESs show a decrease in mass due to a loss of water.⁴⁶ Therefore, DESs are thermally less stable than mineral base oil due in part to the presence of some water.⁴⁷

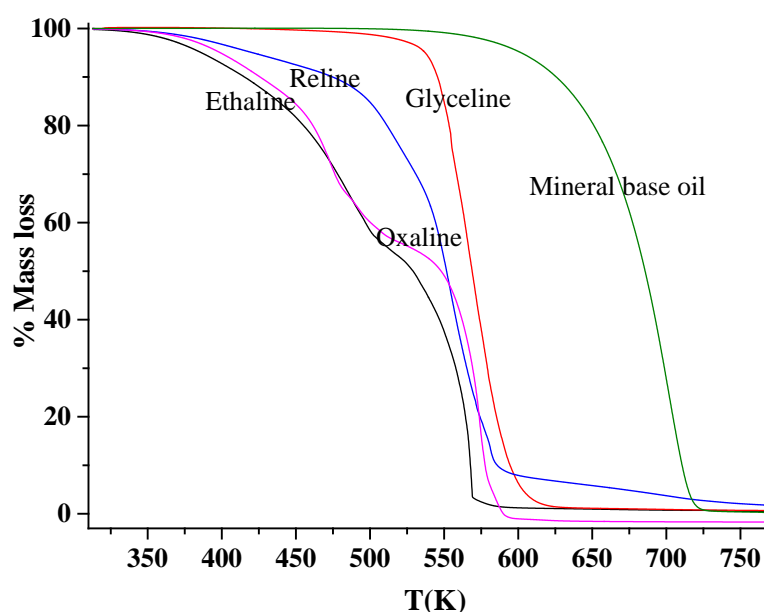
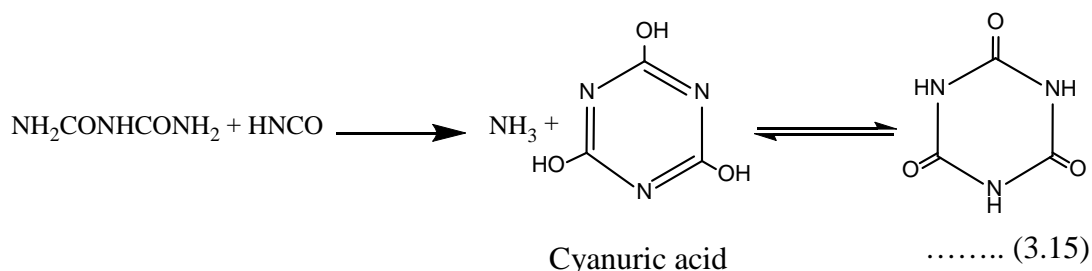
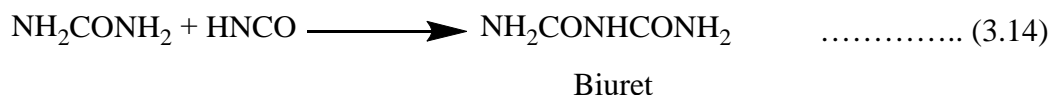
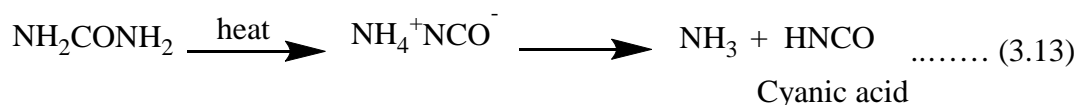


Figure 3-5: Thermal stability of DESs and mineral base oil.

For Reline the change in mass can be attributed to the decomposition of urea as a result of heating it above its melting point. The possible decomposition products are thought to be cyanic acid which reacts with urea to give biuret at 433 K (b.p. 458-463 K) or oligomerises to produce cyanuric acid (1,3,5-triazine-2,4,6-triol) a stable

compound up to 773 K as shown in chemical reactions 3.13 - 3.15.^{48, 49} Therefore, after 573 K the mass of Reline does not go to zero as is the case with the other liquids.



In the case of Oxaline it has been shown that the main decomposition products of oxalic acid are formic acid and carbon dioxide⁵⁰ when Oxaline is heated over about 400 K. However, from the change in mass as a function of temperature, the oxalic acid in Oxaline may sublime followed by decomposition above 423 K so the mass change is more gradual. All of the TG curves show significant loss at around 573 K where ChCl starts to decomposes.⁵¹

Glyceline resists degradation until higher temperatures than the other DESs because glycerol is more thermally stable. For Ethaline after breakdown of hydrogen bonding at about 370 K, ethylene glycol start to evaporate as shown in Figure 3-5 so a sharp decrease in mass is observed over a narrow temperature range. The remaining mass is ChCl which begins to decompose at about 575 K. When mineral base oil thermally breaks down it releases a considerable amount of methane with lesser amounts of ethane and some ethylene.^{23, 24}

3.3 Physical properties

The thermal and thermo-physical properties of lubricants are important for their successful application. The most pertinent properties include viscosity and viscosity index, surface tension, density and conductivity.⁵²⁻⁵⁴ The presence of impurities can lead to considerable changes in its properties; therefore a proper procedure should be

employed to prepare DESs or ILs as they are very sensitive to the presence of impurities such as water, chloride ion and organic solvents.²⁶

3.3.1 Viscosity of ILs

Viscosity is considered as one of the most important properties for a lubricant. While the high viscosity of ionic liquids is undesirable for many applications it plays a favourable role as in the case of lubrication.⁵² The viscosity of liquids are influenced greatly by the strength of Van Der Waals forces and hydrogen bonds therefore, high viscosity of ILs and DESs are due to the strong affinity among their component ions/molecules as a result of hydrogen bonding and Coulombic forces.¹⁵ Consequently the movement of ions or molecules becomes easier at higher temperature and thus the viscosity will be reduced. The change in viscosity with temperature is often described by equation 3.16 which is similar to Arrhenius law.^{55, 56}

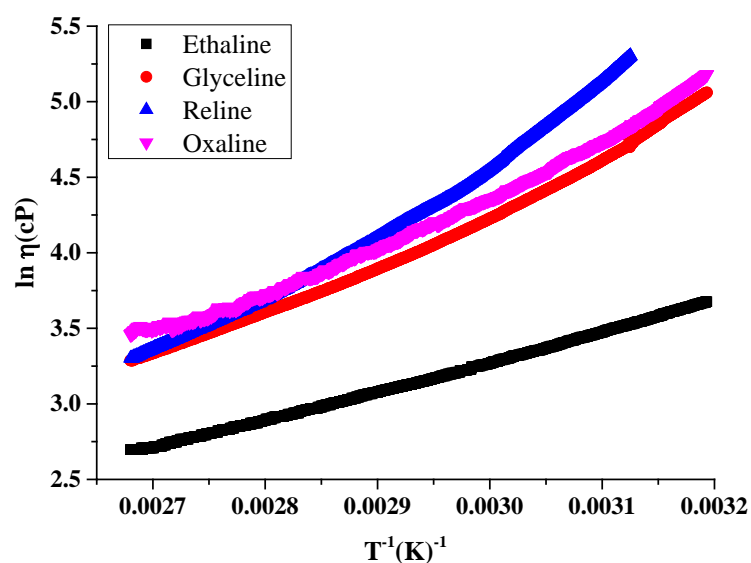


Figure 3-6: Plot of \ln viscosity vs $1/T$ for different DESs.

$$\ln \eta = \ln \eta_o + \frac{E_\eta}{RT} \quad \dots\dots\dots(3.16)$$

Where: E_η is activation energy for viscous movement η is absolute viscosity, T is the absolute temperature, R is the gas constant and η_o is a constant.

Figure 3-6 shows \ln viscosity obtained using a rotating cylinder versus reciprocal temperature for DESs wherein it is possible to calculate viscous flow activation energy. The values of activation energies are 17, 33, 34 and 43 kJ mol⁻¹ for Ethaline, Glyceline, Oxaline and Reline respectively. The values do not correlate solely with the hydrogen bond interaction forces as shown in Table 3-2. It has previously been shown that the flow of ions and molecules in DESs is related to the size of the ions in comparison to the size of the voids as will be discussed later in Table 3-3. In Ethaline the activation energy is lower than the other three DESs which are thought to be due to weaker hydrogen bonding and the larger void volume. Moreover, both Glyceline and Oxaline have similar activation energies. The activation enthalpies for viscous flow do not correlate directly with the enthalpy of hydrogen bonding showing that it is not purely the intermolecular forces that affect the mobility of species in the liquid. Finally, activation energies as studied before for other DESs are directly proportional to the melting point of liquids and the order is in agreement with the order of freezing points as shown later in Table 3-3 in this study.¹³

3.3.1.1 Viscosity measurements using QCM

An alternative method of measuring viscosity is using a high frequency vibrating crystal or wire. A commonly used method is the quartz crystal microbalance (QCM) sensor which is made from a thin AT-cut quartz crystal which is sandwiched between two circular inert electrodes of the same diameter as shown in Figure 3-7. Due to the piezoelectric properties of the quartz crystal, the crystal will oscillate upon application of external potential to the electrodes due to shear deformation of the crystal. The oscillation of the crystal is quite sensitive to mass changes and hence a nano-gram mass change can be detected.⁵⁷⁻⁵⁹ Frequency changes of piezoelectric crystals in response to a solid or liquid deposit is proportional to the ratio of kinetic energies of the exposed crystal and the free crystal.⁶⁰

The relationship between the frequency shift and mass change has been described by Sauerbury who devised equation 3.17 for thin over layer films

$$\Delta f = -\frac{2f_o^2}{p_q v_q} \Delta m = -\frac{f_o}{p_q t_q} \Delta m = -C \Delta m \quad \dots\dots\dots (3.17)^{61}$$

Where; f_o is frequency of free crystal in air

$\rho_q v_q$ is the density and shear wave velocity of quartz crystal

respectively

t_q is the thickness of the quartz crystal and

Δm is the mass added to the crystal

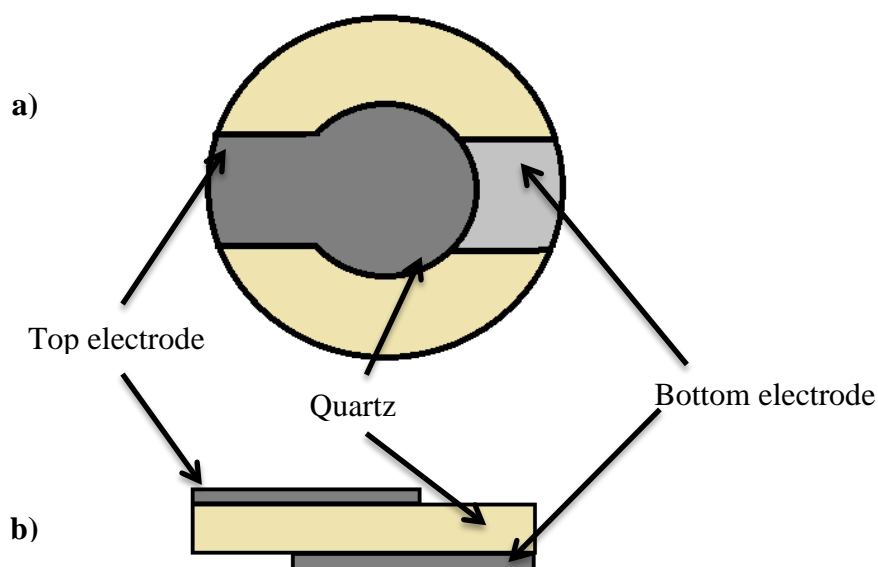


Figure 3-7 : (a) and (b) are top and side view of QCM sensor.⁶²

Exploiting this relationship offers a unique sensitivity (1.1 ng mass change reduces the frequency of a typical crystal by 1 Hz). The technique allows real-time monitoring of what is happening at the electrode-liquid interface which is particularly useful in the course of electrochemical driven processes.⁵⁷

In 1982 it was found that the quartz crystal sensor could be used in liquids as well.⁶³ The use of QCM in liquids is quite useful as a new analytical technique in applications such as monitoring petroleum and lubricant properties, medicine and biotechnology, chemical industry and environment protection.^{61, 62, 64, 65}

The oscillating frequency is sensitive to the contact liquid environment due to a shear motion of crystal and hence a planar-laminar movement which is proportional to the square root of the liquid viscosity and density ($\sqrt{\eta\rho}$).^{57, 66, 67} For instance, shear movement penetrates about 2500 Å in water for a 5 MHz crystal. When the layer close to the quartz crystal thickens the frequency-mass relationship will no longer be linear and the relationship must be modified.⁶⁶

Here the frequency shift is due to energy dissipation by mechanical and electrical boundary conditions in addition to the effects of mass changes. For example, interfacial properties at electrode surface/liquid, density and viscosity of most molecular liquids reduce the oscillating frequency of the crystal by between 3400 and 8000 Hz. The effect of surface roughness can add an additional several kilohertz in comparison to the unloaded crystal frequency. Finally, the effects of pressure and temperature have to be considered in calculations.^{57, 63, 65, 66, 68}

Moreover, when an electrolyte is added to pure solvent it is necessary to include the effects of dielectric constant and conductivity upon the solvent and finally charge, chemistry and roughness of electrode surface are considered as other important factors affecting crystal oscillation.^{58, 59, 61, 63} Therefore, the term thickness-shear mode sensor (TSM) would be more appropriate in liquids instead of QCM⁶⁶. In liquids the relationship between frequency and solution viscosity and density are given by equation 3.18.⁶⁹

$$\Delta f = f_o^{\frac{3}{2}} \sqrt{\left(\frac{\eta p}{\pi \eta_q p_q} \right)} \dots\dots\dots(3.18)$$

Where: η and p are viscosity and density of solvent respectively

For a number of pure solvents the relationship between frequency and $\sqrt{\eta p}$, has been shown to be linear but deviations have been observed for some polymer and salt solutions.⁶⁶

Viscosity measurements made by QCM are presented in Table 3-3 and good agreement is observed between values found with the rotational viscometer at high shear rates showing that QCM is an appropriate method of measuring viscosity.

3.3.1.2 Viscosity index

The viscosity indexes of the DESs and ionic liquids are higher in all cases to the base oil. All four DESs have viscosity indexes which are above the value of the base oil. It should be stressed however, than none of these liquids have additive packages added which would be used in the finished lubricant. Most of the DESs and imidazolium based ionic liquids also have improved freezing points compared to the base oil suggesting improved performance at lower temperatures. The urea based eutectic with choline chloride has too high a freezing point and coupled with the

propensity for urea to break down to form ammonia at high temperatures would probably make it unsuitable for general use.

Table 3-3: Viscosity index data of liquids.

Fluid	Density at 298K /g cm ⁻³	VI		T_f / K
		Rotational viscometer	QCM	
Base oil	0.87	100	91	264
Ethaline	1.12	191	182	212
Glyceline	1.19	147	147	238
Reline	1.20	121	120	285
Oxaline	1.20	144	142	255
C ₂ mim HSO ₄	1.36	130	146	<243
C ₂ mim C ₂ H ₅ SO ₄	1.24	142	173	<243
C ₂ mim SCN	1.11	212	174	223
C ₂ mim CH ₃ COO	1.10	141	141	253

The glycol based liquids are, however better at both high and low temperatures and have high VI values. The benign nature, particularly of glycerol, makes this eutectic an interesting candidate for a marine lubricant because it is totally miscible with water and would disperse if discharged at sea. Since both components are extremely benign they pose negligible threat to aquatic life.⁷⁰ The four imidazolium-based ionic liquids also show high viscosity indexes and thermal properties. They are also miscible with water and C₂mim has been shown to have relatively low toxicity although anions such as SCN are clearly undesirable.⁷¹

3.3.2 Surface Tension

For a number of applications measuring interfacial behaviour of liquids is valued as a core property such as wettability, capability of mass transfer for liquid-liquid or gas-liquid extraction, or in multi-phasic homogeneous catalysis.⁵² Measuring surface tension indirectly is a measure of intrinsic energy between liquid molecules since the surface tension is defined as a measure of cohesion force among liquid

molecules at the surface and it is the quantification of force per unit length. Figure 3-8 shows the surface tension of the 4 liquids listed above as a function of temperature. It can be seen that Glyceline, Oxaline and Reline have high surface tensions which is indicative of the large interactions between the ions and molecules in the liquid.

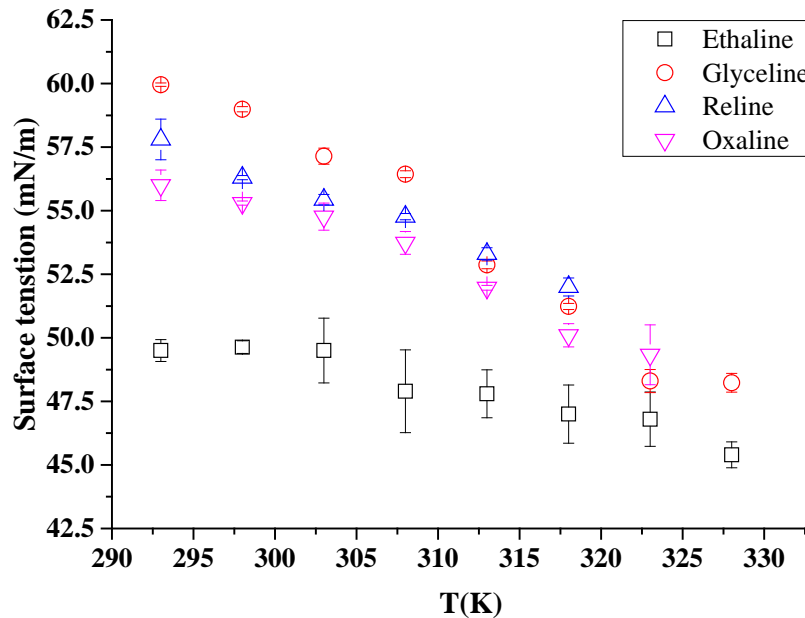


Figure 3-8: Surface tension of some DESs as a function of temperature.

It has previously been shown that the surface tension gives a measure of the interaction between the ions and molecules in a liquid. The surface tension can be related to the average void radius $\langle r \rangle$ by equation (3.19).^{55, 56}

$$4\pi \langle r^2 \rangle = \frac{3.5kT}{\gamma} \quad \text{.....(3.19)}$$

Where, k is Boltzmann constant and T is absolute temperature.

Knowing the size of the voids and the size of the ions it is possible to calculate the probability of finding a hole which is bigger than the ion ($P(r > R_{+/-})$) Equation (3.20). In ionic liquids, the high surface tension and low void size make the probability of finding such a vacancy relatively (10^{-4} - 10^{-7}). It has been shown that there is a good correlation between $P(r > R_{+/-})$ and the viscosity of a fluid.⁵⁵

$$P = 0.602a^{\frac{7}{2}} \left[-\frac{r^5 e^{-ar^2}}{2a} + 2.5 \left\{ \left[-\frac{r^3 e^{-ar^2}}{2a} + \frac{1.5 \left(\frac{r e^{-ar^2}}{2a} + \frac{0.443 \operatorname{erf} \sqrt{ar}}{a^{\frac{3}{2}}} \right)}{a} \right] / a \right\} \right] \quad \text{.....(3.20)}$$

Abbott assumed that a general model should be able to account for the fluidity across the gas liquid phase change and argued that the viscosity of an ideal gas only broke down when applied to non-ideal systems because $P(r > R)$ was not 1 so the ideal gas equation

$$\eta = \frac{m\bar{c}}{\frac{3}{\sqrt{2}}\sigma} \dots\dots\dots(3.21)$$

Where m is the molecular mass (for ionic fluids this was taken as the geometric mean), \bar{c} is the average speed of the molecule ($= (8RT/\pi m)^{1/2}$) and σ is the collision diameter of the molecule ($4\pi R^2$). Could be modified by incorporating the term $P(r > R)$ *i.e.*

$$\eta = \frac{m\bar{c}/2.12\sigma}{P(r > R)} \dots\dots\dots(3.22)$$

The viscosity can therefore be related to the surface tension of the fluid. Using equation 3-19 and the data in Figure 3-8 the average void radius in the liquid can be calculated

Table 3-4: Void radius of some DESs as a function of temperature.

Temperature	Void radius / Å			
/ K	Ethaline	Glyceline	Reline	Oxaline
298	1.52	1.42
303	1.53	1.45	1.44	1.45
308	1.55	1.49	1.46	1.47
313	1.59	1.61	1.48	1.50
318	1.60	1.62	1.51	1.53
323	1.63	1.62	1.55	1.57
328	1.64	1.62

Comparing the data in Figure 3-6 and Table 3-1 it can be seen that the differences in viscosity can be correlated to the differences in their void sizes in the liquids. As shown in Figure 3-1 Reline has the highest surface tension among the liquids and therefore the smallest hole radius thus the ions are least able to move.

3.3.3 Conductivity

Ionic conductivity is an important parameter for understanding the mobility of species in ionic fluids. Despite the high ionic concentration ILs and DESs tend to have relatively low conductivities due primarily to the high viscosity of the liquids.⁷² In aqueous solutions the conductivity is related to the number of charge carrying species as well as their ability to move. Abbott argued that since the viscosity of an ionic liquid was limited by the availability of holes then conductivity can be considered as the migration of voids in the opposite direction to that of the ions.⁵⁶ Since the probability of finding suitably sized voids in ionic liquids at ambient temperature is very low (10^{-6} - 10^{-7}) the voids are essentially at infinite dilution. This is the same as would be experienced in an aqueous electrolyte solution at infinite ion dilution and so the migration of charge carriers (either voids or ions) can be described by the Stokes-Einstein equation

$$\lambda_+ = z^2 F e / 6 \pi \eta R_+ \dots\dots\dots(3.23)$$

Where z is the charge on the ion, F is the Faraday constant and e is the electronic charge.

Many groups have empirically observed that the molar conductivity of an ionic liquid is inversely proportional to the viscosity of a fluid and have invoked the Walden rule which states that for a given electrolyte⁵

$$\Lambda_m^0 \eta^0 = \text{constant} \dots\dots\dots(3.24)$$

They have however forgotten that this is only valid at infinite dilution for a given electrolyte. The rule is clearly a result of equation 3.23, If the holes are at infinite dilution and the hole sizes are relatively similar (which Table 3-4 shows is a valid assumption for DESs) then the reason behind the linear relationship between η^{-1} and Λ_m becomes apparent.

Figure 3-9 shows the conductivity of ChCl in ethylene glycol as a function of composition. Initially there is an increase in conductivity with composition of ChCl as more charge carriers are added to the system. When the ChCl composition exceeds 20 mol% the conductivity decreases due presumably to mass transport limitations arising as the hole size decreases and the fluid becomes more viscous.

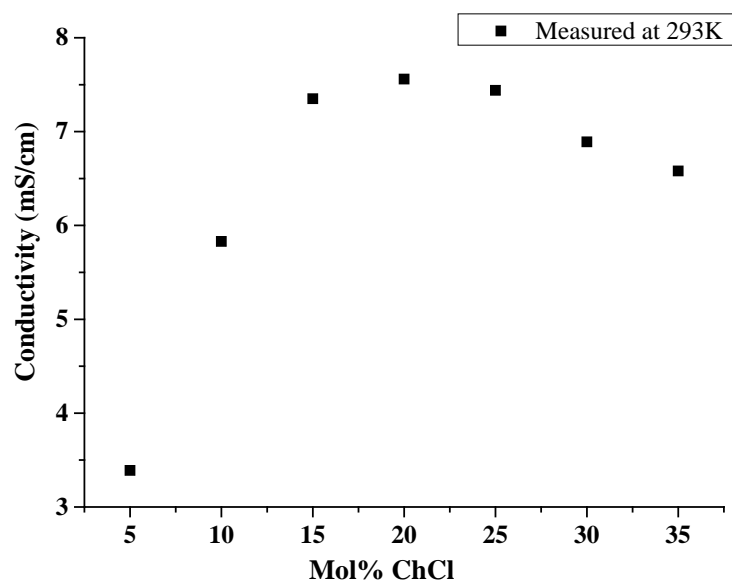


Figure 3-9 : molar % composition of ChCl in ethylene glycol versus conductivity at 293K.⁷³

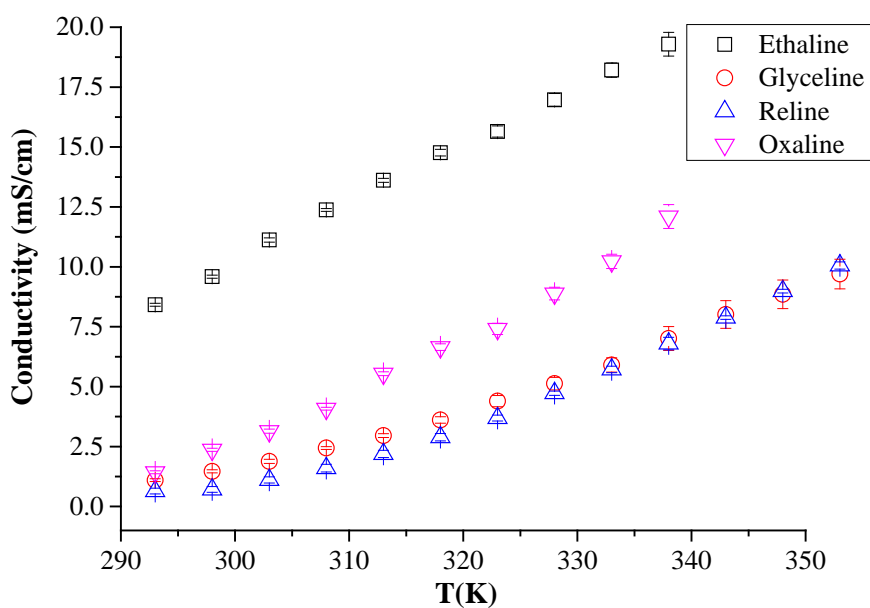


Figure 3-10 : Conductivity versus temperature of different DESs.

Figure 3-10 shows the conductivity of the eutectic compositions of Ethaline, Glyceline, Reline and Oxaline as a function of temperature and it can be seen that for Ethaline the relationship is roughly linear whereas the other fluids show a non-linear increase in conductivity.

To analyse this data in more depth it is better to use the molar conductivity and this allows for differences in concentration. To determine this, the densities of the fluids were measured and these data are shown in Figure 3-12. It is notable that the density of Ethaline is considerably lower than the other 3 liquids.

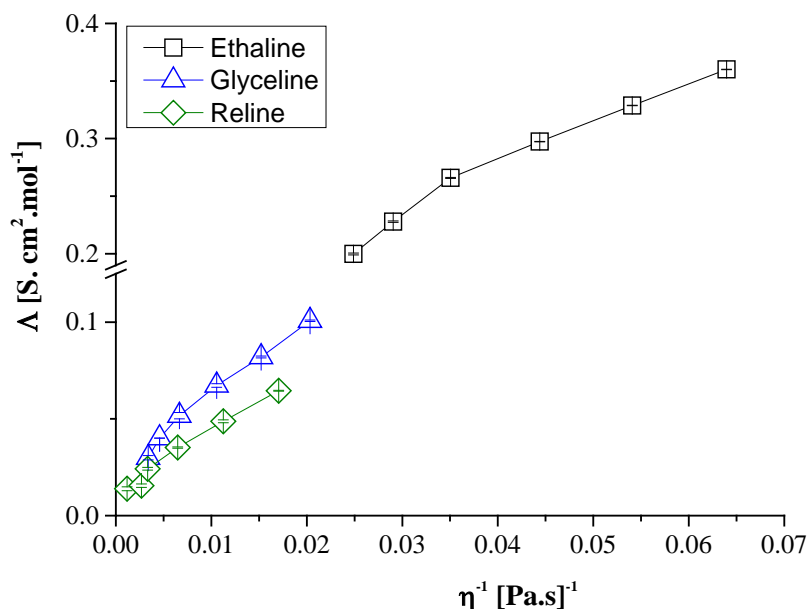


Figure 3-11: Plot of molar conductivity versus fluidity of Ethaline, Reline and Glyceline as a function of temperature.

Direct comparison of Ethaline and Reline is useful as they have the same molar mass and the higher density of Reline must result from the higher packing density of the fluids. This in turn is related to the stronger hydrogen bonds in Reline. The data in Figure 3-11 reflect the surface tension data in Figure 3-8: Ethaline has a low surface tension and therefore has a larger void volume and a lower density.

Plots of molar conductivity vs fluidity can also be useful in analysing the mobile species in mixtures of DESs with water. Figure 3-11 shows a plot of molar conductivity of Ethaline, Reline and Glyceline versus fluidity as a function of temperature. The plot shows a roughly linear relationship. Variability of a relationship at low molar conductivity values for Reline could be due to the liquids being super-cooled and having non-Newtonian behaviour.

3.3.4 Density

The change in density as a function of temperature for DESs and mineral base oil are shown in Figure 3-12. Due to the fact that the mineral base oil is a mixture of different hydrocarbons therefore, the possible cohesive force is thought to be only Van Der Waals which in comparison with hydrogen bonding and dipole-dipole interactions is the weakest.²⁴ However, type III DESs are made from a mixture of ionic molecules or ionic/neutral molecules therefore, the intermolecular forces mostly is hydrogen bonding⁴ this in addition of Coulombic interactions. This difference is more observable from the figure in which the change in density of mineral oil is more significant in comparison with the change in DESs.

When oil is heated the heating energy is mostly consumed in the way of molecular fluctuation without consuming energy which needed for breaking cohesive forces among molecules therefore, the change in density is considerable.

When the void radius was calculated according to equation 3.19 for mineral base oil and compared with the DESs at 298 K and 333 K, there will be a significant difference between their calculated void radius because for mineral oil the void radius are 1.94 Å at 298 K and 2.12 Å at 333 K.

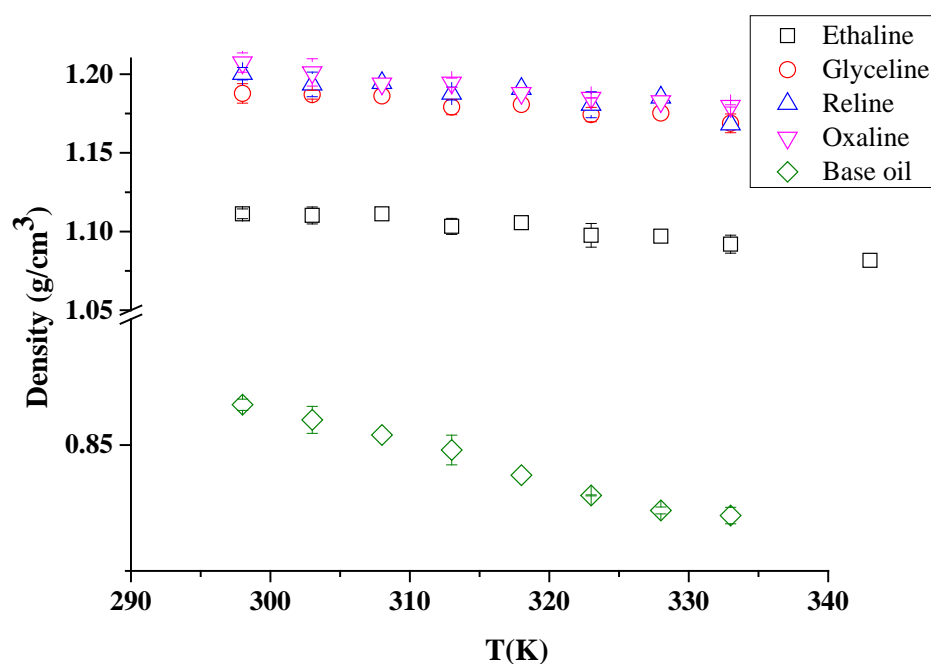


Figure 3-12 : Density of different DESs and mineral base oil versus temperature.

However for Ethaline the void radius is 1.53 Å at 298 K and 1.67 Å at 333 K. Thus the change in void radius is similar for both liquids at about 9.2 %. Therefore, it is thought due to the existing of stronger cohesive forces in DESs makes these liquids to withstand for more heat for molecules to gain enough energy to become free and their viscosity change with temperature is low. However, for mineral oil the temperature raise only makes the long chain molecules expand more and their contribution in viscosity will be higher which possibly explains why in mineral oil has a high viscosity index despite having weak intermolecular forces.⁷⁴

3.4 Rheological properties

3.4.1 Flow characteristics of liquids

Flow characteristics of fluids are classified into two classes dependent on their viscosities. When the viscosity of a fluid is unaffected by changes in the shear rate (flow velocity) the fluids are called Newtonian fluids. Figure 3-13 which shows the typical relation between shear stress (resistance to flow) and shear rate, for these fluids. Some examples of these types of liquids are water, glycerol, liquid honey and olive oil.

On the other hand, liquids where the viscosity changes with a change in shear rate are called non-Newtonian fluids. Some systems have a complex composition which makes their viscosity strongly shear rate dependent. Some examples of non-Newtonian fluids include; waxy crude oil at low temperatures, body fluids, polymeric solutions, creams, paints, and printing ink.⁷⁵⁻⁷⁸

To investigate non-Newtonian behaviour of liquids, it is necessary to quantify its viscosity over a wide range of shear rates. There are several methods to determine the viscosity of liquids but the two most commonly used are rotating viscometers (dragging flow style) and capillary viscometers (pressure driving style).^{75, 76}

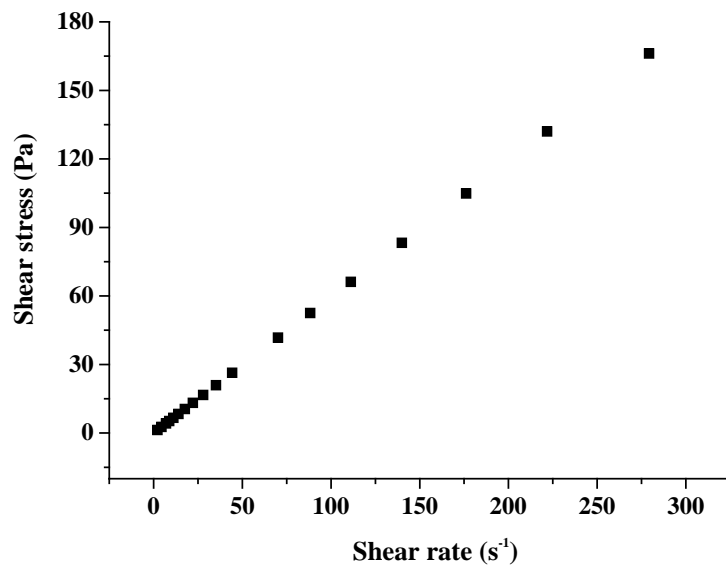


Figure 3-13: An example of Newtonian behaviour of liquids⁷⁹

Despite the fact that capillary viscometers are easy to use, relatively inexpensive, and applicable to most Newtonian liquids, rotational viscometers are preferred for the measuring the behaviour of non-Newtonian liquids as they provide more comprehensive rheological data.^{75, 76, 80, 81}

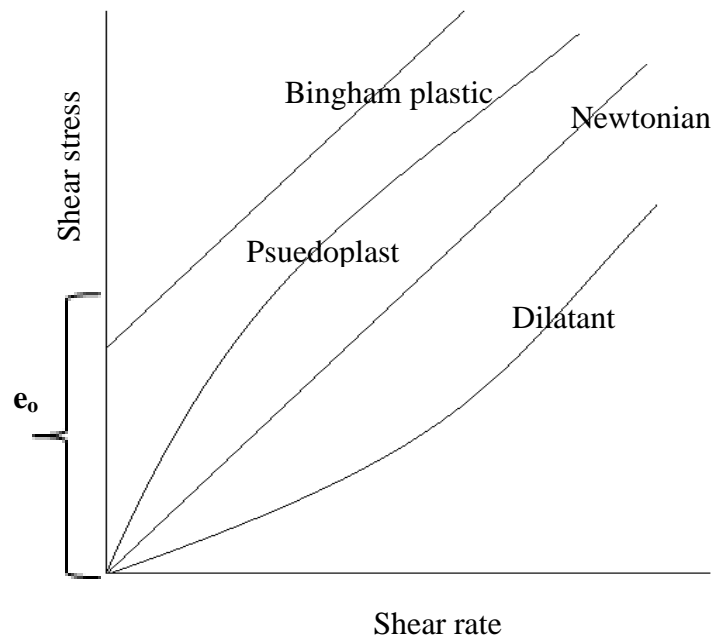


Figure 3-14 : The behaviour of Newtonian and non-Newtonian fluids.^{76, 77}

There are time dependant and independent non-Newtonian liquids. Time independent fluids are categorized as shear thickening (dilatant), shear thinning

(pseudo-plastic) and Bingham plastic types and their flow behaviours are shown in Figure 3-14.^{76, 77} When the viscosity of a liquid increases with increasing shear rate it is termed to be shear thickening, if the viscosity of liquid is decrease with increasing shear rate the liquid classified as shear thinning. However, for some liquids some pressure is necessary before any flow is made (the yield stress) and liquids with this behaviour are termed Bingham plastic liquids. Here the viscosity decreases when the shear rate exceeds 200 s^{-1} .

3.4.2 Flow characteristics of DESs

While the viscosity of DESs has been reported^{13, 15, 16, 82, 83} their Newtonian or non-Newtonian behaviour has not been previously studied. Figure 3-15 shows the viscosity of some types III DESs as a function of shear rate. It can be seen that Ethaline, Glyceline and mineral base oil have a roughly constant viscosity at different shear rates showing that they are approximately Newtonian at 313K. This is probably because the hydrogen bonding between the HBD and chloride anion is considerably weaker than that formed with urea or oxalic acid.

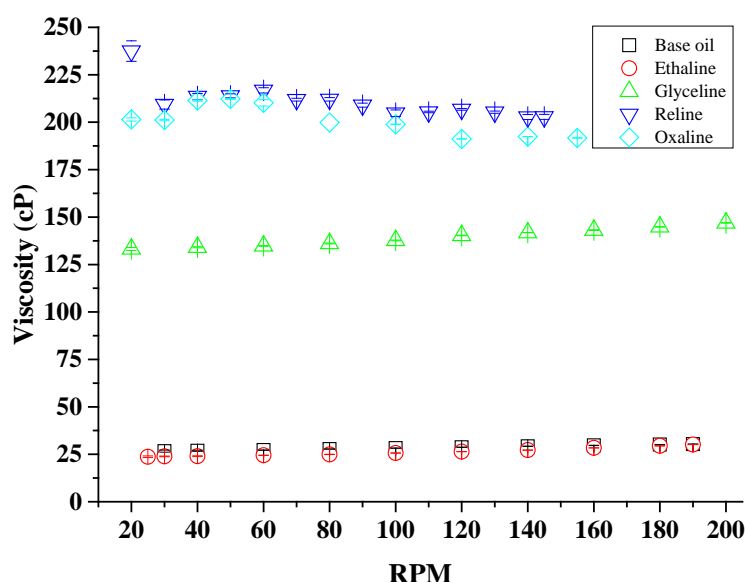


Figure 3-15: Viscosity of DESs as a function of shear rate at 313 K.

In contrast Reline and Oxaline form stronger hydrogen bonds and consequently the viscosity changes more markedly with shear rate. Both liquids decrease their

viscosity with increased rotation rate and so they are shear thinning.⁸⁴ At low shear rates the hydrogen bonds will be more effective at resisting flow and so the viscosity will appear to be higher.

In Oxaline the formation of dimers or long chains dimers of oxalic acid molecules is thought to hinder the mobility even more therefore it may affect the flow behaviour of system and results in non-Newtonian behaviour.⁸⁵ This behaviour has previously been observed using pulsed field gradient NMR spectroscopy for malonic acid.⁸⁶

3.4.2.1 Influence of temperature on flow characteristics

The viscosity of Reline has been measured as a function of shear rate as a function of temperature. Figure 3-16 shows that at low temperatures the viscosity of Reline changes more markedly with shear rate than at high temperatures. Below 323 K Reline has a clear non-Newtonian behaviour. However, above 333 K the viscosity was found to be constant with shear rate showing that it became Newtonian. As above, Newtonian behaviour is observed as the hydrogen interactions break-down.

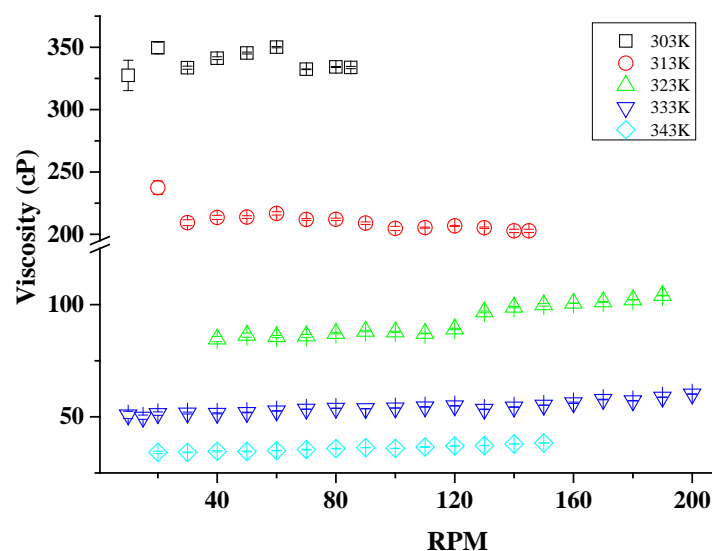


Figure 3-16: Viscosity versus rotation rate for Reline at different temperatures.

3.4.2.2 Influence of water on flow characteristics

The inclusion of water in mineral oils is a significant issue as it leads to a significant change in the properties of the fluid. It is also a major factor affecting

corrosion. In the following section the viscosity of DES-water mixtures is characterized and self-diffusion coefficients were determined to investigate if the mixtures are homogeneous.

Figure 3-17 shows the plot of molar conductivity versus fluidity for eutectic mixtures of Ethaline, Reline and Glyceline as a function of water content. It can be seen that a relatively linear plot is observed for all systems with the exception of Reline at high water content. In all cases the charge carriers should be the same via Ch^+ and Cl^- . In more dilute ionic solutions it would be expected that ionic association would dominate molar conductivity; the linear plot observed in Figure 3-17 suggests viscosity controls charge transport in most systems. As will be shown below, the dilute Reline solution shows evidence of some urea decomposition leading to the formation of NH_4OH which is probably the cause of the increase in molar conductivity at high water content.

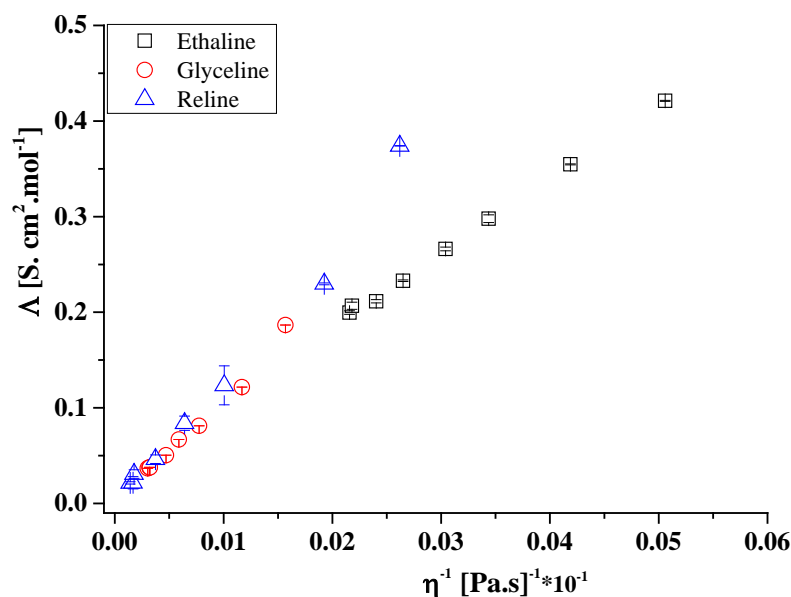


Figure 3-17: Plot of molar conductivity versus fluidity for Ethaline, Glyceline and Reline systems as a function of water content.

The incorporation of water into lubricants is a significant issue as it can change the rheology of the fluid and it significantly affect the corrosion behaviour of metals in

contact with the fluid. The flow characteristics of Reline have been studied in terms of water content and its influence is shown in Figure 3-18.

As shown in Figure 3-18, pure Reline exhibits non-Newtonian behaviour due to complex aggregation as a consequence of complex intermolecular forces among ChCl and urea molecules. With the addition of water the viscosity-shear rate relationship becomes less pronounced but rather than being shear thinning there is a slight shear thickening behaviour at low water contents. When the water content reaches 7.5 wt% the viscosity is unaffected by shear rate. It has been noted previously that DESs are generally unaffected by water contents of up to 5 wt%. As will be shown later there are clear changes which occur in the structure of DESs when water is added.

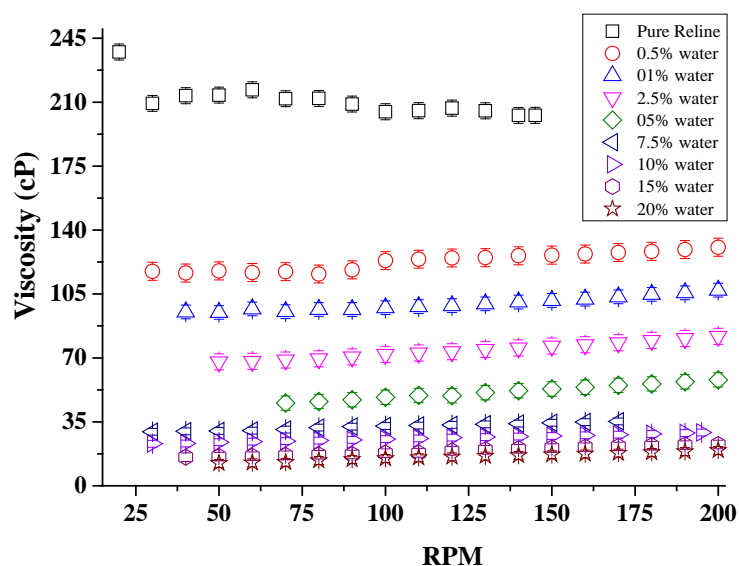


Figure 3-18 : Viscosity versus rotation rate for Reline at 313 K as a function of water content.

3.4.2.3 Diffusion in liquids

Under thermodynamic equilibrium internal thermal energy of species is responsible for random Brownian (or translational) motion in liquids which is defined as self-diffusion.⁸⁷ Mathematically, diffusion has been expressed by Fick's first law of diffusion wherein the flux of species through a given plane is proportional to the gradient of concentration through the plane as shown in equation 3.25.⁸⁸

$$J = -DA \frac{\partial C}{\partial z} \dots\dots\dots(3.25)$$

Where;

A is the area across which diffusion occurs, z the distance J is the flux per unit area; D is diffusion coefficient and $(\frac{\partial C}{\partial z})$ is the concentration difference.⁸⁸ The unit of diffusion constant is (length²/time). The right side of equation has a negative sign indicating the solute is moving toward areas of lower concentration. In above equation there are no considerations for concentration change to happen over time which is very important in the process of diffusion to be counted. In the second Fick's law of diffusion local diffusion flux is correlated to the concentration change over time as shown in equation 3.26.⁸⁸

$$\frac{\partial C}{\partial t} = D(\frac{\partial^2 C}{\partial z^2} + \frac{1}{A} \frac{\partial A}{\partial z} \frac{\partial C}{\partial z} \dots\dots\dots(3.26)$$

The Stokes-Einstein equation^{86, 88, 89} which relates the diffusion coefficient to the species radius and viscosity of medium as shown in equation 3.27.

$$D = \frac{k_B T}{f} = \frac{k_B T}{6\pi\eta R} \dots\dots\dots (3.27)$$

Where k_B is Boltzmann constant, R is the analyte radius and f is frictional force of the solute. In order to understand precise structure characterisation and how mobility of species in DESs and ILs are affecting physical properties in a macroscopic level such as viscosity, freezing point, conductivity, solubility and surface tension it is important to address the mobility of species at molecular levels. Self-diffusion studies provide important knowledge about how the anion or cation interacts with the HBD in DESs.⁸⁶

3.4.2.4 Influence of water on self-diffusivity of DESs

The use of DES in aqueous mixture is of particular significance as aqueous DES mixtures have several practical applications.^{19, 90-92} For example, interactions involving DES, salts and water play an important role when DES are used as extraction media for protein partitioning.⁹¹ Different DESs were shown to have different abilities to extract

and stabilise various proteins. DES plays a key role in determining interactions with the aqueous protein solution, hence affecting the extraction capacity.

Recently⁸⁶, the molecular transport of the HBD and the choline cation (Ch^+) in different pure choline chloride (ChCl) based DES has been investigated. It was found that the structure of the HBD greatly affects the molecular mobility of the whole system; in addition, it was speculated that in the case of Maline, the malonic acid HBD tends to form long chains of dimers which reduces significantly the molecular mobility of the whole system compared to the other DES and leads to a slower diffusivity of malonic acid relative to ChCl , despite its much smaller molecular weight and size. It is therefore clear that, a variety of interactions takes place within such samples, notably ionic interactions and hydrogen bonding interactions which is in agreement with other studies.¹⁸

In principle, if a Stokesian model of diffusion is valid then the diffusion coefficient should be inversely proportional to the viscosity. Self-diffusivity for three DESs (not Oxaline) has been studied using pulsed field gradient nuclear magnetic resonance (PFG-NMR) as a function of water content. The data of self-diffusion have been supplied by Dr D'Agostino at the University of Cambridge. Diffusion coefficient data of Ethaline, Glyceline and Reline are plotted against inverse viscosity as shown in *Figure 3-19*.

Figure 3-19a shows that for the aliphatic protons on choline this behaviour is valid, although there is a slightly different slope for the first three data points (up to 2.5 wt %). In the dry ionic liquids and DESs it has been shown before that diffusion is non-Stokesian and this may be due to the large size of the diffusing species and the lack of suitable spaces for them to diffuse into.⁹³

Application of the Stokes-Einstein equation 3.27 should enable the hydrodynamic radius (R) to be calculated. Figure 3-19a shows also the theoretical line calculated for Ch^+ using Equation (3.27) and assuming the hard sphere radius of 3.29 Å calculated using a Hartree-Fock model and used previously.⁹⁴ It can be seen that the aliphatic protons all give responses very similar to those predicted by the Stokes Einstein equation.

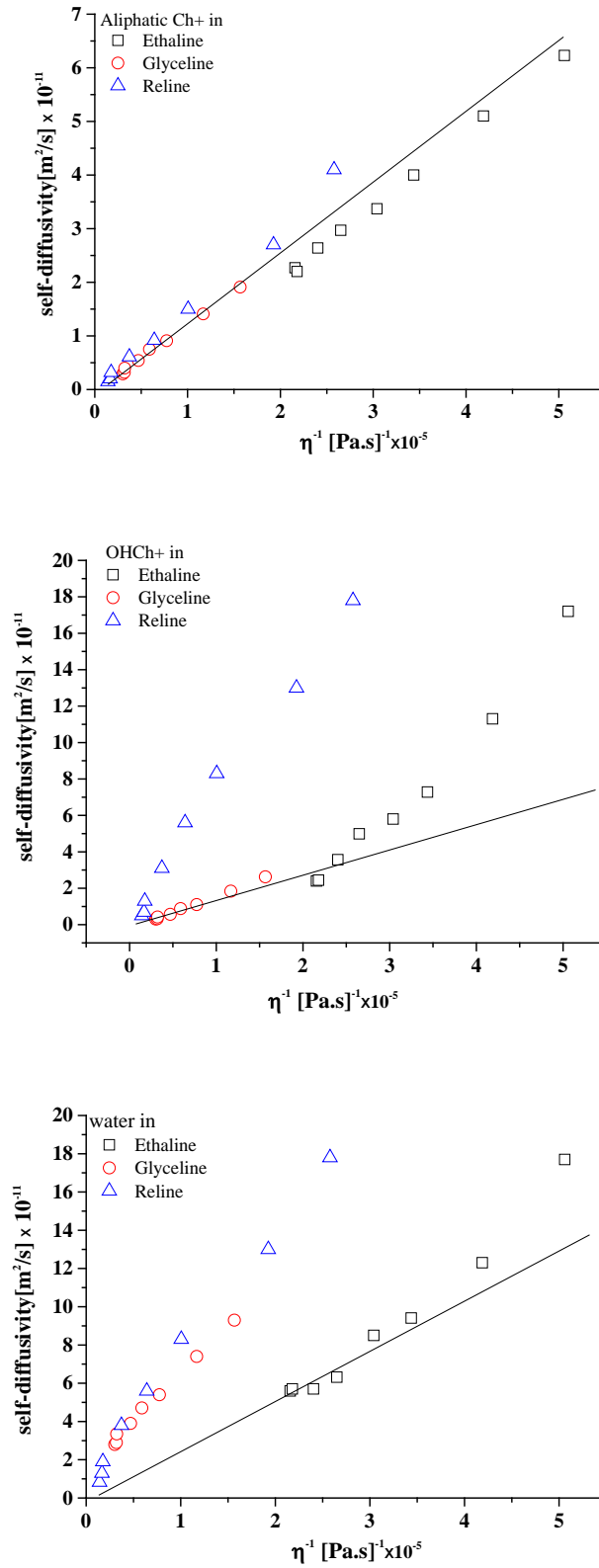


Figure 3-19: Diffusion coefficients as a function of inverse viscosity for a) aliphatic Ch^+ b) OH on Ch^+ and c) water in Ethaline, Glyceline and Reline. Straight lines correspond to ideal Stokesian responses in (a) and (b) for Ch^+ and in (c) for water.

Figure 3-19b shows the response for the OH proton in Ch^+ and it is clear that there is a difference between the behaviour of Glyceline and the other two liquids. At low water concentrations all liquids show a behaviour which is roughly similar to the theoretical slope for Ch^+ but Ethaline and Reline deviate significantly as the water content increases above 2.5 wt% (a 1:1 H_2O : Cl^-). At high water content the diffusion coefficients become similar to those expected for water i.e., at low water content the water associates with the halide anion whereas at higher water contents it acts as essentially free water.

Finally, Figure 3-19c shows the diffusion coefficient for water as a function of fluidity. The responses for Reline and Glyceline are relatively similar and show a high diffusivity for water which is similar in both liquids. The self-diffusion coefficient of pure water is $2.299 \times 10^{-9} \text{ m}^2 \cdot \text{s}^{-1}$ at 25°C .⁹⁵ Using this value and scaling for viscosity produces the solid line seen in Figure 3-19c. It can be seen that the data for Ethaline fit this quite well but the data for Glyceline and Reline are anomalously high. These results are difficult to reconcile if the liquids are homogeneous and it leads to the suggestion that the anomalous behaviour of water/ DES mixtures arise because the water is not homogeneously mixed with the DESs but instead forms separate phases at high water concentrations.

Similar studies have been carried out using hydrophobic ionic liquids. Rollet et al.⁹⁶ used NMR spectroscopy to study water diffusion in 1-n-butyl-3-methylimidazolium bis(triflimide) $[\text{C}_4\text{mim}][(\text{CF}_3\text{SO}_2)_2\text{N}]$ and found diffusion coefficients for water which was 25 times higher than predicted. They concluded that this was due to phase separation at a microscopic scale. This phase separation is one that has been predicted by molecular dynamics simulations and is somewhat unsurprising given the hydrophobicity of the ionic liquids.⁹⁷ The hydrophilicity of DESs might lead to the assumption that aqueous mixtures are homogeneous but these diffusional studies show strongly that microscopic phase separation still occurs. The pH and the ability of water in these mixtures to form separate micro-phases could be responsible for some of the observations in biochemical and mineral processing applications e.g. the stability of enzymes in water DES mixtures.⁹⁸

3.5 Conclusions

The change in viscosity as a function of temperature for DESs are lower than mineral base oil which makes them at least as good at providing a protective film during the operation even at high temperature. With the exception of Reline, all DESs used in this study are shown to be liquid at temperatures below the pour point of most mineral based oils. In terms of their cooling ability Ethaline, Glyceline, and Reline are better than mineral base oil due to their higher heat capacity. From the data of enthalpies of formation it is clear that the hydrogen bonding is responsible for the main intermolecular forces among ChCl and HBDs.

The thermal stability of mineral oil is better than all DESs used in this study. When DESs are heated it is the HBDs that decompose most easily and these limit the thermal stability of the liquid. The conductivity occurs via Ch^+ and Cl^- and the viscosity is the major factor which limits this. Reasonable void radii could be extracted from surface tension-temperature relationships which support the validity of hole theory to describe both conductivity and viscosity in DESs. Finally, the OH proton on Ch^+ does not behave similarly in all liquids. In Glyceline it remains associated when water is added but in Ethaline and Reline is dissociated to some extent.

Molecular liquids do not tend to have good lubricating properties because the intermolecular forces change significantly with temperature. Mineral oils tend to be good lubricants due to the high molecular weight and the change from intra- to intermolecular interactions with temperature (the molecules coil and uncoil when heated). In contrast ionic liquids and DESs have strong interionic and intermolecular forces between them and these are not changed significantly with temperature and so they exhibit high viscosity index values.

3.6 References

1. L. R. Rudnick, *Lubricant Additives: Chemistry and Applications, Second Edition*, Taylor & Francis, 2009.
2. G. E. Totten, *Fuels and Lubricants Handbook*, ASTM international, 2003.
3. S. Glazier, N. Marano and L. Eisen, *J Chem Educ*, 2010, 87, 1336-1341.
4. E. L. Smith, A. P. Abbott and K. S. Ryder, *Chem Rev*, 2014, 114, 11060-11082.
5. J. C. Wedvik, C. McManaman, J. S. Anderson and M. K. Carroll, *J Chem Educ*, 1998, 75, 885-888.
6. G. W. H. Höhne, W. Hemminger and H. J. Flammersheim, *Differential Scanning Calorimetry: An Introduction for Practitioners*, Springer Berlin Heidelberg, 1996.
7. B. P. Woods and T. R. Hoye, *Org Lett*, 2014, 16, 6370-6373.
8. William P. Brennan, Bernard Miller and J. C. Whitwell, *Industrial and engineering chemistry fundamentals*, 1969, 8, 314-318.
9. S. R. Eckhoff and E. B. Bagley, *Anal. Chem.*, 1984, 56, 2868-2870.
10. R. L. Danley, *Thermochim Acta*, 2003, 395, 201-208.
11. M. J. O'Neill, *Anal. Chem.*, 1966, 38, 1331-1336.
12. J. D. Menczel and R. B. Prime, *Thermal Analysis of Polymers: Fundamentals and Applications*, Wiley, 2009.
13. A. P. Abbott, D. Boothby, G. Capper, D. L. Davies and R. K. Rasheed, *Journal of the American Chemical Society*, 2004, 126, 9142-9147.
14. U. B. Patil, A. S. Singh and J. M. Nagarkar, *Rsc Adv*, 2014, 4, 1102-1106.
15. A. P. Abbott, P. M. Cullis, M. J. Gibson, R. C. Harris and E. Raven, *Green Chem*, 2007, 9, 868-872.
16. A. P. Abbott, G. Capper, D. L. Davies, R. K. Rasheed and V. Tambyrajah, *Chem Commun (Camb)*, 2003, DOI: Doi 10.1039/B210714g, 70-71.
17. Shuji Saito, M. Lee and W.-Y. Wen, *Journal of the American Chemical Society*, 1966, 88, 5107-5112.
18. S. L. Perkins, P. Painter and C. M. Colina, *J Chem Eng Data*, 2014, 59, 3652-3662.
19. A. P. Abbott, E. I. Ahmed, R. C. Harris and K. S. Ryder, *Green Chem*, 2014, 16, 4156-4161.

20. P. Atkins and J. de Paula, *Atkins' Physical Chemistry*, OUP Oxford, 2010.
21. X. L. Ge and X. D. Wang, *Ind Eng Chem Res*, 2009, 48, 2229-2235.
22. X. L. Ge and X. D. Wang, *J Solution Chem*, 2009, 38, 1097-1117.
23. E. R. Booser, *CRC Handbook of Lubrication: Theory and Practice of Tribology, Volume II: Theory and Design*, Taylor & Francis, 1983.
24. S. Q. A. Rizvi, *A Comprehensive Review of Lubricant Chemistry, Technology, Selection, and Design*, ASTM International, 2009.
25. C. P. Fredlake, J. M. Crosthwaite, D. G. Hert, S. N. V. K. Aki and J. F. Brennecke, *J Chem Eng Data*, 2004, 49, 954-964.
26. R. Larsson and O. Andersson, *P I Mech Eng J-J Eng*, 2000, 214, 337-342.
27. R. B. Leron and M. H. Li, *Thermochim Acta*, 2012, 530, 52-57.
28. A. Diedrichs and J. Gmehling, *Fluid Phase Equilibr*, 2006, 244, 68-77.
29. J. M. Crosthwaite, M. J. Muldoon, J. K. Dixon, J. L. Anderson and J. F. Brennecke, *J Chem Thermodyn*, 2005, 37, 559-568.
30. M. E. Lepera and G. E. Oswald, *Ind Eng Chem Prod Rd*, 1974, 13, 209-213.
31. M. E. Van Valkenburg, R. L. Vaughn, M. Williams and J. S. Wilkes, *Thermochim Acta*, 2005, 425, 181-188.
32. G. C. G. a. M. M. Judith C. Gomez, presented in part at the Solar PACES Marrakech, Morocco, September 11–14, 2012.
33. N. J. Bridges, A. E. Visser and E. B. Fox, *Energ Fuel*, 2011, 25, 4862-4864.
34. H. C. Hu, A. N. Soriano, R. B. Leron and M. H. Li, *Thermochim Acta*, 2011, 519, 44-49.
35. *USA Pat.*, 6,440,385, , August 27 2002.
36. V. Trisaksri and S. Wongwises, *Renew Sust Energ Rev*, 2007, 11, 512-523.
37. B. Dudda and D. Shin, *Int J Therm Sci*, 2013, 69, 37-42.
38. D. H. Shin and D. Banerjee, *J Heat Trans-T Asme*, 2011, 133.
39. I. C. Nelson, D. Banerjee and R. Ponnappan, *J Thermophys Heat Tr*, 2009, 23, 752-761.
40. S. Q. Zhou and R. Ni, *Appl Phys Lett*, 2008, 92.
41. H. Tiznobaik and D. Shin, *Int J Heat Mass Tran*, 2013, 57, 542-548.
42. H. DeVoe, *Thermodynamics and Chemistry*, Prentice Hall, 2001.
43. J. N. Israelachvili, *Intermolecular and Surface Forces: Revised Third Edition*, Elsevier Science, 2011.

44. Edward S. Blake, William C. Hammann, James W. Edwards, Thomas E. Reichard and M. R. Ort, *J Chem Eng Data*, 1961, 6, 87-98.
45. *USA Pat.*, 1990.
46. J. Zhang, G. A. Lawrance, N. Chau, P. J. Robinson and A. McCluskey, *New J Chem*, 2008, 32, 28-36.
47. N. Meine, F. Benedito and R. Rinaldi, *Green Chem*, 2010, 12, 1711-1714.
48. P. A. Schaber, J. Colson, S. Higgins, D. Thielen, B. Anspach and J. Brauer, *Thermochim Acta*, 2004, 424, 131-142.
49. M. Koebel and M. Elsener, *J Chromatogr A*, 1995, 689, 164-169.
50. Gabriel Lapidus, D. Barton and P. E. Yankwich, *J Phys Chem-U.S.*, 1964, 68, 1863-1865.
51. J. Higgins, X. F. Zhou, R. F. Liu and T. T. S. Huang, *J Phys Chem A*, 1997, 101, 2702-2708.
52. S. Aparicio, M. Atilhan and F. Karadas, *Ind Eng Chem Res*, 2010, 49, 9580-9595.
53. R. B. Leron, A. N. Soriano and M. H. Li, *J Taiwan Inst Chem E*, 2012, 43, 551-557.
54. K. Shahbaz, F. S. Mjalli, M. A. Hashim and I. M. AlNashef, *Fluid Phase Equilibr*, 2012, 319, 48-54.
55. A. P. Abbott, *Chemphyschem*, 2004, 5, 1242-1246.
56. A. P. Abbott, *Chemphyschem*, 2005, 6, 2502-2505.
57. A. R. Hillman, *J Solid State Electr*, 2011, 15, 1647-1660.
58. J. Auge, P. Hauptmann, F. Eichelbaum and S. Rosler, *Sensor Actuat B-Chem*, 1994, 19, 518-522.
59. J. Auge, P. Hauptmann, J. Hartmann, S. Rosler and R. Lucklum, *Sensor Actuat B-Chem*, 1995, 24, 43-48.
60. A. P. M. Glassford, *J Vac Sci Technol*, 1978, 15, 1836-1843.
61. C. G. Marxer, A. C. Coen and L. Schlapbach, *J Colloid Interf Sci*, 2003, 261, 291-298.
62. S. J. Martin, J. J. Spates, K. O. Wessendorf, T. W. Schneider and R. J. Huber, *Anal Chem*, 1997, 69, 2050-2054.
63. T. Nomura and M. Okuhara, *Anal Chim Acta*, 1982, 142, 281-284.
64. M. Rodahl and B. Kasemo, *Sensor Actuat a-Phys*, 1996, 54, 448-456.

65. D. X. Wang, P. Mousavi, P. J. Hauser, W. Oxenham and C. S. Grant, *Colloid Surface A*, 2005, 268, 30-39.
66. C. K. O'Sullivan and G. G. Guilbault, *Biosens Bioelectron*, 1999, 14, 663-670.
67. D. X. Wang, P. Mousavi, P. J. Hauser, W. Oxenham and C. S. Grant, *Ind Eng Chem Res*, 2004, 43, 6638-6646.
68. S. Bruckenstein, M. Michalski, A. Fensore, Z. F. Li and A. R. Hillman, *Anal Chem*, 1994, 66, 1847-1852.
69. K. K. Kanazawa and J. G. Gordon, *Anal Chim Acta*, 1985, 175, 99-105.
70. K. Radosevic, M. C. Bubalo, V. G. Sreck, D. Grgas, T. L. Dragicevic and I. R. Redovnikovic, *Ecotox Environ Safe*, 2015, 112, 46-53.
71. C. Pretti, C. Chiappe, D. Pieraccini, M. Gregori, F. Abramo, G. Monni and L. Intorre, *Green Chem*, 2006, 8, 238-240.
72. Q. Zhang, K. De Oliveira Vigier, S. Royer and F. Jerome, *Chem Soc Rev*, 2012, 41, 7108-7146.
73. R. C. Harris, *PhD Thesis at the University of Leicester*, 2008.
74. L. A. Mikeska, *Industrial and engineering chemistry*, 1936, 28, 970-984.
75. N. Srivastava and M. A. Burns, *Anal Chem*, 2006, 78, 1690-1696.
76. D. S. Viswanath, *Viscosity of Liquids: Theory, Estimation, Experiment, and Data*, Springer, 2007.
77. K. S. Pedersen and H. P. Ronningsen, *Energ Fuel*, 2000, 14, 43-51.
78. S. E. Quinones-Cisneros, K. A. G. Schmidt, J. Creek and U. K. Deiters, *Energ Fuel*, 2008, 22, 799-804.
79. R. P. Chhabra and J. F. Richardson, *Non-Newtonian Flow in the Process Industries: Fundamentals and Engineering Applications*, Butterworth-Heinemann, 1999.
80. M. Dolz, J. Delegido, A. Casanovas and M. J. Hernandez, *J Chem Educ*, 2005, 82, 445-447.
81. D. C. Ash, M. J. Joyce, C. Barnes, C. J. Booth and A. C. Jefferies, *Meas Sci Technol*, 2003, 14, 1955-1962.
82. R. C. Harris, PhD, Leicester, 2008.
83. A. P. Abbott, R. C. Harris and K. S. Ryder, *J Phys Chem B*, 2007, 111, 4910-4913.
84. R. A. Kuharski and P. J. Rossky, *Journal of the American Chemical Society*, 1984, 106, 5786-5793.

85. A. Chmielewska and A. Bald, *J Mol Liq*, 2008, 137, 116-121.
86. C. D'Agostino, R. C. Harris, A. P. Abbott, L. F. Gladden and M. D. Mantle, *Phys Chem Chem Phys*, 2011, 13, 21383-21391.
87. P. T. Callaghan, *Aust J Phys*, 1984, 37, 359-387.
88. E. L. Cussler, *Diffusion: Mass Transfer in Fluid Systems*, Cambridge University Press, 2009.
89. A. W. Taylor, P. Licence and A. P. Abbott, *Phys Chem Chem Phys*, 2011, 13, 10147-10154.
90. Y. H. Hsu, R. B. Leron and M. H. Li, *J Chem Thermodyn*, 2014, 72, 94-99.
91. Q. Zeng, Y. Wang, Y. Huang, X. Ding, J. Chen and K. Xu, *Analyst*, 2014, 139, 2565-2573.
92. R. Esquembre, J. M. Sanz, J. G. Wall, F. del Monte, C. R. Mateo and M. L. Ferrer, *Phys Chem Chem Phys*, 2013, 15, 11248-11256.
93. A. W. Taylor, P. Licence and A. P. Abbott, *Phys. Chem. Chem. Phys.*, 2011, 13, 10147-10154.
94. A. P. Abbott, R. C. Harris, K. S. Ryder, C. D'Agostino, L. F. Gladden and M. D. Mantle, *Green Chem*, 2011, 13, 82-90.
95. M. Holz, S. R. Heil and A. Sacco, *Phys. Chem. Chem. Phys.*, 2000, 2, 4740-4742.
96. A.-L. Rollet, P. Porion, M. Vaultier, I. Billard, M. Deschamps, C. Bessada and L. Jouvensal, *J. Phys. Chem. B*, 2007, 111, 11888-11891.
97. C. G. Hanke and R. M. Lynden-Bell, *J. Phys. Chem. B*, 2003, 107, 10873-10878.
98. E. Durand, J. Lecomte, B. Barea, G. Piombo, E. Dubreucq and P. Villeneuve, *Process Biochem*, 2012, 47, 2081-2089.

CHAPTER FOUR: CORROSION STUDIES

CONTENTS

4 CORROSION STUDIES

4.1	INTRODUCTION.....	92
4.1.1	<i>Corrosion</i>	92
4.1.2	<i>Corrosion Requirements:</i>	93
4.1.3	<i>Corrosion Types</i>	94
4.1.4	<i>Uniform Corrosion</i>	94
4.2	CORROSION PROCESS	94
4.3	ELECTROCHEMICAL STUDIES OF CORROSION.....	95
4.3.1	<i>Linear polarization resistance (LPR)</i>	97
4.3.2	<i>Corrosion rate calculations</i>	99
4.3.3	<i>Results from LSV measurements</i>	100
4.3.4	<i>Effect of water on corrosion</i>	106
4.3.5	<i>Corrosion thermodynamics</i>	108
4.3.6	<i>Electrochemical Impedance Spectroscopy (EIS)</i>	109
4.4	RESULTS FROM IMPEDANCE MEASUREMENTS.....	113
4.5	CHARACTERIZATION OF CORROSION PRODUCTS	117
4.6	CONCLUSIONS	123
4.7	REFERENCES	124

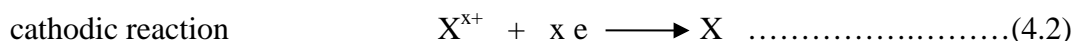
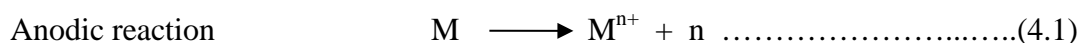
4 CORROSION STUDIES

4.1 Introduction

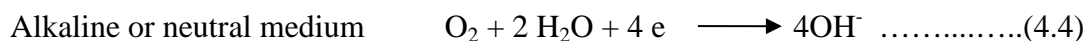
Corrosion is a spontaneous phenomenon which occurs to metals due to the thermodynamic driving force to equilibrate the energy of a system. Corrosion is clearly exacerbated for fully immersed systems. Using liquids made of or containing ions as a lubricant is quite different from liquids made of hydrocarbons. The later as non-conducting media should inhibit corrosion and most formulated oils contains additives to actively prevent corrosion. On the other hand, high conducting media such as ILs or DESs would be thought to behave differently toward metals in contact with them. To date no studies have been made of corrosion in ionic liquids. It is therefore necessary to study the corrosion behavior of DESs or ILs before they can be applied as lubricants. The aim of this chapter is to address the corrosion behavior of some pure type III DESs and imidazolium ILs. Furthermore, the corrosion products will be characterized as a function of time and water content.

4.1.1 Corrosion

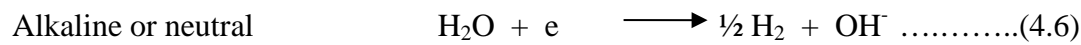
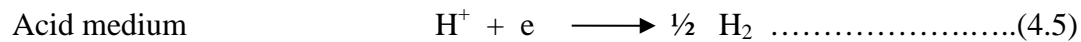
Corrosion is defined as an electrochemical reaction which happens between a metal and its surrounding environment. In terms of thermodynamic stability, most metals are more stable in their ore states than in elemental metallic state thus corrosion is the electrochemical process in which metals revert back to their ore state. As in any electrochemical reactions for corrosion to occur the reaction should involve both electron loss and electron gain in the corrosion process. The common cathodic and anodic reactions are illustrated below in aerated and deaerated solutions.¹⁻³



In aerated



In de-aerated



Where, M=Metal M^+ =Metal ion $\text{X}^{\text{x}+}$ = reduced species

4.1.2 Corrosion Requirements:

For corrosion to occur there needs to be; an anode where oxidation occurs, a cathode where the electrons from the oxidation site are consumed by the reduction of other species, ionic conduction between two sides (electrodes) to connect them by electrolytic path and finally a path for electrons to transfer between anode and cathode Figure 4-1. ^{3,4}

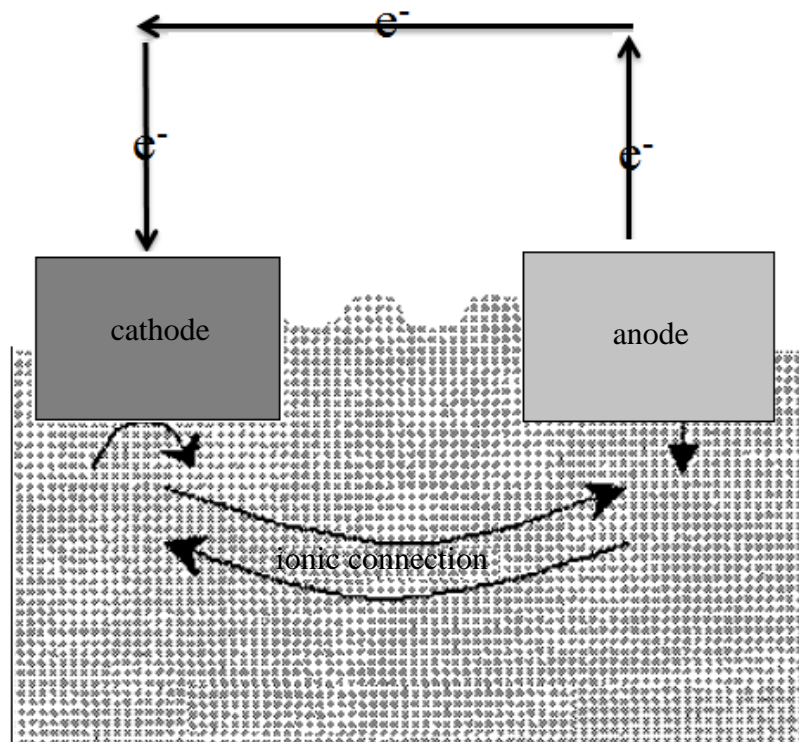


Figure 4-1 : Diagram of conditions required for corrosion. ⁴

4.1.3 Corrosion Types

Corrosion can be categorized into the following types:^{2, 3} uniform corrosion, erosion or abrasion corrosion, stress corrosion cracking, microbial corrosion, selective corrosion, cavitation corrosion, galvanic corrosion, crevice corrosion, inter-granular corrosion, pitting corrosion and fretting corrosion

4.1.4 Uniform Corrosion

Uniform corrosion is the most common form of corrosion and is responsible for a maximum damage of the materials. In uniform corrosion the thickness loss is spread relatively evenly over the surface of the material. Estimation of the corrosion rate can easily be made by electrochemical measurement. Hence it is simple to estimate the lifetime and potential weakness that will occur.^{2, 3}

4.2 Corrosion process

There are two questions that could be asked for a corrosion process; firstly does the reaction occur spontaneously? and secondly if it is spontaneous how fast does the chemical reaction occur between the metal and its environment?

The release of energy during state change of a material or a chemical reaction can be considered as a condition of spontaneity. Its principle value is in providing information on intermediate products from both the anodic and cathodic partial reactions. This condition could be estimated for corrosion process by knowing the Gibbs free energy of a reaction which is related to the corrosion potential of any particular metal-environment system as shown in equation 4.7.

$$\Delta G = -nFE \quad \text{..... (4.7)}$$

Where ΔG is Gibbs free energy, n is the number of electrons involved in the redox reaction, F is the Faraday constant 96484 Coulombs and E is electromotive potential for the corrosion reaction.

The second question could then be answered by knowing the reaction rate from measuring corrosion current density associated with the reaction for a particular corrosion

system. This could be done using the exponential relationship between current and over potential (Tafel principle) equations 4.8 - 4.10 at over potentials > 0 volts.

$$i = ke^{\left(\frac{\Delta G}{RT}\right)} e^{\left(\frac{\alpha z F \eta}{RT}\right)} \dots\dots\dots(4.8)$$

But

$$i_o = ke^{\left(\frac{\Delta G}{RT}\right)} \dots\dots\dots(4.9)$$

Therefore,

$$i = i_o e^{\left(\frac{\alpha z F \eta}{RT}\right)} \dots\dots\dots(4.10)$$

Where i = applied current density (A/cm²)

i_o = corrosion current density (A/cm²)

ΔG = Activation energy or free energy change (J / mol)

k = Chemical reaction constant

z = Oxidation state or valence number

F = Faraday constant

α = symmetry factor ≈ 0.5

η = over potential (volt)

Then using corrosion current density in Faraday equation provides the rate at which the reaction is occurring.

$$R = \frac{i_{corr} A_w}{nF} \dots\dots\dots(4.11)$$

Where R = corrosion reaction rate

A_w = Atomic weight of metal

In the following sections the answer for these two questions will be addressed for some common metals in some type III DESs, ILs and mineral base oil

4.3 Electrochemical studies of corrosion

Various methods have been used for measuring corrosion rates for metals and alloys which are based on the condition of exposure, such as mass loss (gravimetric and quartz crystal microbalance (QCM)), exposed sample dimensional change, solution analysis, electrical resistance and electrochemical methods. Measuring polarization resistance is an

electrochemical method which is considered as a quick way to measure of the exchange current density and determine the corrosion reaction rate from a single experiment. In contrast, the rest of the methods are accompanied by integrated or historical information regarding mass loss over a certain period of time that has happened for the target metal. Hence corrosion rate information must be derived from multiple measurements over periods of time to gain corrosion rate information.^{4, 5}

If DESs are to be suitable base lubricants their corrosion behaviour needs to be characterised for different metals and alloys that they are expected to be exposed to during their service. The corrosion rates of different DESs and ILs were studied by means of linear sweep voltammetry (LSV) wherein, corrosion current densities for Fe, Ni and Al at 298 K were measured. Furthermore, in order to understand whether corrosion rates are changeable over time, impedance spectroscopy studies have been carried out to measure polarization resistance for Fe, Ni and Al at 298 K for time periods between 0 and 48 hours.

Finally, to recognize why liquids behave differently toward metals Raman spectroscopy has been used to record spectra of oxide films on the surface of metals after immersion for long time in these liquids.

In electrochemical corrosion studies a potentiostatic circuit is employed to determine the corrosion rate and corrosion behaviour of different metals and alloys. A polarization cell in potentiostatic circuit is made from a working electrode, counter or auxiliary electrode and reference electrode. The target metal is employed as a working electrode (WE), the auxiliary (counter) electrode (AE) is made preferably of a material that will help redox reactions with reactants in the medium without polluting the solution or contributing to the corrosion process. Finally, the reference electrode (RE) serves to retain a constant potential with respect to the working electrode during measurements.⁶ Figure 4-2 shows a schematic diagram of the corrosion measurement cell.

A polarization curve is determined for both individual cathodic and anodic half-cell reactions happening on the surface of the target metal.⁴⁻⁶

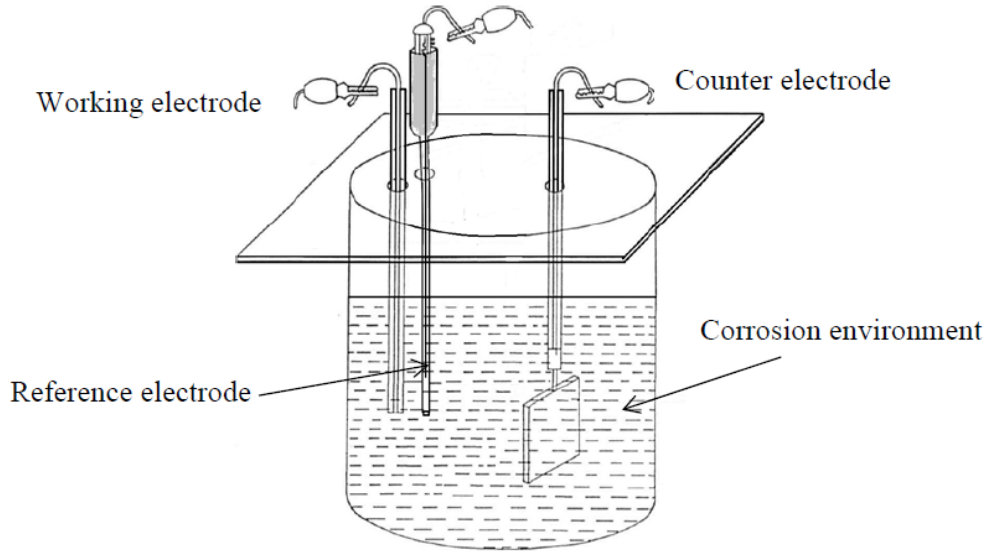


Figure 4-2: Typical cell for measuring corrosion rates.⁶

4.3.1 Linear polarization resistance (LPR)

The Tafel (current-potential) relationship is based on the theory of polarization resistance which is based on electrochemical reactions (electron-transfer).⁷ The rate of general corrosion of a metal is related to polarization resistance near or at their potential of corrosion. Measurement of the polarization resistance is a rapid and accurate method to measure the corrosion rate.^{5, 8} Experimentally the Butler-Volmer equation (4.12) is used to describe the polarisation resistance between the applied potential and the arising current density at the electrode, provided that no other redox reaction occurs at the electrode surface.^{5, 6}

$$i_{app} = i_{corr} \left[\left(e^{\frac{+2.3(E - E_{corr})}{\beta_{ox,M}}} - e^{\frac{-2.3(E - E_{corr})}{\beta_{red,X}}} \right) \right] \quad \text{.....(4.12)}$$

Where, β_{ox} and β_{red} are anodic and cathodic Tafel slopes respectively

$$i_{app} \text{ (applied current density)} = i_{ox} - i_{red}$$

$$\Delta E = E - E_{corr}$$

$$E_{corr} = \text{corrosion potential}$$

$$i_{corr} = \text{corrosion current density}$$

The relationship is a base of electrochemical polarization technique which is applied to corroding sample electrode at E_{corr} .^{6, 8}

It has been observed by many investigators that there is an almost linear relation between few mV polarisations from E_{corr} and i_{app} . Therefore, for small scan rate potentials with respect to the E_{corr} the relation has been linearized by Stern and Geary, when taking the differentiation of the equation with respect to E which provides the following relationship.

$$\frac{di_{app}}{dE} = i_{corr} \left[\frac{2.3}{\beta_{ox,M}} e^{\frac{2.3(E-E_{corr})}{\beta_{ox,M}}} + \frac{2.3}{\beta_{red,X}} e^{-\frac{2.3(E-E_{corr})}{\beta_{red,X}}} \right] \dots\dots\dots(4.13)$$

The exponential terms are unity at $E = E_{corr}$, and after rearrangement, the equation becomes;

$$\left(\frac{dE}{di_{app}}\right)_{E_{corr}} = R_p = \frac{\beta_{ox,M} \beta_{red,X}}{2.3i_{corr}(\beta_{ox,M} + \beta_{red,X})} \dots\dots\dots(4.14)$$

The linear relation is achieved when the following sequence expansion has been applied to the equation.

$$e^x = 1 + X + \frac{X^2}{2!} + \dots + \frac{X^n}{n!} \dots\dots\dots(4.15)$$

As long as the reaction kinetics is controlled by charge transfer and the third and greater terms can be ignored because x is small and equation 4.16 becomes valid.^{4, 6, 8}

$$\left(\frac{E-E_{corr}}{i_{app}}\right) = \frac{\beta_{ox,M} \beta_{red,X}}{2.3i_{corr}(\beta_{ox,M} + \beta_{red,X})} \dots\dots\dots(4.16)$$

i_{app} is commonly almost linear with potential within $\pm 5 - 10$ mV with respect to corrosion potential. The gradient of this plot ($\Delta E / \Delta i$) when determined from a line of the potential vs current curve at the corrosion potential describes the polarization resistance as shown in Figure 4-3a. Hence, this technique is often named as the linear polarization resistance (LPR) method.^{4, 6, 9} The values of β , β_a , β_c and corrosion current are directly calculated from the plot between log absolute current verses potential for redox reactions Figure 4-3b.

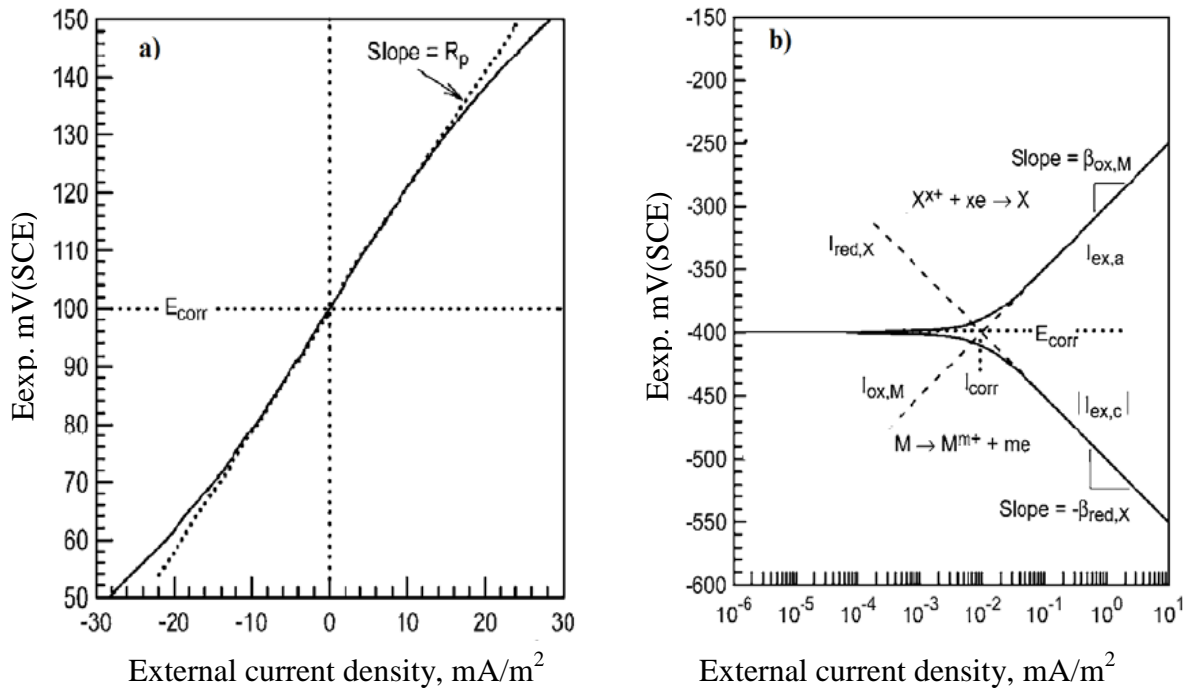


Figure 4-3: Current potential plots a-Polarization resistance b- Tafel slopes.⁶

Consequently, the corrosion current could be directly obtained by re-writing the relationship in the following form:

$$i_{corr} = \frac{1}{(2.3R_p)} \left(\frac{\beta_a \beta_c}{\beta_a + \beta_c} \right) = \frac{B}{R_p} \dots\dots\dots(4.17)$$

Where, R_p = polarisation resistance (ohm.cm²)

B = Stern-Geary coefficient

$\beta_a = \beta_{ox}$ $\beta_c = \beta_{red}$

and

$$B = \left(\frac{\beta_a \beta_c}{2.3 \beta_a + \beta_c} \right) \dots\dots\dots(4.18)$$

4.3.2 Corrosion rate calculations

Corrosion rates (CR) in mm/year for any metal or alloys can be calculated if R_p and the Stern-Geary coefficient B are available by using of the following relationship.⁸

$$CR = 3.27 \times 10^{-3} * \frac{i_{corr} EW}{\rho} \dots\dots\dots(4.19)$$

Where,

CR is the corrosion rate in mm/year, EW is the equivalent weight g/mole, ρ is the density of corroding sample g/cm³

$$i_{corr} (\mu\text{A}/\text{cm}^2) = 10^6 B/R_p \dots\dots\dots(4.20)$$

4.3.3 Results from LSV measurements

It is well known that chloride ions can significantly enhance the corrosion rate in aqueous solution as they break down passive films.^{10, 11} As such it would seem logical that chloride based DESs should be avoided for lubricant applications. Table 4-1 shows the initial corrosion rates as determined using Tafel slopes from slow-rate linear sweep voltammetry for mild steel in some DESs and ionic liquids.

The corrosion rates are particularly low for Ethaline, Reline and Glyceline however extremely high for Oxaline. The origin of this difference could be due to the presence of an insulating film on the metal surface or the kinetics of either the anodic or cathodic processes. As shown in Figure 4.5 the Tafel slope shows that in Ethaline, Reline and Glyceline the cathodic slope is shallow in comparison with Tafel slope for Oxaline suggesting that the cathodic process is rate limiting. In these liquids the cathodic process is the reduction of oxygen i.e.

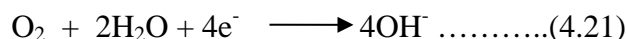


Table 4-1: Corrosion rates of mild steel in different liquids at 298 K.¹²

Fluid	Corrosion of mild steel / $\mu\text{m year}^{-1}$	
	LSV	EIS
Ethaline	1.90	5.02
Glyceline	0.40	2.20
Reline	2.50	2.70
Oxaline	176	65.0
C ₂ mim HSO ₄	2.10	2.30
C ₂ mim C ₂ H ₅ SO ₄	6.05	3.20
C ₂ mim SCN	2.43	1.47
C ₂ mim CH ₃ COO	0.54	3.50

As shown in Figure 4-5a in the oxalic acid based eutectic however the cathodic process is extremely fast as it is just the reduction of protons to form hydrogen gas allowing

much faster corrosion. Interestingly in this liquid bright yellow sheets of iron oxalate form parallel to the metal surface until all the metal is dissolved, which effectively filled the sample tube by the end of the experiment as shown in Figure 4-4b and Figure 4-4c. The corrosion process corresponds to equations 4.22 and 4.23 and Figure 4.4a shows the process clearly.

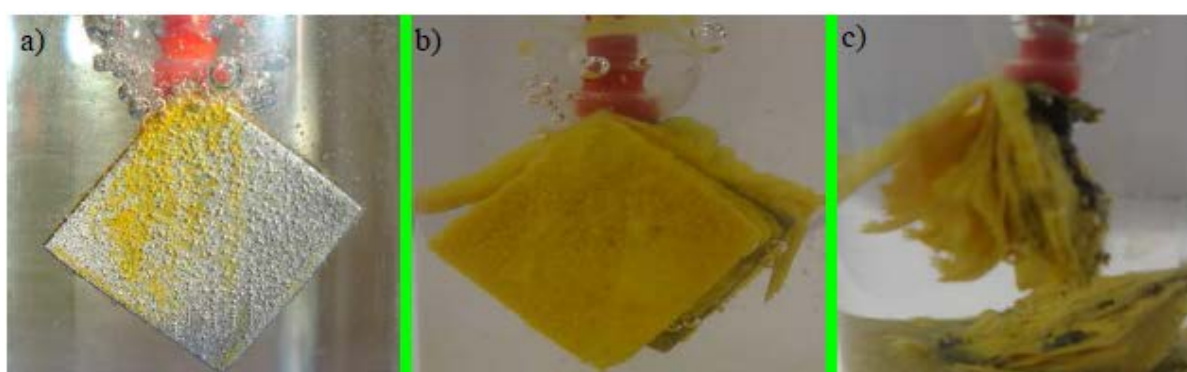
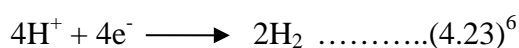
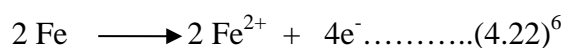


Figure 4-4: Corrosion of mild steel in ChCl/oxalic acid eutectic mixture, a) hydrogen evolution, formation of yellow sheets of iron oxalate and c) insolubility of corrosion products.

The very high chloride concentration will decrease the activity of water as it is highly hydrogen bonded. The very unusual aspect of DESs is their propensity to prevent corrosion even when the liquid is doctored with an aqueous electrolyte solution. Figure 4-6 shows that when 1 wt% water containing 1 wt% NaCl (a mimic of sea water) is added to the mineral oil, significant corrosion is observed of the mild steel immersed in the liquid after 2 weeks. Clearly the aqueous phase partitions to the steel surface where corrosion is caused by the relatively high chloride concentration.

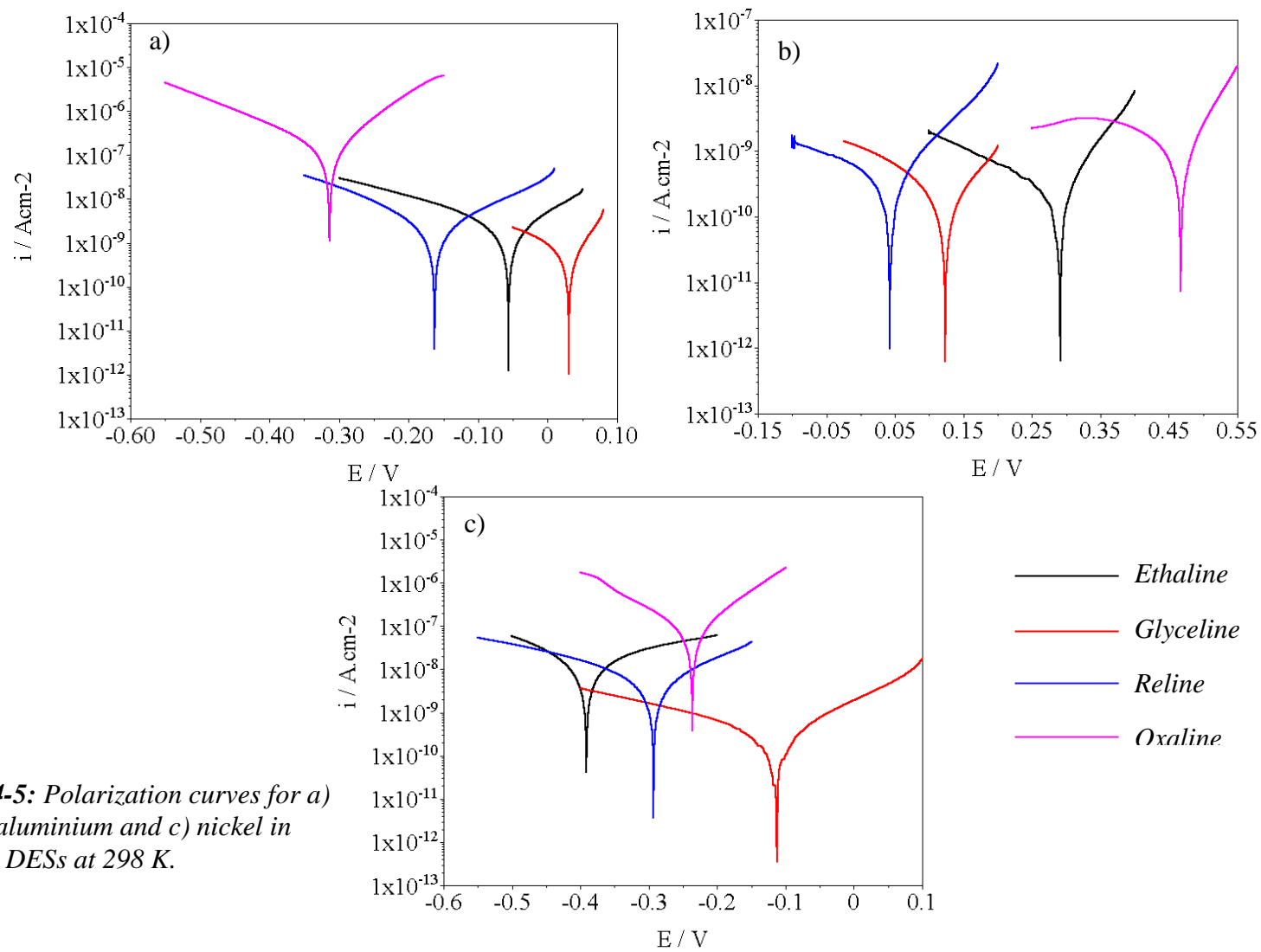


Figure 4-5: Polarization curves for a) iron, b) aluminium and c) nickel in different DESs at 298 K.

Figure 4-6 shows an analogous experiment where choline chloride is added to the aqueous solution in place of sodium chloride and it can be seen that corrosion occurs but to a lesser extent.

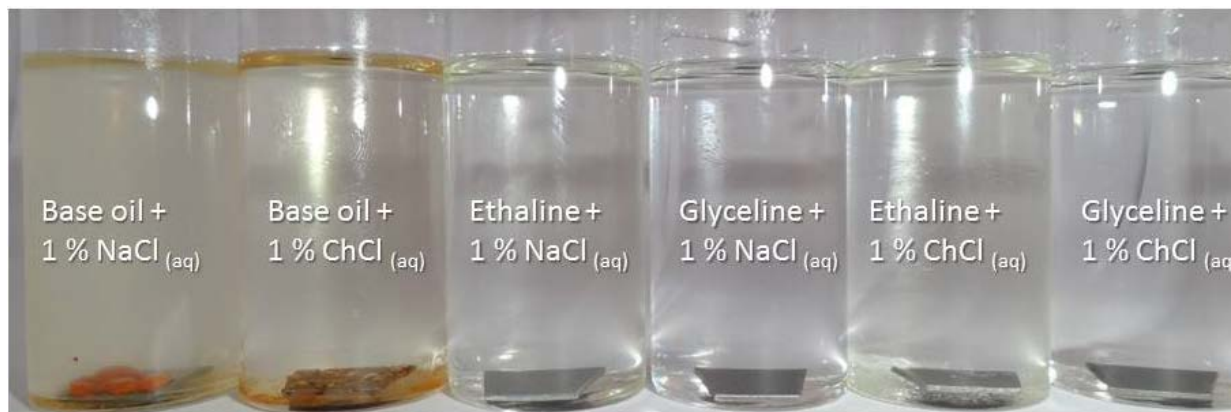


Figure 4-6 : Corrosion behaviour of mild steel in DESs and mineral base oil containing 1% $\text{NaCl}_{(aq)}$ and 1% $\text{ChCl}_{(aq)}$.¹²

This surprisingly shows that there is a cation effect to the corrosion mechanism which is explained in detail in the diffusion section below.

The corrosion rates of metals in Ethaline, Glyceline and Reline have been determined as a function of water content and these are shown in Table 4-1. It can be seen that steel corrodes mildly in wet Ethaline and Reline but was almost inert in wet Glyceline this was ascribed to differences in cathodic reactions in these liquids. The data in Figure 3.19c suggest that aqueous solutions of Ethaline and Reline enable dissociation of the OH proton of Ch^+ which could make the liquids more acidic than Glyceline.

Metal oxides and specifically hydrous ferric oxides are very sensitive to the solution variables such as pH and temperature, wherein a slight change in these causes a significant change in chemical composition. The type of anions and solution are playing similar roles as pH and temperature for metal oxide formation.¹³

Figure 4-1a show the corrosion of mild steel bolts in the wet DESs after 2 weeks and 18 months. After 2 weeks corrosion in the DESs is less than that in wet mineral oil although some colouration of Ethaline and Reline are just visible. In Glyceline there is no visible evidence of corrosion either on the metal surface or from colouration of the liquid.

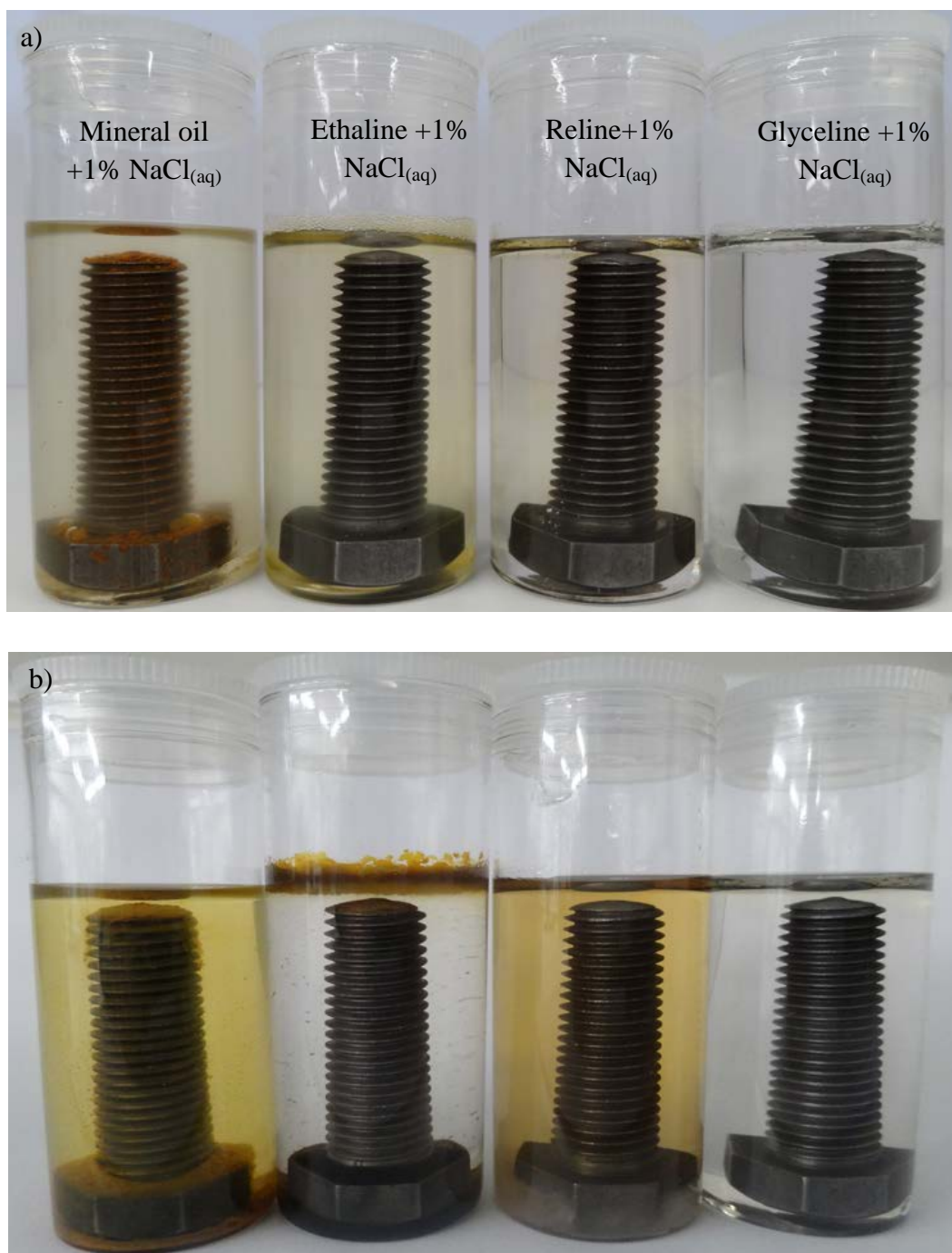


Figure 4-7: visible corrosion of mild steel in mineral oil and DESs containing 1 wt% sea water after a) two weeks, and b) 18 months.

In Ethaline after 6 months the liquid is clear and colourless but the corrosion products (mostly iron glycolate) can be seen floating on the liquid surface since it has lower density than Ethaline. There is also evidence of bubbles forming on the surface of liquid and trapped in the threads of the screws as shown in Figure 4-7a. As will be shown below these are possibly hydrogen as wet Ethaline is mildly acidic. Over the 18 month period atmospheric

oxygen must react with the glycolate to form a green complex $[\text{Fe}(\text{H}_2\text{O})_4(\text{OH})_2]$ which precipitated on the bottom of the bolt in Figure 4-7b therefore after 18 months the colourless Ethaline has remained which supports the formation of neutral iron oxides.¹⁴

In Reline, the oxidation of mild steel occurs but the corrosion products are soluble forming a yellow coloured solution. This could be due to the chloride interacting with the metal centre but it could also form with ammonia ligands. The slow decomposition of urea to form ammonia should lead to a basic solution with water.

In base mineral oil severe corrosion is observed due to water being immiscible with oil. The hydrophilic nature of mild steel means that water will concentrate at the surface and accentuate corrosion. Finally, in Glyceline there is no visible corrosion even after 18 months which could be due to the neutral pH of Glyceline water mixtures.

Figure 4-8 shows solutions of the three DESs containing 20 wt% water and universal indicator paper as a pH indicator. It can clearly be seen that there is a significant difference in the colour of the solutions indicating that Reline is considerably more basic than the other two liquids. Use of a pH electrode shows the pH of the three solutions each with 20 wt% water to be Ethaline = 3.97, Glyceline = 7.02 and Reline = 12.2. The Glyceline solution is roughly neutral confirming that the OH on the Ch^+ remains associated while the Ethaline solution is slightly acidic which is confirmed by the larger diffusion coefficient observed in Figure 3.19c. The pH of Reline can only be explained by the partial decomposition of urea to form $\text{NH}_3/\text{NH}_4\text{OH}$. It should however be noted that the dissociation is relatively small with an OH^- concentration of $0.016 \text{ mol dm}^{-3}$. It is therefore unsurprising that only a trace NMR signal is observed.

These pH data also tie in with the corrosion data for the three liquids *i.e.* almost no corrosion was observed in wet Glyceline (pH 7.02) even after one year as shown in Figure 4.7b however mild corrosion was noted in both wet Reline (pH 12.2) and Ethaline (pH 3.97). The formation of NH_4OH in dilute Reline would also explain the deviation from linear behaviour in Figure 3.17 since there will be more charge carriers, which are considerably smaller and have a larger molar conductivity.



Figure 4-8: Samples of Ethaline (left) Glyceline (middle) and Reline (right) with 20 wt% water and each containing a sample of universal indicator paper.¹⁵

4.3.4 Effect of water on corrosion

In order to elucidate the influence of water on corrosion behaviour of DESs, corrosion rates have been measured for iron, nickel and aluminium in four DESs in the presence of water up to 10 wt%. Table 4-2 shows the initial corrosion rate for these metals in four DESs as a function of water content. It can be seen that the glycol based liquids are relatively insensitive to the addition of water, whereas urea and oxalic acid based liquids are significantly more sensitive to increase the rate of corrosion for iron compared to an aqueous solution. Surprisingly aluminium only shows very slow corrosion when water is added even with a high chloride concentration presumably due to oxalate being able to passivate the metal surface.

Due to the complexity of intermolecular forces in DESs it is thought that addition of water will change these forces since water is able to participate in the formation of new hydrogen bonds with different species in the system. Consequently, a number of physical properties of a liquid will alter upon addition of water. For instance, and most significantly viscosity which is governed by association forces in the liquid, it is thought that it will change greatly upon addition of water and this change should cause a significant increase in the rate of mass transport, hence increasing the rate of cathodic reaction.

For Oxaline the decrease in corrosion rate may be due to the effect of the change in pH of a liquid with addition of water. As Oxaline is made from a mixture of one mole of oxalic acid and one mole of choline chloride the system is very acidic rather than basic or neutral as is visible in Figure 4-5. Hence, the rate of hydrogen evolution will be increased.

Table 4-2: : Corrosion rates of Fe, Al and Ni in four DESs as a function of water content determined using linear sweep voltammetry and Tafel slope analysis.¹²

liquids	Glyceline	Ethaline	Reline	Oxaline
Corrosion rate of Fe ($\mu\text{m}/\text{year}$)				
1% water	0.74	2.51	3.22	169.1
2% water	0.86	3.25	9.69	110.5
5% water	1.72	2.68	12.30	82.78
10% water	2.95	4.35	17.55	206.2
0.1 M aqueous KNO_3	7.32	7.32	7.32	7.32
Corrosion rate of Al ($\mu\text{m}/\text{year}$)				
1% water	1.10	1.55	1.37	2.30
2% water	1.12	1.78	1.36	2.05
5% water	1.19	1.82	1.40	2.40
10% water	1.41	1.94	1.55	2.11
0.1 M aqueous KNO_3	5.86	5.86	5.86	5.86
Corrosion rate of Ni ($\mu\text{m}/\text{year}$)				
1% water	0.23	6.79	1.60	63.1
2% water	0.51	7.96	2.24	58.7
5% water	1.14	9.62	4.64	90.0
10% water	1.53	7.30	8.79	126
0.1 M aqueous KNO_3	8.05	8.05	8.05	8.05

Chloride ions, and to some degree other halogen ions, have a strong tendency to destroy or to prevent the formation of passive oxide films during the process of oxidation. The film on the surface of metals and alloys like Fe, Ni, Cr, Co, Al and stainless steel is made of metal oxides. For instance for Fe the inner film is Fe_3O_4 , and outer film is Fe_2O_3 , and Al has an Al_2O_3 film. The chloride ion is in competition with oxide film or OH^- in the medium to adsorb on the metal surface through the defects and pores which increases the hydration of metal ions and leads to dissolution of ions.¹⁰

4.3.5 Corrosion thermodynamics

Only platinum, gold and silver are found in their metallic form in nature whereas other metals react to form oxides, carbonates, hydroxides, sulphides, silicates and sulphates. To reduce them back to their metallic form it is necessary to apply a large amount of energy. Therefore, a driving force for corrosion in metals to happen is the thermodynamic instability (high-energy content and low entropy) originated from the metallic state. Consequently, metals are corrode as a result of natural tendency to go back to a lower energy level.³ Figure 4-9 shows the concept of the cycle of conversion of ores to iron the corrosion of iron to rust.¹⁶

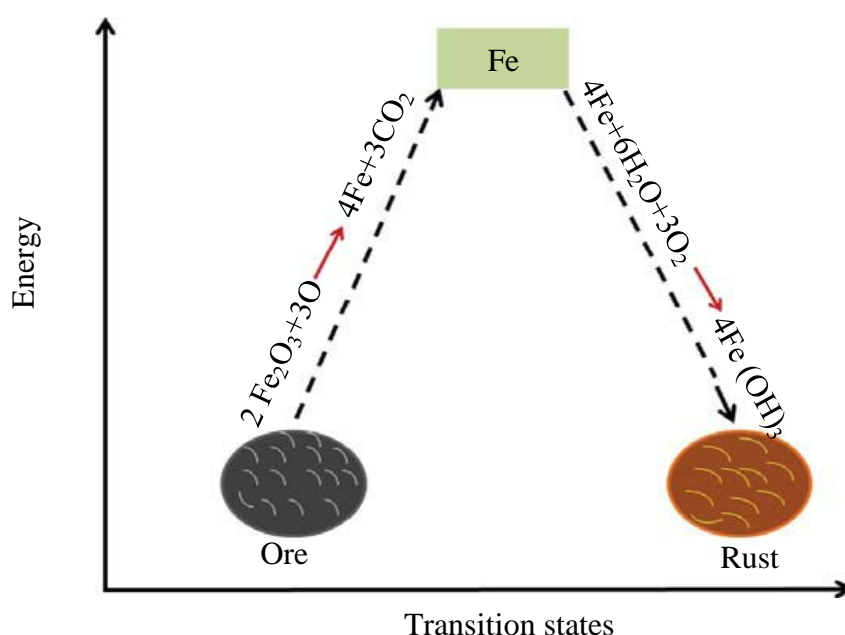


Figure 4-9: Illustration of physical meaning of corrosion and the associated energy is brought out in the figure. Note that energy is supplied to iron ore to convert it into iron and when the latter rusts energy is released.¹⁶

The following is a series of ranking for common metals and alloys according to their resistance to corrosion which is due to their difference in thermodynamic stability.

Na < Mg/ Mg alloys < Zn < Al < Cd < Fe < steel and cast iron < Pb < Sn < Cu < Ni < Cr < stainless steel < Ag < Ti < Au < Pt

According to equation 4.7 if the value of ΔG is negative it means that the metal corrodes spontaneously and if the value is positive it means that some energy is necessary to apply for corrosion reaction to happens. Table 4-3 shows thermodynamic stability of metals in different DESs and ILs at 298 K. It is obvious that iron and nickel do not corrode

spontaneously in all liquids except iron in EMIMEtSO₄ which possess a negative Gibbs energy. On the other hand apart from Reline and Glyceline aluminium corrodes spontaneously in most liquids including Ethaline and Oxaline. Finally, DESs are better than ILs in terms of spontaneous occurrence of corrosion of metals because the values of Gibbs energy of metals in these liquids are positive.

Table 4-3: Thermodynamic stability of metals in different DESs and ILs at 298 K.

Metals	Liquids	Ecorr. (Ag/AgCl 1M)	Ecorr. (SHE)	ΔG (kJmol ⁻¹)
Fe	Ethaline	-0.056	-0.278	80.6
	Glyceline	0.030	-0.192	55.76
	Reline	-0.163	-0.385	111.6
	Oxaline	-0.314	-0.536	155.3
	EMIM HSO ₄	0.169	-0.053	15.5
	EMIM EtSO ₄	0.240	0.017	-5.1
	EMIM SCN	0.100	-0.122	35.4
	EMIM OAc	0.144	-0.078	22.7
Ni	Ethaline	-0.391	-0.613	118.4
	Glyceline	-0.113	-0.335	64.7
	Reline	-0.293	-0.515	99.5
	Oxaline	-0.236	-0.458	88.5
	EMIM HSO ₄	-0.148	-0.370	71.5
	EMIM EtSO ₄	-0.147	-0.369	71.3
	EMIM SCN	-0.267	-0.489	94.5
	EMIM OAc	-0.392	-0.614	118.6
Al	Ethaline	0.291	0.068	-19.9
	Glyceline	0.124	-0.098	28.5
	Reline	0.043	-0.179	51.9
	Oxaline	0.467	0.245	-70.8
	EMIM HSO ₄	0.222	-0.001	0.12
	EMIM EtSO ₄	0.352	0.130	-37.5
	EMIM SCN	0.258	0.035	-10.3
	EMIM OAc	0.251	0.0286	-8.3

4.3.6 Electrochemical Impedance Spectroscopy (EIS)

The technique of electrochemical impedance spectroscopy applies an ac voltage to a dc step over a range of frequencies ($10^4 - 10^{-3}$ Hz) to provide impedance (Z) and phase angle data. The ratio of ac voltage to ac current gives the frequency-dependent impedance. Owing to the fact that the method gives extra information concerning the performance of

electrochemical cell as well as corrosion mechanism, the use of the technique is increasing rapidly.^{5, 6} In this technique for each frequency, the observed external current (I_{ex}), as a function of the applied voltage might be out of phase, as shown in Figure 4.9a.

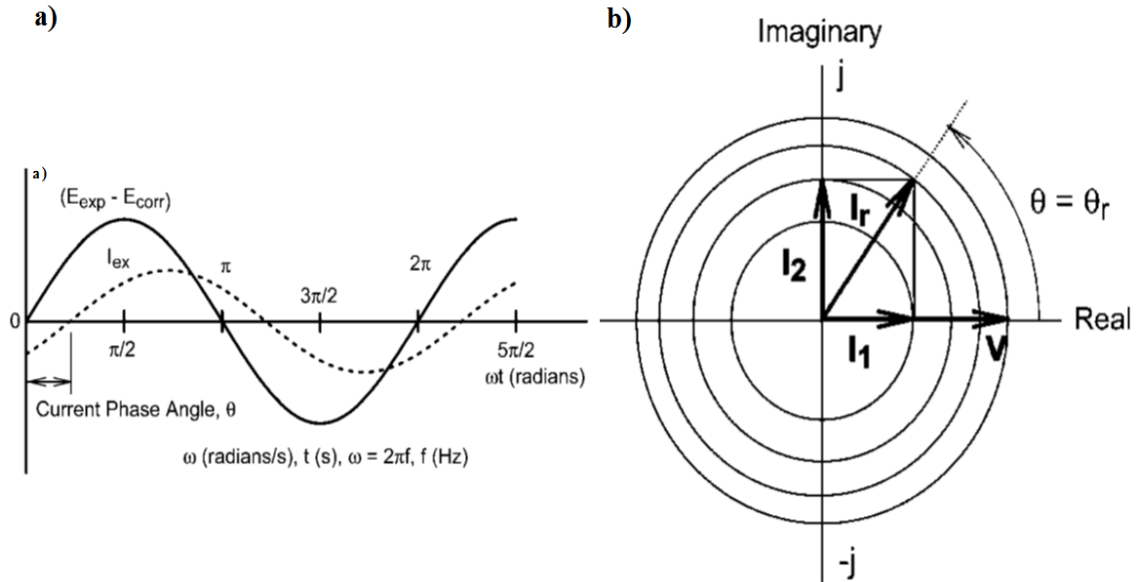


Figure 4-10 : a) External current shift as a result of applied ac voltage b) A description of applied voltage and the response current Stationary-vector.⁶

Hence, the impedance of the system similarly might be out of phase, because the physical processes acts as an inductive or capacitive element instead of resistive element in the circuit Figure 4-10b so it is considered to be “equal in the electrochemical cell”. Variation of the current as a function of the applied ac voltage for a simple parallel resistor and capacitor are shown in Figure 4-11.

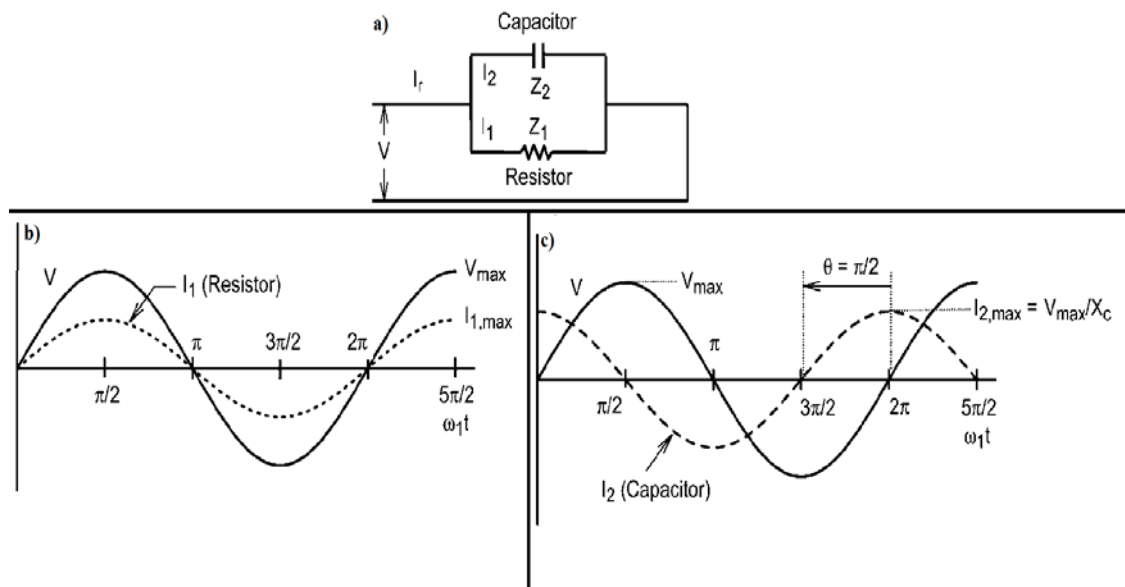


Figure 4-11 : Variation of current as a function of applied ac voltage of a simple circuit.⁶

Figure 4-12 shows the response for a simple corrosion circuit which is used to provide information about a corrosion process. For this situation the circuit is always normalised with respect to the area of the corroded electrode so the impedance has dimensions of resistance times area ($\Omega \cdot \text{cm}^2$).

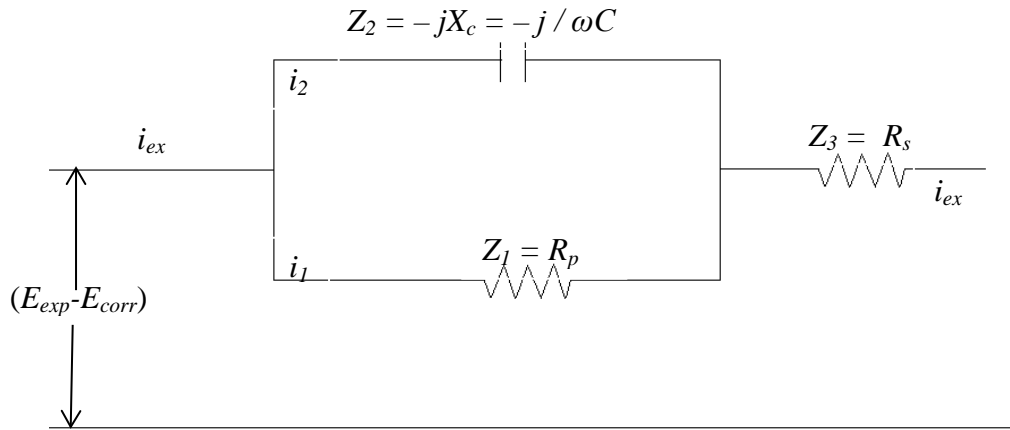


Figure 4-12 : Total impedance parts.⁶

For simplicity as shown in Figure 4-12 a total circuit for corrosion is analysed by treating the voltage, current and impedance as vectors which produce complex numbers giving that the Z is a total impedance of a circuit and $Z_{1,2,3}$ are total impedance fragments.^{6, 17}

$$Z = \frac{Z_1 Z_2 + Z_2 Z_3 + Z_1 Z_3}{Z_1 + Z_2} \dots\dots\dots(4.24)$$

Where, $Z_1 = R_p (R_{ct}) = \text{Polarisation resistance } (\Omega \cdot \text{m}^2)$

$$Z_2 = -jX_c = -j / \omega C$$

$$j = -I^{1/2}$$

$Z_3 = R_s = \text{Resistance of the solution } (\Omega \cdot \text{m}^2)$

$C = \text{is the normalised capacitance } (\text{F} \cdot \text{m}^{-2})$

$\omega = \text{angular frequency (radians/s)} = 2\pi f$

$f = \text{frequency in Hz}$

The current of the circuit takes the following shapes for both resistor and capacitor

For a resistor

$$(E_{exp} - E_{corr}) = i_1 Z_1 + i_{exp} Z_3 \dots\dots\dots(4.25)$$

And for a capacitor

$$(E_{exp} - E_{corr}) = i_2 Z_2 + i_{exp} Z_3 \dots\dots\dots(4.26)$$

But the total I of the circuit (I_{ex}) is the summation of resistor and capacitor currents together so

$$i_{ex} = i_1 + i_2 \dots\dots\dots(4.27)$$

Therefore, if i_1 and i_2 are eliminated from the resistor and capacitor currents and substituted in the impedance equation for the system which is defined as the ratio of applied voltage to the external current then the impedance relation to the current and applied potential becomes as below

$$i_{ex} = \frac{(E_{exp} - E_{corr})}{Z} \dots\dots\dots(4.28)$$

Therefore, if the values of impedance parts are substituted in the above equation the total impedance of the circuit takes the following shape

$$Z = R_s + \frac{R_p}{\omega^2 C^2 R_p^2 + 1} - \frac{j\omega C R_p^2}{\omega^2 C^2 2 R_p^2 + 1} \dots\dots\dots(4.29)$$

Or

$$Z = Z' + jZ'' \dots\dots\dots(4.30)$$

Where,

Z' is a real part and Z'' is an imaginary part of corresponding impedance thus¹⁷,

$$Z' = R_s + \frac{R_p}{\omega^2 C^2 R_p^2 + 1} \quad \text{and} \quad Z'' = \frac{-\omega C R_p^2}{\omega^2 C^2 2 R_p^2 + 1} \dots\dots\dots(4.31)$$

For the purpose of data processing the Nyquist plot ($-Z''$ vs Z') is used to define the components of the total impedance which has the following relationship between the real and imaginary components of the impedance and after elimination of angular frequency

$$(Z'')^2 = 2R_s Z' + R_p Z' - (Z')^2 - R_s^2 - R_s R_p \quad \text{.....(4.32)}$$

The equation is rearranged to give the equation of circle

$$\left[Z' - \left(R_s + \frac{R_p}{2} \right) \right]^2 + (-Z'')^2 = \left(\frac{R_p}{2} \right)^2 \quad \text{.....(4.33)}$$

This equation is used to calculate the value of polarisation resistance R_p , solution resistance R_s and capacitance C value from the semi-circle plot Figure 4-13.

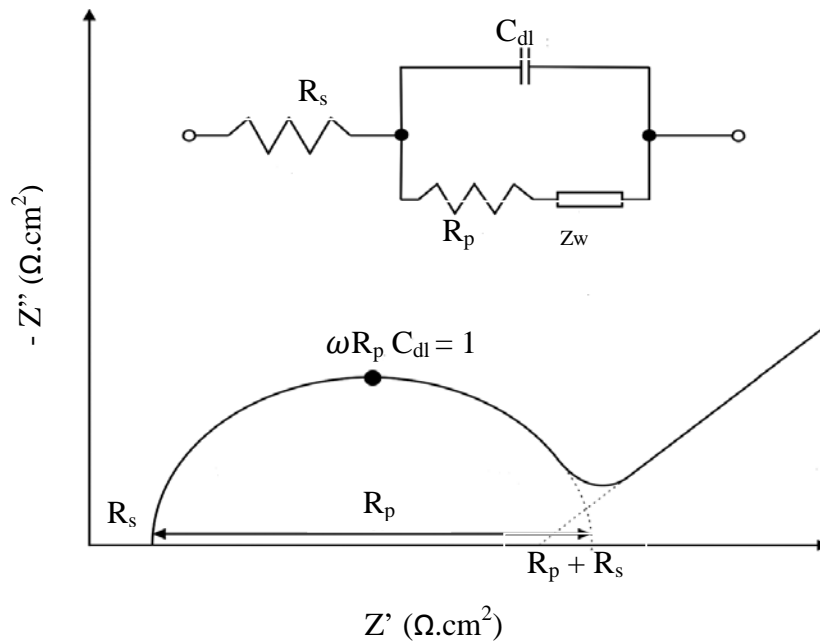


Figure 4-13: Typical Nyquist plot. ⁶

From the figure the value of R_s and R_p are obtained directly on the Z' axis. R_s is obtained at higher frequency values when $-Z'' = 0$, the polarization resistance is the diameter of semi-circle and the value of C is calculated according to equation 4.34 at maximum value of $|-Z''|$

$$C = \frac{1}{\omega R_p} \quad \text{.....(4.34)}$$

4.4 Results from impedance measurements

As well as measuring corrosion currents it is important to address the passivation behaviour of metals. By measuring impedance as a function of time (1- 48 hours) Nyquist plots can give information about the formation of passivating films. Figure 4-14 shows an

example of growing semi-circles overtime for Ni metal in a eutectic mixture of ChCl/ urea, in which the diameter of semi circles shows the polarization resistance. This was done for 3 metals in 4 DESs at 298 K. These data are shown in Figure 4-15, 4.15 and 4.16. Then to make it easier for comparison the log of polarization resistance values have been plotted versus time to show their behaviour overtime.

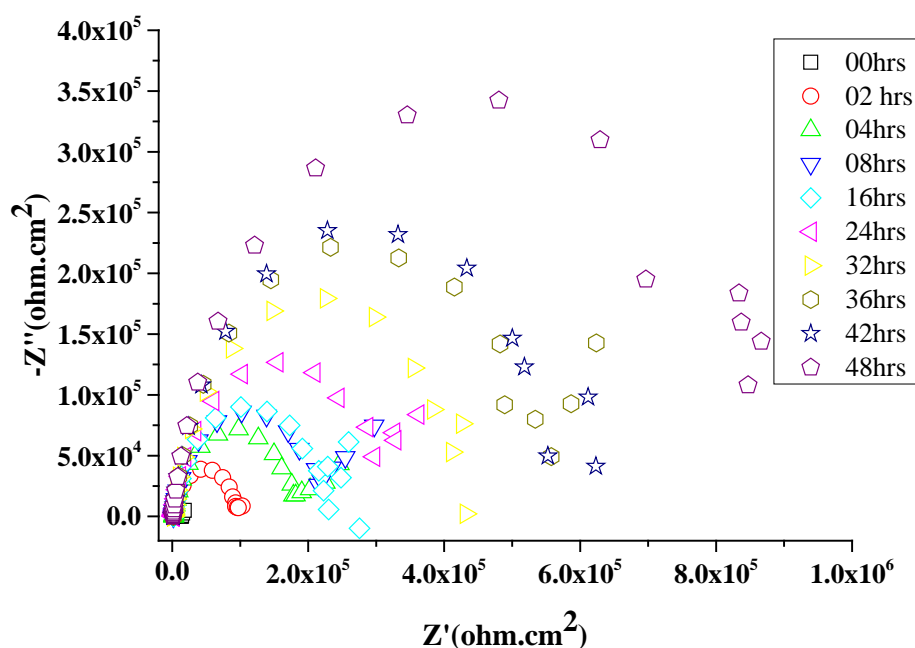


Figure 4-14: Nyquist plots of Ni in Reline at different times at 298 K.

In addition to the thermodynamics of corrosion the kinetics of corrosion can be strongly affected by film formation at the metal-solution interface. Figure 4-15 shows the effect of immersion time on the polarisation resistance of Fe in various eutectic mixtures.

The corrosion of iron in eutectic mixture of ChCl/ (urea, ethylene glycol and glycerol) decreases over time as seen in their resistance polarization values which have been increase. This means the corrosion becomes slower over time. In Ethaline there is an initial increase in the corrosion rate (decrease in R_p) in the first few hours which is followed by a decrease afterward. Corrosion is similar to the electropolishing process where applied potential leads to the controlled dissolution of the metal.

The electropolishing of steel in Ethaline has been studied in depth¹⁸ and despite iron oxide being relatively soluble¹⁹ it was found that a yellow layer forms on the steel surface during electropolishing. This was thought to be a glycoxylate complex although this was not formally proven. Figure 4-15 shows that after about 2 hours the R_p value increase by

approximately and order of magnitude which would cause the corresponding decrease in the corrosion rate. It is therefore likely that this results from a passive layer forming on or close to the electrode surface.

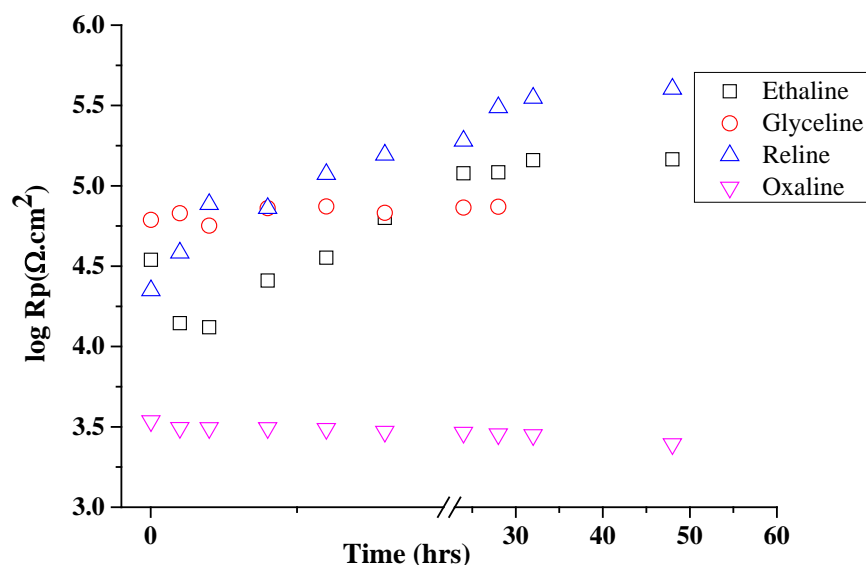


Figure 4-15: Polarisation resistance of Fe in different DESs at 298 K.

Figure 4-4 clearly shows that a layer forms rapidly on iron in Oxaline but it is unable to slow the overall corrosion rate over time, as the data in Figure 4-15 shows that the polarization resistance of iron decreases gradually with time.²⁰ The fast corrosion rate is clearly due to the cathodic reaction which is hydrogen evolution. The corrosion rate in Glyceline remains constant and slow due probably to the low concentration of a cathodic reagent. If equation 4.4 is dominant then the activity of water will be low due to the high ionic strength. If equation 4.3 dominates then the concentration of H^+ will be low due to the neutral pH.

Figure 4-16 shows the corrosion rate of Al in different DESs at 298 K. By comparing these data with those in Figure 4-15 it can be seen that aluminium corrodes more slowly than iron in ChCl/urea and ChCl/glycerol. This would suggest that the protective film of aluminium oxides is relatively stable in these liquids. However, in Ethaline aluminium corrodes faster than iron. This could be due to the activity of the chloride ions in Ethaline

which is thought to be higher than in the other liquids as the hydrogen bonding between ethylene glycol and the chloride ion are thought to be weaker.

This enables the chloride to interact more strongly with the aluminium oxide decreasing its ability to passivate the metal surface. In Oxaline the corrosion rate of aluminium is similar to that of iron in the same liquid which is again thought to be due to the inability of the corrosion product to passivate the electrode surface.

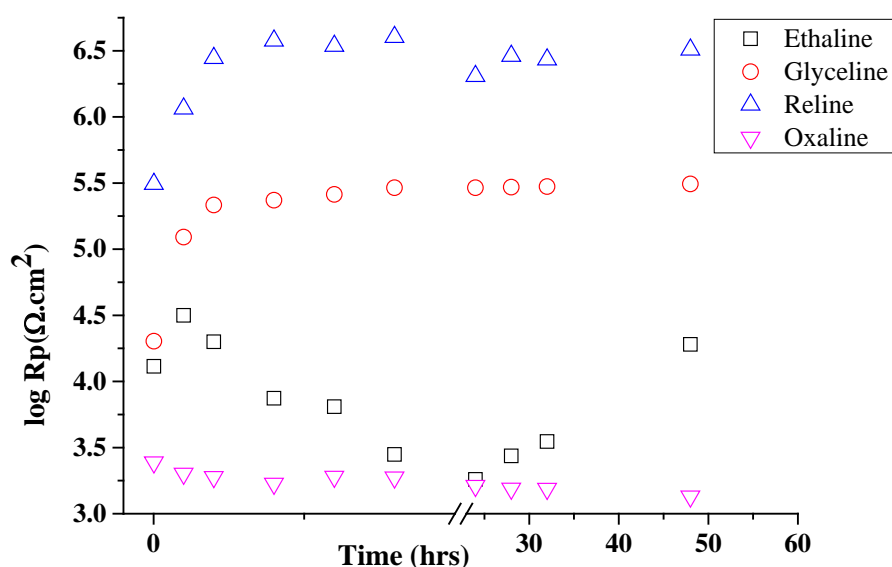


Figure 4-16 : Polarisation resistance of Al in different DESs at 298 K.

Figure 4-17 shows the corresponding polarisation resistance values for nickel as a function of time in the same four DESs. The behaviour of Ni is different to the other two metals. Firstly, the polarization resistance in Reline starts to increase and then remains roughly constant over time suggesting that a passivating layer is forming on the metal surface.

In Glyceline the polarization resistance is an order of magnitude higher for Ni than either Fe or Al. The reason for this is not immediately obvious as it will also have the same issues of the lack of a cathodic reactant. Nickel corrodes considerably slower in Oxaline than the other two metals and this must be due to some form of passive layer on the metal surface.

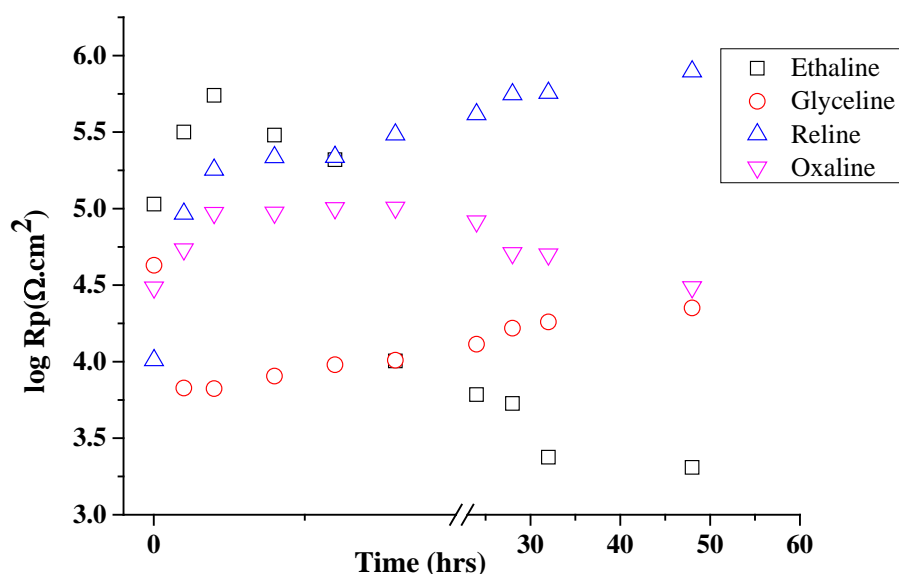


Figure 4-17 : Polarisation resistance of Ni in different DESs at 298 K.

In summary, the corrosion rates of metals in Glyceline and Reline remain almost constant for the metals studied here; whilst Ethaline has variable corrosion activity toward different metals which may be refers to the effect of mass transport, higher chloride activity and acidity of hydroxyl proton on ChCl. In Oxaline Ni is almost passive but Fe and Al corrodes rapidly.

4.5 Characterization of corrosion products

Characterisation of either corrosion products or a liquid layer directly adsorbed on the surface of metallic materials will provide some important information about the way in which metals corrode or passivate when they are in contact with liquids for a long time. Measuring vibrational spectra for chemical species is one way to gain information concerning a thin film of metal oxides or a liquid which is in direct contact with metal surfaces.

Characterization of corrosion products by Raman spectroscopy has been used for about two decades and in the last 10 years the technique has become more widely used due to two significant advantages. Sample preparation is easy and it is possible to probe the interface between liquids and solids in-situ.^{11, 21} In addition it is possible to decrease the overlap between broad peaks of corrosion products which occur with some other techniques such as IR spectroscopy.²²

In Raman spectroscopy when chemical species or polyatomic molecules are irradiated with monochromatic light such as a laser a small proportion of the photons are scattered due to their interaction with molecular vibrational states in a crystal lattice (phonons). In this technique the incident photons will be scattered in three different modes which are Stokes, anti-Stokes and Rayleigh scattering. As shown in Figure 4-18 if the energy of the scattered photons are less than the energy of incident photons the scattering is said to be Stokes scattering, however, if the energy of the incident and scattered photons are the same the signal is said to be Rayleigh scattered. Finally, if the scattered photons possesses more energy than the incident photons this situation is called anti-Stokes scattering.^{23, 24}

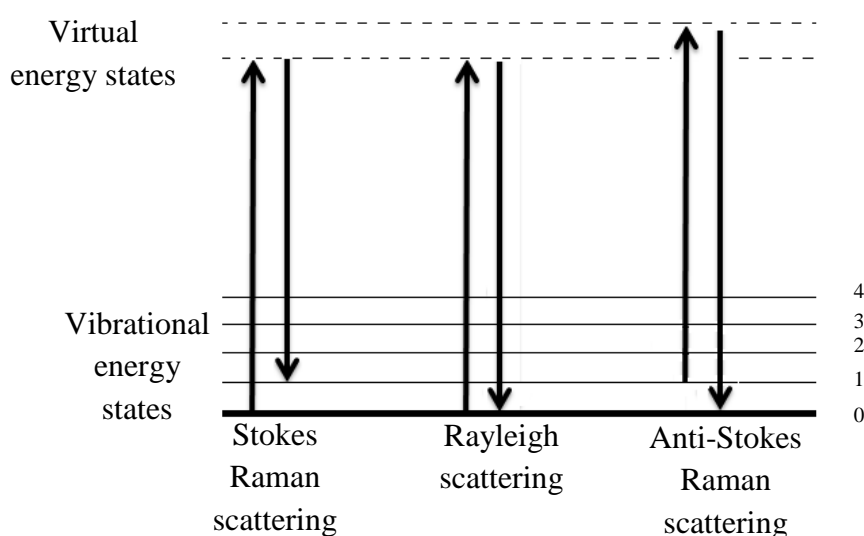


Figure 4-18: Scattering modes of Raman signals.²³

Stokes scattering is the form which is mostly exploited in Raman spectroscopy but only a small number of photons are involved in this form as shown in Figure 4-19 using cyclohexane as an example. As a consequence a spectrum consists of different peaks referring to the different vibrational energies of the molecule.^{11, 23, 24}

Raman spectroscopy has been widely used to characterize corrosion products taking advantages of a number of different crystal orientations. More specifically oxides of iron and aluminium have been characterized. Oxides of these metals are shown to have bands in the range $200\text{-}1400\text{ cm}^{-1}$ as illustrated in Table 4-4:

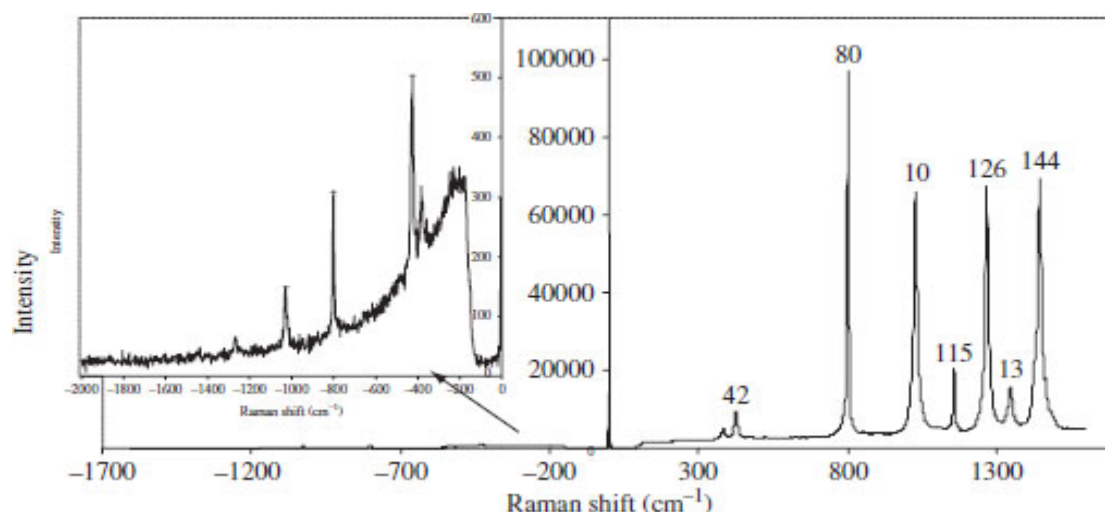


Figure 4-19: Raman intensity of Stokes and anti-Stokes scattering of cyclohexane.²³

Some shifting and broadening in the position and shapes of some peaks is observed in these studies. This is thought to arise from the use of different laser beam powers in comparison with other cited references which is responsible for this phenomenon.^{11, 21, 24, 25} Moreover, the peak intensities of some corrosion products are very low compared with other peaks therefore the peaks may be hidden by other stronger signals. For instance, magnetite possess a very weak signal intensity in comparison with haematite despite a relative abundance of only ~10%.²² It can therefore be difficult to distinguish between these two oxides easily if they exist together.^{21, 26}

Table 4-4: Oxidation products of iron and aluminium and their corresponding bands in Raman spectroscopy.

Corrosion products	Observable peaks in Raman spectra
Aluminium oxide (Al ₂ O ₃)	315-335, 371-385, 418, 432-451, 490-502, 524- 526, 544-547, 559-591, 600-612, 645-678, ~700, 719-770 cm ⁻¹ ¹²⁷⁻²⁹
Goethite (α-FeOOH)	203-206, 244-250, 298-304, 385-399, 414-418, 474-482, 549-560, 675-685, 997-1003, 1113, 1304-1320 cm ⁻¹ ^{1, 11, 22, 26, 30-32}
Akaganeite (β-FeOOH)	139, 308-331, 380-400, 420, 499, 539-549, 609, 720-725, 1410 cm ⁻¹ ^{28, 31, 33}
Lepidocrocite (γ-FeOOH)	166, 212-219, 245-252, 302-311, 343-350, 375-380, 521-529, 648-662, 713, 1050-1055, 1300-1312 cm ⁻¹ ^{1, 11, 21, 22, 24, 31-34}
feroxyhite (δ-FeOOH) ^{21, 28}	700 cm ⁻¹ ¹³¹
Magnetite (Fe ₃ O ₄)	300-308, 513, 532-550, 550, 616, 662-675 cm ⁻¹ ^{1, 21, 22, 30-33, 35}
Maeghemite (γ-Fe ₂ O ₃)	339-386b, 460-510b, 660-720b, 1200, 1430-1440, 1600 cm ⁻¹ ^{21, 28, 31, 33, 34}
Heamatite (α-Fe ₂ O ₃)	222-228, 244-250, 292-299.3, 410.9-414, 495-502, 611-625, 670, 806, 1318-1330 cm ⁻¹ ^{1, 21, 22, 24, 25, 31, 33}
Wustite (FeO) ^{21, 22, 24, 31}	471, 616, 653, 663 cm ⁻¹ ^{121, 31}

In this study Raman spectroscopy has been used to characterise the corrosion products formed on iron and aluminium after being left in DESs for long time. Characteristic peaks observed for iron are shown in Figure 4-20 and for aluminium in Figure 4-20.

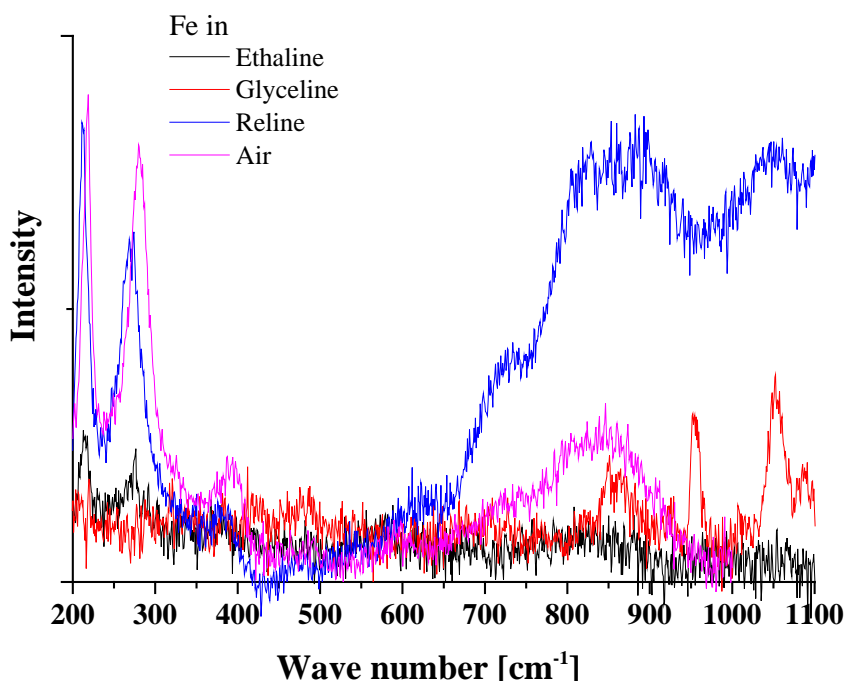
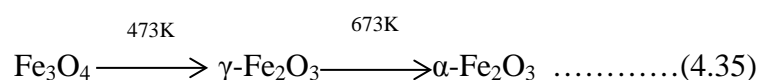


Figure 4-20: The Raman spectrum of mild steel tested in DESs and air.

Figure 4-20 shows the Raman spectra of mild steel corroded in different DESs and in moist air. From the figure it is obvious that some peaks are common in Glyceline Ethaline, Reline and air *i.e.* 212 -220 cm^{-1} . These peaks correspond to the presence of lepidocriocite which is often produced at the early stages of corrosion wherein oxygen supply is not limited. Figure 4.19 also shows some peaks between 284-322 cm^{-1} , 470-488 cm^{-1} , 575-597 cm^{-1} , 667 cm^{-1} , 954-1009 cm^{-1} and 1052 cm^{-1} in these liquids and air which are mostly related to the presence of goethite, lepidocriocite and ackaganite.^{1, 11, 22, 26, 28, 30-33}

However, as haematite possess peaks at around 226 cm^{-1} , 292-300 cm^{-1} and 806 cm^{-1} it is also thought that the haematite is exist in the corrosion products as well.^{1, 21, 22, 24, 25, 31, 33} It is unusual for haematite to form in a liquid unlike in air where it is common. If haematite is formed there are only two routes; either oxygen in the liquid is consumed as a result of a cathodic reaction and haematite is formed as a consequence of oxygen deficiency. Magnetite can thermally transform to maghaemite at about 473 K and then to haematite at 673 K in a

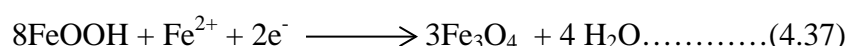
second route as shown in equation 4.35 but it is not possible at room temperature even with very high laser power.²¹



The presence of some peaks around 470-474 cm⁻¹ and 620-667 cm⁻¹ in both Glyceline and Ethaline are similar to peaks of maeghemite and magnetite at 460-510 cm⁻¹ and 662-675 cm⁻¹ this may arise from the fact that magnetite sometimes forms in the early stages of corrosion due to the air oxidation of green rust Fe(OH)₂ as shown in equation 4.36.¹



However, green rust has not been observed on any samples studied here so if magnetite or maeghemite have formed it is probably by a different mechanism from that shown above. As the metal samples were left in liquids for a long time in carefully sealed condition which reduces the chance of air getting into the samples another mechanism may play a role to form magnetite. One potential mechanism could be that shown in equation 4.37. In this case probably oxygen decreases overtime due to the cathodic reaction and this result in an alternative cathodic process other than equation 4.4:¹



When the bands are broad it means that the iron corrosion has occurred and the product has low crystallinity which makes the spectrum difficult to interpret.¹¹ A common band exists for feroxite, maeghemite, ferri-hydrate and magnetite at about 700 cm⁻¹.³¹ A broad band at around 710 cm⁻¹ is often observed for the atmospheric corrosion of iron.³⁴ Wustite is unstable under 843 K²⁴ therefore, it is not possible to exist at room temperature in any liquids studied here.

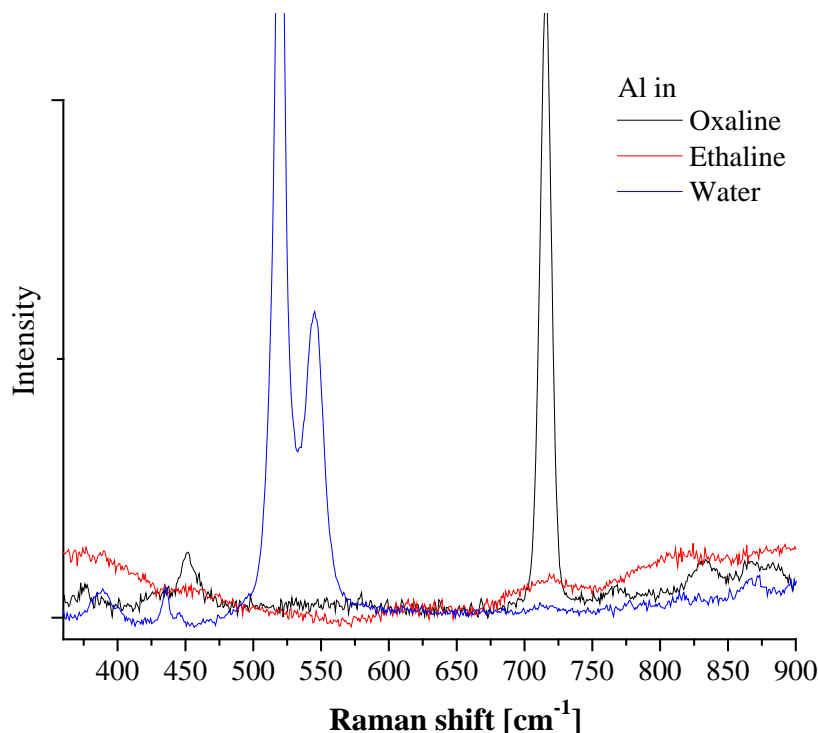


Figure 4-21: The Raman spectrum of aluminium tested in DESs and water.

Figure 4-21 shows the Raman spectrum of aluminium after corroding in DESs and water. Raman peaks in the range of $377\text{--}452\text{ cm}^{-1}$ are observed for oxidation products of aluminium which has been corroded in Oxaline, Ethaline and water. The peaks seem to be similar to the spectrum of $\gamma\text{-Al}_2\text{O}_3$ crystal studied before.²⁷ In this spectrum the light which entered the Al_2O_3 corrosion product via the (z) axis is then polarized in the (x) direction and the scattered light is polarized parallel to the (x) axis which is collected along the (y) axis.

Aluminium oxides are in a variety of structural forms including amorphous anodic alumina which contains (AlO_4 , AlO_5 , and AlO_6),^{36, 37} a quasi-crystal (θ , δ , η , γ - Al_2O_3) and crystalline structure (α - Al_2O_3).^{37, 38} This difference in crystal structure arises from O-Al-O bond angle differences which originated from the ionic character of the Al-O bond. To point out which band correlates to which crystalline structure it is important to recognize how the coordination number of cation influences the vibrational frequency of Al-O bonds. For Al corrosion products because the bond length is directly proportional to the coordination number whereas the vibrational frequency inversely correlated to the coordination number.^{38, 39} Hence as the coordination number is increased Raman peaks occur in lower frequency ranges. Raman peaks at 377 , 389 , 417 , 435 , 452 and 520 cm^{-1} for aluminium observed in liquids seem to be correlated to the condensed octahedral crystals of aluminium oxide AlO_6 which is considered as the most ordered crystal form.³⁸ Peaks at $716\text{--}720$ and $800\text{--}870\text{ cm}^{-1}$

in Ethaline, water and especially in Oxaline probably indicates the presence of tetrahedral Al-O containing structures.³⁸ Finally, as peaks are observed in both tetrahedral and octahedral ranges the corrosion layers are thought to be a mixture of both structures.

4.6 Conclusions

The corrosion rates for Fe, Ni and Al in Glyceline and Reline are small and remain almost constant overtime which is due to slow cathodic reaction rates resulting from different processes occurring due to differences in pH. Ethaline has variable corrosion activity toward different metals as a consequence of mass transport and higher chloride activity in addition to the acidity of the hydroxyl proton on ChCl. In Oxaline the corrosion rate for Fe and Al are high due to it being acidic. Ni, however appears to passivate due to the formation of an insoluble salt on the metal surface.

It is proposed that the corrosion products of iron in Ethaline to be iron glycolate which reacts slowly with oxygen from the air forming insoluble iron oxides. In Reline iron appears to produce complexes with urea or with ammonia which forms as a result of urea dissociation. Glyceline does not show any visible corrosion products even after 18 months which thought to be due to its neutrality resulting from hydrogen associated in both ChCl and glycerol hydroxyl groups. Iron does not corrode in dry mineral base oil however, when 1 wt% aqueous NaCl was added a significant amount of undissolved corrosion products is observed which precipitates on the surface of metal.

The corrosion products of Fe were studied using Raman spectroscopic measurements and were shown to contain a variety of products including Goethite (α -FeOOH) Akaganeite (β -FeOOH) Lepidocrocite (γ -FeOOH) and feroxyhite (δ -FeOOH). For Al the corrosion product is thought to be a mixture of amorphous aluminium oxides. From these studies it can be concluded that for most metals Glyceline is the most compatible lubricant as the corrosion rates with most metals is very low due to the non-acidic protons and therefore the slow cathodic reaction rate.

4.7 References

1. X. Zhang, K. Xiao, C. F. Dong, J. S. Wu, X. G. Li and Y. Z. Huang, *Eng Fail Anal*, 2011, **18**, 1981-1989.
2. V. Cicek and B. Al-Numan, *Corrosion Chemistry*, Wiley, 2011.
3. V. Cicek, *Cathodic Protection: Industrial Solutions for Protecting Against Corrosion*, Wiley, 2013.
4. R. G. Kelly, J. R. Scully, D. W. Shoesmith and R. G. Buchheit, *Electrochemical Techniques in Corrosion Science and Engineering*, Marcel Dekker Incorporated, 2002.
5. G. S. Frankel, *Journal of ASTM International*, 2001, **5**, 1-27.
6. E. E. Stansbury and R. A. Buchanan, *Fundamentals of Electrochemical Corrosion*, ASM International, 2000.
7. D. A. D. Ming-Kai Hsieh, Radisav D. Vidic, *Ind. Eng. Chem. Res.*, 2010, **49**, 9117–9123.
8. ASTM, *Annual Book of ASTM Standards*, ASTM International, West Conshohocken, PA, 2004.
9. R. B. Leron, D. S. H. Wong and M.-H. Li, *Fluid Phase Equilibria*, 2012, **335**, 32-38.
10. R. W. Revie, *Corrosion and Corrosion Control*, Wiley, 2008.
11. M. Criado, S. Martinez-Ramirez, S. Fajardo, P. P. Gomez and J. M. Bastidas, *Mater Corros*, 2013, **64**, 372-380.
12. A. P. Abbott, E. I. Ahmed, R. C. Harris and K. S. Ryder, *Green Chem*, 2014, **16**, 4156-4161.
13. E. Matijevi and S. Cima, *Colloid and Polymer Science*, 1987, **265**, 155-163.
14. J. Clark, *Calculations in AS/A Level Chemistry*, Longman, 2000.
15. C. D'Agostino, L. F. Gladden, M. D. Mantle, A. P. Abbott, E. I. Ahmed, A. Y. M. Al-Murshedi and R. C. Harris, *Phys Chem Chem Phys*, 2015, **17**, 15297-15304.
16. K. Elayaperumal and V. S. Raja, *Corrosion Failures: Theory, Case Studies, and Solutions*, Wiley, 2015.
17. E. P. Randviir and C. E. Banks, *Anal Methods-Uk*, 2013, **5**, 1098-1115.
18. A. P. Abbott, G. Capper, K. J. McKenzie, A. Glidle and K. S. Ryder, *Phys Chem Chem Phys*, 2006, **8**, 4214-4221.

19. A. P. Abbott, G. Capper, D. L. Davies, K. J. McKenzie and S. U. Obi, *J Chem Eng Data*, 2006, **51**, 1280-1282.
20. Q. Zhang, K. De Oliveira Vigier, S. Royer and F. Jerome, *Chem Soc Rev*, 2012, **41**, 7108-7146.
21. D. L. A. deFaria, S. V. Silva and M. T. deOliveira, *J Raman Spectrosc*, 1997, **28**, 873-878.
22. R. J. Thibeu, C. W. Brown and R. H. Heidersbach, *Appl Spectrosc*, 1978, **32**, 532-535.
23. E. Smith and G. Dent, *Modern Raman Spectroscopy: A Practical Approach*, Wiley, 2005.
24. E. Hazan, Y. Sadia and Y. Gelbstein, *Corros Sci*, 2013, **74**, 414-418.
25. I. R. Beattie and T. R. Gilson, *Journal of chemical Society A*, 1970, 980-986.
26. F. Dubois, C. Mendibide, T. Pagnier, F. Perrard and C. Duret, *Corros Sci*, 2008, **50**, 3401-3409.
27. S. P. S. Porto and R. S. Krishnan, *Journal of chemical physics*, 1967, **47**, 1009-1012.
28. N. Boucherit, A. H. L. Goff and S. Joiret, *Corros Sci*, 1991, **32**, 497-507.
29. J. D. Ramsey and R. L. McCreery, *J Electrochem Soc*, 1999, **146**, 4076-4081.
30. D. Neff, S. Reguer, L. Bellot-Gurlet, P. Dillmann and R. Bertholon, *J Raman Spectrosc*, 2004, **35**, 739-745.
31. A. Demoulin, C. Trigance, D. Neff, E. Foy, P. Dillmann and V. L'Hostis, *Corros Sci*, 2010, **52**, 3168-3179.
32. Renato Altobelli Antunes, I. Costa and D. L. A. d. Faria, *Materials research*, 2003, **6**, 403-408.
33. Sei J. Oh, D. C. Cook and H. E. Townsend, *Hyperfine Interactions*, 1998, **112**, 59-66.
34. D. Neff, L. Bellot-Gurlet, P. Dillmann, S. Reguer and L. Legrand, *J Raman Spectrosc*, 2006, **37**, 1228-1237.
35. T. Ohtsuka, *Mater T Jim*, 1996, **37**, 67-69.
36. Y. Oka, T. Takahashi, K. Okada and S. I. Iwai, *J Non-Cryst Solids*, 1979, **30**, 349-357.
37. R. Manaila, A. Devenyi and E. Candet, *Thin Solid Films*, 1984, **116**, 289-299.
38. P. V. Thomas, V. Ramakrishnan and V. K. Vaidyan, *Thin Solid Films*, 1989, **170**, 35-40.
39. P. TARTE, *SpectrochimActa*, 1967, **23A**, 2127-2143.

CHAPTER FIVE: MECHANICAL PROPERTIES AND ADDITIVE STUDIES

CONTENTS

5 LUBRICATION STUDIES

5.1	INTRODUCTION.....	127
5.2	FRICTION	127
5.2.1	<i>FRICTION COEFFICIENT</i>	128
5.2.2	<i>FRICTION COEFFICIENT RESULTS</i>	129
5.2.3	<i>WEAR AND WEAR VOLUME</i>	132
5.3	WETTABILITY	134
5.3.1	<i>CONTACT ANGLE</i>	136
5.4	SURFACE ENERGY AND INTERFACIAL TENSION.....	139
5.4.1	<i>THERMODYNAMICS OF WETTING</i>	140
5.4.2	<i>SURFACE ROUGHNESS</i>	142
5.5	ADDITIVE STUDIES	144
5.5.1	<i>SURFACTANTS</i>	144
5.5.2	<i>ADSORPTION OF SURFACTANTS</i>	146
5.5.3	<i>VISCOSITY INDEX</i>	147
5.5.4	<i>CONDUCTIVITY</i>	148
5.5.5	<i>DENSITY</i>	150
5.5.6	<i>CONTACT ANGLE</i>	151
5.5.7	<i>FRICTION COEFFICIENT</i>	152
5.5.8	<i>WEAR VOLUMES</i>	154
5.6	CONCLUSIONS.....	155
5.7	REFERENCES	157

5 LUBRICATION STUDIES

5.1 Introduction

Using lubricants between moving contacted surfaces is important in reducing energy and material loss arising from friction. Lubrication of surfaces can reduce energy consumption and extend the life of engines. It has been estimated that 30-50% of energy is expended and lost due to frictional forces during operation.¹

A major environmental focus is designing environmentally friendly lubricants. The hydrophobicity of oils makes them environmentally incompatible and this is considered as one of the most important reasons to study non-oil based lubricants.^{2, 3} Therefore, for a specific system a suitable lubricant needs not only a given mechanical durability but it should also have greener credentials than what it is replacing.¹ The increasing demands in lubricant specification particularly for automotive and aerospace applications have led to improvements in efficiency and performance.⁴

Nowadays formulated lubricants based on biodegradable materials for applications such as marine and industrial gear oil, hydraulic fluids and tractor transmission oils are becoming more common.⁵ In this chapter some DESs and some ILs have been evaluated as base lubricants and their performance characteristics are compared with the same properties of standard mineral base oil. In these studies no additives have been considered so that the characteristics of the base material could be considered. This clearly will not produce lubricants which can be compared with commercial products but it provides a baseline for comparison sake.

5.2 Friction

Friction is defined as a force resisting or hindering the relative motion between two contacting bodies. As friction is responsible for movement it can be either beneficial or detrimental depending on the application. High friction is important in applications such as braking, or tire traction on a road however, in engines or equipment having gears or bearings low friction is essential. The frictional force largely depends on the magnitude of the contact zone, the properties of the substrate, the pressure or load and the roughness of the surface (asperities) as well as the type of motion e.g. whether it is rolling or sliding.⁶⁻⁹

Originally, friction arises from a complex mechanical and molecular interaction between contacting bodies while they are in relative motion. The interaction will generate wear which is followed by frictional heat whereby in addition to energy loss it makes operative machine parts initiate failure. Generally there are two types of friction when two bodies are in contact, solid or dry friction is the case when bodies are in direct contact and fluid friction is the case when bodies are separated by a gaseous, liquid or solid medium. When some parts of the two contacting bodies are separated by fluid film and the rest is in direct contact the situation said to have mixed friction.⁷

5.2.1 Friction coefficient

Commonly to represent friction force a unit-less term friction coefficient (μ) is used which is given by;

$$\mu = F / N \quad \dots\dots\dots (4.1)$$

Where; F represents frictional force which two contacting bodies are undergoing in their relative motion and N represents the normal force pressing together the same two contacting bodies.

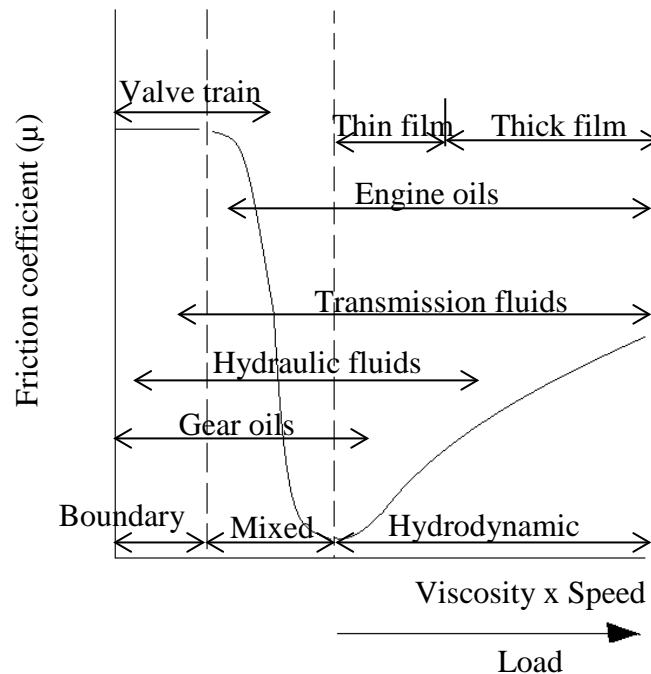


Figure 5-1: A Stribeck curve showing the relationship between the friction coefficient and the function (speed x viscosity/load).⁷

The friction coefficient is in the range of 0 to 1 and it has been found that the value is broadly variable according to the operational variables involved between contacting bodies.

The greater the value of μ the greater motion is hindered and the more energy is lost. There are two kinds of frictional constants; static or starting friction coefficient (force necessary to initiate sliding) and dynamic or kinetic friction coefficient (force required to sustain sliding). During cessation, contacting surfaces are welded together therefore the static or starting friction coefficient is generally larger than the so-called kinetic friction coefficient. The static friction coefficient increases with contact time because the bonding of contact points diffuses gradually overtime which rationalises the friction coefficient decrease with increases in sliding speed.^{7, 9}

Figure 5-1 shows that there are three different regions; boundary lubrication, mixed lubrication and hydrodynamic lubrication. Their possible occurrence for different applications are shown in the same Figure.¹⁰

5.2.2 Friction coefficient results

Figure 5-2 shows the measured friction coefficient for DESs and mineral base oil for steel/steel couples. The average frictional coefficients for various DES, ILs and mineral base oil with different sliding surfaces are studied here which summarised in Table 5-1. The data in the table are measured under the following condition; number of strokes are 2000, applied load was 30N and reciprocating velocity was 5mm/s at 293-298K.

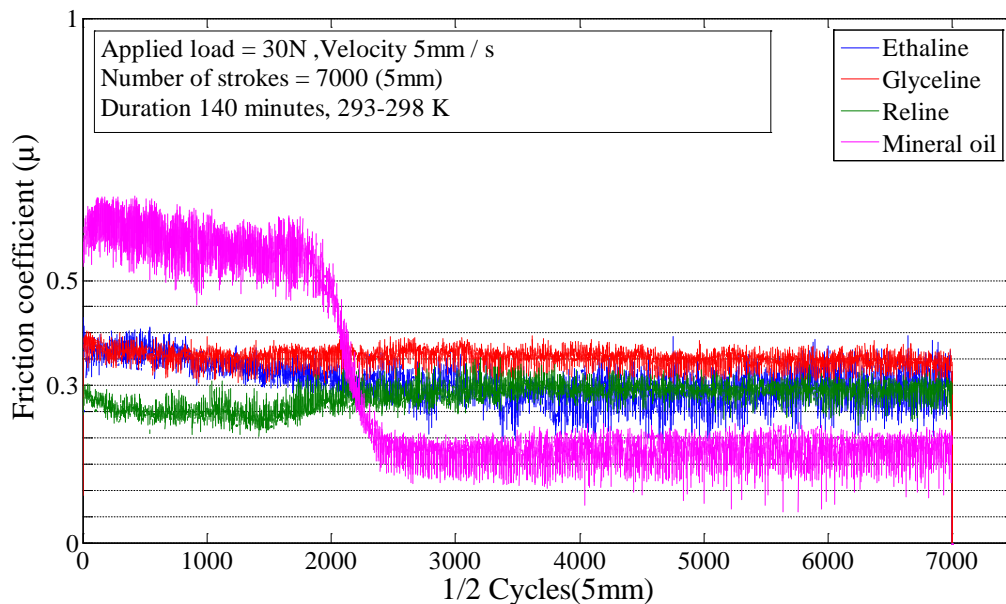


Figure 5-2: Friction coefficient graph of DES and mineral base oil on stainless steel substrate.

As shown in table 5.1 the friction coefficients for DESs are lower than for the mineral base oil with mild and stainless steel, but they are slightly higher values for the aluminium couples. However as shown in Figure 5-2 after 2000 strokes the behaviour of mineral base oil changed for steel/steel couples with a decrease in friction coefficient. The reason for this is not fully understood but it could be due to initial increased wear which produces a smoother surface which oil can wet better. In the beginning the oil may wet the surface poorly but it may become more entrapped with wear.

Previously it has been shown that adding quaternary ammonium electrolytes to ethylene glycol can significantly reduce the friction coefficient which shows that the ionic component has an interfacial preference which allows it to interact with the metal and produce an interfacial barrier. It was found that the friction coefficient was also dependent upon the concentration of quaternary ammonium salt and the optimum lubrication was obtained at the eutectic composition.¹¹

The efficacy of a liquid lubricant depends upon its interaction with a surface. For example a mineral base oil is made from a mixture of hydrocarbon molecules including saturates (normal straight chains or branched molecules), naphthenic molecules and some aromatic hydrocarbons. The interactions of these kinds of molecules with the metal surface are in general quite weak comprising only van der Waals interactions and do not guarantee strong adhesion of the hydrocarbon to the surface. Consequently, the separation of surfaces from each other by additive free mineral base oil is only possible for lightly loaded surfaces due to the ease of removing the liquid from the surface.

In contrast to the hydrophilic molecules in mineral oils, DESs and ILs should have much stronger interactions with most metallic surfaces. The inter-molecular and inter-ionic interactions in DESs are much larger than the van der Waals attractive forces into mineral oils. The presence of polar functional groups such as OH, CONH₂ and COOH in DESs will enable adsorption on the surface through either by hydrogen bonding or chemical reaction with surface consequently forming a thin layer of a lubricant on the surface and reducing friction and wear as well.⁷

In addition to the above discussion, the presence of high chloride content in DESs, could change any surface films and affect the way that the liquid interacts with the surface during the wear test. The abrasion produces fresh and active surface atoms which come into contact with the liquid. This kind of reaction may cause the formation of a tribo-film having low shear strength. The formation of this kind of films is considered as requirements of

lubricants to provide during the service.^{7, 12} For example a chemical reaction between chloride and copper or copper containing compounds yields CuCl and CuCl₂. Furthermore, alloys containing chromium such as stainless steel are producing CrCl₃ which are stable up to 973 K to protect the surface from wear.¹³

Studies in pure imidazolium based liquids have shown that the metal liquid interface is highly structured with most probably alternating layers of cations and anions.^{14, 15} The ability of ammonium based ILs to form structured layers at an interface depend upon the type of cation; it's orientation in the interfacial layer, the surface charge and the type of surface.^{14, 16}

Table 5-1: Friction coefficient data of different contact pairs under 30 N load and at 298 K.¹⁷

ILs	Friction coefficient				
	Substrate metals against stainless steel				
	Al	Bronze	Cu	Mild Steel	Stainless Steel
Ethaline	0.15	0.58	0.59	0.30	0.31
Glyceline	0.55	0.40	0.45	0.28	0.35
Reline	0.31	0.26	0.21	0.32	0.30
Oxaline	0.25	0.29	0.18	0.38	0.30
Emim SCN	0.29	0.33	0.23	0.47	0.28
Emim HSO ₄	0.30	0.42	0.20	0.48	0.23
Emim EtSO ₄	0.43	0.50	0.30	0.22
Emim OAc	0.45	0.50	0.28	0.23
Base oil	0.12	0.23	0.37	0.40	0.55

In a similar way as ammonium based ILs are acting to form a multi solvation layer on the charged surfaces^{14, 18} it is thought that DESs, will form a strong solvation layer on high surface energy surfaces such as mild steel and stainless steel. Even though the DESs were carefully prepared they still contain some water (typically 0.05 to 1 wt%).¹⁸ In general the DESs wet the surfaces well which can be seen from their lower friction coefficient values in comparison with mineral base oil for the same surfaces. The exception seems to be

aluminium where they are not as good as mineral oils. The product of this electrostatic interaction between DESs and high surface active metals yields more tightly bound more enriched and more compact ionic layer on the surface which consequently provides better lubrication.^{15, 19}

Although surface roughness has an important role as a partial determinant in lubrication ability, the cation in association with the surface activity and surface structure also play a significant role.¹⁸ It is possible to conclude therefore that wetting ability alone is not enough to decide about how the surface will be lubricated because as will be shown below the wettability of mineral base oil is the better for all surfaces. The oil based lubricant is not, however always the best at minimizing friction.

5.2.3 Wear and wear volume

Unless a lubricant is used between two contacting bodies while they are in a relative motion, a gradual removal of the surface takes place as a result of friction and this is known as wear.²⁰ This happens due to the fact that most surfaces are not perfectly smooth but are covered with irregularities of different shapes and sizes known as asperities. In addition most surfaces have a significant presence of adsorbed materials or variability of surface layers. Wear depends in addition to the normal load and sliding velocity together with the properties of a material under investigation.²⁰ Wear volume (V) for a scratched surface is related directly to the variables of the experiment such as normal applied load (p), the sliding distance (d) number of cycles and wear coefficient (k). However it is inversely related to the hardness (h) of a substrate as shown in equation 5.2.²¹

$$V = k. p. d / H \dots \dots \dots (5.2)$$

The anti-wear number is commonly used to define the properties of a lubricated surface.^{20, 22}

$$\text{Anti-wear number (AWN)} = - \log k \dots \dots \dots (5.3)^7$$

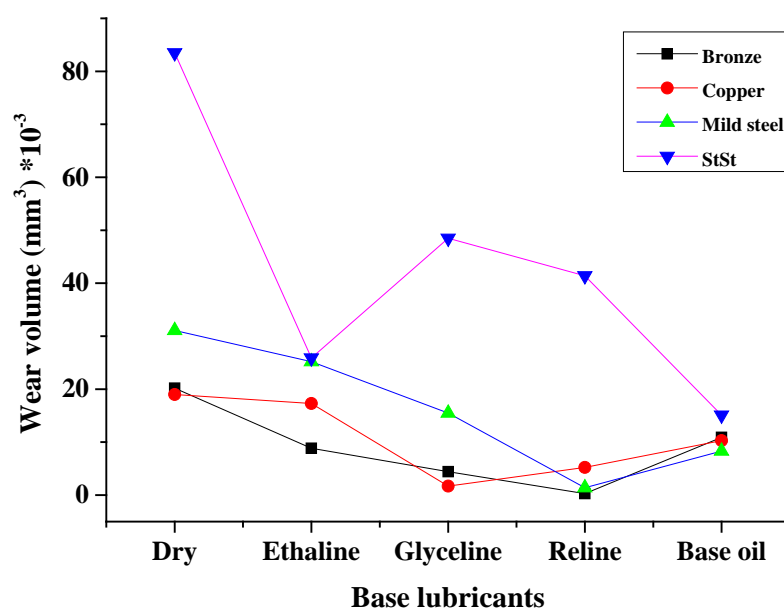


Figure 5-3: The wear volume of scratched dry and lubricated surfaces

Figure 5-3 shows the wear volume data for scratched surfaces after measuring the friction coefficients. The figure shows that the wear volume is significantly reduced for the lubricated surfaces compared to the dry couples.

Table 5-2: Anti-wear number for dry surfaces and compared with using lubricants.

Lubricants	Anti-wear number (AWN)			
	bronze	copper	mild steel	stainless steel
dry surface	4.68	4.86	4.50	3.87
Ethaline	5.03	4.90	4.59	4.38
Glyceline	5.33	5.91	4.80	4.11
Reline	6.53	5.42	5.85	4.18
base oil	4.94	5.13	5.07	4.61

In some cases the wear volumes for the DESs are lower than for the mineral base oil but this is specific to the metal couples. The wear volume should be inversely proportional to the lubrication behaviour of a liquid and this is observed for all of the metal surfaces except

for stainless steel in which the wear volume for mineral base oil is less than that for most DESs.

Since lubrication is a complex process it is not possible to decide which single property determines the lubrication behaviour of a liquid over all surfaces. For each liquid and solid the interactions will be different in each case. Table 5-2 lists the anti-wear number for the DESs and mineral base oil which were calculated using equations 5.2 and 5.3.

The anti-wear number for all liquids is under 6 except for Reline with bronze. This means that these liquids, just like the mineral base oil, are not effective enough to do the role of formulated oil. Therefore to be acceptable as a lubricant anti-wear agents and friction modifier additives are necessary to improve their lubrication efficiency. The wear volume is generally the highest between pairs of contact materials which are the same. In general the wear volume is reduced between dissimilar materials. It is also clear from the table that the anti-wear number for steel/steel contact is lower than any other couples. This is due to adhesive wear which is always worse for identical pairs as a result of strong affinity of the metals to each other.⁷

5.3 Wettability

The topic of wetting has received significant interest from both a fundamental and application point of view. The wettability of solids has a significant role in processes like lubrication, adhesion, detergency, liquid coating, spray quenching, printing, treatment of waste water and oil recovery.²³⁻²⁸ There are a number of techniques employed to assess wettability of liquids which includes, two phase separation, micro-flotation, bubble pickup and contact angle measurements.^{29, 30} Wettability is usually characterised by measuring the contact angle of liquid-solid contact.

The wettability of surfaces is favoured for some applications and not favoured for others. For instance, in the case of printing inks, stain repellent fabrics, seals or gaskets and oil recovery, surface wetting is undesirable. On the other hand, in processes such as lubrication, detergency, emulsion and coating surface wetting is needed.^{27, 30, 31}

It has been suggested that if the surface tension of a liquid is lower or equal to that of the substrate solid, the liquid should wet the surface easily. Accordingly, in some applications, active surface agents are incorporated into a liquid either to enhance spontaneous wetting of solid surfaces or to terminate foam formation due to lowering of the

surface tension of a liquid. For instance, polydimethyl siloxane is added to mineral base oils for this purpose.³²

As shown in Figure 5-4, when the liquid-solid interface is close to zero (surface tension of liquid = surface tension of solid) the liquid spreads spontaneously over the solid surface.³³ This situation is referred to as ‘total wetting’ because the spreading parameter (S) is greater than zero.^{29, 34, 35}

$$S = \gamma_{sv} - (\gamma_{sl} + \gamma_{lv}) > 0 \dots\dots\dots (5.4)$$

or

$$\gamma_{sv} - \gamma_{sl} > \gamma_{lv} \dots\dots\dots (5.5)$$

This means that when $\theta = 0$ the drop of liquid has a tendency to spread entirely on the surface as in the case of silicon oil which spreads on a number of surfaces such as steel, plastics and glasses.³⁶ The reason behind this stems from the fact that the surface tension of silicone oil is very low *c.a.* 20 mNm^{-1} . Therefore, to improve the wettability of liquids surfactants are added to mineral base oil or paints to reduce liquid-vapour interfacial tension. This situation is energetically favourable and a solid surface will be covered by a thick layer of liquid.³⁴ On the other hand, if

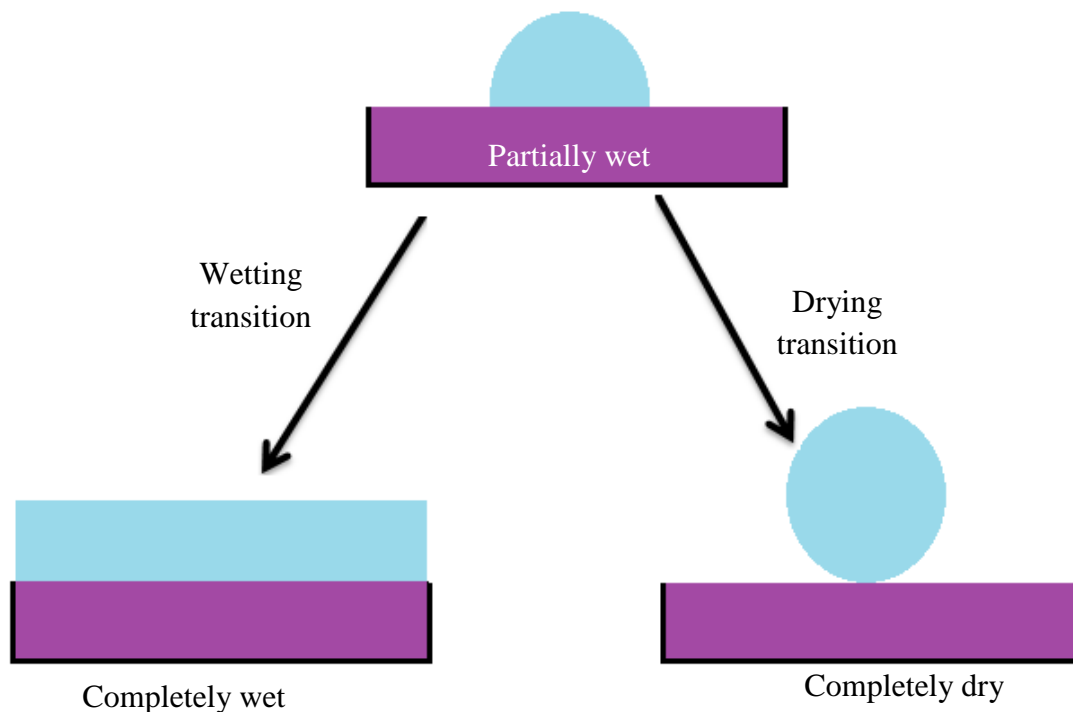


Figure 5-4 : Different possible wetting situations.²⁷

$$\gamma_{sl} - \gamma_{sv} > \gamma_{lv} \dots \dots \dots (5.6)$$

This means that a drop of liquid will be sitting on the surface (Complete drying situation) and have a contact angle of 180°. ³⁶ However, there is no real system which realises this kind of situation even with water on a surfaces with low wettability e.g. PTFE, a contact angle of 120°-130° is observed. ³⁶

Consequently the spreading parameter is usually less than zero;

$$S = \gamma_{sv} - (\gamma_{sl} + \gamma_{lv}) < 0 \dots \dots \dots (5.7)$$

Therefore either partial wetting is the case where the contact angle is smaller than 90° or non-wetting happens where the contact angle is larger than 90° and the liquid does not spread freely over the solid surface and remains as a droplet which finally reaches to equilibrium formula in which it is possible to measure its contact angle. ^{24, 34, 36}

5.3.1 Contact angle

Mostly it is seen that when a liquid droplet is placed on the surface of a solid it will not spread on the surface but remains as a drop owning a certain contact angle between the liquid and solid phases. ³⁷ The angle made between intersection of solid-liquid and liquid-vapour interfaces as shown in Figure 5.5 is defined as the contact angle. The value of the contact angle is governed by the equilibrium between interfacial tensions of (solid-liquid (γ_{sl}), solid-vapour (γ_{sv}) and liquids-vapour (γ_{lv})). These tensions are related to each other by Young's equation. ^{23, 29, 38}

$$\gamma_{sv} = \gamma_{sl} + \gamma_{lv} \cos \theta \dots \dots \dots (5.8)$$

The Young equation is only valid for ideal surfaces (homogeneous with no roughness). A new equilibrium will arise in the case of any changes in theses stabilities. ^{23, 29}

Contact angles can be measured in different ways such as methods based on photographs or projected images or indirect measurements based on calculations of sessile drop measured mass or dimensions. ^{24, 29} There is an inverse relationship between the contact angle and wettability; if the contact angle is smaller than 90° (partial wetting) it means the surface has a high wettability and contact angles bigger than 90° imply a low wettability (non-wettability situation). ^{24, 28}

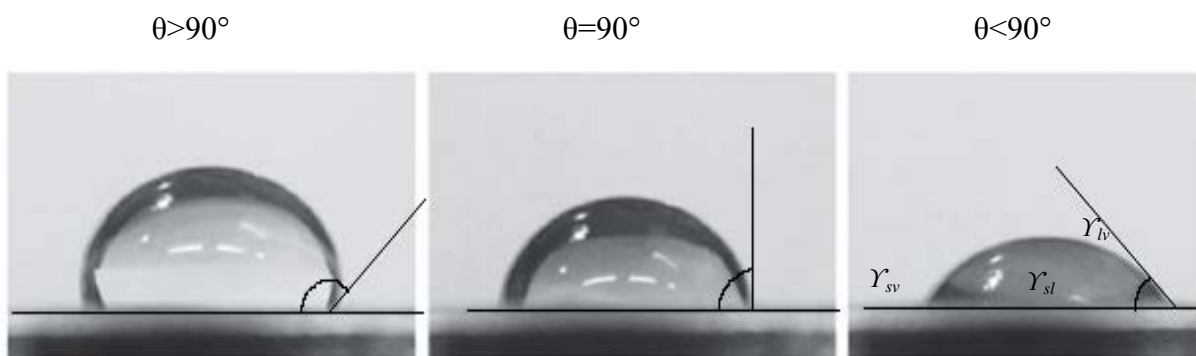


Figure 5-5 : Types of contact angles (θ .)

The concept of wettability and its influence on wear results was tested by measuring the contact angle of different metals and alloys with different liquids. The value of contact angle depends on the surface tension of a liquid, the solid surface energy and the interfacial tension between the solid and the liquid. A common mode of assessing contact angle is to observe the drop in profile from the side.

Table 5-2 shows contact angle and surface tension data for different DESs, ILs and mineral base oil on different substrates. The data obviously illustrates that the contact angle is governed mostly by the surface tension of a liquid more than other factors. Since DESs have high surface tensions they show higher contact angles than other ILs and mineral base oil which means their wettability should be lower than oils and other ionic liquids. Furthermore, since Glyceline and Reline are more viscous than Ethaline they are show contact angles much bigger than contact angles of Ethaline even though their surface tensions are similar. Therefore, if they provide better lubrication to some extent it should be related to some degree to their ability to provide thicker films.

In this study obviously if only the surface tension is considered as a determinant for contact angle and friction constant, DESs must show lower lubrication behaviour than other liquids. However, as DESs are providing better lubrication than mineral base oil under these conditions even if mineral base oil has a better wettability. Therefore, this difference in behaviour is thought to be related to some extent to surface activity and lubrication film quality.

Table 5-3 : Contact angle of different liquids with different metals and alloys at 298 K.¹⁷

Liquids	Surface tension /mN m ⁻¹	Contact angles / °				
		Al	Cu	Bronze	Mild Steel	Stainless Steel
Ethaline	50	85.2	78.2	86.6	75.0	74.5
Glyceline	59	100.7	92.4	106.9	95.9	95.5
Reline	58	111.9	102.9	94.3	103.1	80.1
Oxaline	56	76.5	28.7	30.4	40.8	51.7
C ₂ mim SCN	38	61.4	64.3	50.3	60.4	68.7
C ₂ mim HSO ₄	48	85.2	58.3	77.6	57.2	71.2
C ₂ mim C ₂ H ₅ SO ₄	45	52.0	62.4	70.9	56.4	62.4
C ₂ mim CH ₃ COO	45	67.9	62.2	57.3	54.9	69.2
Base oil	31	7.6	12.8	18.0	11.7	11.3

The contact angle is the angle which is made between a liquid and the surface it is in contact to. This angle is governed by the equilibrium between how strong liquid molecules are bound to each other and how these molecules can spread on the surface. In mineral base oil the wetting ability is not controlled by the strong interaction between oil and the surface but rather due to the weak intermolecular force (low surface tension) the liquid can spread over the surface and this does not necessarily guarantee a strong interaction with the surface.

For DESs and ILs the strong interaction between these liquids with the surface means that their spreading is mostly governed by the strong affinity toward the surface making a stronger protecting lubricant film than for mineral base oil. In conclusion the contact angle and wettability of any liquid with a solid does not mean that it is a good lubricant as the strength of the interaction with the surface and the viscosity-temperature relationship also need to be considered.

5.4 Surface energy and interfacial tension

To achieve an appropriate lubricating film along with suitable tribological properties it has been recognized that knowledge of the surface energy is important to better understand the interaction between the liquid and solid phases which characterise the wetting ability.

The surface energy is considered as one of the most important properties of metals and alloys so it is vital to understand surface phenomena such as growth rate, catalytic behaviour, crystal faceting, vacancy formation, crack propagation, adhesion and wetting.^{39, 40} In comparison to atoms located in the bulk of metals, surface atoms have fewer neighbouring atoms therefore; their physical properties including surface activity are quite different from atoms inside the bulk.⁴¹⁻⁴³

Surface energy is defined as the energy required to yield a new surface area unit and hence is proportional to the change in energy (number of broken bonds) which originates from the process of solid partition in which the solid separated into two cuts along a plane for a given area.⁴¹ In order to achieve good wetting it is important to reduce the interface energy by using solids and liquids which have a strong affinity to each other.⁴⁴

The surface energy for pure metals are taken from the literature⁴⁵ however, the surface energy data for alloys have been calculated by considering the data of pure metals and their elemental composition in alloys. Figure 5-6 shows the calculated interfacial energy determined using equation 5.8 for liquids and metals / alloys in this study. Here, the observed contact angle, surface tension of liquids and calculated surface energy of metals have been taken into consideration for calculations. Figure 5-6 shows that the interfacial energy between surfaces with mineral base oil generally is slightly higher in comparison with other liquids.

This is thought to be mostly related to the composition and polarity of surfaces which are reconcile more with DESs than mineral base oil because lubricated surfaces are often covered with a polar film of metal oxides which have adhesion affinity more with polar liquids than nonpolar liquids such as mineral oil.^{43, 46, 47} Gravity will also have an effect on wetting because more dense liquids will adsorb better on surfaces than less dense liquids.⁴⁸

The friction data in Table 5-1 suggests that the high surface energy of iron and iron based alloy in combination with the high surface tension of DESs enables them to provide better interactions and hence better lubrication with these surfaces than mineral oil

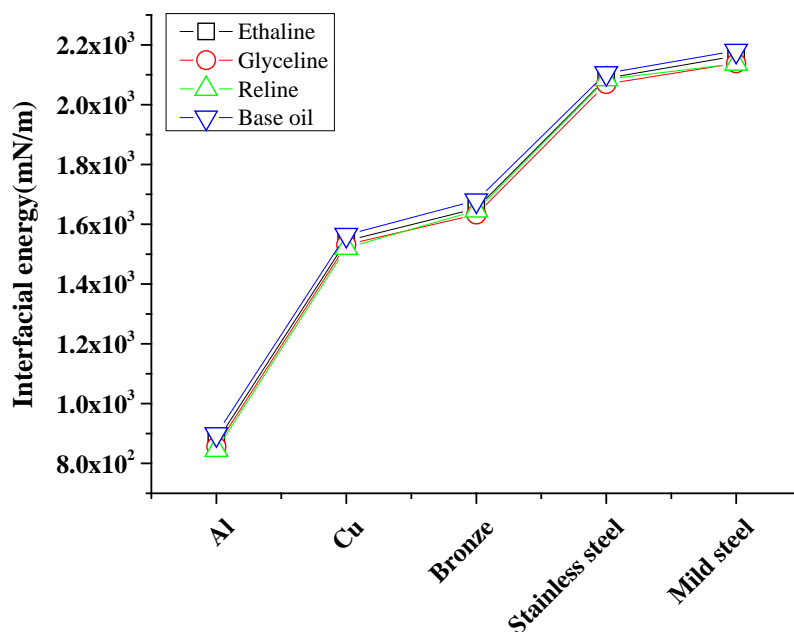


Figure 5-6: Interfacial tension between liquids and surfaces.

Figure 5-6 shows that aluminium has a low surface energy whereas iron based alloys have a higher surface activity which is an indicator of the hydrophilicity of the surface.⁴⁵ It seems logical therefore that ionic liquids with high surface tensions and high contact angles should show have improved friction coefficients over base oils with iron based alloys whereas the reverse is the case for aluminium and copper alloys. In summary, it could be concluded that for a lubricant to work effectively it is necessary to show both strong interactions with the lubricated surface and it should also possess suitable bulk properties. Both mineral oil and ionic fluids (DESs or ILs) have the correct thermophysical properties but for different reasons. However, to interact strongly with the surface mineral base oils have to be mixed with film forming additive which is not always necessary for DESs.

5.4.1 Thermodynamics of wetting

The Gibbs energy of wetting which is also the energy of immersion⁴⁹ could be used to determine if the wetting of a surface is favourable by a particular liquid. To do this it is possible to combine equations of Gibbs energy of immersion and Young's equation to extract a fundamental and straightforward equation to predict wetting process from knowledge of only contact angle and surface tension of a liquid as follows;

The equation of Gibbs energy of wetting is

$$\Delta G = \gamma_{sl} - \gamma_{sv} \dots\dots\dots(5.9)^{50}$$

And from Young's equation

$$\gamma_{sl} - \gamma_{sv} = -\gamma_{lv} \cos\theta \dots\dots\dots (5.10)$$

Therefore,

$$\Delta G = -\gamma_{lv} \cos\theta \dots\dots\dots (5.11)$$

Equation 5.11 is a fundamental equation used to predict liquid/solid wetting.

Table 5-4 shows the Gibbs energy data for some DESs and mineral base oil on different surfaces. It is worth noting that there is a considerable variability in data of DESs. Ethaline shows similar negative Gibbs energy as mineral base oil which means their wettability occurs spontaneously which is mostly due their low viscosity in comparison with Glyceline and Reline. Ethaline and mineral oil have viscosities six times lower than Glyceline and Reline therefore their spreading over the surface is much easier.

Table 5-4: Gibbs energy of wetting of DESs and mineral base oil on different surfaces.

Substrates	Gibbs energy of wetting (mJ m ⁻²)			
	Ethaline	Glyceline	Reline	Base oil
Al	-4.2	11.0	21.6	-30.7
Cu	-10.2	2.5	12.9	-30.2
Bronze	-3.0	17.2	4.3	-29.5
St. Steel	-13.4	8.9	-10.0	-30.4
Mild steel	-12.9	11.6	13.1	-30.4

This implies that the adhesive force for mineral base oil and Ethaline with the surface is stronger than the cohesive forces among molecules. On the other hand for Glyceline and Reline the reverse is the case. Surface wetting of Ethaline and mineral oil is better than Reline and Glyceline however the two latter liquids are able to provide enough lubrication film thickness to separate contact couples much better than Ethaline and mineral base oil due to their higher viscosity.⁷

5.4.2 Surface roughness

Surface roughness can have some effect on the contact angle and wettability of a surface thus affecting lubrication phenomena. Moreover, for contacted surfaces in relative motion, if the surfaces are not perfectly smooth it is only the contacting asperities which represent the real area of contact between two surfaces and this consequently affects the overall coefficient of friction results.^{7, 21, 51}

To illustrate the importance of roughness on the lubrication process especially for applications such as in gear failure studies, the film thickness necessary for lubricant is given by equation 5.12. The so-called Dowson and Hamrock's equation⁵² is used to correlate lubricant film thickness and average surface roughness.^{7, 22}

$$\lambda = \frac{h_o}{\sigma} \dots \dots \dots (5.12)$$

Where: (λ) is the film thickness, (h_o) is the thickness of lubrication film and (σ) is the average roughness of combined surfaces. From equation 5.12 it can be seen that if $\lambda \leq 1$ it means that the contact occurs and the lifetime of surface is reduced and the lubrication is considered as boundary lubrication because asperities will be in direct contact. If λ is between 1 and 3 then mixed lubrication is the case. Finally, if λ is between 3 and 10 then hydrodynamic lubrication will occur.²² Therefore, the knowledge of λ is important as it enables the type of lubrication to be defined.

Since the surfaces of the metals/alloys used in this study have different roughness and hardness values it is not possible to make a direct comparison between all these surfaces. Consequently, the effect of surface roughness on wear volume and wear area for only one surface is investigated here. It must be pointed out that the effect of roughness on friction coefficient was not observed here which is in agreement with other studies carried out for other given kind systems.⁵³⁻⁵⁵

Figure 5-7 shows the effect of using different surface roughnesses on wear volumes and wear areas for lubricated steel /steel couples with Glyceline under 30 N applied load for 35 min. with a sliding velocity of 5 mm s^{-1} using a 5 mm stroke length. The figure shows that the wear volume and wear area decrease gradually with decreasing average surface roughness down to a surface roughness of 0.7 to $0.85 \text{ }\mu\text{m}$.

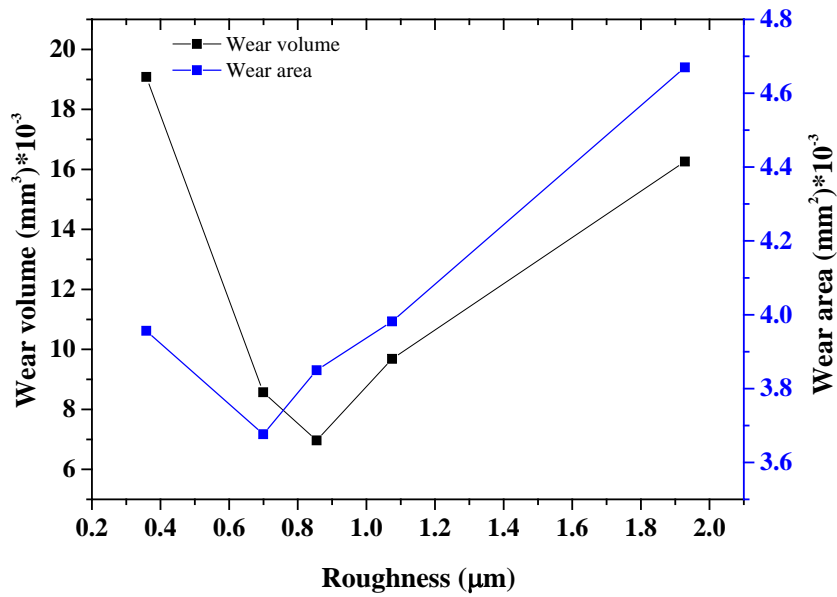


Figure 5-7: Wear volume and wear area as a function of surface roughness of mild steel.

When the surface roughness is less than $0.7 \mu\text{m}$ the wear volume and wear area have increased. The change in wear as a function of roughness could be explained in terms of the ability of a liquid to form thicker lubrication film than the average surface roughness which is depend strongly on the viscosity of a liquid and the surface roughness. For rough surfaces when the local load acting upon asperities is higher than the surface yield stress as a result of plastic deformation, asperities will become flat and causes more adhesion to occur because the contact area between contact couples has increased. This is followed by the formation of welded junctions as a result of high pressure on these areas which becomes much difficult to separate from each other without transfer of one surface with the other.⁷

In contrast, for very smooth surfaces on one hand the contact area is already high while on the other hand, there is no chance for a liquid to stay on the surface because there are not enough asperities or groves to entrap liquid.⁵⁶ Here only cohesive forces are present to bind liquid to the surface therefore, higher wear volumes occur for very smooth surfaces.

Finally, for intermediate surface roughness local hydrodynamic lubrication is provided by trapping some lubricant within space between asperities which explains why some roughness is necessary for better lubrication to occur.⁵⁷ Surface roughness does enable a physical interaction between surfaces with the liquid through trapping of a liquid film within surface irregularities however this is not enough for a lubricant to sufficiently lubricate

the interface. It does however provide some help for a liquid to be stay on the surface for very low loaded systems which is not compensate for the low adsorption strength between the lubricant and the surface.

5.5 Additive Studies

The use of lubricating oils on a large scale dates back to the 1860s following the first extraction of crude oil. Improvements in lubricant properties only really started in the early 20th century when the fatty oils were added to mineral base oil in order to improve its lubrication under loads. In the 1930s the use of additive became common in military use with the development of faster and more compact engines during and after the Second World War.⁷

Based on their structural characterization or their functions, additives are classified into film forming agents, deposit control/stabilizers, polymeric additives and miscellaneous additives.¹⁰ The behaviour of additives in lubricants is a very complex topic and is outside the scope of this study. In this chapter, the effect of just one type of common additive, surfactants, will be addressed. These were chosen because the properties of surfactant aggregates will be dominated by the charge of the head-group and this could change in an ionic medium. The study uses two common surfactants; sodium dodecylsulfate (SDS), an anionic surfactant and cetyltrimethylammonium bromide (CTAB), a cationic surfactant. Both of these are studied in Ethaline, Glyceline and Reline. The effect on the viscosity index, electrical conductivity, density, wettability, friction coefficient and anti-wear number for steel/steel couples are covered.

5.5.1 Surfactants

Surfactants as amphipathic and surface active compounds are used in a number of important applications such as in lubrication, cleaning, detergents, corrosion inhibition, pharmaceuticals, emulsifications, petroleum prospecting and flotation agent.⁵⁸⁻⁶⁰ Their importance comes from the fact that they are able to adsorb at various interfaces. Consequently, the formation of surfactant films at the interface between solid and liquid have been studied in detail.^{58, 59} In lubrication surfactants play a multi-functional role because they are able to solubilizing polar and non-polar constituents, disperse debris, prevent foam formation and reduce friction and wear.¹⁰

Surfactants are able to produce different meta-stable aggregate structures within the solution and different structures at the interfaces.^{12, 58, 61, 62}

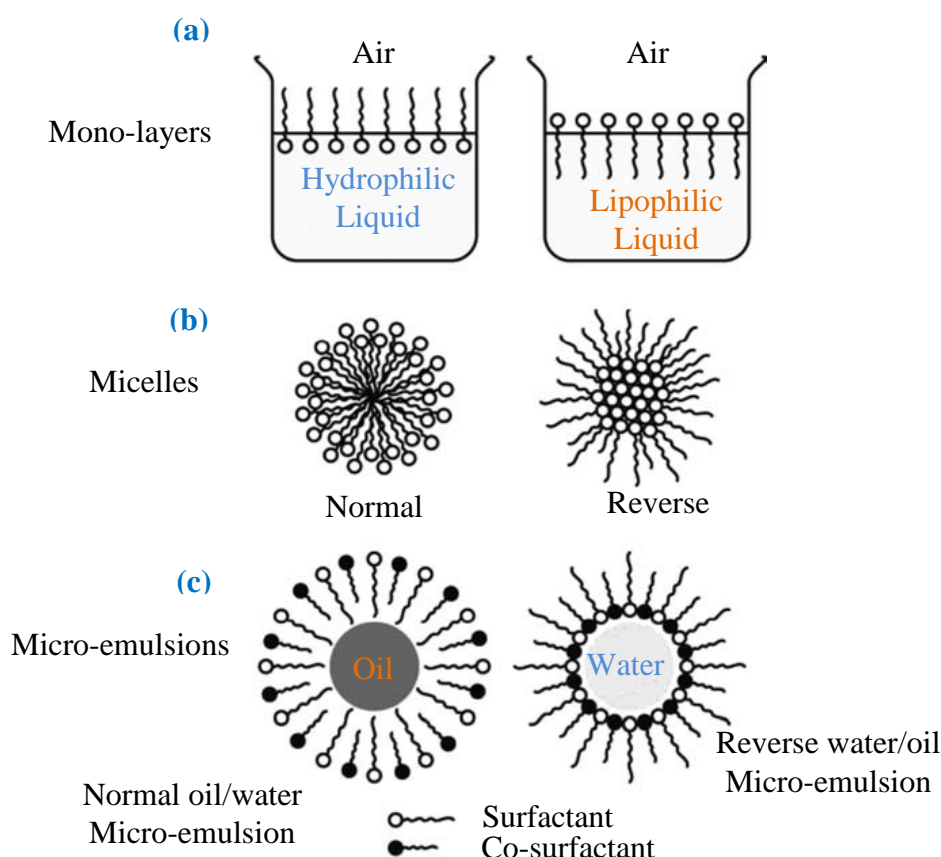


Figure 5-8: Microstructures of surfactant assemblies in solution: (a) monolayers, (b) normal and reverse micelles, (c) micro-emulsions.¹⁰

Figure 5-8 shows common aggregate structures of surfactants in aqueous and non-aqueous liquids. It will be assumed that aggregate structures are formed in DESs with inclusion of surfactants, their structure thought to be more similar to what forms in aqueous based liquids because they are entirely miscible with water and obviously their intermolecular forces should be altered considerably. The type and the number of these assembly structures depend on the size of both hydrocarbon tail and polar group since the interaction of surfactant with the liquid depends significantly on the variability of both groups.

5.5.2 Adsorption of surfactants

Adsorption of surfactant molecules at the solid-liquid interface is affected by a number of factors such as the structure of surfactant and its concentration, the pH of a medium and the presence of other additives.⁵⁹ The change in Gibbs energy in aqueous solutions containing surfactants has been found to be negative which means that micelles occurred spontaneously.¹²

Addition of surfactant to a liquid causes the change in equilibrium Gibbs energy as a result of the change in Gibbs energy for all components in the system. Among factors which are thought to contribute to the change in equilibrium energy change are the various surfactant-solvent, surfactant-surfactant and surfactant-surface interactions.^{12, 62}

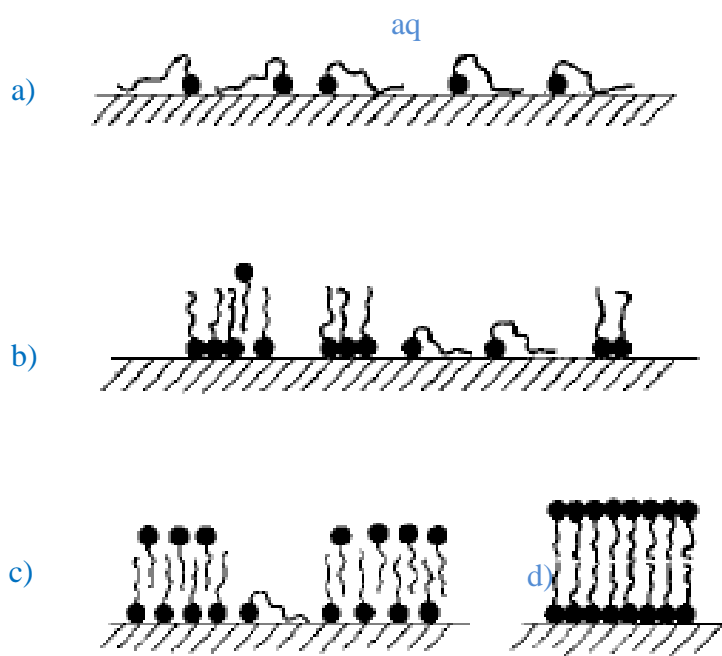


Figure 5-9: Organisation possibilities of ionic surfactant adsorbed on hydrophilic substrate, a) low concentration, b) intermediate concentration and c) hemi-micelle and d) non-interpenetrating bilayer.⁶³

Figure 5-9 shows an example to illustrate how the adsorption of surfactant on polar surfaces occurs as a function of surfactant concentration. Here when the concentration is low Figure 5-9a surfactant molecules are isolated and the polar head of the molecules are bound to the oppositely charged groups of the surface and the hydrocarbon chain is close to the surface.

At higher concentration, Figure 5-9b the hydrocarbon chain takes a position perpendicular to the surface and associates with other neighbour chains to reduce the contact with water. In the region where the concentration is high Figure 5-9c the molecules are organized to a hemi-micelle shape which known contains some molecules antiparallel with other adsorbed molecules and subsequently decreases the contact of hydrocarbon tail for both adsorbed and antiparallel with molecules water. Finally, for large polar head surfactants Figure 5-9d the molecules in the second layer do not penetrates the first layer and a bilayer is formed.⁶³

5.5.3 Viscosity index

To improve the durability and efficiency of an engine it is important to take into consideration how additive packages affect all of the properties of a lubricant.⁶⁴ There are a number of macroscopic interfacial properties influenced significantly by the association of surfactant's molecular interaction within monolayer and multilayers such as lubrication, wetting, stability and cohesion as average film properties and transport properties such as diffusion of ions within the layer.⁶⁵

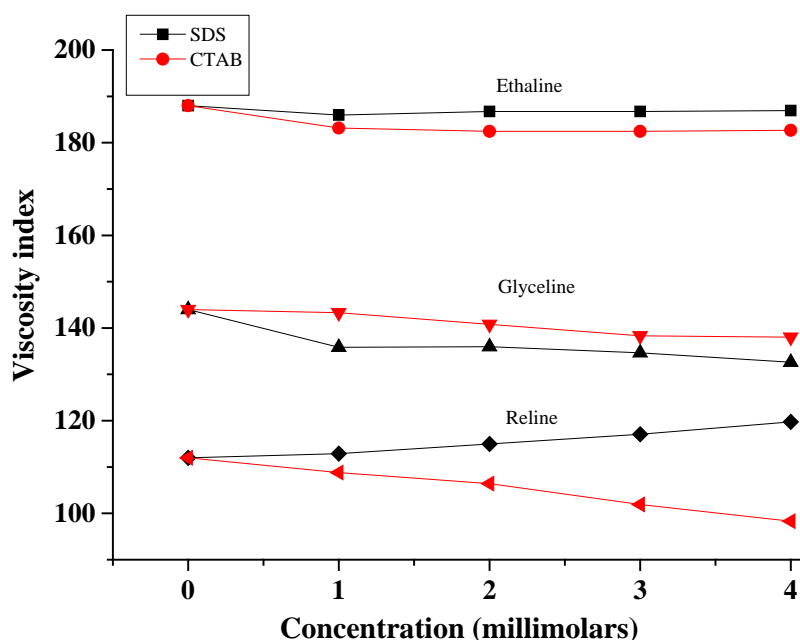


Figure 5-10: Viscosity index change as a function of concentration of surfactant in Ethaline, Glyceline and Reline.

In addition to interfacial properties, inclusion of surfactant causes some changes to the bulk properties of a liquid, due to changes in intermolecular forces.¹² Here, the interaction between a surfactant and a solvent is considered predominantly to be responsible for the change in viscosity of DESs.

Figure 5-10 shows the change of VI as a function of molar concentration for 1 to 4 millimolar (mM) of SDS and CTAB in Ethaline, Glyceline and Reline. From the figure it is shown that the viscosity index of Ethaline, Glyceline, and Reline are reduced by the addition of CTAB and the reduction is continued with increase in concentration.

The reduction in VI by addition of surfactant is thought to happen due to the breakdown of intermolecular force in these liquids as a result of formation of surfactant aggregations which subsequently results in the decrease of attraction force among ions and molecules especially at high temperature. In other word high VI means the viscosity which resulted from strong intermolecular force in DESs is not going to be change considerably as a function of temperature however, addition of CTAB minimizes the attractive forces among molecules and hence the change in viscosity will be higher at higher temperature.

Similarly, addition of SDS to Ethaline and Glyceline has a similar effect to CTAB however, for Reline the addition of SDS results in an increase in the viscosity index. This means that the interaction between SDS and Reline is different to that observed in Ethaline and Glyceline. The behaviour of surfactants in DESs has previously been studied by Azam who studied the surface tension in these two surfactants in Ethaline and Reline.⁶⁶ It was found that SDS caused a significant decrease in surface tension whereas CTAB had little effect. It could therefore be concluded that SDS forms micelles at the concentrations studied in Figure 5-10 whereas CTAB is still below the cmc.⁶⁷

5.5.4 Conductivity

Figure 5-11 shows the effect of addition of 1-4 mM of SDS and CTAB to Ethaline, Glyceline and Reline on electrical conductivity at different temperatures. Firstly, it is clear that the addition of both SDS and CTAB has very little effect on the conductivity of Ethaline.

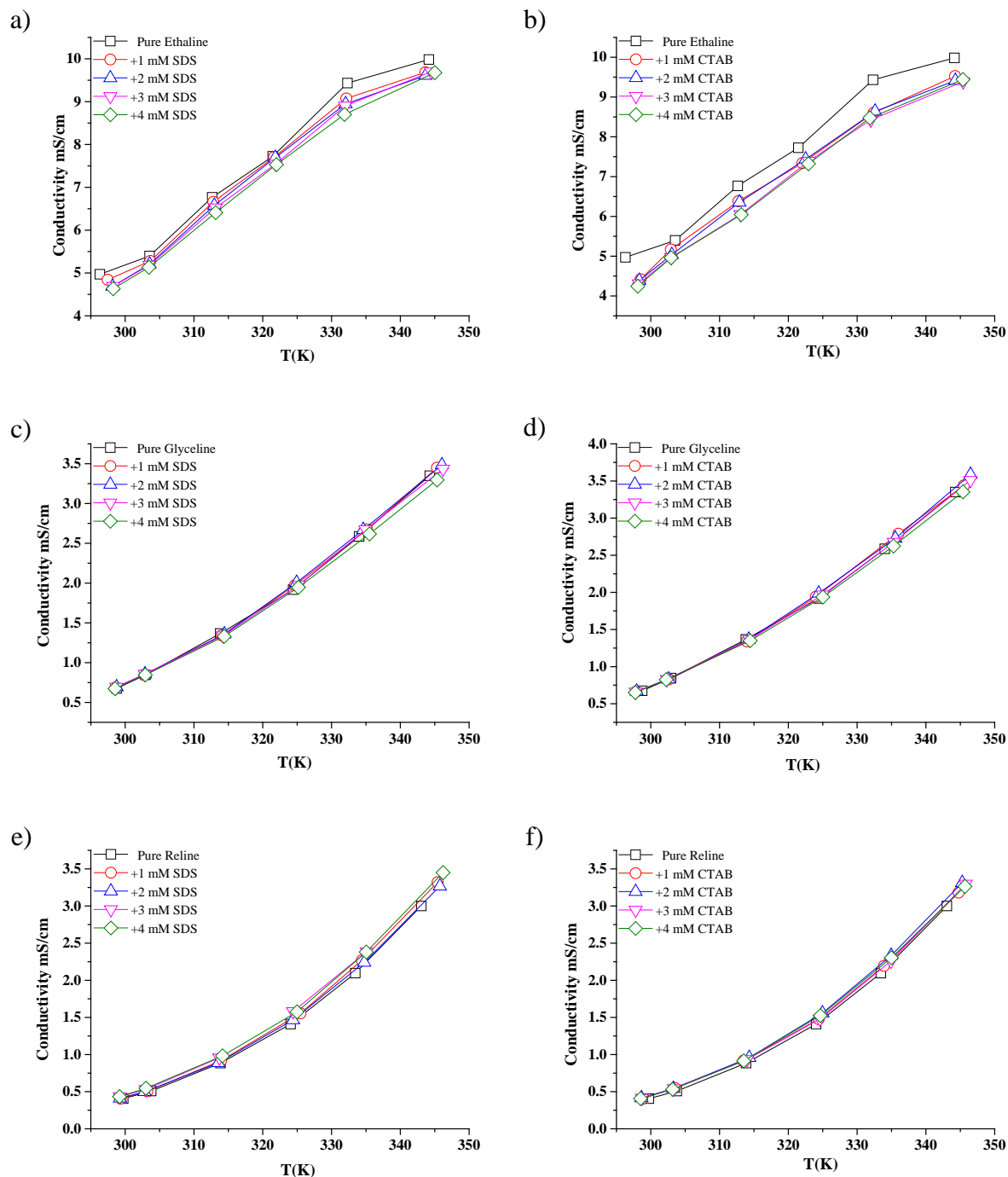


Figure 5-11: Conductivity change as a function of surfactant mM at different temperatures [a), c), e) are SDS, b), d), f) are CTAB] in Ethaline, Glyceline and Reline respectively.

If anything there is a slight reduction of conductivity for all concentrations which could be due to small increases in viscosity. It can therefore be concluded that if micelles do form their effect on charge mobility will be minimal at the concentrations used here.

5.5.5 Density

If surfactants do result in the formation of micelles then it would be expected that there could be a change in solution density. Table 5-5 shows the data of DESs containing low concentration SDS and CTAB. The decrease of density as a function of additive concentration is an indicator to the destruction of cohesive forces in the liquid which causes the liquid to occupy lower volume. The data in Table 5-5 show that for Ethaline and Glyceline both surfactants have a negligible change in the density of the solution. For Reline SDS does cause a significant decrease in the density which is indicative that micelles could be responsible. There is a smaller but still significant decrease for CTAB in Reline. These data could explain the observations in Figure 5-10.⁶⁸

Table 5-5: *Density change of DESs as a function of molar concentration of surfactants.*

Liquids	SDS		CTAB	
	Density	Uncertainty	Density	Uncertainty
Pure Ethaline	1.103	±0.005	1.103	±0.005
1mM	1.103	±0.006	1.103	±0.001
2mM	1.103	±0.004	1.103	±0.005
3mM	1.102	±0.003	1.101	±0.002
4mM	1.100	±0.003	1.103	±0.001
Pure Glyceline	1.179	±0.005	1.179	±0.005
1mM	1.178	±0.001	1.177	±0.007
2mM	1.174	±0.004	1.174	±0.007
3mM	1.175	±0.003	1.175	±0.005
4mM	1.175	±0.002	1.174	±0.008
Pure Reline	1.188	±0.004	1.188	±0.004
1mM	1.184	±0.002	1.185	±0.007
2mM	1.183	±0.002	1.184	±0.002
3mM	1.179	±0.004	1.182	±0.004
4mM	1.178	±0.002	1.180	±0.004

The formation of spherical micelles for fully extended hydrocarbon tail do not tend to form at high concentrations but it is commonly agreed that spherical micelles are formed at low concentration in aqueous media.^{12, 69} In this study only small amount of surfactants are added to DESs, and hydrogen bonding as intermolecular force is thought to exist in DESs, and these liquids are fully miscible with water which mean they thought to show the similar behaviour toward surfactants and finally, the change in some properties have been observed such as density as shown in Table 5-5 and VI in Figure 5-10. Broadly speaking, the

conditions for the formation of surfactant aggregates in general depends on the relation of the hydrocarbon chain volume (v) to the area of polar group (a) and the optimal length of hydrocarbon chain (l).⁶¹

Thus if $(v / a l) < 1/3$ the formation of spherical micelles is possible, if $1/3 < (v / a l)$ cylindrical micelle will be formed and finally, if $1/2 < (v / a l)$ vesicles or bilayer will be produced. For CTAB and SDS regardless of the type of DESs the value of $v / a l$ for both surfactants are 0.16 and 0.18 respectively which are lower than $1/3$, hence the formation of spherical micelles is more favourable than other possibilities. The only issue is whether the surfactants are present above their cmc in solution.

One reason that surfactants are added to oil based lubricants is to act as a dispersant, particularly for water so the formation of micelles is important. In DESs water is miscible and so the ability for a surfactant to form micelles is less important. A more important role therefore is to affect wettability and modify the friction coefficient. To quantify the interfacial properties the contact angle of surfactant solutions was determined.

5.5.6 Contact angle

The change in wettability of stainless steel surface by measuring contact angle was carried out for pure Ethaline, Glyceline and Reline and with the addition of 1-4 mM SDS and CTAB and the results are listed in Table 5-6.

The table show that in Ethaline the addition of SDS has only a small effect on the contact angle with stainless steel whereas CTAB has almost no effect. Ethaline has the lowest surface tension and so it is not surprising that its effect is the smallest. Both Glyceline and Reline have much larger surface tensions and so the initial contact angles tend to be higher. The effects of adding surfactant to the DESs are different in each case showing that the different HBDs clearly affect the aggregation of surfactants at the metal-DES interface.

CTAB in Reline causes the highest contact angles suggesting that the surfactant induces stronger intermolecular forces in the liquid. The reverse is the case for Glyceline where CTAB causes a significant decrease in the intermolecular forces. The clearest trend is observed for the addition of SDS to Reline where changing the SDS concentration from 1 to 4 mM changes the contact angle by approximately 25° .

Table 5-6: Contact angle of pure DESs and with 1-4mM of SDS.

Solutions	Contact angle/ °					
	Ethaline	Uncertainty	Glyceline	Uncertainty	Reline	Uncertainty
Pure DESs	74.5	±1.11	95.5	±1.3	80.1	±7.7
DESs with SDS						
+1 mM	81.5	±0.92	85.3	±0.52	82.4	±0.39
+2 mM	80.6	±1.08	77.8	±0.93	72.4	±2.56
+3 mM	78.0	±1.05	87.4	±0.91	60.6	±1.71
+4 mM	75.3	±0.36	89.1	±0.56	58.5	±1.3
DESs with CTAB						
+1 mM	74.8	±1.02	73.5	±0.35	90.9	±2.16
+2 mM	77.1	±0.64	68.5	±1.02	90.3	±0.45
+3 mM	74.6	±2.3	67.3	±0.23	90.2	±0.44
+4 mM	77.8	±1.16	63.0	±0.91	83.1	±3.01

While very little is known about the aggregation of surfactants in DESs a recent study by Arnold et al. using X-ray reflectivity (XRR) and Small Angle Neutron Scattering (SANS) suggests the behaviour of SDS in Reline is significantly different from that in water.⁷⁰ They found that the cmc was 2 mM and suggested that rod shaped micelles were formed which were significantly larger than in aqueous solutions. XRR measurements showed that a layer of surfactant between 12 and 20 Å thick, formed at the solid-solution interface showing that the surfactant is surface active.

With the exception of CTAB in Ethaline the results in Table 5-6 suggest that the surfactants affect the wettability of steel in most DESs. This change in contact angle is similar, although to a different extent, to what occurs for surfactant in water. To determine the effect of this surface activity on the surface wetting the friction coefficient and wear volume were determined for the various surfactant solutions.

5.5.7 Friction coefficient

Theoretically, the friction reducing ability of a lubricant should be changed when friction reducing agents such as surfactants are added, because these additives are able to form a thin film on the surface of lubricated metal as a result of physisorption. This adsorbed

layer avoids direct contact between rubbing surfaces.¹⁰ However, it has to be realised the formation of thin films due to the physisorption does not guarantee the complete separation of sliding couples because the surfactant is too weakly bound. Consequently the reduction of friction constant and wear values are generally only changed by a small amount unless extreme pressure is observed.^{7, 10}

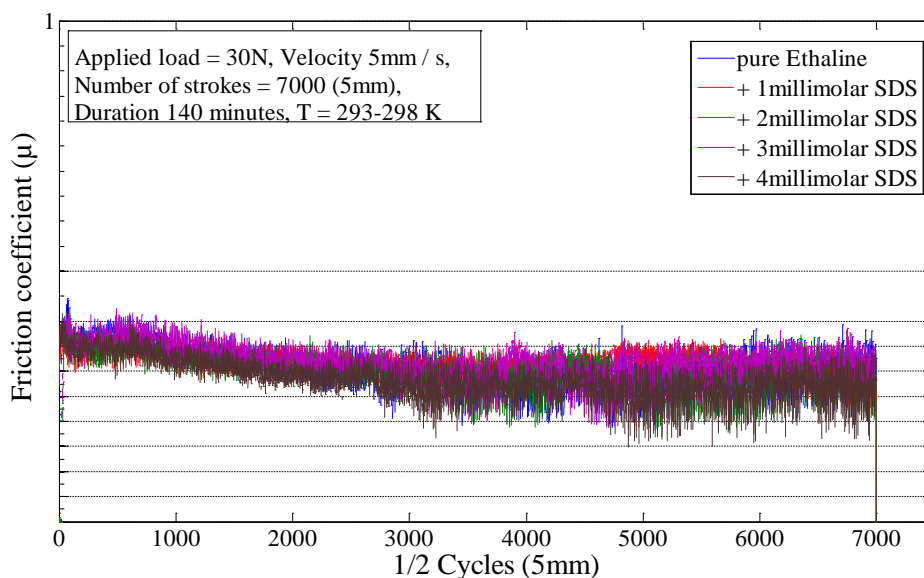


Figure 5-12: Friction coefficient change as a function of concentration of SDS.

Figure 5-12 shows an example of the friction coefficient change for different concentrations of SDS in Ethaline. The figure shows only a small change in the friction coefficient with increasing surfactant concentration. The friction coefficient remains roughly constant for the first 1000 cycles and then it gradually decreases until about 5000 cycles when it levels off again. This behaviour thought to occur due to the surface of steel being covered with a thin oxide layer where the friction constant between steel and oxide layer is higher than steel/steel or the oxide layer is not as active as pure steel to the surfactant molecules. Over time when this oxide layer has been removed as a result of scratching, a new active layer of steel should be made and the film forming ability of surfactant starts to increase which decreases the friction constant slightly over time.

The effect of SDS and CTAB in all DESs is almost similar that observed in Figure 5-12 however the change is a little smaller. These results are shown in the Appendix.

5.5.8 Wear volumes

Table 5-7 shows the data of wear volume for dry and lubricated steel/steel couples by pure Ethaline, Glyceline and Reline in addition to the same liquids containing SDS and CTAB. As shown in the table there is a significant change of wear volumes from dry to lubricated surfaces in which almost the value is halved for Glyceline and Reline and the value lowered to less than one third for Ethaline in comparison with dry surface which may be due to the effect wettability.

This variability as mentioned before thought to go back to the different activity of these liquids to lubricate the surface. For example the fluidity of Ethaline is high and its surface tension is lower than Glyceline and Reline therefore its wettability is better. On the other hand, viscosity of Reline is higher than Glyceline and Ethaline and hence thicker film on the surface will be provided which consequently prevents direct contact for fluid film lubrication.³²

Table 5-7: *Wear Volume of scratched surfaces in the presence of surfactants.*

Liquids	Wear volume (mm ³) *10 ⁻³		
	Ethaline	Glyceline	Reline
No liquid	83.5 ±0.4	83.5±0.4	83.5±0.4
Pure DESs	25.2 ±0.7	48.5 ±0.9	41.4 ±0.3
DESs with SDS			
+1 mM	12.9 ±2.2	37.5 ±0.8	29.4 ±0.8
+2 mM	20.4 ±1.1	34.6 ±0.4	35.2 ±1.2
+3 mM	25.3 ±0.3	38.1 ±0.6	35.9 ±1.6
+4 mM	18.5 ±0.4	36.3 ±0.5	30.6 ±0.8
DESs with CTAB			
+1 mM	21.5 ±1.1	35.6 ±0.6	34.3 ±0.1
+2 mM	20.5 ±2.1	34.1 ±0.6	27.5 ±1.3
+3 mM	21.7 ±1.0	23.9 ±1.3	30.3 ±0.2
+4 mM	31.0 ±0.3	24.8 ±0.8	31.6 ±0.8

Comparison of the wear volumes with and without surfactants in Table 5-7 shows that both surfactants have an effect in all DESs demonstrating that wettability plays important role in the interaction between liquids and the surface which are responsible for these change in

wear volumes. The concentration of surfactants does not significantly affect the wear volume showing that it is surface active at or below 1 mM. In most cases the surfactants cause a 10 to 25 % decrease in the wear volume showing that they are a useful and active additive even in very low concentrations.

The adsorption of alkylammonium ions on silica surface has shown that these ions are adsorbing on the surface physically due to coulombic interactions and they are able to form hemi-micelles in the same way as they form micelles in the bulk solutions.⁷¹ A similar phenomenon is thought to occur for DESs on the surface of steel.

5.6 Conclusions

In summary, the lubrication of a surface is influenced by both intermolecular interactions which determines how the liquid behaves thermally and with mechanical forces and by the interaction of liquid with the lubricated surface. This explains why there is a disparity between the friction constant and wear values reported in this study. In addition, the experimental conditions have a significant impact in controlling wear. Surface tension considerably influences wettability of surfaces. Furthermore, surface roughness and surface energy are elements which have been shown to have some effects on wear values.

Wettability alone does not correlate with the friction coefficient or wear volumes in this study since highly viscous liquids such as Reline and Glyceline provide better lubrication than Ethaline even though they have lower wettability than Ethaline. This is because these liquids offer adequate film thickness under experimental conditions to separate the contacting surfaces and reduce wear. Surfactants were found to affect the wettability of all DESs studied and in most cases they decreased the contact angles between the DESs and stainless steel.

The results in this chapter suggest that Ethaline is not viscous enough and Reline is too viscous to lubricate the interface successfully. For aluminium however, mineral base oil provides better lubrication than DESs due to its better surface wettability. The addition of surfactants were found to decrease the friction coefficients of DESs as a result, lower wear volumes were observed for steel-steel couples clearly demonstrating that the surfactants are surface active and can act as active additives even at very low concentrations. Inclusion of surfactants to DESs is shown to bring about small changes in the physical properties of the DESs. None of the surfactants bring about significant changes in density and conductivity of the DESs and the slight change observed thought to be caused by the formation of different

surfactant aggregates which affect intermolecular forces in the DESs. In most cases there is a small decrease in the VI although SDS in Reline appears to bring about a small increase in VI.

Finally, this study has shown that DESs provide a more constant lubrication over shorter time scales (c.a. 1 hour) than mineral base oil for iron based alloys however; after this period mineral base oil have lower friction coefficients. In general it can be concluded that Glyceline is the optimum DES for lubrication not only from a lubrication and corrosion standpoint but also from a sustainability and cost perspective.

5.7 References

1. V. Khare, M. Q. Pham, N. Kumari, H. S. Yoon, C. S. Kim, J. I. Park and S. H. Ahn, *Acs Appl Mater Inter*, 2013, 5, 4063-4075.
2. F. Zhou, Y. M. Liang and W. M. Liu, *Chem Soc Rev*, 2009, 38, 2590-2599.
3. M. D. Bermudez, A. E. Jimenez, J. Sanes and F. J. Carrion, *Molecules*, 2009, 14, 2888-2908.
4. M. R. Cai, R. S. Guo, F. Zhou and W. M. Liu, *Sci China Technol Sc*, 2013, 56, 2888-2913.
5. Ines Otero, Enriqueta R. Lopez, Manuela Reichelt, María Villanueva, Josefa Salgado and a. J. Fernández, *Appl. Mater. Interfaces* 2014, 6, 13115–13128.
6. R. Van Basshuysen and F. Schäfer, *Internal Combustion Engine Handbook: Basics, Components, Systems, and Perspectives*, SAE International, 2004.
7. S. Q. A. Rizvi, *A Comprehensive Review of Lubricant Chemistry, Technology, Selection, and Design*, ASTM International, 2009.
8. D. Klamann and R. R. Rost, *Lubricants and related products: synthesis, properties, applications, international standards*, Verlag Chemie, 1984.
9. E. R. Booser, *CRC Handbook of Lubrication: Theory and Practice of Tribology, Volume II: Theory and Design*, Taylor & Francis, 1983.
10. L. R. Rudnick, *Lubricant Additives: Chemistry and Applications, Second Edition*, Taylor & Francis, 2009.
11. S. D. A. Lawes, S. V. Hainsworth, P. Blake, K. S. Ryder and A. P. Abbott, *Tribol Lett*, 2010, 37, 103-110.
12. Z. Pawlak, *Tribochemistry of Lubricating Oils*, Elsevier Science, 2003.
13. B. J. Hamrock, S. R. Schmid and B. O. Jacobson, *Fundamentals of Fluid Film Lubrication*, Taylor & Francis, 2004.
14. R. Atkin, S. Z. El Abedin, R. Hayes, L. H. S. Gasparotto, N. Borisenko and F. Endres, *J Phys Chem C*, 2009, 113, 13266-13272.
15. R. Hayes, N. Borisenko, M. K. Tam, P. C. Howlett, F. Endres and R. Atkin, *J Phys Chem C*, 2011, 115, 6855-6863.
16. R. Atkin and G. G. Warr, *J Phys Chem C*, 2007, 111, 5162-5168.
17. A. P. Abbott, E. I. Ahmed, R. C. Harris and K. S. Ryder, *Green Chem*, 2014, 16, 4156-4161.

18. R. G. Horn, D. F. Evans and B. W. Ninham, *J Phys Chem-Us*, 1988, 92, 3531-3537.
19. Y. D. Liu, Y. Zhang, G. Z. Wu and J. Hu, *Journal of the American Chemical Society*, 2006, 128, 7456-7457.
20. A. Zmitrowicz, *Journal of theoretical and applied mechanics*, 2006, 44, 219-253.
21. J. F. Archard, *Journal of Applied Physics*, 1953, 24, 981-988.
22. G. E. Totten, *Fuels and Lubricants Handbook*, ASTM international, 2003.
23. B. A. Starkweather, X. G. Zhang and R. M. Counce, *Ind Eng Chem Res*, 2000, 39, 362-366.
24. K. S. Lee, N. Ivanova, V. M. Starov, N. Hilal and V. Dutschk, *Adv Colloid Interfac*, 2008, 144, 54-65.
25. R. Zhang and P. Somasundaran, *Langmuir*, 2005, 21, 4868-4873.
26. E. Bertrand, T. D. Blake, V. Ledauphin, G. Ogonowski, J. De Coninck, D. Fornasiero and J. Ralston, *Langmuir*, 2007, 23, 3774-3785.
27. D. Bonn, J. Eggers, J. Indekeu, J. Meunier and E. Rolley, *Rev Mod Phys*, 2009, 81, 739-805.
28. D. Duvivier, T. D. Blake and J. De Coninck, *Langmuir*, 2013, 29, 10132-10140.
29. P. Somasundaran and L. Zhang, *J Petrol Sci Eng*, 2006, 52, 198-212.
30. A. J. Meuler, S. S. Chhatre, A. R. Nieves, J. M. Mabry, R. E. Cohen and G. H. McKinley, *Soft Matter*, 2011, 7, 10122-10134.
31. S. L. Perkins, P. Painter and C. M. Colina, *J Chem Eng Data*, 2014, 59, 3652-3662.
32. US patent, 5,962,381,1999.
33. K. Szymczyk, M. L. Gonzalez-Martin, J. M. Bruque and B. Janczuk, *J Colloid Interf Sci*, 2014, 417, 180-187.
34. L. Leger and J. F. Joanny, *Rep Prog Phys*, 1992, 55, 431-486.
35. R. J. Good, *J Adhes Sci Technol*, 1992, 6, 1269-1302.
36. D. Quere, *Physica a Statistical Mechanics and Its Applications*, 2002, 313, 32-46.
37. A. W. Adamson and A. P. Gast, *Physical chemistry of surfaces*, Wiley, 1997.
38. X. S. Wang, S. W. Cui, L. Zhou, S. H. Xu, Z. W. Sun and R. Z. Zhu, *J Adhes Sci Technol*, 2014, 28, 161-170.
39. J. G. Eberhart and S. Horner, *J Chem Educ*, 2010, 87, 608-612.
40. H. L. Skriver and N. M. Rosengaard, *Phys Rev B*, 1992, 46, 7157-7168.
41. J. Heinrichs, *Phys Rev B*, 1975, 11, 3637-3643.
42. J. C. W. Swart, P. van Helden and E. van Steen, *J Phys Chem C*, 2007, 111, 4998-5005.

43. C. Noguera and J. Goniakowski, *Chemical Reviews*, 2013, 113, 4073-4105.
44. M. G. Norton, *J Adhes Sci Technol*, 1992, 6, 635-651.
45. N. Eustathopoulos, G. Nicholas and B. Drevet, *Wettability at High Temperatures*, Elsevier Science, 1999.
46. J. Goniakowski, F. Finocchi and C. Noguera, *Rep Prog Phys*, 2008, 71, 1-55.
47. S. M. Liu, S. A. Wang, J. D. Guo and Q. L. Guo, *Rsc Adv*, 2012, 2, 9938-9943.
48. T. P. Silverstein, *J Chem Educ*, 1993, 70, 253-253.
49. R. G. Craig, J. J. Van Voorhis and F. E. Bartell, *J Phys Chem-Us*, 1956, 60, 1225-1230.
50. C. Rulison, *Two-component surface energy characterization a predictor of wettability and dispersability*, Kruss technical note, 2000.
51. A. R. A. Al-Samarai, Haftirman, K. R. Ahmad and Y. Al-Douri, *Procedia Engineer*, 2013, 53, 616-623.
52. L. Lin, *Komatsu technical report*, 2013 59 1-7.
53. S. Wang, Y. Z. Hu, W. Z. Wang and H. Wang, *J Tribol-T Asme*, 2007, 129, 809-817.
54. P. L. Menezes, Kishore and S. V. Kailas, *Sadhana-Acad P Eng S*, 2008, 33, 181-190.
55. P. L. Menezes, Kishore and S. V. Kailas, *J Mater Process Tech*, 2008, 208, 372-382.
56. K. Yamaguchi, C. Sasaki, R. Tsuboi, M. Atherton, T. Stolarski and S. Sasaki, *The Journal of Engineering Tribology*, 2014, 228, 1015-1019.
57. U. Pettersson and S. Jacobson, *Tribology International*, 2003, 36, 857-864.
58. M. Grossutti, J. J. Leitch, R. Seenath, M. Karaskiewicz and J. Lipkowski, *Langmuir*, 2015, 31, 4411-4418.
59. M. Alkan, M. Karadas, M. Dogan and O. Demirbas, *J Colloid Interf Sci*, 2005, 291, 309-318.
60. A. Zdziennicka and B. Janczuk, *J Colloid Interf Sci*, 2008, 317, 44-53.
61. B. W. Nlnham, D. F. Evans and G. J. Well, *J Phys Chem-Us*, 1983, 87, 5020-5025.
62. S. A. Morton, D. J. Keffer, R. M. Counce, D. W. DePaoli and M. Z. C. Hu, *J Colloid Interf Sci*, 2004, 270, 229-241.
63. T. Arnebrant, K. Backstrom, B. Jonsson and T. Nylander, *J Colloid Interf Sci*, 1989, 128, 303-312.
64. J. Qu, D. G. Bansal, B. Yu, J. Y. Howe, H. M. Luo, S. Dai, H. Q. Li, P. J. Blau, B. G. Bunting, G. Mordukhovich and D. J. Smolenski, *Acs Appl Mater Inter*, 2012, 4, 997-1002.
65. L. Askadskaya, C. Boeffel and J. P. Rabe, *Ber Bunsen Phys Chem*, 1993, 97, 517-521.

66. M. Azam, PhD, Leicester, 2011.
67. M. Pal, R. Rai, A. Yadav, R. Khanna, G. A. Baker and S. Pandey, *Langmuir*, 2014, 30, 13191-13198.
68. D. Das and K. Ismail, *J Colloid Interf Sci*, 2008, 327, 198–203.
69. H. Schott, *J Pharm Sci*, 1971, 60, 1594-&.
70. T. Arnold, A.J. Jackson, A. Sanchez-Fernandez, D. Magnone, A.E. Terry and K.J. Edler, *Langmuir*, In press
71. P. Somasundaran, Thomas W. Healy and D. W. Fuerstenau, *J Phys Chem-U.S.*, 1964, 68, 3562-3566.

CHAPTER SIX: CONCLUSIONS

CONTENTS

6 CONCLUSIONS AND FUTURE WORKS

6.1	CONCLUSIONS	162
6.2	FURTHER WORK.....	165
6.3	APPENDIX.....	166

6 CONCLUSIONS AND FUTURE WORKS

6.1 Conclusions

The lubricant properties of Deep Eutectic Solvents (DESs) have not been studied in any depth previously. This investigation has looked at the thermo-physical properties, corrosion behaviours, rheology and mechanical properties of these liquids and has compared their properties to mineral base oil.

In principle the thermo-physical and rheological properties of DESs and hydrocarbon based liquids should be significantly different as the former has both Coulombic and hydrogen bonding interactions whereas the latter has only van der Waals forces. The observation that both fluids have similar thermo-physical properties shows that they must originate from different phenomena. In DESs the small void size resulting from a high surface tension and the large ion size means that the liquids are viscous. The intermolecular interactions are not significantly affected by temperature resulting in a high viscosity index. In mineral oils the molecules are large and so mobility is limited at low temperatures. At higher temperatures the molecules uncoil and inter-molecular interactions increase which affects the viscosity resulting in a high viscosity index. The other physical properties of DESs such as surface tension, electrical conductivity and density are fundamentally different from hydrocarbons and are mostly related to the cohesive forces resulting from strong Coulombic interactions.

Most of DESs except Reline are fluid at temperatures below the pour point of most mineral oils which makes them suitable base lubricant without the need to add pour point depression additives. Heat capacity measurements show that Ethaline, Glyceline, and Reline are better than mineral base oil at dissipating heat from lubricated equipment. Enthalpies of formation show that the hydrogen bonding is responsible for the new intermolecular forces among ChCl and HBDs and it governs the depression of freezing point of the eutectic mixtures.

The viscosity-temperature relationship for DESs is generally higher than mineral base oil which makes them at least as good at providing a protective film during the operation even at high temperature. This study has shown for the first time that some DESs display non-Newtonian behaviour at low temperatures. The study has also shown the ability to use QCM as a technique to determine the viscosity of DESs and it shows that comparable results

can be obtained to rotational viscometers only using a much smaller volume of liquid (typically 100 times less). The mineral base oil is, however thermally more stable than all DESs and when DESs are heated beyond break down of intermolecular forces the constituents are thought to decompose to form different compounds. The conductivity occurs via Ch^+ and Cl^- and the viscosity has a great impact on its value. Reasonable void radii could be extracted from surface tension-temperature relationships which support the validity of hole theory to describe both conductivity and viscosity in DESs.

In this study mixtures of DESs with water were studied and it was shown that the OH protons both on choline and the polyols behave differently in the different liquids. In Ethaline the protons on both species are labile resulting in slightly acidic solutions whereas in Glyceline both are associated resulting neutral pH solutions. It was also shown that aqueous DES mixtures are non-homogeneous producing bicontinuous microemulsions.

In order to determine the corrosion behaviour of DESs for common metals which are used in engine blocks and engine parts, corrosion studies of iron, aluminium and nickel has been carried out in some DESs, ILs and mineral base oil using linear sweep voltammetry, electrochemical impedance spectroscopy and Raman spectroscopy. The corrosion rates of Fe, Ni and Al in Glyceline and Reline were found to be small and remain almost constant over time. However, as a consequence of mass transport, higher chloride activity and mild solution acidity Ethaline has a variable corrosion activity toward different metals. In Oxaline corrosion rate for all metals are high due to the acidity of the liquids.

Visibly, corrosion products of iron in Ethaline thought to be iron glycolate having low density and then when their product reacts with the air it forms undissolved iron oxides. In Reline possibly iron produces complexes with urea or with ammonia formed as a result of urea dissociation. Glyceline does not show any visible corrosion products even after 18 months which thought to be due to its neutrality. Dry mineral base oil does not corrode iron however, when it contains 1% aqueous sodium chloride a significant amount of undissolved corrosion products is observed which precipitates on the surface of metal.

Raman spectroscopy data demonstrates that the corrosion products of iron are products which thought to be made under low oxygen concentration and for Al the product may consist of a mixture of amorphous oxidation products. Oxaline is not suitable as a lubricant due to its high corrosion rate. Finally, the data suggests that Glyceline does not show any sign of corrosion for any metals and could be suitable as a base lubricant.

The mechanical properties, friction coefficient, wettability, wear volume and wear number were studied for Ethaline, Glyceline, Reline and mineral oil for dissimilar sliding couples. It can be concluded that lubrication is a complex process in which it is difficult to decide which of the lubrication elements dominates the friction constant and wear values. Both the properties of the lubricant and lubricated surface in addition to the experimental conditions contribute to the overall results. All of surface tension, surface roughness and surface activity elements appear to influence the contact angles between the liquid and solid.

Wettability alone does not determine the friction coefficient or wear volumes in this study because some other factors such as viscosity of DESs play an important role. For example, viscous liquids such as Reline and Glyceline are much powerful than non-viscous liquid such Ethaline to provide an adequate lubricant film under experimental conditions even though they have a lower VI than Ethaline.

The results in lubrication studies suggest that Ethaline has too low a viscosity and Reline too high a viscosity to lubricate the interface successfully. Furthermore, mineral base oil provides better lubrication than DESs for aluminium surfaces. On the other hand, DESs are provide a more constant lubrication overtime which is better than mineral base oil for iron based surfaces where the friction coefficient of mineral oil changes with time. In general it can be concluded that Glyceline is the optimum DES for lubrication not only from a lubrication standpoint but also from a sustainability and cost perspective.

The studies concerning the effect of surfactants upon Ethaline, Glyceline and Reline as lubricant additive show that; their inclusion has only a small effect on the thermo-physical and mechanical properties. VI has been decreased for most DESs with the addition of CTAB and SDS shows the same effect on Ethaline and Glyceline however, addition of SDS to Reline displays inverse effect on VI which thought to be due micelle formation.

Both surfactants were found to affect the wettability of a steel surface for all DESs. The contact angle was affected in all cases although sometimes this was small. The biggest effect was observed for SDS in Reline. The friction coefficients of steel in DESs were found to be slightly lower when surfactants were added. This appears to be related to the increased wettability. Finally, as a result of lower friction coefficients in the presence of surfactants, lower wear volumes for steel-steel couples have been observed in all cases. The decrease in wear volume was significant (10 to 25 %) despite the surfactant only being present in small concentrations.

Overall, Glyceline seems to be the best candidate among all DESs because it has very low corrosion rates for common metals, a high viscosity index, fluidity at low temperature,

low friction coefficient and wear volumes. Glyceline is also environmentally the best liquid to use. It has almost no toxicity as both compounds are found in most living creatures. It is miscible with water and therefore spillages will be easily dissipated. Finally glycerol is a useful starting material as it is a common waste material from the soap manufacture and biodiesel synthesis which has few other applications.

6.2 Further Work

This study has only shown that some DESs have suitable properties that may be useful as base lubricants. Considerably more work is required to be able to produce a finished lubricant. The following are areas that should be studied;

- 1- Measurement of friction coefficients for liquids as a function of temperature which was not possible with our available wear testing equipment.
- 2- Measurement of friction tests on real engine parts such as camshaft, bearings, piston, cylinder, and crankshaft.
- 3- Investigation of bimetallic corrosion to address the effect of other constituent metals in the engine alloys which thought to make local corrosion cells due to the DESs are high conductive mediums.
- 4- Study of the effect of temperature on corrosion for metals studied here and for other metals which are exists in engine alloys constituents as additives.
- 5- Studies of additives in detail such as effect of anti-corrosion, extreme pressure/friction modifying agents, detergents, and pour point depression and foam inhibitors additives.

6.3 Appendix

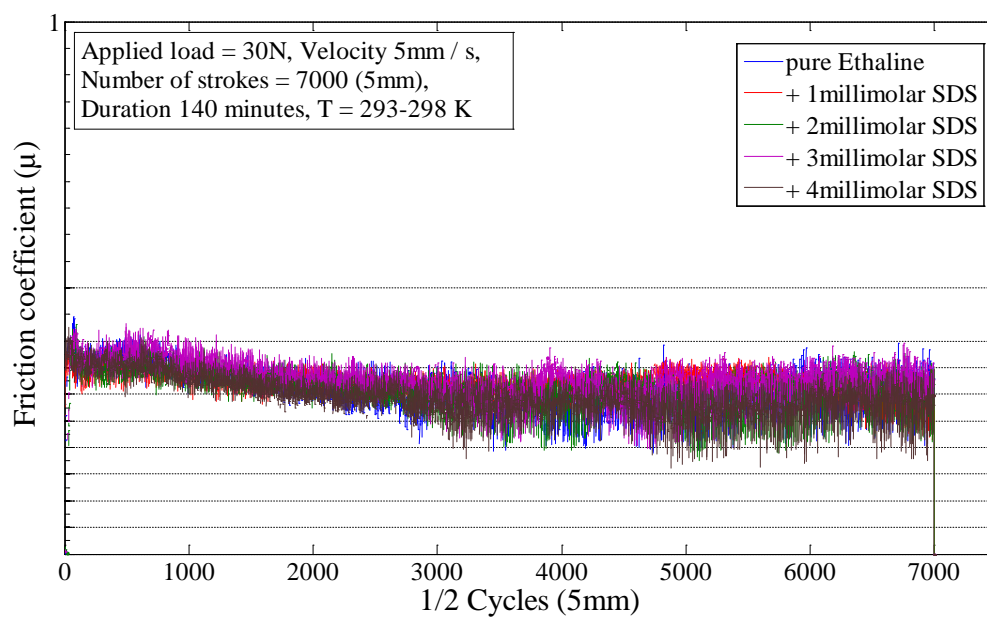


Figure 6-1 : Friction coefficient of Ethaline containing 1-4mM SDS for steel/steel contact couples.

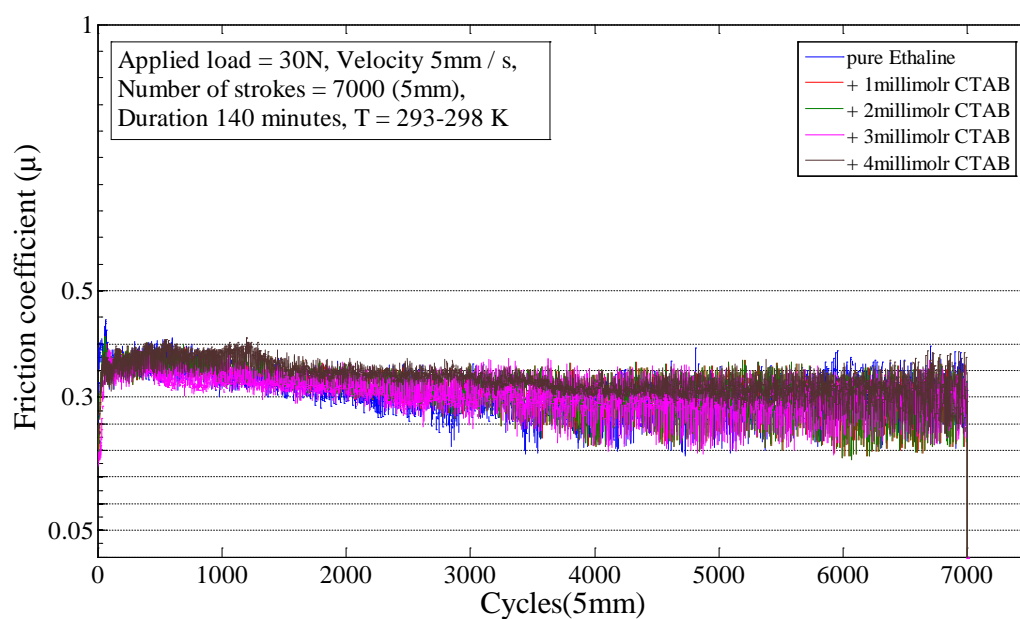


Figure 6-2: Friction coefficient of Ethaline containing 1-4mM CTAB for steel/steel contact couples.

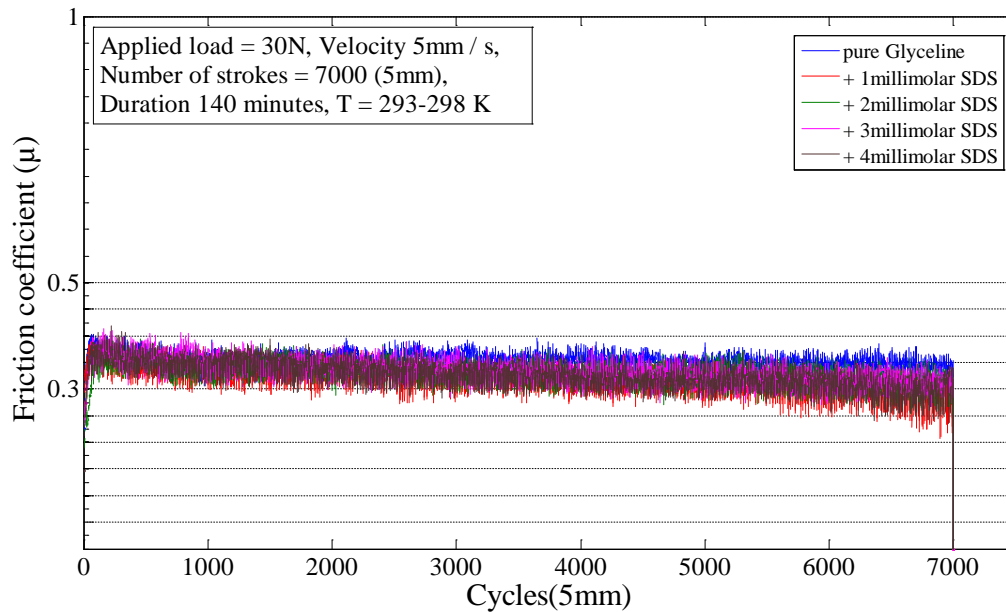


Figure 6-3 : Friction coefficient of Glyceline containing 1-4mM SDS for steel/steel contact couples.

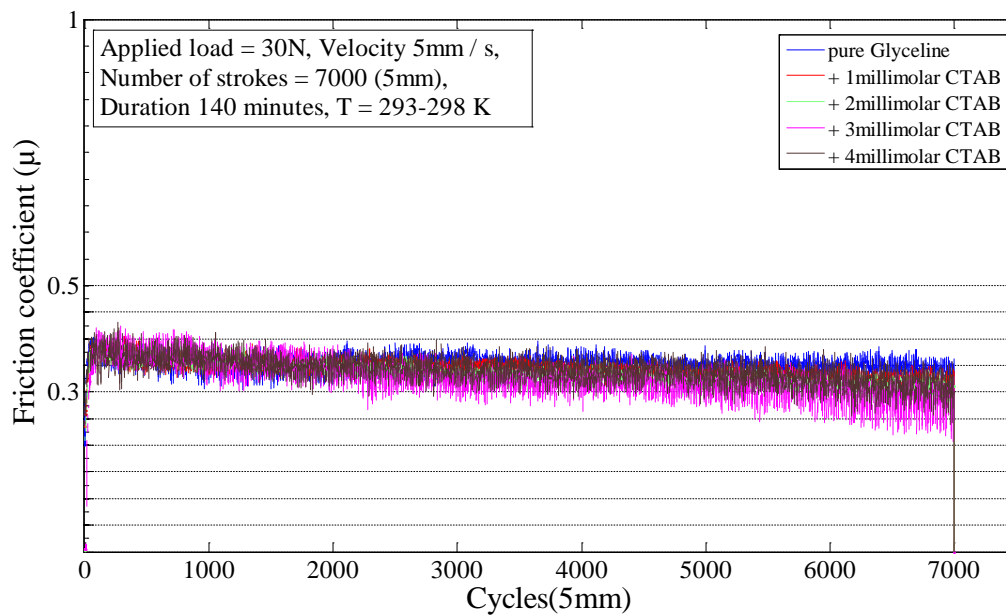


Figure 6-4: Friction coefficient of Glyceline containing 1-4mM CTAB for steel/steel contact couples.

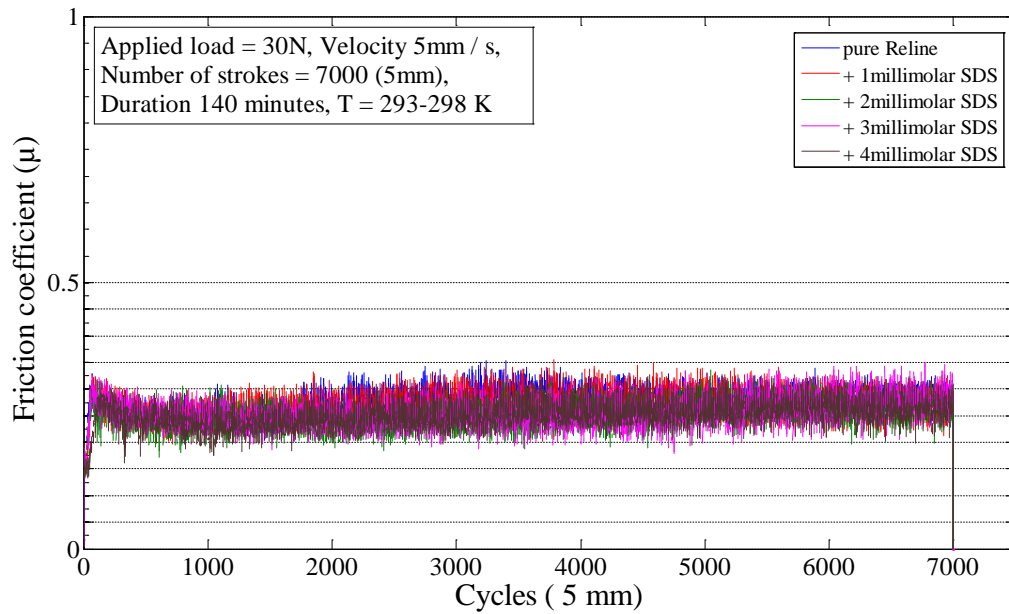


Figure 6-5: Friction coefficient of Reline containing 1-4mM SDS for steel/steel contact couples.

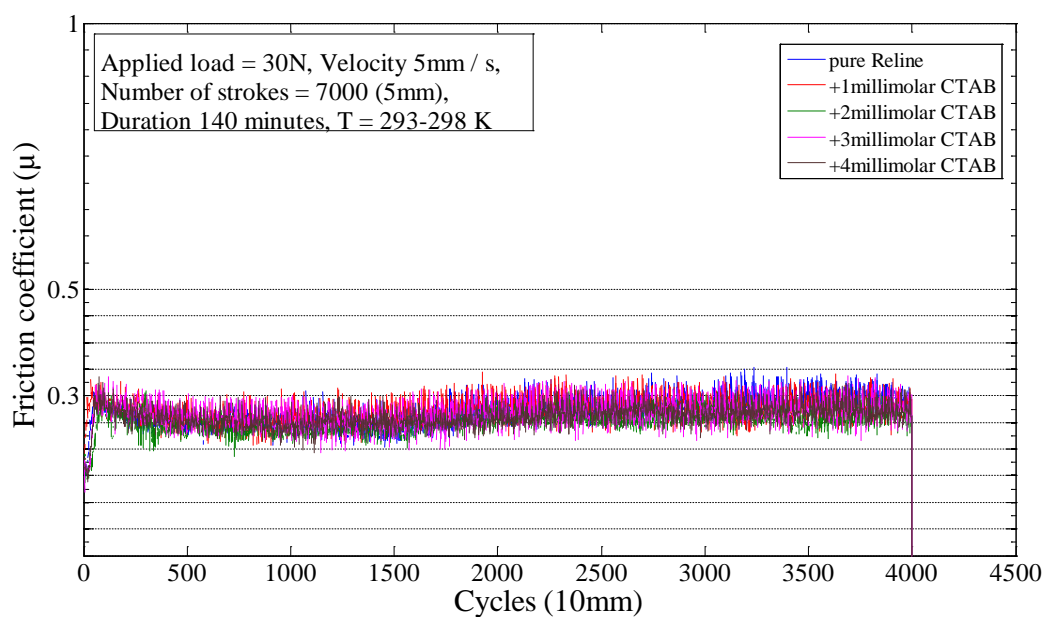


Figure 6-6: Friction coefficient of Reline containing 1-4mM CTAB for steel/steel contact couples.

Table 6-1: Cathodic and anodic constants for iron in pure and water containing DESs.

Fe								
DESs	Ethaline		Glyceline		Reline		Oxaline	
	b _c	b _a	b _c	b _a	b _c	b _a	b _c	b _a
Pure liquids	0.120	0.091	0.048	0.060	0.101	0.105	0.123	0.121
+ 0.01 water	0.065	0.055	0.049	0.062	0.131	0.132	0.140	0.080
+ 0.02 water	0.057	0.045	0.089	0.046	0.078	0.058	0.146	0.077
+ 0.05 water	0.147	0.106	0.117	0.074	0.098	0.094	0.126	0.101
+ 0.1 water	0.113	0.118	0.144	0.094	0.158	0.138	0.139	0.064

Table 6-2: Cathodic and anodic constants for aluminium in pure and water containing DESs.

Al								
DESs	Ethaline		Glyceline		Reline		Oxaline	
	b _c	b _a	b _c	b _a	b _c	b _a	b _c	b _a
Pure liquids	0.125	0.155	0.038	0.036	0.103	0.099	0.056	0.035
+ 0.01 water	0.092	0.048	0.069	0.046	0.223	0.097	0.078	0.038
+ 0.02 water	0.209	0.174	0.044	0.031	0.141	0.065	0.076	0.081
+ 0.05 water	0.106	0.090	0.066	0.043	0.165	0.054	0.099	0.049
+ 0.1 water	0.222	0.114	0.080	0.064	0.130	0.056	0.094	0.052

Table 6-3: Cathodic and anodic constants for nickel in pure and water containing DESs.

Ni								
DESs	Ethaline		Glyceline		Reline		Oxaline	
	b _c	b _a	b _c	b _a	b _c	b _a	b _c	b _a
Pure liquids	0.071	0.078	0.100	0.088	0.101	0.098	0.123	0.121
+ 0.01 water	0.052	0.051	0.109	0.134	0.253	0.144	0.140	0.081
+ 0.02 water	0.069	0.081	0.126	0.126	0.104	0.116	0.146	0.076
+ 0.05 water	0.052	0.056	0.043	0.043	0.144	0.077	0.126	0.101
+ 0.1 water	0.165	0.268	0.090	0.087	0.093	0.084	0.139	0.064

Table 6-4: Cathodic and Anodic constants for iron in pure and water containing EMIM ILs.

Fe								
ILs	EMIM HSO ₄		EMIM EtSO ₄		EMIM SCN		EMIM OAc	
	b _c	b _a	b _c	b _a	b _c	b _a	b _c	b _a
Pure liquids	0.146	0.089	0.097	0.069	0.120	0.083	0.031	0.029
+ 0.01 water	0.118	0.100	0.147	0.105	0.106	0.090		
+ 0.02 water	0.133	0.094	0.059	0.410	0.105	0.115		
+ 0.05 water	0.075	0.085	0.086	0.056	0.120	0.093		
+ 0.1 water	0.073	0.095	0.076	0.060	0.073	0.096		

Table 6-5: Cathodic and anodic constants for aluminium in pure and water containing EMIM ILs.

Al								
ILs	EMIM HSO ₄		EMIM EtSO ₄		EMIM SCN		EMIM OAc	
	b _c	b _a	b _c	b _a	b _c	b _a	b _c	b _a
Pure liquids	0.103	0.106	0.063	0.168	0.039	0.041	0.091	0.166
+ 0.01 water	0.077	0.155	0.135	0.069	0.075	0.023		
+ 0.02 water	0.198	0.119	0.146	0.069	0.074	0.023		
+ 0.05 water	0.181	0.076	0.157	0.086	0.111	0.040		
+ 0.1 water	0.172	0.061	0.172	0.085	0.037	10.463		

Table 6-6: Cathodic and anodic constants for nickel in pure and water containing EMIM ILs.

Ni								
ILs	EMIM HSO ₄		EMIM EtSO ₄		EMIM SCN		EMIM OAc	
	b _c	b _a	b _c	b _a	b _c	b _a	b _c	b _a
Pure liquids	0.083	0.090	0.065	0.072	0.056	0.063	0.085	0.077
+ 0.01 water	0.090	0.106	0.156	0.097	0.052	0.051		
+ 0.02 water	0.095	0.091	0.192	0.104	0.083	0.101		
+ 0.05 water	0.064	0.060	0.060	0.097	0.058	0.048		
+ 0.1 water	0.191	0.075	0.092	0.217	0.084	0.070		

Table 6-7: Corrosion rate and corrosion potentials for iron in pure and water containing DESs.

Fe								
ILs	Ethaline		Glyceline		Reline		Oxaline	
	Ecorr. (V)	CR ($\mu\text{m yr}^{-1}$)	Ecorr. (V)	CR ($\mu\text{m yr}^{-1}$)	Ecorr. (V)	CR ($\mu\text{m yr}^{-1}$)	Ecorr. (V)	CR ($\mu\text{m yr}^{-1}$)
Pure liquids	-0.056	1.04	0.03	0.33	-0.163	1.50	-0.314	120
+ 0.01 water	-0.130	1.98	-0.046	0.60	-0.169	1.88	-0.325	108
+ 0.02 water	-0.050	0.86	-0.102	0.69	-0.239	4.66	-0.300	79.5
+ 0.05 water	-0.071	1.77	-0.163	1.02	-0.272	7.67	-0.221	28.0
+ 0.1 water	-0.109	2.24	-0.169	1.38	-0.241	5.00	-0.321	128

Table 6-8: Corrosion rate and corrosion potentials for aluminium in pure and water containing DESs.

Al								
ILs	Ethaline		Glyceline		Reline		Oxaline	
	Ecorr. (V)	CR ($\mu\text{m yr}^{-1}$)	Ecorr. (V)	CR ($\mu\text{m yr}^{-1}$)	Ecorr. (V)	CR ($\mu\text{m yr}^{-1}$)	Ecorr. (V)	CR ($\mu\text{m yr}^{-1}$)
Pure liquids	0.291	0.60	0.124	0.47	0.043	1.01	0.467	3.12
+ 0.01 water	0.316	0.82	0.144	0.59	0.059	0.70	0.482	1.98
+ 0.02 water	0.318	0.96	0.136	1.25	-0.008	0.95	0.457	0.74
+ 0.05 water	0.222	0.84	0.133	0.97	0.002	0.82	0.467	3.82
+ 0.1 water	0.211	0.98	0.168	1.12	0.005	0.80	0.465	0.63

Table 6-9: Corrosion rate and corrosion potentials for nickel in pure and water containing DESs.

Ni								
ILs	Ethaline		Glyceline		Reline		Oxaline	
	Ecorr. (V)	CR ($\mu\text{m yr}^{-1}$)	Ecorr. (V)	CR ($\mu\text{m yr}^{-1}$)	Ecorr. (V)	CR ($\mu\text{m yr}^{-1}$)	Ecorr. (V)	CR ($\mu\text{m yr}^{-1}$)
Pure liquids	-0.391	2.06	-0.113	0.04	-0.293	0.97	-0.236	16.72
+ 0.01 water	-0.417	2.74	-0.309	0.09	-0.305	0.39	-0.205	31.11
+ 0.02 water	-0.420	3.31	-0.319	0.23	-0.395	1.52	-0.296	45.84
+ 0.05 water	-0.403	5.83	0.453	2.07	-0.347	1.23	-0.291	51.38
+ 0.1 water	-0.422	2.31	-0.394	0.68	-0.430	4.49	-0.239	86.00

Table 6-10: Corrosion rate and corrosion potentials for iron in pure and water containing EMIM ILs.

Fe								
ILs	EMIM HSO ₄		EMIM EtSO ₄		EMIM SCN		EMIM OAc	
	Ecorr. (V)	CR ($\mu\text{m yr}^{-1}$)	Ecorr. (V)	CR ($\mu\text{m yr}^{-1}$)	Ecorr. (V)	CR ($\mu\text{m yr}^{-1}$)	Ecorr. (V)	CR ($\mu\text{m yr}^{-1}$)
Pure liquids	0.169	2.095	0.240	6.05	0.100	2.426	0.144	0.5413
+ 0.01 water	0.108	2.95	0.144	2.814	0.04	2.98
+ 0.02 water	0.124	2.96	0.039	2.239	0.049	4.734
+ 0.05 water	0.097	2.46	0.073	3.163	0.113	2.487
+ 0.1 water	0.062	2.76	0.072	2.352	0.072	2.96

Table 6-11: Corrosion rate and corrosion potentials for aluminium in pure and water containing EMIM ILs.

Al								
ILs	EMIM HSO ₄		EMIM EtSO ₄		EMIM SCN		EMIM OAc	
	Ecorr. (V)	CR ($\mu\text{m yr}^{-1}$)	Ecorr. (V)	CR ($\mu\text{m yr}^{-1}$)	Ecorr. (V)	CR ($\mu\text{m yr}^{-1}$)	Ecorr. (V)	CR ($\mu\text{m yr}^{-1}$)
Pure liquids	0.222	0.85	0.352	2.94	0.258	2.03	0.251	1.76
+ 0.01 water	0.294	1.66	0.392	3.54	0.308	9.76
+ 0.02 water	0.246	1.47	0.403	4.64	0.313	13.3
+ 0.05 water	0.317	2.15	0.432	4.72	0.425	5356
+ 0.1 water	0.343	2.72	0.427	4.83	0.416	4188

Table 6-12: Corrosion rate and corrosion potentials for nickel in pure and water containing EMIM ILs.

Ni								
ILs	EMIM HSO ₄		EMIM EtSO ₄		EMIM SCN		EMIM OAc	
	Ecorr. (V)	CR ($\mu\text{m yr}^{-1}$)	Ecorr. (V)	CR ($\mu\text{m yr}^{-1}$)	Ecorr. (V)	CR ($\mu\text{m yr}^{-1}$)	Ecorr. (V)	CR ($\mu\text{m yr}^{-1}$)
Pure liquids	-0.148	0.39	-0.147	9.96	-0.267	3.43	-0.392	0.32
+ 0.01 water	-0.119	2.3	-0.113	22.6	-0.320	8.94
+ 0.02 water	-0.098	3.2	-0.122	23.2	-0.208	7.92
+ 0.05 water	-0.143	17.8	-0.185	24.5	-0.320	24.3
+ 0.1 water	-0.180	87.4	-0.106	21.1	-0.258	19.5



Cite this: *Green Chem.*, 2014, **16**, 4156

Evaluating water miscible deep eutectic solvents (DESSs) and ionic liquids as potential lubricants

Andrew P. Abbott,^{*a} Essa I. Ahmed,^{a,b} Robert C. Harris^a and Karl S. Ryder^a

Although mineral oils are commonly used as lubricants their emission particularly in marine environments can cause significant impact. In the current study the properties of water miscible deep eutectic solvents and ionic liquids are compared with a typical mineral base oil to ascertain their efficacy for potential marine lubricants. The environmental compatibility of some of the liquids, particularly choline chloride and glycerol, makes it an interesting potential base lubricant. Surprisingly some DESSs showed very low corrosion rates with steel, nickel and aluminium even when the liquids contained water. This is a surprising result given that the chloride ion concentration is approximately 5 mol dm⁻³.

Received 23rd May 2014,
Accepted 18th June 2014

DOI: 10.1039/c4gc00952e

www.rsc.org/greenchem

Introduction

Lubricants are ubiquitous and perform a variety of functions such as cooling of surfaces, avoidance of corrosion, power transfer, offering a liquid seal at sliding contacts in addition to removal and suspension of wear products. Generally lubricating oils are formulated from a mixture of two or more base stocks (mineral oil, bio-based oil or synthetic oil) together with a variety of additives.¹ Most common additives which are used in lubrication are intended to perform several roles, some of them are used to protect the surface of sliding solids, while other are aimed to enhance the performance of the lubricant itself and others are used to maintain the lubricant's properties. Examples of common additives include dispersants, antioxidants, friction modifiers, anti-wear agents, detergents and viscosity index improvers.² While they generally have low toxicity on a small scale emission at sea in particular has significant environmental consequences. An additional issue for marine lubricants is the enhanced corrosion resulting from the incorporation of sea water in mineral oil based systems.³

Nowadays, the development of new products from renewable bio-based materials has become an important potential in the area of lubricant manufacturing. Triglyceride derivatives from seed oils are valued as important alternatives to conventional petroleum based base stocks as they are sustainable, generally environmentally compatible, nontoxic, biodegradable as well as small changes in viscosity as a function of temperature. Additionally, they are able to adhere to the metal surface giving them a great boundary lubrication role. Moreover,

vegetable oils are readily able to dissolve additives and polar contaminants. However, their drawbacks are associated with their high sensitivity to oxidation, hydrolysis and high pour points.^{4,5} There are, however several polyalkylene glycol based water miscible lubricants which are also available although they have tended to be used for specialist applications.⁶

While most lubricants are non-polar and have low surface tension there have recently been a significant number of publications using ionic liquids as lubricants.⁷ It has been shown that these neoteric liquids have viscosity indexes which are superior to many mineral base oils and comparable to many semi-synthetic base oils. They have also been studied as additives for a range of base fluids particularly where the ionic liquids have surfactant properties. Under extreme wear conditions some ionic liquids can break down to produce tribofilms which protect the surface. Naturally there are some environmental issues with selected ionic liquids and the complex synthesis means that the cost of production limits their use to small volume specialised applications. The numerous combinations of cations and anions allow the physical and mechanical properties to be tailored for the application. Their wide liquid range, lack of flammability, high thermal stability and non-volatility makes them interesting candidates as lubricants.⁸ Most of the studies have been carried out using imidazolium, BF₄⁻ and PF₆⁻ due to their availability although other cations and anions are now being studied. These include sulfonates and phosphates which have lower eco-toxicity.^{9–12}

In an alternative approach we have previously demonstrated that eutectic mixtures of quaternary ammonium salts and hydrogen bond donors form liquids with properties similar to ionic liquids.^{13,14} These so-called deep eutectic solvents (DESSs) have physical properties which would make them useful as lubricants. The base lubricant needs to have specific pro-

^aChemistry Department, University of Leicester, Leicester, LE1 7RH, UK.
E-mail: apa1@le.ac.uk

^bChemistry Department, College of Education, Salahaddin University, Hawler, Iraq

erties, including high viscosity index (VI), good friction coefficient reduction (μ), low pour point and low corrosivity. In this study deep eutectic solvents are compared with other water soluble ionic liquids and a mineral base oil and it is shown that the ionic fluids have enhanced thermophysical properties, corrosion resistance and wear resistance.^{1–3} It is interesting to note that while the hydrophobic oil and hydrophilic ionic liquids have similar molar masses the relative intermolecular or interionic forces are very different. While mineral oils are good at wetting hydrophobic metal surfaces such as aluminium we show that ionic liquids and DESs show improved wear characteristics with iron based alloys.

Experimental

The DESs were made by the method reported in the literature.^{13,14} The ionic liquids listed in Table 1 were used as received from BASF. Mobil Therm 605 was used as a standard heavy paraffinic petroleum distillate, solvent-dewaxed mineral base oil. The viscosity of all DESs was measured using both Ubbelohde and rotational (Brookfield DV-II+ Pro) viscometers. For rotating viscometer the spindle was rotated in each liquid between 5 and 200 rpm to ensure the appropriate torque and the resultant dynamic viscosities have been converted to kinematic viscosity using their densities at the same temperature.

Both density and surface tension were measured with a Krüss Tensiometer K9 model K9MK1. A liquid sample was placed in a glass dish surrounded by a water jacket. The temperature was controlled by a thermostat connected to the jacket. Surface tension measurement was recorded using a Pt–Ir alloy plate (Krüss, part number PL01). Contact angle measurements were performed using CAM 100 contact-angle meter from (Edmund industrial optics). Droplets of base oil, DESs and ILs

have been formed at the end of a needle and brought into contact with specimen surfaces.

The corrosion studies were carried out using AUTOLAB instruments (Autolab PGSTAT12 and FRA2 μ AUTOLAB Type III). In all experiments the metal samples (Al, Fe and Ni) were used as a working electrode and Pt electrode as a counter electrode however, the reference electrode used was (Ag/AgCl in 1 M KCl concentration). The working electrodes were made from discs of Fe, Al and Ni. For corrosion rate measurements using a.c. impedance the electrodes were polished initially with alumina (0.05 μ m) and then left in the liquids at open circuit potential for between 1 and 48 hours without polishing. Corrosion rates were calculated using ASTM G 59-97

$$i_{\text{corr}} = \frac{1}{(2.3 R_p)} \left(\frac{\beta_a \beta_c}{\beta_a + \beta_c} \right) = \frac{B}{R_p}$$

where i_{corr} is the corrosion current density, B is the Stern–Geary constant and R_p is the polarisation resistance. The value of i_{corr} was obtained automatically from software and converted to corrosion rates by inserting equivalent weights and density values of each element in LSV and adjusted for the electrode surface area (cm^2). For electrochemical impedance spectroscopy, EIS, values of (R_p) have been derived from semi-circular Nyquist plots and converted to i_{corr} using following equation

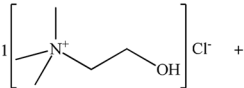
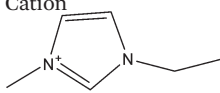
$$i_{\text{corr}} (\mu\text{A cm}^{-2}) = 10^6 B / R_p$$

Then, values are converted to corrosion rates in mm per year from this equation

$$\text{CR} = 3.27 \times 10^{-3} + \frac{i_{\text{corr}} \text{EW}}{\rho}$$

where CR is the corrosion rate in mm per year, EW is the equivalent weight (g mol^{-1}) and ρ is the density of corroding sample g cm^{-3} .

Table 1 Structures and compositions of liquids used in this study

Deep eutectic solvents	Ionic liquids
 2 $\text{H}_2\text{N}-\text{C}(=\text{O})-\text{NH}_2 \longrightarrow$ Reline Urea	Cation  C ₂ mim ⁺ Anions HSO ₄ [−] C ₂ H ₅ SO ₄ [−] SCN [−] CH ₃ COO [−]
2 $\text{HO}-\text{CH}_2-\text{CH}_2-\text{OH} \longrightarrow$ Ethaline Ethylene Glycol	
2 $\text{HO}-\text{CH}_2-\text{CH}(\text{OH})-\text{CH}_2-\text{OH} \longrightarrow$ Glyceline Glycerol	
1 $\text{HO}-\text{C}(=\text{O})-\text{C}(=\text{O})-\text{OH} \longrightarrow$ Oxaline Oxalic acid	

Friction coefficient data were determined using the standard pin on disc technique using a Teer Coatings ST-200 wear tester. In all cases the friction coefficient-time profile remained flat over (2000 cycles) and 1 hour at 0.005 ms^{-1} under a load of 30 N at $293 \pm 1 \text{ K}$.

Results and discussion

Thermophysical data

To be suitable as lubricants fluids need to retain an appropriate viscosity profile over a wide range of temperature. This is generally expressed through the viscosity index (VI) which is defined as;

$$VI = 100(L - U)/(L - H)$$

where U is the kinematic viscosity at 40°C of the unknown oil; L is the kinematic viscosity at 40°C of an oil ($VI = 0$) having the same viscosity at 100°C as the unknown oil; H is the kinematic viscosity at 40°C of an oil ($VI = 100$) having the same viscosity at 100°C as the unknown oil.¹⁵

It has previously been shown that the addition of quaternary ammonium salts lead to a decrease in the friction coefficient of fluids and the minimum friction occurs at the eutectic composition.¹⁶ In the current study four DESs were tested at their eutectic composition using choline chloride as the quaternary ammonium salt together with different hydrogen bond donors. These are compared with four water-miscible, imidazolium-based ionic liquids as shown in Table 1.

Table 2 shows thermo-physical and corrosion data for four DESs, four ionic liquids and a standard mineral base oil. It should be highlighted that this study is comparing the properties of the ionic fluids to those of the base lubricating fluid. The properties of finished lubricating fluids are usually superior to those in Table 2 due to complex additive packages.

The viscosity index is usually calculated using a U-tube viscometer to measure the kinematic viscosity. This method is only valid for truly Newtonian fluids where the viscous stress is proportional to the local shear rate. It is known that some ionic liquids have some non-Newtonian character.¹⁷ Most liquids in Table 2 showed Newtonian behaviour and good correlation was observed between the viscosity obtained from the

Ubbelohde and rotating cylinder techniques. Reline and oxaline showed non-Newtonian behaviour and so to give comparable results the average viscosity at a series of rotation rates was calculated. It should therefore be stressed that the VI data in Table 2 are comparative for some of the DESs. The viscosity indexes of the DESs and ionic liquids are higher in all cases to the base oil. All four DESs have viscosity indexes which are above the value of the base oil. It should be stressed however, than none of these liquids have additive packages added which would be used in the finished lubricant.

Most of the DESs and imidazolium based ionic liquids also have improved freezing points compared to the base oil suggesting improved performance at lower temperatures. The urea based eutectic with choline chloride has too high a freezing point and coupled with the propensity for urea to break down to form ammonia at high temperatures would probably make it unsuitable for general use. The glycol based liquids are, however better at both high and low temperatures and have high VI values. The benign nature, particularly of glycerol, makes this eutectic an interesting candidate for a marine lubricant because it is totally miscible with water and would disperse if discharged at sea. Since both components are extremely benign they pose negligible threat to aquatic life. The four imidazolium-based ionic liquids also show high viscosity indexes and thermal properties. They are also miscible with water and C_2mim has been shown to have relatively low toxicity although anions such as SCN are clearly undesirable.¹⁸

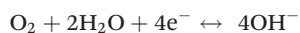
Corrosion rate data

Viable lubricants must also be non-corrosive which is why mineral oils have been widely used. While viscosity data exists for most ionic liquids very little data exists on their compatibility with metals.¹⁹ Table 2 shows the corrosion rates for mild steel in 4 DESs and four ionic liquids. The corrosion was studied using both linear sweep voltammetry and electrochemical impedance spectroscopy (EIS) and Table 2 shows that both had similar trends and magnitudes. It is well known that chloride based media can significantly enhance the corrosion rate in aqueous solution as it breaks down passive films.²⁰ As such it would seem logical that it should be avoided for lubricant applications. Table 2 shows the initial corrosion rates as

Table 2 Thermo-physical properties and corrosion rate data for four DESs, four imidazolium based ionic liquids and a mineral base oil

Fluid	Viscosity/ $\text{mm}^2 \text{ s}^{-1}$		Density at $25^\circ\text{C}/\text{g cm}^{-3}$	VI	$T_f/^\circ\text{C}$	Surface tension/ mNm^{-1}	Corrosion of mild steel/ $\mu\text{m per year}$	
	At 40°C	At 100°C					LSV	EIS
Base oil	30	5	0.87	100	−9	30.6	—	—
Ethaline	20	5	1.12	191	−61	49.2	1.9	5.02
Glyceline	118	23	1.19	147	−35	55.4	0.4	2.2
Reline	218	24	1.20	121	12	86.4	2.5	2.7
Oxaline	149	28	1.20	144	−18	75.3	176	65
$\text{C}_2\text{mim HSO}_4$	160	30	1.36	130	<−30	46.7	2.1	2.3
$\text{C}_2\text{mim C}_2\text{H}_5\text{SO}_4$	80	13	1.24	142	<−30	45.1	6.05	3.2
$\text{C}_2\text{mim SCN}$	15	7	1.11	212	−50	37.9	2.43	1.47
$\text{C}_2\text{mim CH}_3\text{COO}$	75	13	1.10	141	−20	45.4	0.54	3.5

determined using Tafel slopes from slow-rate linear sweep voltammetry. These are extremely low for ethaline, glyceline and reline but extremely high for oxaline. The origin of this difference could be due to the presence of an insulating film on the metal surface or the kinetics of either the anodic or cathodic processes. The Tafel slope shows that in ethaline, reline and glyceline the cathodic slope is shallow suggesting that the cathodic process is rate limiting. In these liquids the cathodic process is the reduction of oxygen *i.e.*



The very high chloride concentration will decrease the activity of water as it is highly hydrogen bonded. In the oxalic acid based eutectic however the cathodic process is extremely fast as it is just the reduction of protons to form hydrogen gas allowing much faster corrosion. Interestingly in this liquid bright yellow sheets of iron oxalate form parallel to the metal surface until all the metal is dissolved, which effectively filled the sample tube by the end of the experiment.

The very unusual aspect of DESs is their propensity to prevent corrosion even when the liquid is doctored with an electrolyte solution. Fig. 1 shows that when 1 wt% water containing 3 wt% NaCl (a mimic of sea water) is added to the mineral oil, significant corrosion is observed of the mild steel immersed in the liquid after 2 weeks. Clearly the aqueous phase partitions to the steel surface where corrosion is caused by the relatively high chloride concentration. Fig. 1 shows an analogous experiment where choline chloride is added to the aqueous solution in place of sodium chloride and it can be seen that corrosion occurs but to a lesser extent. This surprisingly shows that there is a cation effect to the corrosion mechanism which is not fully understood at present but may be related to the relative solubility of the corrosion products. Fig. 1 also shows corrosive effect of ethaline and glyceline to which the same aqueous electrolytes were added in the same amounts. No visible signs of corrosion were detected on mild steel even after 6 months whereas in wet base oil corrosion was clearly visible within two days. This unusual observation shows that, counter to perceived wisdom, mild steel does not

show signs of corrosion in a high chloride medium (approximately 5 mol dm^{-3}).

Table 3 shows the initial corrosion rate for iron, nickel and aluminium in four DESs as a function of water content. It can be seen that the glycol based liquids are relatively insensitive to the addition of water, whereas the urea and oxalic acid significantly increase the rate of corrosion for iron compared to an aqueous solution. Surprisingly aluminium only shows very slow corrosion when water is added even with a high chloride concentration presumably due to oxalate being able to passivate the metal surface. The formation of a passivating film can clearly be observed using a.c. impedance spectroscopy.

The low corrosion rate of common metals with glycol-based DESs even with significant water content suggests that they

Table 3 Corrosion rates of Fe, Al and Ni in four DESs as a function of water content determined using linear sweep voltammetry and Tafel slope analysis

	Glyceline	Ethaline	Reline	Oxaline
Corrosion rate of Fe (μm per year)				
Pure DES	0.40	1.98	2.503	176.4
1% water	0.74	2.51	3.220	169.1
2% water	0.86	3.25	9.688	110.5
5% water	1.72	2.68	12.30	82.78
10% water	2.95	4.35	17.550	206.2
0.1 M aqueous KNO_3	7.32	7.32	7.32	7.32
Corrosion rate of Al (μm per year)				
Pure DES	0.68	1.02	1.99	3.82
1% water	1.10	1.55	1.37	2.30
2% water	1.12	1.78	1.36	2.05
5% water	1.19	1.82	1.40	2.40
10% water	1.41	1.94	1.55	2.11
0.1 M aqueous KNO_3	5.86	5.86	5.86	5.86
Corrosion rate of Ni (μm per year)				
Pure DES	0.09	4.18	1.59	25.9
1% water	0.23	6.79	1.60	63.1
2% water	0.51	7.96	2.24	58.7
5% water	1.14	9.62	4.64	90.0
10% water	1.53	7.30	8.79	126.8
0.1 M aqueous KNO_3	8.05	8.05	8.05	8.05

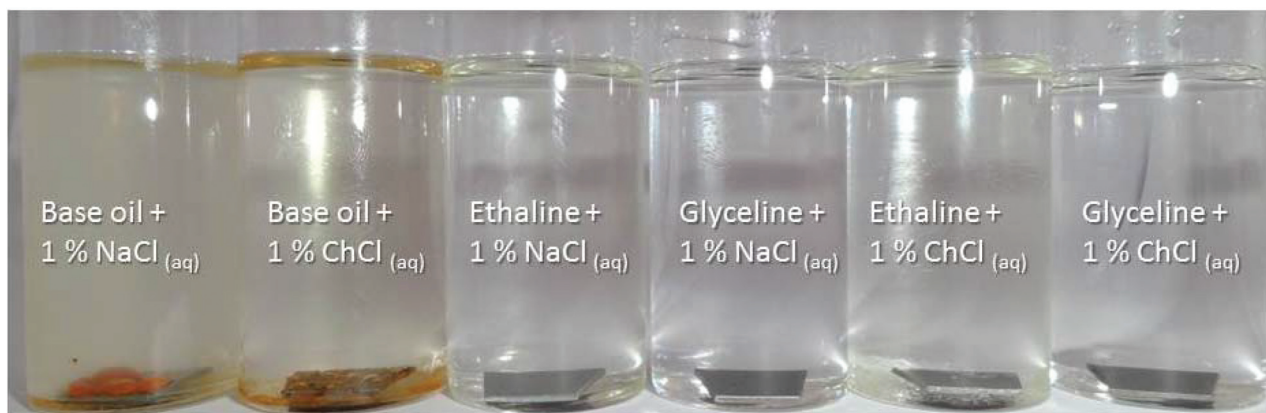


Fig. 1 Corrosion behaviour of mild steel after 2 weeks immersed in DESs and mineral base oil containing 1% $\text{NaCl}_{(\text{aq})}$ and 1% $\text{ChCl}_{(\text{aq})}$.

Table 4 Coefficient of kinetic friction, μ_k , and contact angles of various water miscible ionic liquids and DESs for several metal contacts with mild steel. Surface activity values were calculated for alloys using linear combinations of the values of the individual components

	Properties	Substrate metals against stainless steel				
		Al	Bronze	Cu	Mild steel	Stainless steel
ILs	Surface activity (mJ m^{-2})	867	1534	1650	2150	2075
Ethaline	Contact angle	66.1	72.7	88.3	70.9	82.4
	μ_k	0.15	0.58	0.59	0.30	0.37
Glyceline	Contact angle	79.5	77.5	84.7	92.2	86.3
	μ_k	0.55	0.40	0.45	0.28	0.38
Reline	Contact angle	74.4	93.2	94.9	90.5	90.7
	μ_k	0.31	0.26	0.21	0.32	0.28
Oxaline	Contact angle	76.52	30.4	28.7	40.8	51.7
	μ_k	0.25	0.29	0.18	0.38	0.30
Emim SCN	Contact angle	61.4	50.3	64.3	60.4	68.7
	μ_k	0.29	0.33	0.23	0.47	0.28
Emim HSO ₄	Contact angle	85.2	77.6	58.3	57.2	71.2
	μ_k	0.30	0.42	0.20	0.48	0.23
Emim EtSO ₄	Contact angle	52.0	70.9	62.4	56.4	62.4
	μ_k		0.43	0.50	0.30	0.22
Emim OAc	Contact angle	67.9	57.3	62.2	54.9	69.2
	μ_k		0.45	0.50	0.28	0.23
Base oil	Contact angle	7.6	18.0	12.8	11.7	11.3
	μ_k	0.12	0.23	0.37	0.40	0.45

may be useful media as base lubricants particularly for marine applications.

Electrochemical a.c. impedance spectroscopy shows that while slow corrosion occurs initially and a passivating layer appears to form for a range of metals including Ni and Al. Comparing the corrosion rates for the imidazolium based ionic liquids with those for the DESs and base oil shown in Table 2 it can be seen that the corrosion rate of mild steel in the most hydrophobic anion, ethylsulfate, is considerably higher than either hydrogen sulfate or SCN presumably due to its inability to bind traces of water. The acetate anion showed the lowest rate of corrosion. It appears to hold that ionic fluids with more Lewis basic anions tend to demonstrate enhanced corrosion resistance.

Wear resistance

We have previously shown that adding quaternary ammonium electrolytes to glycerol can significantly reduce the friction coefficient which shows that the ionic component has an interfacial preference which allows it to interact with the metal and produce an interfacial barrier.¹⁶ Studies in pure imidazolium based liquids have shown that the metal liquid interface is highly structured with most probably alternating layers of cations and anions.^{21,22} Friction modifying additives which decrease the friction coefficients for base oils tend to be relatively polar and include fatty acid derivatives such as glycerol monooleate² or the correspond oleylamide. The polar functional groups are thought to chemisorb onto the metal surface through the mechanical wear of one surface with another. An alternative additive is an organometallic compound such as zinc dialkyldithio phosphate which forms a complex insoluble film of 10–200 nm thickness this acts as an anti-wear layer.² Previous studies have shown that glycolate films form from the electrooxidation of iron and nickel in DESs. These tend to have

characteristic a.c. impedance spectra²³ which are similar in magnitude to those observed on prolonged contact with the DESs and iron electrodes.

Table 4 shows that the DESs show lower friction coefficients than base oil with stainless steel, but slightly higher values for aluminium couples. This is thought to result from the relative abilities of the liquids to wet the different surfaces. This concept was tested by measuring the contact angle of the metals with different DESs. Clearly mineral oils with their low surface tension and low contact angles should be able to better wet surfaces but it depends to some extent on the nature of the surface. An indicator of the hydrophilicity of the surface activity of the liquid metal and Table 4 shows that aluminium has a low surface energy whereas iron based alloys have a high surface activity.²⁴ It seems logical therefore that ionic liquids with high surface tensions and high contact angles should show improved friction coefficients over base oils with iron based alloys whereas the reverse is the case for aluminium and bronze alloys.

Conclusion

This study has shown that DESs, particularly those based on glycols, together with choline chloride have the correct lubricity, toxicity and corrosivity to be viable options for base lubricants. Their ability to be miscible with water in all proportions and to suppress corrosion even when slightly wet means that they could be of particular use for marine lubricants. Friction coefficient measurements suggest that they have improved tribological properties with respect to mineral oils for iron-based alloys which are clearly the important materials for lubrication whereas the converse is the case for more hydrophobic surfaces such as aluminium.

Acknowledgements

The authors would like to thank the Higher Committee for Education Development in Iraq and Salahaddin University for a studentship (E.I. Ahmed).

References

- 1 Z. Pawlak, *Tribochemistry of Lubricating Oils*, Elsevier Science, 2003.
- 2 L. R. Rudnick, *Lubricant Additives: Chemistry and Applications*, CRC Press, Boca Raton, USA, 2nd edn, 2009.
- 3 R. M. Mortier, M. F. Fox and S. T. Orszulik, *Chemistry and Technology of Lubricants*, Springer, Dordrecht, 3rd edn, 2010.
- 4 A. Adhvaryu, B. K. Sharma, H. S. Hwang, S. Z. Erhan and J. M. Perez, *Ind. Eng. Chem. Res.*, 2006, **45**, 928–933.
- 5 B. K. Sharma, J. M. Perez and S. Z. Erhan, *Energy Fuels*, 2007, **21**, 2408–2414.
- 6 W. H. Millett, *Ind. Eng. Chem.*, 1950, **42**, 2436–2441.
- 7 A. E. Somers, P. C. Howlett, D. R. MacFarlane and M. Forsyth, *Lubricants*, 2013, **1**, 3–21.
- 8 F. Zhou, Y. Liang and W. Liu, *Chem. Soc. Rev.*, 2009, **38**, 2590–2599.
- 9 W. Morales, K. W. Street, R. M. Richard and D. J. Valco, *Tribol. Trans.*, 2012, **55**, 815–821.
- 10 I. Minami, T. Inada, R. Sasaki and H. Nanao, *Tribol. Lett.*, 2010, **40**, 225–235.
- 11 A. S. Wells and V. T. Coombe, *Org. Process Res. Dev.*, 2006, **10**, 794–798.
- 12 T. P. T. Pham, C.-W. Cho and Y.-S. Yun, *Water Res.*, 2010, **44**, 352–372.
- 13 A. P. Abbott, G. Capper, D. L. Davies, R. K. Rasheed and V. Tambyrajah, *Chem. Commun.*, 2003, 70–71.
- 14 A. P. Abbott, D. Boothby, G. Capper, D. L. Davies, R. Rasheed and V. Tambyrajah, *J. Am. Chem. Soc.*, 2004, **126**, 9142.
- 15 ASTM, “Standard Practice for Calculating Viscosity Index From Kinematic Viscosity at 40 and 100 °C” ASTM Standard D 2770, *Annual Book of ASTM Standards*, American Society for Testing Materials, ASTM International, West Conshohocken, PA, 2004.
- 16 S. D. A. Lawes, S. V. Hainsworth, P. Blake, K. S. Ryder and A. P. Abbott, *Tribol. Lett.*, 2010, **37**, 103–110.
- 17 G. L. Burrell, N. F. Dunlop and F. Separovic, *Soft Matter*, 2010, **6**, 2080–2086.
- 18 C. Pretti, C. Chiappe, D. Pieraccini, M. Gregori, F. Abramo, G. Monni and L. Intorre, *Green Chem.*, 2006, **8**, 238–240.
- 19 Y.-C. Wang, T.-C. Lee, J.-Y. Lin, J.-K. Chang and C.-M. Tseng, *Corros. Sci.*, 2014, **78**, 81–88.
- 20 R. W. Revie, *Corrosion and Corrosion Control*, Wiley, New York, 2008.
- 21 R. Atkin, S. Z. El Abedin, R. L. Hayes, L. H. S. Gasparotto, N. Borisenko and F. Endres, *J. Phys. Chem. C*, 2009, **113**, 13266–13272.
- 22 R. L. Hayes, N. Borisenko, M. K. Tam, P. C. Howlett, F. Endres and R. Atkin, *J. Phys. Chem. C*, 2011, **115**, 6855–6863.
- 23 A. P. Abbott, G. Capper, K. J. McKenzie and K. S. Ryder, *Electrochim. Acta*, 2006, **51**, 4420–4425.
- 24 *Wettability at High Temperatures*, ed. N. Eustathopoulos, M. G. Nicholas and B. Drevet, Elsevier Science Ltd., Oxford, 1999.



Cite this: *Phys. Chem. Chem. Phys.*,
2015, 17, 15297

Molecular and ionic diffusion in aqueous – deep eutectic solvent mixtures: probing inter-molecular interactions using PFG NMR

Carmine D'Agostino,^{*a} Lynn F. Gladden,^a Mick D. Mantle,^a Andrew P. Abbott,^{*b} Essa, I. Ahmed,^b Azhar Y. M. Al-Murshedi^b and Robert C. Harris^b

Pulsed field gradient (PFG) NMR has been used to probe self-diffusion of molecular and ionic species in aqueous mixtures of choline chloride (ChCl) based deep eutectic solvents (DESs), in order to elucidate the effect of water on motion and inter-molecular interactions between the different species in the mixtures, namely the Ch^+ cation and hydrogen bond donor (HBD). The results reveal an interesting and complex behaviour of such mixtures at a molecular level. In general, it is observed that the hydroxyl protons (^1H) of Ch^+ and the hydrogen bond donor have diffusion coefficients significantly different from those measured for their parent molecules when water is added. This indicates a clear and significant change in inter-molecular interactions. In aqueous Ethaline, the hydroxyl species of Ch^+ and HBD show a stronger interaction with water as water is added to the system. In the case of Glyceline, water has little effect on both hydroxyl proton diffusion of Ch^+ and HBD. In Reline, it is likely that water allows the formation of small amounts of ammonium hydroxide. The most surprising observation is from the self-diffusion of water, which is considerably higher than expected from a homogeneous liquid. This leads to the conclusion that Reline and Glyceline form mixtures that are inhomogeneous at a microscopic level despite the hydrophilicity of the salt and HBD. This work shows that PFG NMR is a powerful tool to elucidate both molecular dynamics and inter-molecular interactions in complex liquid mixtures, such as the aqueous DES mixtures.

Received 13th March 2015,
Accepted 11th May 2015

DOI: 10.1039/c5cp01493j

www.rsc.org/pccp

Introduction

Deep Eutectic Solvents (DES) are mixtures of quaternary ammonium salts and hydrogen bond donors such as amides and polyols, having properties which are analogous to ionic liquids. The interaction between the two species leads to a lowering of the melting point and the formation of a eutectic. DESs are attracting considerable attention in many applications such as catalysts,^{1–3} solvents,^{4–6} electro-plating,⁷ purification media⁸ and others.^{9,10}

In many of these applications, the addition of water has little effect upon the chemical properties but significantly improves the mass transport characteristics of the liquids. In the applications listed above water is often added to improve conductivity and aid filtration; the amount of water added often being chosen empirically. It has been empirically noted that DESs change their properties to those of ionic solutions when between

5 and 10 wt% water has been added.¹¹ The addition of water introduces a second HBD and the relative interactions between the anion/cation and both HBDs will change the diffusion coefficients of each component.

Due to the complexity of such mixtures, a fundamental understanding of the interactions involved between the different species of a DES is of significant importance. Hydrogen bonds and ionic interactions play a key role in determining the macroscopic behaviour. The HBD is known to form a complex with the anion of the salt, resulting in the formation of a bulky asymmetric anion, which decreases the lattice energy thus decreasing the freezing point of the system.¹² The whole picture could potentially be more complex as some HBDs may also ionise to some extent, leading to the presence of multiple ions within the mixtures. The bulk properties of the whole system, such as viscosity, ionic conductivity and density have provided some insight into the behaviour of these liquids;^{5,6,12,13} however, a microscopic approach can provide insights regarding the individual species, which affect the macroscopic behaviour of the system. In particular, a more detailed understanding of the mobility of the individual component of the mixture allows an understanding of the relative interactions in the mixture. In this

^a Department of Chemical Engineering and Biotechnology, University of Cambridge, Pembroke Street, Cambridge CB2 3RA, UK. E-mail: cd419@hermes.cam.ac.uk

^b Department of Chemistry, University of Leicester, Leicester LE1 7RH, UK. E-mail: apa1@le.ac.uk

context, pulsed-field gradient (PFG) NMR is one technique that can provide significant insight. The method allows self-diffusion coefficients of NMR active species to be determined and has the advantage of being non-invasive and chemically selective, which makes it possible to investigate simultaneously the diffusion behaviour of different species within a mixture, including different moieties within each molecular species.

In a recent study,¹⁴ the molecular transport of the HBD and the choline cation (Ch^+) in different pure choline chloride (ChCl) based DESs was investigated. It was found that the structure of the HBD greatly affects the molecular mobility of the whole system. In addition, it was speculated that in the case of Maline, the malonic acid HBD tends to form long chains of dimers, which reduces significantly the molecular mobility of the whole system compared to the other DES and leads to a slower diffusivity of malonic acid relative to ChCl , despite its much smaller molecular weight and size. It is therefore clear that, a variety of interactions takes place within such samples, notably ionic interactions and hydrogen bonding interactions.

The use of DESs in aqueous mixtures is of particular significance as aqueous DES mixtures have several practical applications.^{15–18} For example, interactions involving DESs, salts and water play an important role when DESs are used as extraction media for protein partitioning.¹⁶ Different DESs were shown to have different abilities to extract various proteins. A clear explanation of the extraction performances of the different DES samples was not given; however, from such results one can infer that the steric hindrance of the hydrophobic moieties around the positive nitrogen centre of the DES used in this study plays a key role in determining interactions with the aqueous protein solution, hence affecting the extraction capacity. Abbott *et al.*¹⁸ used water miscible DESs as potential “green” lubricants and investigated the corrosion rate for different metals. It was shown that steel corroded mildly in wet Reline but was almost inert in wet Glyceline. This was ascribed to differences in cathodic reactions in the liquids. It is clear that additional details on the molecular interactions involved in aqueous DES systems would certainly contribute to a better understanding of the microscopic behaviour of such systems in several applications, such as separation and reaction processes in general.

In this study PFG NMR has been used to study the molecular mobility of three ChCl based DESs in the presence of water in order to understand the effect of water composition on the molecular mobility of the different species involved in the system. The hydrogen bond donors studied are those most commonly used in the literature, namely glycerol (Glyceline), urea (Reline) and ethylene glycol (Ethaline). This information obtained shows that all three DESs have different speciation and characteristic interactions from those previously assumed.

Experimental

Materials

Choline chloride [$\text{HOC}_2\text{H}_4\text{N}(\text{CH}_3)_3\text{Cl}$] (ChCl) (Aldrich 99%) was recrystallized from absolute ethanol, filtered and dried under

vacuum. Ethylene glycol (EG), glycerol and urea (all Aldrich +99%), were dried under vacuum. The two components of the DES were mixed together by stirring (in a 1:2 molar ratio of ChCl : hydrogen bond donor) at 60 °C until a homogeneous, colourless liquid formed. Viscosity measurements were obtained as a function of temperature using a Brookfield DV-E Viscometer (Brookfield Instruments, USA) fitted with a temperature probe. A variety of spindles (LV1, LV2 and LV3) were used with rotation rates of 5–200 rpm to obtain appropriate viscosity data. The conductivity of the liquids were measured at 20 °C using a Jenway 4510 conductivity meter fitted with a temperature probe (cell constant = 1.01 cm^{-1}). A Krüss Tensiometer/Densitometer model K9MK1 was used to measure the density data for all liquids.

The water content is quoted in wt% but the table below describes the corresponding approximate mole equivalents of water.

Wt% H_2O	2.5	5	7.5	10	12.5	15	17.5	20
Mol eq. water: DES	0.37	0.76	1.17	1.60	2.06	2.55	3.06	3.61

PFG NMR measurements

PFG NMR diffusion measurements were conducted on a Bruker DMX 300 spectrometer, equipped with a diffusion probe capable of producing magnetic field gradient pulses up to 11.76 T m^{-1} in the z-direction and using a pulsed gradient stimulated echo (PGSTE) sequence with a homospoil gradient, which is usually preferred to the standard pulsed gradient spin echo or PGSE sequence, resulting in a better signal-to-noise ratio. The NMR signal attenuation, $E(g)/E_0$, is related to the experimental variables and the diffusion coefficient D according to:¹⁹

$$\frac{E(g)}{E_0} = \exp \left[-D \gamma_{\text{H}}^2 g^2 \delta^2 \left(\Delta - \frac{\delta}{3} \right) \right] \quad (1)$$

In eqn (1), $E(g)$ and E_0 are the NMR signal in the presence and absence of the gradient pulse, respectively; γ_{H} is the gyromagnetic ratio of the nucleus being studied (*i.e.*, ^1H in our case), g is the strength of the gradient pulse of duration δ , and Δ is the observation time. The measurements were performed by fixing $\Delta = 50 \text{ ms}$ and δ with values in the range 1–4 ms. The magnitude of g was varied with sixteen linearly spaced increments. In order to achieve full signal attenuation, maximum values of g of up to 11.50 T m^{-1} were necessary. The diffusion coefficients D can be calculated by fitting eqn (1) to the experimental data. More details on the experimental set-up can be found elsewhere.¹⁴

Results and discussion

Fig. 1 shows the viscosity of 3 different DESs, Reline (HBD = urea), Ethaline (HBD = ethylene glycol) and Glyceline (HBD = glycerol). The viscosity of each liquid was determined using both a rotating cylinder and a quartz crystal microbalance and the data from both techniques deviated from each other by less than 1%. Data for Reline and Glyceline were in accordance with

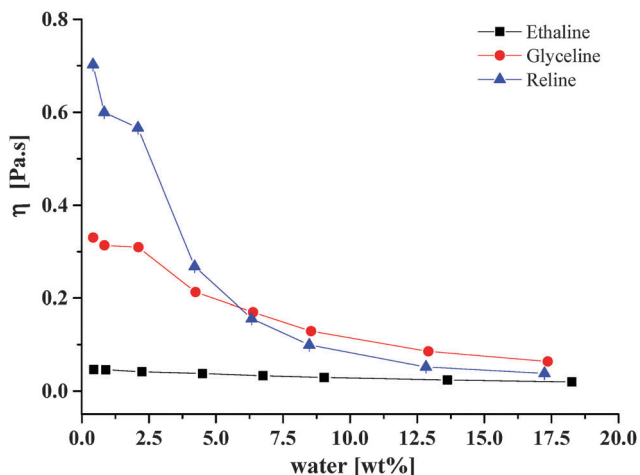


Fig. 1 Viscosity of the three DESs at 20 °C as function of water content as determined by rotating cylinder technique. Note error bars are all within the size of the plot symbol.

those published previously, albeit the Reline data was at higher temperatures.^{20,21} In the anhydrous state all liquids showed some non-Newtonian behaviour but all became Newtonian when the water content rose above 2.5 wt%. The non-Newtonian behaviour was observed through a larger error bar in the low water content data but is not discussed further in this study; all of the error bars are smaller than the plot symbol in Fig. 1. In all liquids a decrease in viscosity is observed with increasing water content; however, this is not a steady decrease and there is a pronounced and reproducible shoulder at 2.5 wt% for Glyceline and Reline, which corresponds to approximately 1 mole equivalent of water to each chloride anion, which may be significant.

It is important to notice from Fig. 1 that the effect of water on the viscosity of Reline is greater than for the other two liquids. At higher water content, Glyceline has a higher viscosity than Reline, followed by Ethaline. This suggests that glycerol is the strongest HBD due solely to the fact that it has 3 OH functionalities. This is consistent with the hydrogen bond donating parameters, α , previously determined for these three liquids.²² The α -values for Reline (0.922) and Glyceline (0.937) are relatively similar to those of water (1.17) but the value for Ethaline (0.903) is lower showing that the water will preferentially solvate the chloride anion. As will be discussed later, this may also explain why there is no apparent change in the diffusion coefficient for water in Ethaline at low water content as it is bound with the chloride. This can be clearly seen by inspection of Fig. 5a, shown later.

Fig. 2 shows the plot of molar conductivity *versus* fluidity for the systems shown in Fig. 1. It can be seen that a relatively linear plot is observed for all systems with the exception of Reline at high water content. In all cases the charge carriers should be the same *viz* Ch^+ and Cl^- . In more dilute ionic solutions, it would be expected that ionic association would dominate molar conductivity; the linear plot observed in Fig. 2 suggests viscosity controls charge transport in most systems. As will be shown below, the dilute Reline solution shows evidence

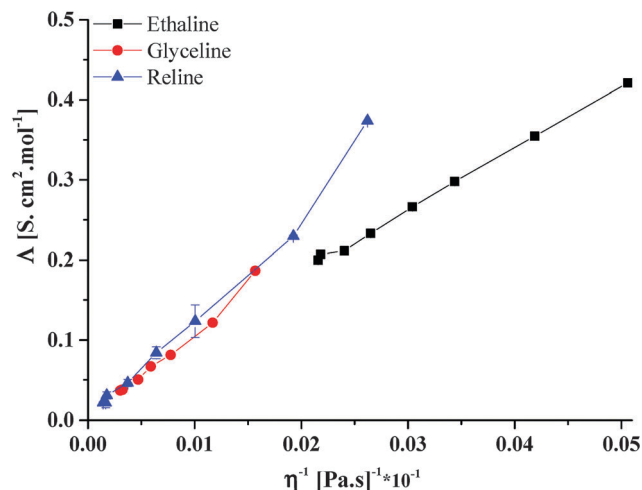


Fig. 2 Plot of molar conductivity *versus* fluidity for the data in Fig. 1.

of some urea decomposition leading to the formation of NH_4OH , which is probably the cause of the increase in molar conductivity at high water content.

To probe the mobility of the charged and uncharged species further the self-diffusion coefficients were determined using NMR spectroscopy. Fig. 3 reports a typical NMR spectrum for the samples used in this study, together with the peak assignment. The peak assignment is consistent with the spectra previously reported for choline chloride-based DES.¹⁴ The NMR peaks are rather broad (typical linewidth values of approximately 25–30 Hz at FWHM) and this is expected given the high viscosity of such samples.

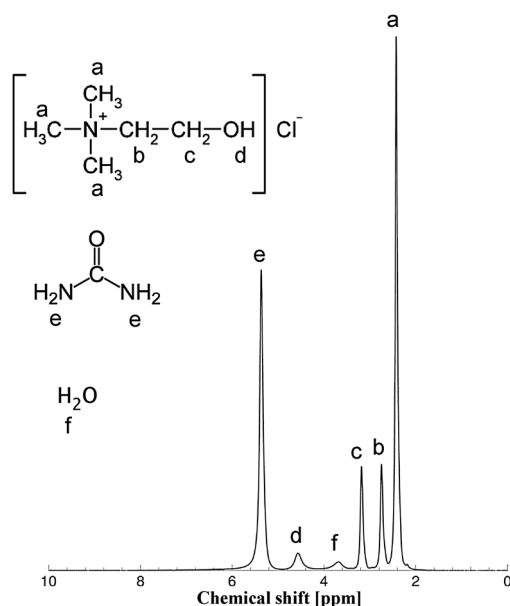


Fig. 3 ^1H NMR spectrum of aqueous Reline at 1 wt% water content at 20 °C. The NMR peak positions are (in ppm): $a = 2.43$; $b = 2.75$; $c = 3.18$; $d = 4.59$; $e = 5.38$; $f = 3.69$. All resonances are quoted relative to the ^1H resonance of tetramethylsilane (TMS).

The NMR spectrum and relative peak assignment for aqueous Glyceline, with a 13 wt% fraction of water, is shown in Fig. 4a. Fig. 4b reports the PFG NMR attenuation plots for the various resonances in this sample. The much steeper slope for the water resonance indicates a much faster diffusion of water in the mixture relative to the diffusion of the chemical species of Glyceline. From Fig. 4 it is also possible to observe that the two moieties of glycerol (*i.e.*, the hydroxyl proton and the aliphatic carbon backbone) have diffusivity values that are almost identical to the diffusivity of the hydroxyl proton of the Ch^+ species, hence their PFG NMR plots overlap. The Ch^+ ion is the species with the slowest diffusivity, as it can be seen by its PFG NMR plot, which shows the lowest slope amongst all species probed.

The experimental data in Fig. 4b were fitted using eqn (1), which allows the determination of the numerical values of self-diffusivity. In the current work we are not only interested in probing the self-diffusion coefficients of the three main components of the mixture (*i.e.*, ChCl , HBD and water) but we are also interested in probing the diffusivities of the hydroxyl protons in both Ch^+ and HBD molecules. The particular advantage of PFG NMR is that it can probe the diffusion of a certain species by measuring the signal attenuation of the NMR resonances of that species. In the absence of any exchange/interactions with other species, both aliphatic and hydroxyl ^1H resonances of the molecule should yield the same diffusion coefficients (*i.e.*, the molecule/ion moves as a whole). However, if phenomena such as interaction/pairing/exchange between hydroxyl protons of different molecules become significant, one may expect a very large difference in the diffusion coefficient values of the aliphatic and hydroxyl protons of the same

molecule. In this context, PFG NMR diffusion measurements become a powerful tool to elucidate interactions between the different species within the liquids, besides their motion characteristics.²³

In Fig. 5, the values of self-diffusion coefficients as a function of water content are reported for the different species present in the three different aqueous DES mixtures. It is noted that the only species that cannot be probed with our current experimental PFG-NMR set-up is the Cl^- anion; this is because its detection *via* PFG-NMR is complicated by several factors such as the low sensitivity of chloride anions and the presence of nuclear quadrupolar interactions.

Ethaline

In the pure liquid (*i.e.*, in the absence of any water) the diffusivity of ethylene glycol is higher than that of Ch^+ . This is in agreement with previous findings¹⁴ on pure DES studies and is attributed to the larger size of the Ch^+ cation relative to ethylene glycol. It can also be seen that, in each species (*i.e.* Ch^+ and ethylene glycol) the diffusivity of the hydroxyl proton is the same as that measured for the rest of the molecule, which clearly suggests that there is no significant exchange of hydroxyl protons between the two species in the pure Ethaline sample (*i.e.*, the hydroxyl proton remains bound to the rest of the molecule as it diffuses).

When water is added to the DES, the diffusivities of both Ch^+ and ethylene glycol both increase. However, we now observe a significant deviation for the hydroxyl protons diffusivity of both Ch^+ and ethylene glycol relative to the diffusivity of their parent molecules; for each of these species, the hydroxyl proton diffuses faster than rest of the molecule and such a difference

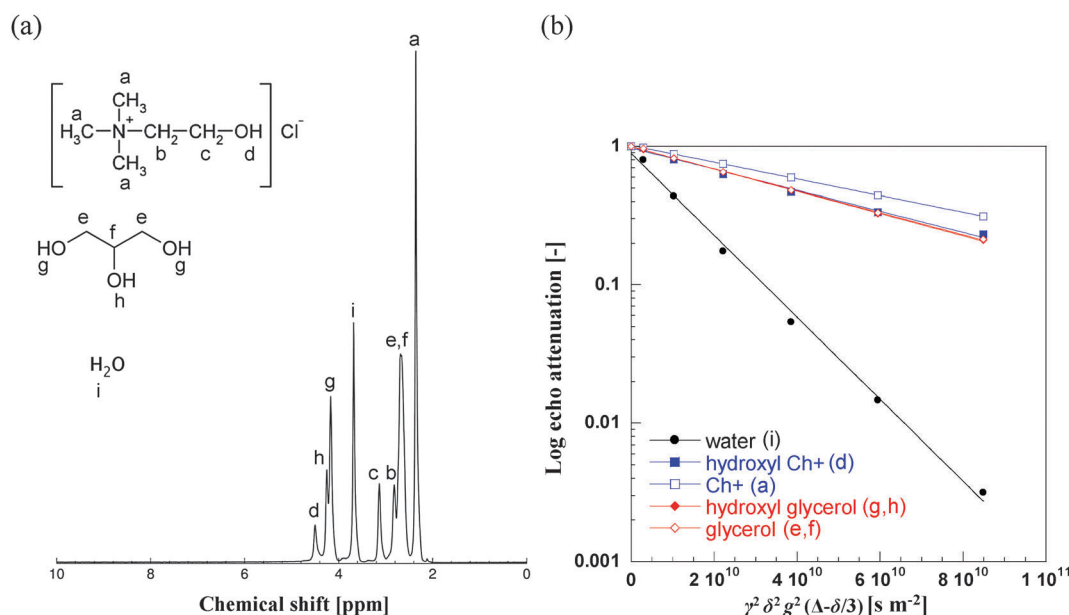


Fig. 4 (a) ^1H NMR spectrum of aqueous Glyceline at 13 wt% water content at 20 °C. The NMR peak positions are (in ppm): a = 2.40; b = 2.81; c = 3.13; d = 4.50; e, f = 2.67; g = 4.17; h = 4.25; i = 3.68. All resonances are quoted relative to the ^1H resonance of tetramethylsilane (TMS). (b) PFG NMR log attenuation plots for the various species in aqueous Glyceline with a 13 wt% fraction of water. The letters in brackets in the legend refer to the peak assignment made on Fig. 4a. Note the distinctive diffusion attenuation of water relative to the other species. Solid lines are fittings using eqn (1).

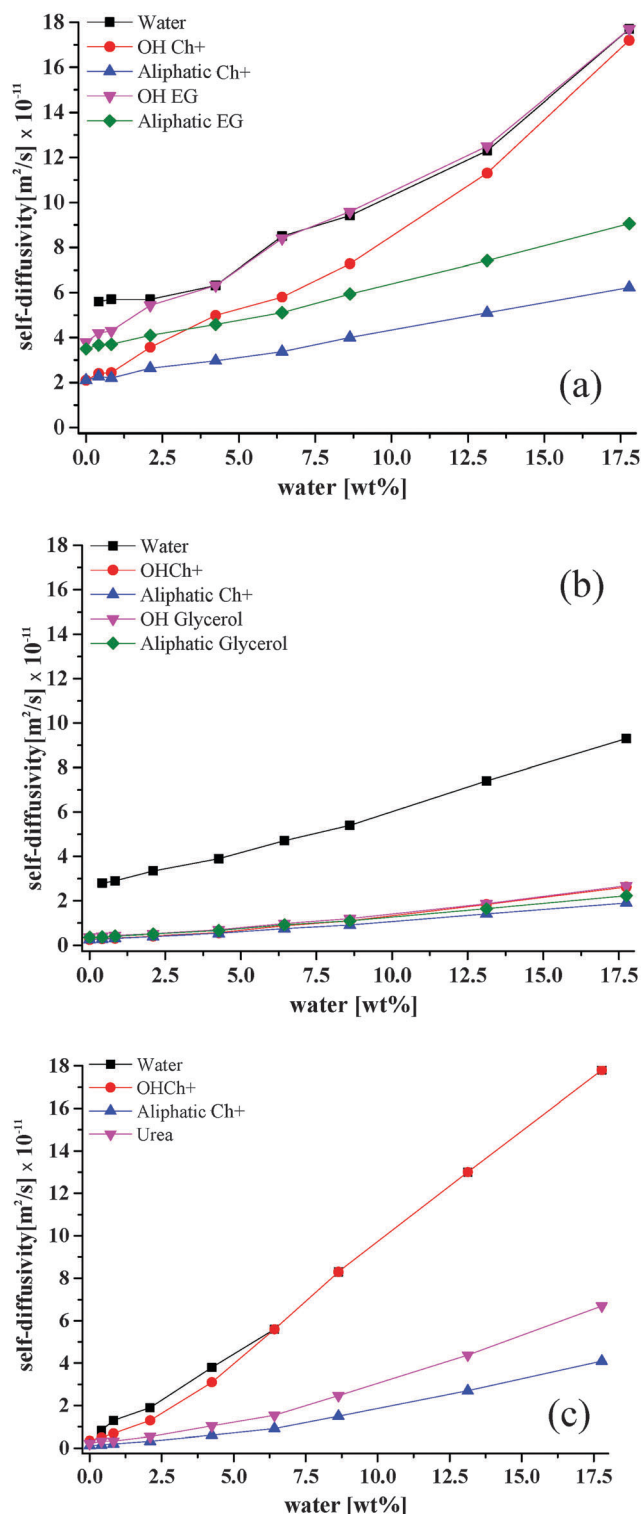


Fig. 5 Self-diffusivity coefficients for different species in (a) Ethaline, (b) Glyceline and (c) Reline as a function of water content at 20 °C.

becomes more significant as the water content increases, with values approaching those measured for pure water. Indeed, for the highest water content, the diffusion coefficients of the hydroxyl protons of Ch^+ and ethylene glycol are almost identical to that measured for water. This suggests that at higher water

content both Ch^+ and ethylene glycols are in equilibrium with some negatively charged species, with their hydroxyl counterpart in strong exchange with water. If that was not the case, then there should be no difference between self-diffusion of hydroxyl proton and that of the rest of the molecule, which is clearly not the case. It is noted that for the highest water content the $-\text{OH}$ resonance of the HBD and water overlap and the diffusivity reported is the average diffusivity of both species.

Glyceline

In the pure liquid the diffusivity of glycerol is slightly higher than that of Ch^+ , again reflecting the differences in molecular size; however, compared to the case of Ethaline, the diffusivity of the glycerol is similar to that of Ch^+ and this is also consistent with previous findings.¹⁴ Water has a significantly higher and distinct diffusion coefficient in Glyceline relative to all the other species of the DES, including the hydroxyl species of the DES components (*i.e.*, Ch^+ and HBD). This suggests that the hydroxyl protons of Ch^+ and glycerol forming Glyceline do not show any significant interaction with water, otherwise a different diffusion coefficient for such protons would be observed due to chemical exchange of protons, as previously observed in alcohol–water mixtures.²⁴ Conversely, the hydroxyl protons of both Ch^+ and glycerol have a similar value of self-diffusivity, particularly for low water content. As the water content increases, a deviation of the hydroxyl proton diffusivities in both Ch^+ and glycerol is observed, with values becoming higher than those measured for the rest of the molecules; however, such values are nowhere close to the values measured for water. For example, in pure Glyceline (*i.e.*, no water added) the hydroxyl proton of Ch^+ and its parent molecule (*i.e.*, Ch^+) have both a diffusivity value of $2.7 \times 10^{-12} \text{ m}^2 \text{ s}^{-1}$; the hydroxyl proton of glycerol and its parent molecule (*i.e.*, glycerol) have both a diffusivity value of $3.6 \times 10^{-12} \text{ m}^2 \text{ s}^{-1}$. Conversely, for the Glyceline sample with the highest water content, the hydroxyl proton of Ch^+ has a diffusivity of $2.6 \times 10^{-11} \text{ m}^2 \text{ s}^{-1}$, which is higher than the $1.9 \times 10^{-11} \text{ m}^2 \text{ s}^{-1}$ value measured for the Ch^+ ; the hydroxyl proton of glycerol has a diffusivity of $2.7 \times 10^{-11} \text{ m}^2 \text{ s}^{-1}$, which is higher than the $2.2 \times 10^{-11} \text{ m}^2 \text{ s}^{-1}$ value measured for the rest of the glycerol molecule. However, both hydroxyl protons have diffusivities that are still significantly slower than that of water, the latter having a diffusivity of $9.3 \times 10^{-11} \text{ m}^2 \text{ s}^{-1}$. This suggests that the interaction of Ch^+ and the glycerol with water is minimal compared to the Ethaline case; conversely, a much stronger correlated motion between Ch^+ and glycerol is observed. This could be attributed to differences in steric hindrance effects between ethylene glycol and glycerol.

Reline

A major difference in Reline compared to Ethaline and Glyceline is that urea does not have any hydroxyl protons that may interact with other species. In pure Reline, similar considerations to those made for pure Glyceline can be made in terms of differences in diffusion coefficients between the HBD and Ch^+ ; the diffusivity of urea is faster than that observed for Ch^+ ,

reflecting again the difference in molecular size. As water is added to the system, the diffusivity of the hydroxyl proton of Ch^+ starts deviating significantly relatively to the diffusivity of the rest of the Ch^+ molecule and approaches the larger diffusivity values observed for water. Above 10 wt% water, the resonances of the hydroxyl proton of Ch^+ and water become closer and eventually overlap. Above this water content, the reported diffusivity values for water and the hydroxyl proton of Ch^+ is that of the overlapping NMR peaks. The coalescence of these two NMR peaks indicates a fast exchange between the water protons and the hydroxyl protons of Ch^+ ,²⁵ in addition to the finding that the diffusion coefficients of such peaks become similar, this suggests a strong interaction between water and the hydroxyl proton of Ch^+ .

To compare the systems more clearly the data from Fig. 1 and 5 are combined in Fig. 6. In principle, if a Stokesian model of diffusion is valid then the diffusion coefficient should be inversely proportional to the viscosity. Fig. 6a shows that for the aliphatic protons on choline this behaviour is valid, although there is a slightly different slope for the first three data points (up to 2.5 wt%). In the dry ionic liquids and DESs we have previously shown that diffusion is non-Stokesian and this may be due to the large size of the diffusing species and the lack of suitable spaces for them to diffuse into.¹³ Application of the Stokes-Einstein equation:

$$D = kT/6\pi\eta R \quad (2)$$

where k is the Boltzmann constant and T the absolute temperature should enable the hydrodynamic radius, R to be calculated.

Fig. 6 shows also the theoretical line calculated for Ch^+ using eqn (2) and assuming the hard sphere radius of 3.29 Å calculated using a Hartree-Fock model and used previously.¹ It can be seen that the aliphatic protons all give responses very similar to those predicted by the Stokes Einstein equation. In a previous study¹⁴ it was shown that the diffusion coefficient for choline in pure Glyceline was lower than that expected from the Stokes Einstein Equation and this was related to the fact that the mass transport mechanism was limited by the availability of holes. When water is added to the liquid the smaller water molecules are able to move between these small voids and the availability of holes becomes less of an issue in mass transport.

Fig. 6b shows the response for the OH proton in Ch^+ and it is clear that there is a difference between the behaviour of Glyceline and the other two liquids. At low fluidities (*i.e.*, low water concentrations) all liquids show a behaviour which is similar to the theoretical slope for Ch^+ but Ethaline and Reline deviate significantly as the water content increases above 2.5 wt% (a 1:1 $\text{H}_2\text{O}:\text{Cl}^-$). At high fluidities (*i.e.*, high water content) the diffusion coefficients become similar to those expected for water (see Fig. 6c) *i.e.*, at low water content the water associates with the halide anion whereas at higher water contents it acts as essentially free water.

The data in Fig. 6b also suggest that aqueous solutions of Ethaline and Reline enable dissociation of the OH proton of

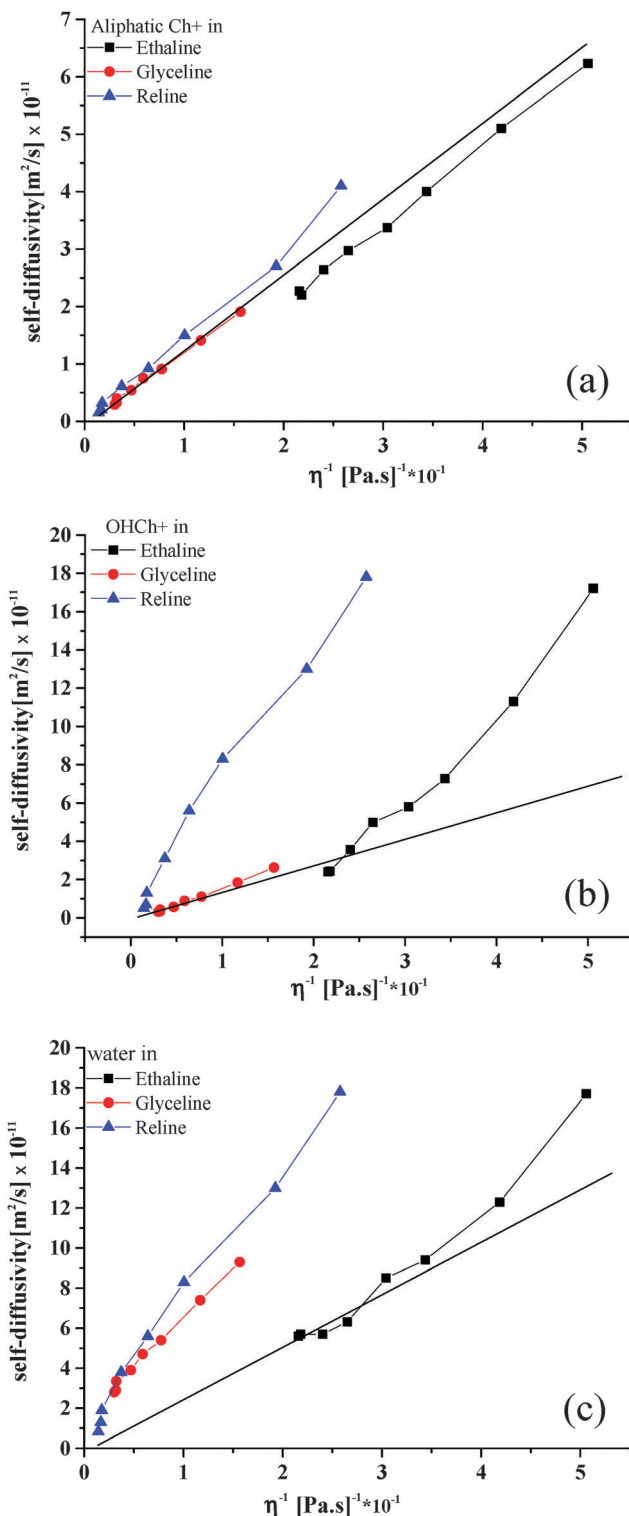


Fig. 6 Diffusion coefficients at 20 °C as a function of inverse viscosity for (a) Ch^+ , (b) OH of Ch^+ and (c) water in Ethaline, Glyceline and Reline. The linear solid black line corresponds to ideal Stokesian responses in (a) and (b) for Ch^+ and in (c) for water.

Ch^+ , which could make the liquids more acidic than Glyceline. This, together with the much faster mobility of the hydroxyl proton of Ch^+ in aqueous Ethaline and Reline, relatively to



Fig. 7 Samples of Ethaline (left) Glyceline (middle) and Reline (right) with 20 wt% water and each containing a sample of universal indicator paper.

Glyceline, as shown in Fig. 5, would explain the recently reported corrosion data for steel in these solutions, which showed negligible corrosion rate for steel in aqueous Glyceline compared to aqueous Ethaline and Glyceline. Fig. 7 shows solutions of the 3 DESs containing 20 wt% water and universal indicator paper as a pH indicator. It can clearly be seen that there is a significant difference in the colour of the solutions indicating that Reline is considerably more basic than the other two liquids. Use of a pH electrode shows the pH of the three solutions each with 20 wt% water to be Ethaline = 3.97, Glyceline = 7.02 and Reline = 12.2. The Glyceline solution is approximately neutral confirming that the OH proton on the Ch^+ remains associated, as shown in Fig. 5b, while the Ethaline solution is slightly acidic which is confirmed by the dissociation and larger diffusion coefficient of the OH proton relative to the Ch^+ , observed in Fig. 5a. The pH of Reline can only be explained by the partial decomposition of urea to form $\text{NH}_3/\text{NH}_4\text{OH}$. It should however be noted that the dissociation is relatively small with an OH^- concentration of $0.016 \text{ mol dm}^{-3}$. It is therefore unsurprising that only a trace NMR signal is observed.

These pH data also tie in with the corrosion studies recently reported for the three liquids,¹⁸ where it was shown that almost no corrosion was observed in wet Glyceline even after one year whereas mild corrosion was noted in both wet Reline and Ethaline. The formation of NH_4OH in dilute Reline would also explain the deviation from linear behaviour in Fig. 2 since there will be more charge carriers, which are considerably smaller and have a larger molar conductivity.

Fig. 6c shows the diffusion coefficient for water as a function of fluidity. The responses for Reline and Glyceline are similar and show a high diffusivity for water, which is similar in both liquids. The self-diffusion coefficient of pure water is $2.299 \times 10^{-9} \text{ m}^2 \text{ s}^{-1}$ at 25°C .²⁶ Using this value and scaling for viscosity produces the solid line seen in Fig. 6c. It can be seen that the data for Ethaline fit this quite well but the data for Glyceline and Reline are anomalously high. These results are difficult to reconcile if the liquids are homogeneous and it leads to the suggestion that the anomalous behaviour of water-DES mixtures arise because the water is not homogeneously mixed with the DESs but instead forms separate “microscopic” phases at

high water concentrations. Similar studies have been carried out using hydrophobic ionic liquids. Rollet *et al.*²⁷ used NMR spectroscopy to study water diffusion in 1-*n*-butyl-3-methylimidazolium bistriflimide $[\text{C}_4\text{mim}][(\text{CF}_3\text{SO}_2)_2\text{N}]$ and found diffusion coefficients for water which was 25 times higher than predicted. They concluded that this was due to phase separation at a microscopic scale. This phase separation is one that has been predicted by molecular dynamics simulations and is somewhat unsurprising given the hydrophobicity of the ionic liquids.²⁸ The hydrophilicity of DESs might lead to the assumption that aqueous mixtures are homogeneous but these diffusional studies show strongly that microscopic phase separation still occurs. The pH and the ability of water in these mixtures to form separate micro-phases could be responsible for some of the observations in biochemical and mineral processing applications *e.g.* the stability of enzymes in water DES mixtures.²⁹

Conclusions

This study has shown that in anhydrous DESs the HBD and OH on Ch^+ are associated and the fluidity of the liquid is controlled by the hydrogen bond interaction between the HBD and the halide anion. When water is added to the liquid the viscosity of all liquids decrease but a discontinuity is observed for all systems at about 2.5 wt% which corresponds to a 1:1 mole equivalent of water:chloride. This is the typical water content where changes in the behaviour of DESs have been observed. PFG NMR diffusion experiments revealed new insights into these liquids at a microscopic level. This study has shown that the choline cation diffuses in a Stokesian manner. However it has been shown for the first time that the addition of water can lead to the exchange of the OH proton on Ch^+ , which leads to mildly acidic solutions for Ethaline, *i.e.*, when ethylene glycol is used as the HBD. Conversely, for Reline, *i.e.*, when urea is the HBD, decomposition leads to the formation of basic solutions when NH_4OH is formed. Self-diffusion data for water strongly suggest that the liquids are not homogeneous and contain distinct microscopic water-rich phases when a significant amount of water is added. In conclusion, this study show that PFG NMR diffusion measurements are a powerful tool that combined with other characterisation methods may give new microscopic insights into complex liquid mixtures, such as the DES-water mixtures used in this work and yield information on both molecular dynamics and molecular/ionic interactions between the different species within the mixture.

Acknowledgements

Carmine D'Agostino would like to acknowledge Wolfson College, Cambridge, for supporting his research activities. The authors would also like to thank Salahaddin University (EIA) and the University of Kufa (AYMA) for funding studentships.

References

- 1 A. P. Abbott, R. C. Harris, K. S. Ryder, C. D'Agostino, L. F. Gladden and M. D. Mantle, *Green Chem.*, 2011, **13**, 82–90.
- 2 V. Krishnakumar, N. G. Vindhya, B. K. Mandal and F. R. N. Khan, *Ind. Eng. Chem. Res.*, 2014, **53**, 10814–10819.
- 3 U. N. Yadav and G. S. Shankarling, *J. Mol. Liq.*, 2014, **195**, 188–193.
- 4 A. P. Abbott, G. Capper, D. L. Davies, K. J. McKenzie and S. U. Obi, *J. Chem. Eng. Data*, 2006, **51**, 1280–1282.
- 5 H. G. Morrison, C. C. Sun and S. Neervannan, *Int. J. Pharm.*, 2009, **378**, 136–139.
- 6 A. P. Abbott, G. Capper, D. L. Davies, R. K. Rasheed and V. Tambyrajah, *Chem. Commun.*, 2003, 70–71.
- 7 E. L. Smith, C. Fullarton, R. C. Harris, S. Saleem and A. P. Abbott, *Trans. Inst. Met. Finish.*, 2010, **88**, 285–293.
- 8 A. P. Abbott, P. M. Cullis, M. J. Gibson, R. C. Harris and E. Raven, *Green Chem.*, 2007, **9**, 868–872.
- 9 H.-R. Jhong, D. S.-H. Wong, C.-C. Wana, Y.-Y. Wang and T.-C. Wei, *Electrochem. Commun.*, 2009, **11**, 209–211.
- 10 A. M. M. Sousa, H. K. S. Souza, N. Latona, C. K. Liu, M. P. Goncalves and L. S. Liu, *Carbohydr. Polym.*, 2014, **111**, 206–214.
- 11 A. P. Abbott, G. Frisch and K. S. Ryder, *Annu. Rev. Mater. Res.*, 2013, **43**, 335–358.
- 12 A. P. Abbott, D. Boothby, G. Capper, D. L. Davies and R. K. Rasheed, *J. Am. Chem. Soc.*, 2004, **126**, 9142–9147.
- 13 A. W. Taylor, P. Licence and A. P. Abbott, *Phys. Chem. Chem. Phys.*, 2011, **13**, 10147–10154.
- 14 C. D'Agostino, R. C. Harris, A. P. Abbott, L. F. Gladden and M. D. Mantle, *Phys. Chem. Chem. Phys.*, 2011, **13**, 21383–21391.
- 15 Y. H. Hsu, R. B. Leron and M. H. Li, *J. Chem. Thermodyn.*, 2014, **72**, 94–99.
- 16 Q. Zeng, Y. Wang, Y. Huang, X. Ding, J. Chen and K. Xu, *Analyst*, 2014, **139**, 2565–2573.
- 17 R. Esquembre, J. M. Sanz, J. G. Wall, F. del Monte, C. R. Mateo and M. L. Ferrer, *Phys. Chem. Chem. Phys.*, 2013, **15**, 11248–11256.
- 18 A. P. Abbott, E. I. Ahmed, R. C. Harris and K. S. Ryder, *Green Chem.*, 2014, **16**, 4156–4161.
- 19 J. E. Tanner, *J. Chem. Phys.*, 1970, **52**, 2523–2526.
- 20 A. Yadav and S. Pandey, *J. Chem. Eng. Data*, 2014, **59**, 2221–2229.
- 21 A. Yadav, S. Trivedi, R. Rai and S. Pandey, *Fluid Phase Equilib.*, 2014, **367**, 135–142.
- 22 R. C. Harris, PhD thesis, University of Leicester, Leicester, 2008.
- 23 P. S. Pregosin, *Prog. Nucl. Magn. Reson. Spectrosc.*, 2006, **49**, 261–288.
- 24 R. Li, C. D'Agostino, J. McGregor, M. D. Mantle, J. A. Zeitler and L. F. Gladden, *J. Phys. Chem. B*, 2014, **118**, 10156–10166.
- 25 P. J. Hore, S. G. Davies, R. G. Compton, J. Evans and L. F. Gladden, *Nuclear Magnetic Resonance*, Oxford Science Publications, Oxford, UK, 1995.
- 26 M. Holz, S. R. Heil and A. Sacco, *Phys. Chem. Chem. Phys.*, 2000, **2**, 4740–4742.
- 27 A.-L. Rollet, P. Porion, M. Vaultier, I. Billard, M. Deschamps, C. Bessada and L. Jouvencal, *J. Phys. Chem. B*, 2007, **111**, 11888–11891.
- 28 C. G. Hanke and R. M. Lynden-Bell, *J. Phys. Chem. B*, 2003, **107**, 10873–10878.
- 29 E. Durand, J. Lecomte, B. Barea, G. Piombo, E. Dubreucq and P. Villeneuve, *Process Biochem.*, 2012, **47**, 2081–2089.